Development of State of Charge Estimation Method and Power Optimization Strategies for Hybrid Electric Vehicles

THESIS

Submitted in partial fulfilment
of the requirements for the degree of

DOCTOR OF PHILOSOPHY

By

AISHWARYA PANDAY
ID No. 2011PHXF001P

Under the Supervision of

Prof. Hari Om Bansal

BITS Pilani
Pilani | Dubai | Goa | Hyderabad

BIRLA INSTITUTE OF TECHNOLOGY AND SCIENCE, PILANI

2016

Dedication

To my dear parents

Wonderful Brothers

Amazing Bhabhi

Cute little Punnu

and

Best ever friends

for

their unconditional love and encouragement over the years.

BIRLA INSTITUTE OF TECHNOLOGY AND SCIENCE, PILANI

CERTIFICATE

This is to certify that the thesis entitled **"Development of State of Charge Estimation Method and Power Optimization Strategies for Hybrid Electric Vehicles"** and submitted by **Aishwarya Panday,** ID No. **2011PHXF001P** for award of Ph.D. of the Institute embodies original work done by her under my supervision.

_____

Signature of the Supervisor

Name: Dr. HARI OM BANSAL

Designation: Associate Professor

Date: / / 2016.

Acknowledgements

I would like to take this opportunity to convey my heartfelt gratitude and indebtedness to my supervisor, Prof. Hari Om Bansal for all his support, guidance and supervision during my research tenure.

The time spent at BITS-Pilani was very enjoyable and inspiring. I wish to thank all my colleagues in creating a great working environment for in-depth technical discussions and valuable suggestion to cope with all sorts of difficulties. I owe a debt of gratitude to my Doctoral Advisory Committee members Prof. H. D. Mathur and Prof. Rajneesh Kumar, whose well-versed comments have shed a new light on several aspects and feedback in stratifying the research work. I heartily thank to Prof. Surekha Bhanot for unveiling the meaning of life with positive reflections at every juncture. I owe my sincere gratitude to HOD Prof. Anu Gupta and Prof. V. K. Chaubey for providing me the requisite facility to carry out my doctoral research. I would like to show my gratitude to Prof. Navneet Gupta, convener, Doctoral Research Committee for all their support and useful suggestions.

I wish to express my humble gratitude to Vice Chancellor, Director, Deputy Directors, Deans, BITS Pilani, Pilani Campus for providing me the opportunity to pursue my doctoral studies. I express my gratitude to Prof. S. K. Verma, Dean-ARD, Prof. H. R. Jadhav, Associate Dean-ARD and Prof. S. Kumar, Associate Dean-SRCD, for their official support and encouragement. I extend my thanks to SRCD and ARD staff for their valuable support.

There have been several inspiring individuals I would like to acknowledge. My interest in mathematics is one way or another reflection of the interesting lessons given by Mr. Arun Kumar Singh in my high school days. I would like to express my earnest gratitude to Prof. Pankaj Rai to craft control systems fascinating for research exercise. My desire to pursue PhD is cultivated by Dr. A. K. Singh and I cannot thank him enough the way he helped me.

I would also like to thank my mom and dad in inspiring and imparting the faith that created crave for knowledge, whether humanity or science. I wish to thank my brothers and bhabhi for all their love, emotional support and inspiring words to

complete thesis and a humble surrender before the almighty who blessed me with a little nephew whose cute smile makes my day.

During my teaching assistantship, I got unflinching support from Mr. Manoj Jangir, Mr. Ravindra Kumar, Mr. Tulsiram Sharma, Mr. Ashok Saini, Mr. Mahesh Chandra and Mr. Amitabh Jangir for the successful course delivery. I extend my sincere gratitude to Mr. Bridi Chand and Mr. Sanjay Bhargava to deal with all the documentation required for a research scholar. They always made cumbersome processes trouble-free.

I would like to thanks all my pears and seniors for their support and inspiration during the gamut of adverse time and to help me to overcome from such impasses. I would cherish happy moments spent with my friends at BITS Pilani campus for the whole life.

Aishwarya Panday

Abstract

Automobiles have provided a great freedom to the society in terms of mobility and convenience. On the other hand, the price has been paid in terms of ecological imbalance. The conventional Internal Combustion Engine (ICE) based vehicles emit copious measure of toxic gasses; strangling the environmental balance and are serious threat to human life. The availability of petroleum resources are limited and need to be consumed sagely to run for a longer incumbency. Hasty usage of fossil fuels has resulted in rapid depletion of natural resources and price inflation. These concerns encourage the modern society to ascertain new alternatives for the sustainable future transportation. One prominent solution could be to adopt hybrid vehicles as part of the modern transportation scheme. These vehicles can be the path-breaker to reshape the transportation arena and face of the market with poise between petroleum consumption and toxic emissions. Various aspects like sources of pollution, decreasing level of fossil fuel, dependency on oil energy are discussed in this thesis. Several government schemes to focus on securing its energy resources, trim down reliance on fossil fuels and to promote hybrid vehicles on roads are discussed. Hybrid vehicles employ two power sources namely, ICE and an alternative/renewable energy source; spruce down the usage of petroleum. By introducing hybrid vehicles on road brings many techno-economical challenges in accepting them. Remedies to these challenges are also suggested before inviting them on roads.

Hybrid Electric Vehicles (HEVs) use ICE and an electrical energy source (battery); therefore batteries play a vital role in HEV's proficient performance. Various types of rechargeable batteries are available in market and a wise and worthy choice is of utmost importance. Hence, proper selection of battery is of prime concern. The base of this thesis work is to identify relevant battery using multi criteria decision making methods for HEV applications. Ashby's methodology, Technique for Order Preferences by Similarity to an Ideal Solution (TOPSIS) and VIse Kriterijum-ska Optimizacija Komprominsno Resenje (VIKOR) methods are employed to assess various battery attributes like specific energy, energy density, electrical efficiency, self-discharge rate, nominal cell voltage, energy per cycle, cost and durability of the battery. On the basis of battery selection charts, it is found that Li-ion and Ni-MH batteries outperform and would serve the purpose.

Today, the major challenge is to utilize battery power efficiently without deteriorating its health while minimizing fuel consumption for HEVs. Hence, accurate information about battery operating conditions and State of Charge (SOC) level are essential. Therefore, analysis of suitable battery model and SOC calculation are required to predict its characteristics. Since battery performance greatly depends on the temperature and SOC level, a generalized thermo electric model is proposed to predict its I-V characteristic and dynamic behavior of battery. Three battery models namely, model 1, model 2 and model 3 presented here represent cover the resistance offered by electrolyte, diffusion and double layer effects developed at the contact points of electrode and electrolyte to realize its operational characteristic. Temperature alters the operating conditions and self discharge rate affect the shelf life of battery; thus both are given attention while calculating current and voltage. The conventional SOC estimation method (based on current) is emended and a modified SOC estimation method is deduced. Proposed method, observe both voltage and current and blend them using a weighting factor to calculate precise SOC. A correction factor is also formulated to read absolute SOC useful for varying temperature and different loading circumstances. Thermal behavior of Li-ion battery is investigated for wide temperature range and its effect on resistance, capacity and open circuit voltage (OCV) is analyzed.

In HEVs, presence of ICE and battery together inevitably postulates for power split between these. Different optimization techniques available in literature for energy management of HEVs are detailed in depth. These techniques with its features and limitations are presented and a comparison of all the control strategies to optimize the power split is carried out.

In this thesis work, efficient energy management strategies are developed to split power between ICE and battery. The vehicle performance is analyzed using different battery models using proposed modified SOC estimation method are employed to analyze the vehicle performance. HEVs' governing parameters are optimized using DIviding RECTangle (DIRECT) method firstly considering default SOC estimation algorithm and fuel economy is determined. Further, to improve the performance of the vehicle, Genetic Algorithm (GA) based control strategy is used. It is observed that the vehicle performance is altered due to varying temperature

conditions because battery charging/discharging efficiency, resistance, capacity and OCV varies. Effect of temperature is analyzed to restrict the operating range of the vehicle to achieve the fuel efficient performance along with the longer battery life. The GA based method proves to be better as compared to DIRECT. GA based control strategy is applied to various battery models to opt for the best model. The engine is operated in its most efficient region during the analysis promises for fuel consumption diminution. Further, Pontryagin's Minimum Principle (PMP) is articulated, features with a lesser computation time and real time implementable. To decide the threshold power level at which engine should be turned on/off, optimal values of various governing parameters from GA are fed to PMP and promising improvement in fuel efficiencies are found.

The Indian market is very emerging in almost all the sectors and for vehicle fleets, it ranks second after China. Hence, an smart analysis of HEVs' performance before casting them on road can lead to strategized and successful projection. It is imperative to check the nature and response of a hybrid vehicle on different driving cycles because road profile parameters play an important role in determining the fuel efficiency. Typical parameters of road profile are reduced to a useful smaller set using size reduction techniques and then various considered driving cycles are ranked in order of their fuel economy using multi criterion optimization methods. These results are further validated using GA based intelligent power split control strategy. The results reveal that Indian city driving cycle offers higher fuel economy for an HEV as compared to other countries' driving cycles. This may attract more HEV manufacturing giants and would lead to further reduction in toxic emissions and improvement in the economic growth of the country.

Finally the overall conclusion and future scope of further research work is hashed out.

Table of Contents

List of Figures

List of Tables

List of Symbols

Symbols	Notation
ω_s	Sun angular speeds
ω_c	Carrier angular speeds
r_r	Ring radii
r_s	Sun radii
T_c	Torques acting on carrier gear
T_s	Torques acting on sun gear
T_r	Torques acting on ring gear
ω_e	Engine speed
ω_m	Motor speed
ω_g	Generator speed
N_r	Tooth number in ring gear
N_s	Tooth number in sun gear
ω_r	Ring angular speeds
$T_{M/G1}$	Torque provided by M/G1
$T_{M/G2}$	Torque provided by M/G2
$\omega_{M/G1}$	Speed of M/G1
$\omega_{M/G1}$	Speed of M/G2
T_{req}	Requested torque at wheels
ω_{req}	Requested speed at wheels
Z	Final drive ratio
R_g	Gear ratio
ω_{e_max}	Maximum allowable speed of engine
ω_{e_min}	Minimum allowable speed of engine
ω_{ring}	Speed requested at ring gear
$\omega_{g_{max}}$	Maximum speed of generator
$\omega_{g_{min}}$	Minimum speed of generator
V(t)	Open circuit voltage at time t
V'(t)	Output voltage at time t
i(t)	Current at time t
R_{int}	Internal resistance of battery
R_1	Diffusion resistances
R_2	Double layer resistances
C_1	Diffusion capacitance
C_2	Double capacitances
a_0	Battery terminal voltage when SOC = 0%
a_1	Battery terminal voltage when SOC = 100%
$\frac{dV}{dT}$	Temperature coefficient
T	Temperature
$SOC_v(T)$	Open circuit voltage based SOC at temperature T
$SOC_i(T)$	Current based SOC at temperature T
C_P	Battery capacity in Ah
$i_{(s-d)}$	Self discharge current

$\mathbf{K_0}$	Reaction constant
R	Gas constant
$\mathbf{E_a}$	Activation energy
ΔT	Change in temperature
$\mathbf{W}$	Weighting factor
$\mathbf{H}$	Correction factor
$\mathbf{A_f}$	Frontal area
$\mathbf{C_D}$	Aerodynamic drag
$\boldsymbol{\rho}$	Air density
$\mathbf{V}$	Vehicle speed
$\mathbf{V_w}$	Component of wind speed
$\mathbf{f_r}$	Rolling resistance
$\boldsymbol{\delta}$	Road angle
P	force acting on the center of a standstill tire
$\mathbf{T_p}$	Torque output from the power plant
$\boldsymbol{\eta_t}$	Efficiency of driveline from power plant to the driven wheels
$\mathbf{m_{ep}}$	Mean effective pressure
$\mathbf{V_d}$	Volumetric density
$\mathbf{T_l}$	Load toque when mechanical load is applied
J	Moment of inertia
B	Viscous friction
$\frac{\mathbf{d\theta}}{\mathbf{dt}}$	Rotation speed
$\mathbf{r_w}$	Wheel radius
$\mathbf{i_{rw}}$	Gear ratio of the ring gear to drive train wheels
$\mathbf{i_{mw}}$	Gear ratio from the traction motor to the driven wheels
$\mathbf{n_{tm}}$	Traction motor speed
$\mathbf{V_L}$	Vehicle low speed threshold
$\mathbf{V_H}$	Vehicle high speed threshold
V	Vehicle speed
$\mathbf{K}$	Kelvin
$\mathbf{P_b}$	Battery power
$\mathbf{V_{oc}}$	Open circuit voltage of battery
$\mathbf{R_b}$	Battery resistance
$\mathbf{I_b}$	Current flowing in battery
$\dot{\mathbf{SOC}}$	Time rate of SOC
Subscript 'min'	Minimum value
Subscript 'max'	Maximum value
Mpgge	Miles per gallon gasoline equivalent
Eq.	Equivalent

Chapter 1
Introduction

Internal combustion engine (ICE) based vehicles are the backbone of the modern transport sector. These vehicles use fossil fuels as a source of energy to propel it and emit toxic gases. These noxious gases harm the environment and causes human health problems. Hasty usage of fossil fuels results in rapid depletion of these resources and price inflation. These concerns encourage the modern society to discover alternatives for sustainable future transportation. This chapter discusses about various aspects like sources of pollution, decreasing level of fossil fuel, society's dependency on oil energy and need of green vehicles. A broad literature analysis and statistics compilation is carried out to emphasize the move towards green vehicles (EVs and HEVs). It suggests to adopt fuel efficient technologies, tells the challenges in accepting them as part of the transportation system and their remedies also. The status of hybrid vehicles on the roads worldwide and initiatives taken by different governments are discussed in lucent manner. This chapter deliberately describes governments' schemes to focus on securing its energy resources, trim down reliance on fossil fuels and to promote hybrid vehicles on roads to make pollution free world.

1.1 Background

Call forth of the automobiles and its pulsation towards development and economic growth has liberated the society with greater mobility and convenience. The growth of modern society relies on efficient modes of transportation and satisfied many needs of everyday life. The automobile industry plays an imperative function in leading world's economy and has an effect on each level of population. ICE is the strength of automobile sector and uses fossil fuels as a source of energy. These ICE based transportation causes large amount of toxic emissions of carbon dioxide (CO_2), carbon monoxide (CO), nitrogen oxides (NO_x) and unburned hydrocarbons (HCs) which results in environmental pollution and global warming. Exponential rise in population and increase in personal

transportation interest have amplified the number of automobiles around the globe. It has caused and prolong to cause severe environmental problems and a hazard to human life.

Due to several reasons, i.e. air pollution, greenhouse gas emissions, rapid depletion, cutting level of natural resources and rise in oil prices; humanity need to move towards the a greener solution for transportation. These issues are described here in detail.

1.1.1 Air Pollution

As a result of chemical reaction between fuel and air, ICE produces heat as well as CO_2 and unburned HCs. Jos et al. revealed that air pollution is a major environmental jeopardy to health and causes approximately two million premature deaths worldwide per year. Around 620,000 premature deaths occur in India due to air pollution-related diseases [1].

1.1.2 CO_2 Emission

Emission of CO_2 is the main cause of global warming. It has reached to a dangerous amount of 34 billion tonnes globally in 2011. After China, the United States, the European Union, the Russian Federation; India is fifth with a 6 percent contribution to CO_2 emission [2]. According to the 'Ministry of environment and forests' report, toxic emissions are contributed by road transport, aviation, railways and navigation. In 2007, Indian transport sector contributed 142.04 million tonnes of CO_2 eq. in which road transport contributed 87 percent and aviation sector added 7 percent [3]. Energy sector emitted 1100.06 million tonnes of CO_2 eq., of which 719.31 million tonnes are emitted from electricity generation and 142.04 million tonnes from the transport sector [4]. 'Centre for Science and Environment' expects that CO_2 emissions on Indian roads will reach to a hazardous level of 1212 million tonnes by 2035. Figure 1-1 shows CO_2 emission in India since 1980 [5]**.**

23 percent of total CO_2 emissions in the world is caused by the transport sector. Automobiles and light trucks contribute over 60 percent of emissions from the transport sector [6]. The upper safety limit for atmospheric CO_2 is 350 parts per million (ppm) which has stayed higher than 350 ppm since early 1988 [7].

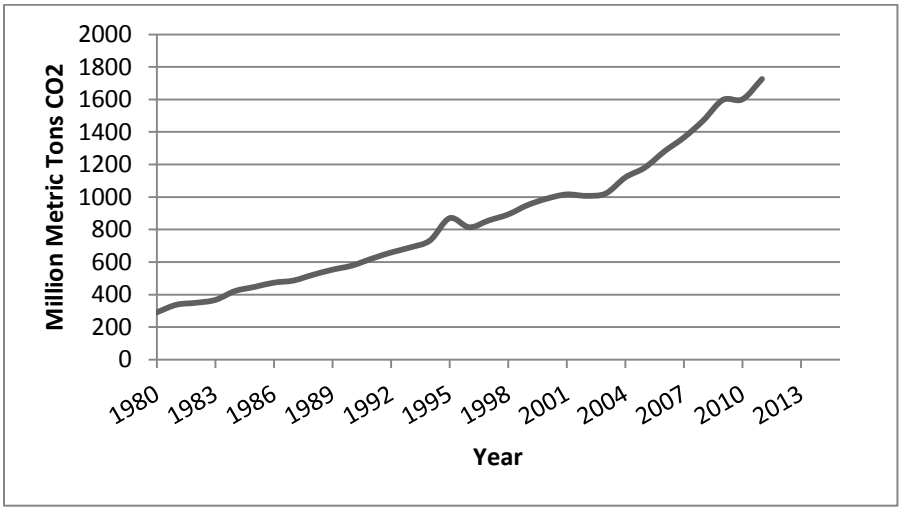

Figure 1.1: Increasing CO_2 emission in India

CO_2 emission from liquid fuel consumption worldwide has increased by approximately 0.9 percent per year which results in an increment of 3.5 billion metric tons from 2010 to 2040. The coal related CO_2 emission has decreased for 'Organization of Economic co-operation and Development' (OECD) countries by 0.1 percent per year, whereas, an increase of 1.7 percent per year is observed for non-OECD. As a result, the OECD's CO_2 emissions from liquid fuels will decline from 52 percent (2010) to 39 percent (2040) as shown in figure 1.2 [8].

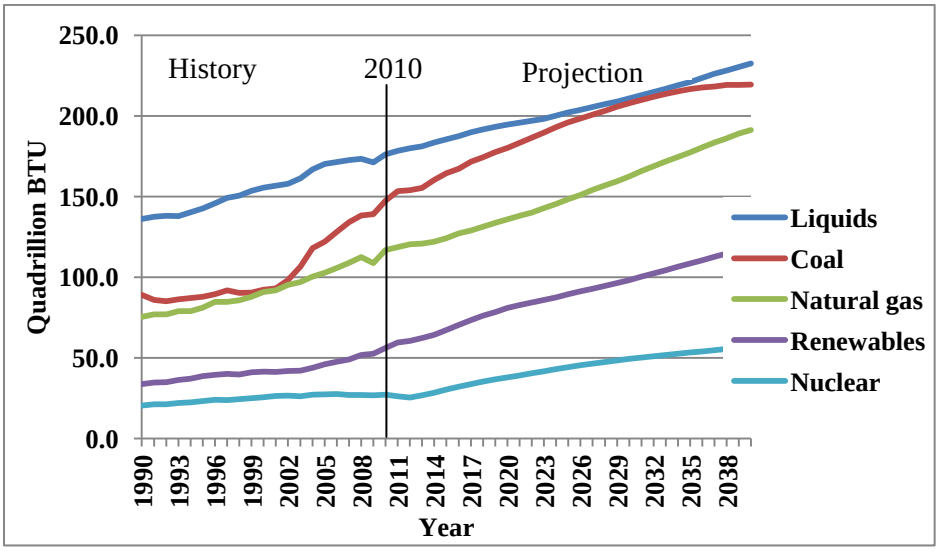

Figure 1.2: World energy consumption by fuel type

The use of energy sources is increasing over the time horizon. In non-OECD countries, with increasing gross domestic product (GDP) and a rise in living standard; an increase in the travel and freight transport is expected to happen. This will result in high

energy demand. Figure 1.3 shows the comparison of energy consumption between OECD and non-OECD countries.

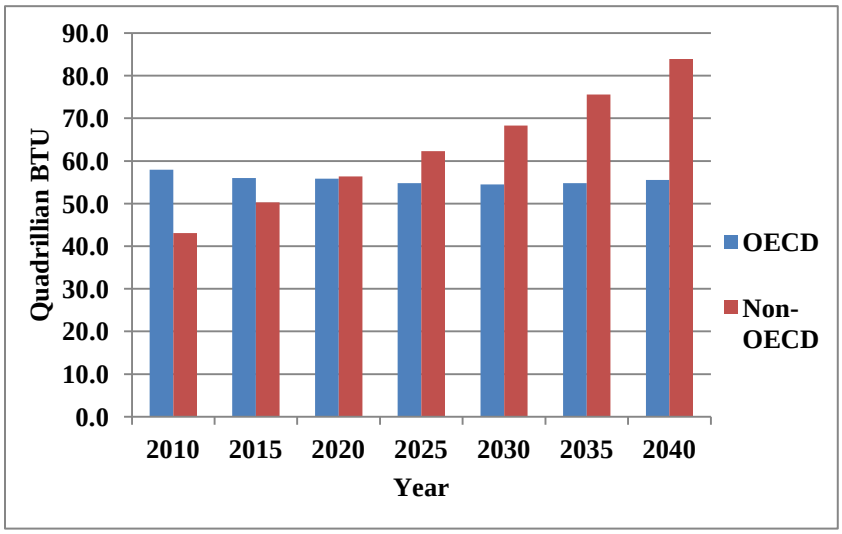

Figure 1.3: Energy consumption by OECD and non-OECD countries

2.0-2.5 percent growth in transportation energy use is recorded per year globally since 1971-2006 and road transport sector alone has used most of the energy. Rapid transport growth is expected to rise continuously in non-OECD countries if the income rise continues. Population growth is also much more rapid in non-OECD countries than in OECD countries [9]. In contrast, there are signs of saturation of some types of travel in OECD countries.

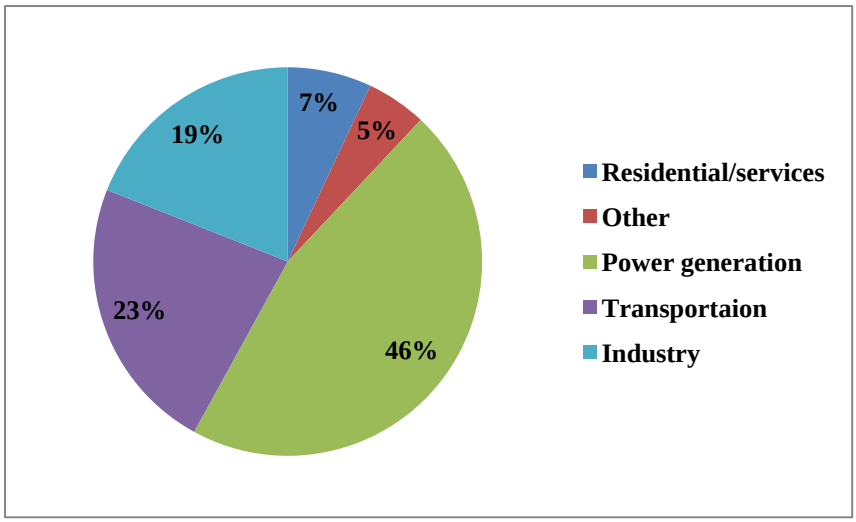

Figure 1.4: Sector wise CO_2 emission per year

In figure 1.4, percentage contribution of different sectors is shown. Expanding motorization across the globe has caused a steady increase in CO_2 emission in the

transport sector, which accounted for about 23 percent of total worldwide CO_2 emissions in 2005, of which roughly 73 percent was generated by road transport [10].

1.1.3 Green House Gas Emission

Due to the greenhouse effect, earth's atmosphere is slightly warmer than it should be. The greenhouse gases (GHG) trap the heat and increase earth's temperature. CO_2 emission along with other gases like CO, NOx, etc. is the major contributors to GHGs. It has been investigated that, within the time period of 1980 to 2000, number of vehicles increased by nine times and gasoline/diesel consumption for road transportation became quadrupled [11]. The road transport sector in India is the largest consumer of liquid fuel and accounts for nearly 35 percent of it. India's GHG emissions increased by 4.2 percent in 2000 with the quantity of 1301.21 million tonnes compared to the data recorded in 1994 [12]. Report of 'Ministry of Environment and forests' state, net GHG emissions from India in 2007 was 1727.71 million tonnes of CO_2 eq. of which, CO_2 was 1221.76 million tonnes, CH_4 was 20.56 million tonnes and nitrous oxide (N_2O) was 0.24 million tonnes [3].

1.1.4 Increasing Oil Prices

According to Silicon India, on an average approximately 30 percent of worldwide energy consumption is by the transportation sector, of which 95 percent is supported by liquid fuel. By the report of Business Line, it is estimated that a sustained $10 increase in oil prices leads to a 1.5 percent reduction in the GDP of developing countries.

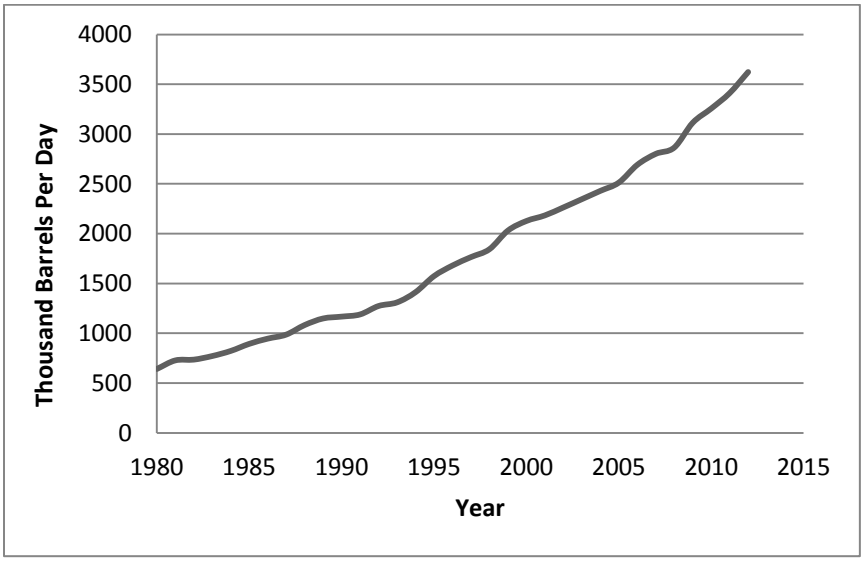

Figure 1.5: Petroleum oil consumption in India

From the updates of Commodity Online, oil imports during April-October, 2012-13 are valued at $95569.0 million, which is 9.99 percent higher than the oil imports of $86887.7 million in the corresponding period last year. Today, over 80 percent of India's requirements of petroleum products is being imported which is likely to increase continuously. India's oil import bill leaped 40 percent to a record of $140 billion in 2011-12. In 2011, 3426 thousand barrels of petroleum per day are recorded in India, which is the fourth largest amount of consumption in the world [13]. Petroleum oil consumption since 1980 to 2011 in barrels per day is shown in figure 1.5 for India.

Global economic conditions are highly dependent on oil demand and pricing. According to the IEA, negative impact on the global economy is measured due to increase in oil prices. According to [14], price path assumptions are made on the basis of possible production levels and the world oil price path and it will be approximately $160 per barrel in 2035. Figure 1.6 shows the consumption of petroleum by different sectors from 1990-2040 with projections. It is projected that total liquid consumption peak at 19.8 million barrels per day in 2019 whereas it falls to 18.9 million barrels per day in 2040. And it can be easily analyzed that the largest share of total consumption is accounted by the transport sector. It is expected to fall in 2040 to 68 percent from the 72 percent in 2012. The reason behind this may be the improvement in vehicle efficiency by following the 'Corporate Average Fuel Economy' (CAFE) standards [15].

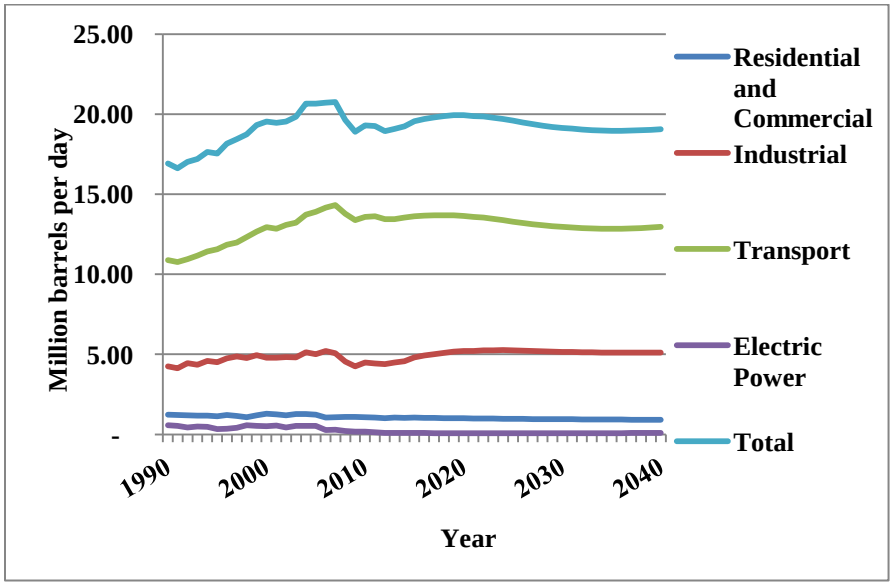

Figure 1.6: Consumption of petroleum and other liquids by sector (1990-2040)

An Increment in the crude oil prices has been observed all the time. The average U.S. retail price of regular gasoline rose from $3.25 per gallon on December 17, 2012 to $3.78 per gallon on February 25, 2013. Over the past ten years, the 'Chained Consumer Price Index' (C-CPI-U) which is a measure of change in the cost of living has approximately tracked the movements of the international Brent crude oil price [16].

1.1.5 Extraction of Natural Resources

Ever-increasing consumption of liquid fuel is causing hasty extraction of crude oil throughout the world. In 1980, extraction of crude oil was less than 200 thousand barrels per day in India and became 782.34 thousand barrels per day in 2011. Crude oil consumption per day in India is shown in figure 1.7 for period of 1980-2011. India ranks 24th position in total crude oil production in the world. India's petroleum production per year is very less as compared to its demand; therefore its net export/import decreases year after year.

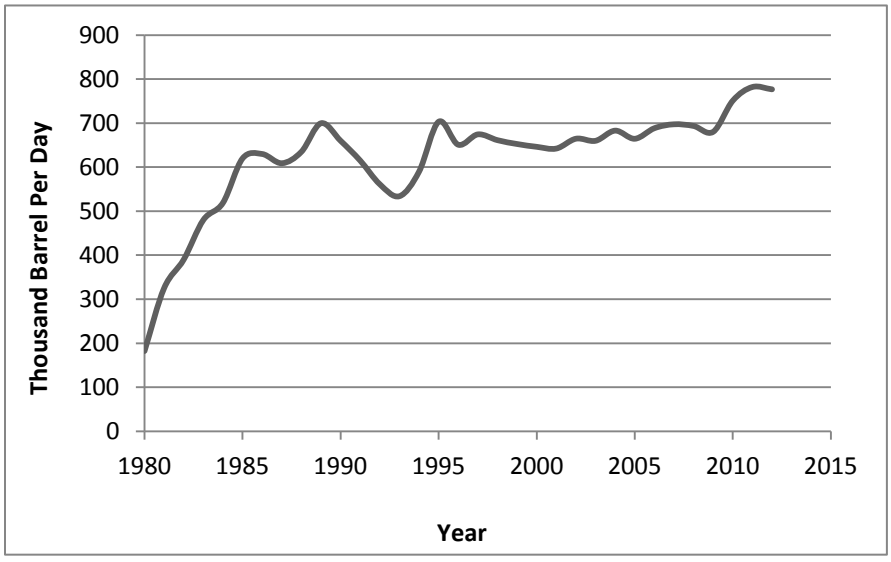

Figure 1.7: Crude oil consumption in India

In 2011, 89 million barrels of oil and liquid fuel were consumed per day worldwide, which accounts around 32 billion barrels per year. It is expected, China will demand almost half of the global oil and it will continue up to 2035. Whereas for OECD countries demand will decrease because their governments' are implementing the required policies on fuel efficiency and high vehicle prices. From the figure 1.8, it is clearly shown that the crude oil production worldwide increasing year after year.

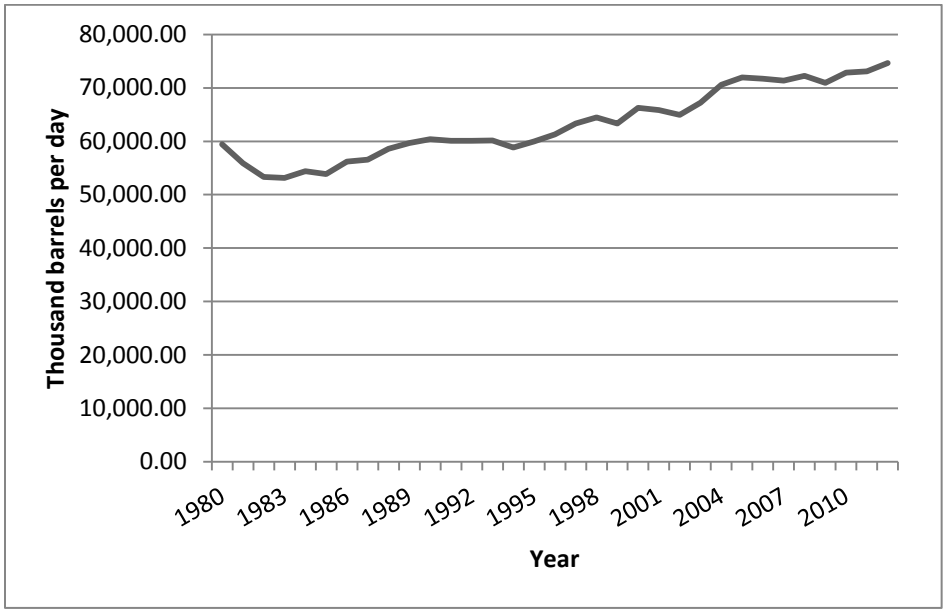

Figure 1.8: World crude oil production year wise

Saudi Arabia is on the 1st position by producing the highest amount of crude oil. United states, Russia, China, Canada, Iran, United Arab Emirates, Iraq, Mexico, Kuwait, Brazil, Nigeria, Venezuela, Norway and Algeria are following Saudi Arabia and are in the list of top producers of crude oil [5].

International Energy Outlook (IEO) reveals that overall energy consumption in the world will rise from 523.9 quadrillion British Thermal Units (BTU) in 2010 to 629.8 quadrillion BTU in 2020 and is expected to reach the amount of 819.6 quadrillion BTU in 2040 as shown in figure 1.9 [17].

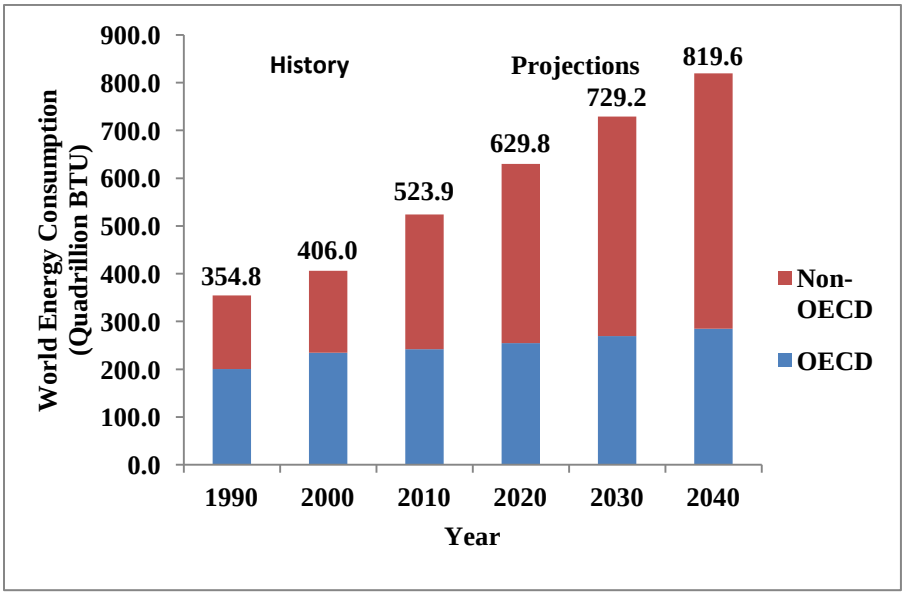

Figure 1.9: World energy consumption

Much of the growth in energy consumption occurs in countries outside the non-OECD, where demand is driven by strong long-term economic growth. Energy usages in non-OECD nations increased by 85 percent whereas only 18 percent increase is observed for the OECD economies.

1.1.6 Dependence on Oil Energy

World use of petroleum and other liquids has increased from 85.7 million barrels (2008) to 97.6 million barrels (2011) per day. Existing studies reveal, despite of rising fuel prices, use of liquids for transportation is increasing by an average of 1.4 percent per year, or 46 percent overall from 2008 to 2035. Figure 1.10 represents the oil consumption for various sectors, i.e., transportation, industrial, buildings and electrical power generation. The use of liquids will increase for transport sector.

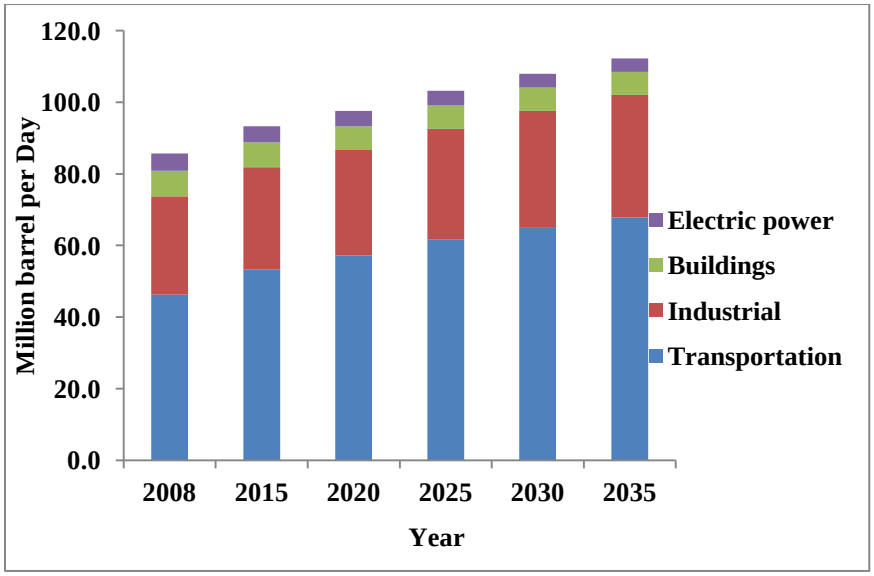

Figure 1.10: Sector wise world liquid fuel consumption

1.1.7 Import

Despite of the slowing global economy, India's liquid fuel demand continues to rise. In India, vehicle ownership is expanding so the petroleum demand also. India's domestic energy resource base is substantial, still country relies on imports of a considerable amount of energy to fulfil its demand. According to IEA Country Analysis Briefs' transportation accounts for the majority of India's energy use. Together, coal and oil shares about two-third of total energy usages. Natural gas accounts around 7 percent

share, which is expected to grow with the discovery of new gas deposits. Figure 1.11 shows the energy contribution of different sources [18].

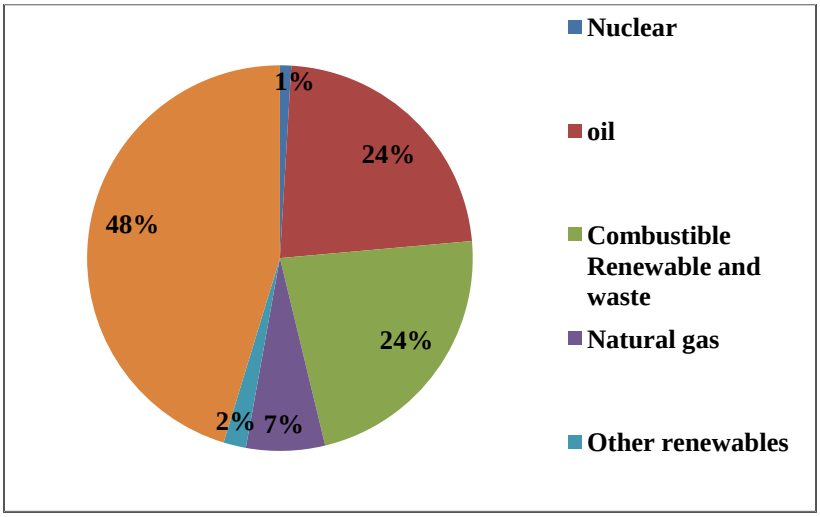

Figure 1.11: Share of different energy sources

1.2 Solution

In the near future oil production will fall, but its consumption will continue to rise, so it is essential to find an alternative, preferably green and sustainable. Considering environmental and economical challenges, a new concept of transportation should be included to reduce petroleum consumption and toxic emissions with better efficiency. Based on the detailed evaluation of probable costs and GHG emission consequences, various strategies like improvement in vehicle efficiencies through fuel economy standards (for manufacturers), improving fuel quality, encouragement for the cleaner fuels and mode shifting may be used. Transport sector should eradicate the complete dependence on oil by adapting the new transportation medium. This concept has introduced new vehicles such as Electric Vehicles (EVs), HEVs and Plug-in Hybrid Electric Vehicles (PHEVs) which are clean, economical, efficient and environment friendly.

1.2.1 Worldwide Initiatives for Hybrid Vehicles

Exposure to air pollutants is beyond the control of individuals and requires a lot of involvement of public authorities at the regional, national and even international levels to control. For better economic growth along with environmental and energy security, U.S. 'Department of Energy' (DOE) has started a clean city program since 1993 [19]. DOE

supported National Renewable Energy Laboratory (NREL) is working to improve supportive energy sources for hybrid vehicles. A lot of research is in progress to improve the performance of Li-ion battery. NREL expects significant role of the battery based vehicles in coming 30 years [20].

'International Council on Clean Technology' is working to improve the environmental performance and efficiency of cars, trucks, buses and transportation systems in order to protect and improve public health, environment and quality of life. In July 2012, the 'European Commission' proposed regulations for new passenger cars and light-commercial vehicles and labelled it mandatory to achieve year 2020 CO_2 emission targets. The IEA provides support for over 40 international co-operation and collaboration agreements in energy technology research and development, deployment and information dissemination.

In 2012, the global sales of hybrid vehicles have tripled to 2.2 million units. Germany, France, Norway, Netherlands, United Kingdom and Sweden will be the top six European countries to use Battery Electric Vehicles (BEVs) in the year 2020 and these will capture more than 67 percent of the total market. In case of PHEVs, only four countries are expected to exceed a volume greater than 100,000 vehicles. In this case Germany, France, Italy and United Kingdom will have 52 percent of total hybrid vehicles across the globe [21]. According to Pike Research forecast more than 1.8 million BEVs, 1.2 million PHEVs and 1.7 million HEVs will be on Europe's roadways by 2020 [22].

By taking a step forward IEA is conducting huge research and analysis for the transportation area to reduce GHGs and policy making to have a healthy environment in the future. IEA efforts in analyzing transport system to reduce GHG emissions and oil dependency.

Several projects are led by IEA and other external stakeholders to have a greener tomorrow.

1.2.1.1 The Mobility Model Partnership

Since 2003, a global transport spreadsheet model has been developed, known as Mobility Model (MoMo). For transport sector's energy and GHG emission implications, MoMo collects historical data by mode, by fuel, and by region and provides projection for 2050.

It performs the quantitative analysis and contributes in publishing 'Energy Technology Perspectives' and 'World Energy Outlook' and shares with other partners. The MoMo is divided into 29 regions covering all modes of transportation. It analyses the future fuel pathways and the impact of new technologies on energy use, GHG emission, vehicle and fuel cost and other concerned matters.

1.2.1.2 Global Fuel Economy Initiatives

According to 'Global Fuel Economy Initiatives' (GEFI) which includes the 'United Nations Environment Program' (UNEP), 'International Transport Forum' (ITF) and 'Federation International Automobile' (FIA) foundation claims that improved fuel economy will decrease CO_2 emission by half by 2050 and a 6 billion barrel oil per year can be saved.

1.2.1.3 The Electric Vehicle Initiatives

Electric Vehicle Initiatives (EVI) is a multi-government policy forum dedicated to rapid introduction and adoption of EVs worldwide. EVI is adopted by the 'Clean Energy Ministerial' (CEM). CEM involves the world's major economies' energy ministers. Fifteen member governments from Africa, Asia, Europe, North America and EIA are included in EVI. It aims to deploy around 20 million passenger car EVs, including PHEVs and fuel cell electric vehicle (FEV) globally by 2020. EVI is planning to launch a 'World EV cities and ecosystem web portal' which will be able to capture deployment progress all over the world. EVI include China, Denmark, Finland, France, Germany, India, Italy, Japan, Netherlands, Portugal, South Africa, Spain, Sweden, the United Kingdom and the United States. The IEA facilitates and coordinates the collection, analysis and dissemination of EVI data.

1.2.1.4 The Partnership on Sustainable, Low Carbon Transport

To improve the knowledge of developing countries (government and business) about sustainable, low carbon transport and to help them to develop better policies regarding greener transport, 'Partnership on sustainable, low Carbon Transport' (SLoCat) is formed. Over 50 organizations including United Nations, multilateral development banks, Technical co-operation agencies, non-government organizations and research

organizations are part of SLoCaT. More than 350 million conventional vehicles are expected to be on the road of OECD and non-OECD countries by 2020. It will increase to 400 million by 2030 for non-OECD whereas conventional vehicles are estimated to decrease for OECD countries and hundred million hybrid vehicles are expected to be on the roads.

1.2.2 Scenario in India

In India, transport sector accounts for about one-third of the total crude oil consumption and 80 percent of this is utilized for road transport. By Indian Transport Portal, the Indian automobile market is the second fastest growing in the world and has shown nearly 30 percent of growth in 2011-12. The government is also keen in electric-operated vehicles to avoid over dependency on scarce fossil fuel. The Indian government is carrying out encouraging policies to entice eco-friendly hybrid car manufacturers and started many plans to make these vehicles more popular in India and reachable to all [23]. Das explores that investment in greener cars; capitalization of under-utilized area (hybrid vehicle industry) and development of the infrastructure will enhance economic growth and reduce emissions. This initiative of Indian government will promote the Indian automotive industries to shift to newer and cleaner technologies for environmental sustainable products, innovation and knowledge [24].

An Indian government initiative for 'National Electric Mobility Plan' deals with cash subsidy and financing facilities for the end consumers. To create a network for vehicles' charging is under consideration of this plan. These policies will actuate automobile companies for research and development of cheaper, greener and better mileage vehicles. Since battery is the vital component of HEVs, more research is required to develop batteries with lower running cost, lesser maintenance and higher efficiency.

Department of Heavy Industry is going ahead with the 'National Mission for Electric Mobility' (NMEM) to have a significant number of EVs and HEVs on road by 2020. To encourage manufacturing and selling of alternative fuel-based vehicles 'National Mission for Hybrid and Electric Vehicles', 'National Board on Electric Mobility' and 'National Automotive Board' have set up a body to facilitate interaction between government and automotive industries for the growth of HEVs.

Societies of Indian Automotive Manufactures and Ministry of New & Renewable Energy Sources have initiated a 'National Hybrid Propulsion Program' to develop high energy density batteries for the best performance.

In a move to reduce the dependency on fossil fuels for vehicles, India has set up a target to produce six million green vehicles by 2020 and four to five million are expected to be two-wheelers. At present, only about 1,500 electric four-wheelers and four lacs electric two-wheelers are on roads. Live mint reports that the government will save Rs 30,0000 million in fuel by giving Rs 14,0000 million subsidy to industries for manufacturing EVs and the industrial contribution would be about Rs 8,0000 million.

The Budget of 2011-12, proposed to reduce excise duty from 10 percent to 5 percent of development and manufacturing of hybrid vehicle kits as well as a full exemption on customs and counter-veiling duty on import of special hybrid parts.

An autonomous research body under the 'Union Ministry of Petroleum and Natural Gas', 'Petroleum Conservation and Research Association' signed a memorandum of understanding with the 'Bureau of Energy Efficiency' to develop fuel economy standards under the 'Energy Conservation Act 2001'. The fuel efficiency standard is applicable for all types of vehicles including cars, trucks and buses. According to government projections, the country would be saving up to $36 billion, if fuel efficiency can be improved by 50 percent by 2030 in all sectors [25].

1.3 Challenges

For the greener tomorrow in terms of automotive solutions, hybrid vehicles are one of the promising and feasible options. Leaping into the era of hybrid vehicles, will benefit the humanity and the environment both. But at the same time, many challenges are waiting to get resolved. Adaptation, dissemination and penetration of hybrid vehicles will not be an easygoing job. Despite of enormous research, they have numerous weaknesses in terms of fuel efficiency, refuelling, price and many others. Few issues are listed here.

1.3.1 Battery Concern

The battery is one of the power sources in HEV and has following issues:

- It is heavy, expensive and generally affected by the atmospheric temperature. Temperature variation causes to change in behavior of the battery. Hence an efficient battery management system is required.
- It takes long charging time as well as is sensitive to overcharge/undercharge.
- It contains toxic heavy metals; hence disposal of waste becomes a challenge to face.

Resolving these issues will allow the BEVs to run on the road. A powerful energy support system for BEVs should be provided with extensive research in the domain of advanced electrodes, efficient electrolytes and best suited battery modeling. Li-ion batteries are widely used now-a-days due to their higher specific energy and energy density, durability as well as low self discharge rate.

1.3.2 Development of Energy Management Strategies

Power split between engine and battery is of utmost importance to minimize the fuel consumption without affecting the vehicle speed. Due to complex structure of HEVs/PHEVs, the design of control strategies is a challenging task. The preliminary objective of the control strategy is to satisfy the driver's power demand with minimum fuel consumption and toxic emissions with optimum vehicle performance. Moreover, fuel economy and emissions minimization are conflicting objectives; a smart control strategy should satisfy a trade-off between them.

1.3.3 Public Awareness and Participation

Public awareness and participation is very important to penetrate any policy into their lives. To relate pollution and social health, a widespread environmental education program will promote public involvement. As far as the case of India is concerned where literacy rate is around 74 percent and larger part of the population lives in villages, to conduct a mass awareness program is very challenging. For developed countries, the mass awareness program for the vehicular pollution control will be bit easier. Government and private sector participation with lucrative and cost-effective schemes will attract the consumer and encourage the hybrid usage. Participation of media will also help in spreading the responsiveness about the causes of pollution, impact on human life and the environment.

1.3.4 Smart Charging Infrastructure

Development of roads, expressways, flyovers and bridges will ease the vehicle motion on roads and hence less pollutant emission. Hybrid vehicles should be considered as the future vehicles. For the greener tomorrow, a supportive and smart infrastructure must be proposed. To bring green vehicles on road, smart charging is inevitable. The smart infrastructure should consist of sensitive and smart charging stations, billing and metering system to facilitate the user. The concept of two way communication is employed to exchange such information. To attract towards the green vehicle, user preferences should be considered. Infrastructure should be sensitive to collect/send the data between grid and user. "Better Place", a California based venture is building the world's first large scale public EV charging network in Israel and planning to expand it in Denmark, Hawaii, Australia and California [26].

1.3.5 Impact on Grid

As PHEVs/EVs are charged from power plugs in several hours to run uninterruptedly on roads, so append additional electricity demand on the grid. With the increase in the number of these vehicles on the road, the power demand will also increase. The conventional modes of power generation may not suffice the demand. Worldwide countries should focus to generate power through alternative energy sources like wind, hydro and solar power to meet the demand and develop the smart grids. Vehicle to grid (V2G) concept can be entertained here. This concept works on the balance of the 'off-peak' and 'peak' demand. With this facility during ‘off-peak’ hours user can fulfil his own demand and can store the power in batteries. And, during ‘peak’ hours when power demand is very high, user can sell it back to the grid, thus satisfy the need of own and other's. Smart grid projects have been started across the globe including India to address this issue. Morgan very nicely explains the potential barriers of V2G and concludes that V2G is likely to develop more slowly than grid to vehicle (G2V). But smart grid technologies certainly have the potential to meet future power demand, which will support V2G.

1.3.6 Cost

High price of an efficient battery hikes the market price of hybrid vehicles. Due to higher prices, hybrids are not affordable to middle income group who are the major portion of the population. Development of vehicle control strategy, a good battery management system and less costly component utilization can decrease the purchase and operational cost. Government should provide subsidies in purchasing and maintaining the hybrid vehicles. The fuel saving is very attractive feature of hybrids and can be compensated with tax relaxation and other incentives provided by the government. Involvement of feature like 'regenerative braking' and 'idle stopping' will benefit the various components of the vehicles. Electric accessories reduce load on the engine and hence reduce the maintenance cost.

1.4 Motivation and Scope of Research

Based on available literature, the scope and motivation of the research work carried out is briefed as follows:

- Battery is a complex system and very important component of HEV. Analyzing a battery on cell level reveals that it may go under various effects like diffusion and double layer at the contact points of electrolyte and electrode. The hindrance in current flow may be contributed by electrolyte which opposes the charge movements through it. These phenomena need to be incorporated while modeling a chosen battery to analyze its behaviour.
- Battery performance is affected by handling, charging/discharging pattern, loading, heat exposure and its calendar life. It gets discharged even when not in use. The battery is one of the most expensive components of the vehicle. Its performance is generally characterized by State of Charge (SOC) level which is left charge in the battery. Thus, an accurate knowledge of SOC level is important while propelling a vehicle to estimate how long a vehicle can run on battery power. In the available literature on HEVs, SOC estimation is performed only using ampere hour counting method. Although several available literature on batteries says that open circuit voltage consideration is also important for SOC calculation. Here, a modified SOC estimation method incorporating both, ampere hour counting and open circuit voltage is proposed. During current calculation, self discharge current is also considered because it affects the battery life even

when kept on the shelf. As battery performance is greatly affected by temperature, therefore temperature effect is also incorporated while calculating current and voltage. Hence, an adaptive SOC estimation method is developed to follow up the charge level while in use.

- Both engine and battery together or alone need to power the vehicle to fulfil driver's demand. At the same instant, it is required to restrict the engine to work in its efficient region only and use the battery capability to its fullest without deteriorating its health. Hence, a power split between these two sources is of great importance to minimize the fuel consumption and maximize the power utilization. Thus, an intelligent energy management strategy development to split power demand between these two sources is an important consideration for HEV manufacturers and engineers. So, development of control strategy and optimization requires a lot of efforts to make HEV work with its supreme performance achievements.

Battery modeling and development of energy management strategies are the major issues in an HEV. The subsequent chapters will elaborate these in detail.

1.5 Objectives

Based on the literature review and research gaps, the research endeavors to develop battery models, synthesize the modified SOC estimation method and power optimization strategies to improve the fuel economy of HEV are performed. The objectives are elaborated as follows:

1. Selection of the best suitable battery for HEV application and its modeling involving diffusion, double layer effects with self discharge current and temperature variation.
2. Development of adaptive SOC estimation method using Ampere hour counting and open circuit voltage and determination of threshold SOC level to deplete the battery during operation without deteriorating its health.
3. Exploring the optimization techniques to calculate the thresholds of various vehicle parameters responsible to turn on/off the engine for optimal power split and maximum fuel efficiency using developed battery models and SOC estimation method.

4. Feature extraction of various driving cycles and analyze the vehicle performance over these including Indian road conditions.

1.6 Structure of Thesis

The research work carried out in this thesis is organized as follows:

Chapter 1: Elaborate the problems caused by ICE based vehicle and leads towards the solution. The inspiration to carry out a research in the area of HEVs is the outcome of the study performed.

Chapter 2: Performs study for the selection of the suitable battery for HEV applications using multi criterion optimization methods like, Ashby, VIKOR and TOPSIS.

Chapter 3: Modeling of Li-ion battery is performed in this chapter incorporating temperature effect and self discharge current. A modified SOC estimation method is proposed and a threshold SOC level determination is performed.

Chapter 4: Various architectures of HEVs are discussed in this chapter. A detailed literature survey of various existing energy management strategies is performed to choose a suitable method to optimize the power split between engine and battery.

Chapter 5: Elaborates the various developed energy optimization strategies to minimize fuel consumption in HEVs. DIRECT, genetic algorithm and Pontryagin's minimum principle is used to determine the fuel economy. The developed battery models and proposed modified SOC estimation methods are incorporated in 'ADvance VehIcle SimulatOR' (ADVISOR). Effect of temperature on vehicle performance is studied.

Chapter 6: Feature extraction of several driving cycles is performed using independent component analysis and principle component analysis. HEV performance on various driving cycles is analyzed and fuel economies are calculated. Indian road conditions are studied to check the feasibility of using HEVs on it.

Chapter 7: Finally the main findings of the research work are summarized and future scope is discussed.

Chapter 2
Battery Selection for Hybrid Electric Vehicle Applications

The main component behind the HEV's efficient performance is presence of rechargeable battery. The power delivered by the battery is mainly dependent on its SOC. Being a key component, battery performance and cost plays a vital role in manufacturing efficient and economical HEVs hence the selection of a proper battery for HEV application becomes inevitable.This chapter proclaims the battery selection for HEV applications using multi-objective optimization techniques. Ashby's methodology, 'Technique for Order Preferences by Similarity to an Ideal Solution' (TOPSIS) and 'VIse Kriterijum-ska Optimizacija Komprominsno Resenje' (VIKOR) methods are employed here for the assessment. Various considered attributes, specific energy, energy density, electrical efficiency, self-discharge rate, nominal cell voltage, energy per cycle, cost and durability are considered here for investigation. The batteries considered for analysis are Li-ion, Ni-MH, Ni-Cd and Pb-acid. Based on the performance indices and battery attributes, selection charts are plotted and influential data are tabulated. Ashby's method, TOPSIS and VIKOR converge to unique outcome, i.e. Li-ion. It is observed, Li-ion batteries are most suitable for hybrid vehicle applications followed by Ni-MH batteries. The results obtained are also matched up with actual practices in automobile industries.

2.1 Types of Batteries

The batteries available in the market are basically of two types, primary and secondary. Primary batteries produce current immediately and are most commonly used in portable devices with lower current drawn. Primary cells cannot be recharged, since the chemical reactions are not easily reversible and active. These batteries have high energy density, but are expensive in terms of cost per kilowatt hour [27]. Secondary batteries, also known as rechargeable batteries, are composed of active materials and get (re)charged by applying electric currents. The chemical reactions are reversible hence battery can be charged and recharged subsequently. The most commonly used secondary cells are Lead-

Acid (Pb-acid), Nickel-Cadmium (Ni-Cd), Nickel-Metal Hydride (Ni-MH) and Lithium-ion (Li-on). The market has shifted towards secondary cells because of its lower unit prices, useable time and repetitive charging/discharging. The batteries chosen for analysis are explained below.

2.1.1 Lead-Acid Battery

Pb-acid battery is the oldest type of rechargeable battery. Pb-acid batteries are designed for high power applications and are inexpensive, safe and reliable [28]. They have low specific energy, short calendar life and temperature sensitive performance. The Pb-acid cell contains electrodes of Pb metal and lead oxide (PbO_2) in the sulfuric acid (H_2SO_4) electrolyte. The chemical reaction results in potential or voltage. The overcharging of Pb-acid cell causes emission of hydrogen and oxygen. The following reactions occur at the electrodes.

At anode: $Pb + HSO_4^- + H_2O \rightarrow PbSO_4 + H_3O + 2e^-$

At cathode: $PbO_2 + 3H_3O^+ + HSO_4^- + 2e^- \rightarrow PbSO_4 + 5H_2O$

2.1.2 Nickel-Cadmium Battery

The Ni-Cd battery came into the market to compete with Pb-acid batteries in 1899. It has a significantly higher energy density than Pb-acid battery. It contains Nickel Oxide Cadmium Hydroxide as the positive electrode, Cadmium (Cd) as the negative electrode and potassium hydroxide as the electrolyte. Potassium hydroxide is not consumed in the reaction. Cd is heavy metal and is highly toxic. Ni-Cd batteries are costlier that Pb-acid and have negative temperature coefficients [29]. These exhibit thermal runaway hence avoided by car manufacturers.

At anode: $2NiO(OH) + Cd + 2H_2O \rightarrow 2Ni(OH)_2 + Cd(OH)_2$

At cathode: $2\ NiO(OH) + 2H_2O + 2e^- \rightarrow 2Ni(OH)_2 + 2OH^-$

2.1.3 Nickel-Metal Hydride Battery

Ni-MH batteries have 2 to 3 times higher capacity than equivalent Ni-Cd cell and have a much higher life than Pb-acid batteries. These batteries have been used successfully in

electric vehicles. Metal hydride, as anode, $Ni(OH)_2$ as the cathode and potassium hydroxide as the electrolyte are used in Ni-MH cell. The active material is hydrogen in the cell. The issues with Ni-MH are high self discharge rate, heat generation at higher temperature and higher cost. The chemical reactions are as given:

At anode: $OH^- + MH \rightarrow H_2O + M + e^-$

At cathode: $Ni(OH) + H_2O + e^- \rightarrow Ni(OH)_2 + OH^-$

2.1.4 Lithium-Ion Battery

Li-ion battery with higher energy per unit mass, high energy efficiency, better performance at all temperatures and low self discharge rate is dominating the current market. One of the best features of Li-ion battery is that it can be recycled. These batteries use carbon anode and oxides of cobalt, manganese and nickel as cathode. The chemical reaction equations are as given:

At anode: $Li_xC_6 \rightarrow xLi^+ + xe^- + 6C$

At cathode: $Li_{1-x}CoO_2 + xL^+ + xe^- \rightarrow LiCoO_2$

Firstly, it is required to understand which battery will serve the purpose of high power demand with good life span for hybrid vehicle applications. For that, battery attributes like energy density, specific energy, electrical efficiency, durability, energy/cycle, self-discharge rate and cost are considered and studied in detail. Using Ashby's approach, TOPSIS and VIKOR methods, best suitable battery for HEV is chosen.

2.2 Battery Indices

The performance indices of batteries vary with respect to a range of variables, i.e. energy density, specific energy, electrical efficiency, self discharge rate, energy per cycle, cost, durability etc. These are described here in detail:

2.2.1 Specific Energy and Energy Density

The energy density of fuel per unit mass is known as specific energy of that fuel. Specific energy is the amount of electrical energy stored for every kilogram of battery mass. More

the energy can be stored or transported for the same amount of volume, it is said to have high energy density. Mass is the greatest source of energy as $E = mc^2$, where m is mass, c is the speed of light, and E is the energy stored/released. Energy density is the amount of electrical energy stored per cubic meter of battery volume. To maximize energy density and specific energy, specific energy density can be calculated and higher value shows the efficient energy storage [30].

2.2.2 Electrical Efficiency

This is another very important parameter and it is defined as the ratio of electrical energy supplied by a battery to the amount of electrical energy required to return it to the state before discharge. Higher efficiency will prove a better battery type.

2.2.3 Self Discharge Rate

The batteries discharge when not in use, this phenomenon is called self discharge. This reduces the charge level of the battery without any use even. The discharge rate varies with battery type and temperature. The self discharge rate is a measure of how quickly a cell will lose its energy while sitting on the shelf due to unwanted chemical actions within the cell [31]. These side reactions can be reduced to some extent by storing the battery at lower temperature [32].

2.2.4 Energy/Cycle

Energy delivered per cycle has a significant impact on choosing a battery. The amount of energy in every discharge cycle should be high and it should be continued for larger numbers of cycles with repetition.

2.2.5 Cost

The initial cost and lifetime cost of batteries may vary. The installation and initial purchase of Li-ion battery is high as compared to the other batteries of the same capacity, but durability and high performance of Li-ion battery repay it back in terms of good performance. Different chemistries need a different type of charger to charge it; this also leads to the cost raise.

2.2.6 Durability

Number of charge/discharge decides the durability of the battery. It varies with the type of battery and how it has been used in the past. This is a significant attribute of battery which decides the life of the battery and performance duration. Good durability with high installation cost may repay back to the customer in terms of economy.

Table 2.1 shows the numerical values of different attributes of the related battery [33, 34].

Table 2.1: Attributes of different material battery

Battery attributes	Unit	Li-ion	Ni-MH	Ni-Cd	Pb-acid
Specific energy	Wh/kg	180	70	50	35
Energy density	Wh/l	180	140	100	70
Electrical efficiency	Percent	85	66	90	90
Self-discharge rate	Percent/month	5	30	10	20
Nominal voltage	Volts	3.6	1.2	1.2	2.0
Energy /cycle	Wh	8.6	7.5	4.5	24
Cost/kWh	$	24	18.5	11	8.5
Durability	Cycles	1200	1000	2000	800

2.3 Different Methods used for Battery Selection

Ashby's method, TOPSIS and VIKOR are used here to rank the batteries on the basis of their attributes. These are described in detail as follows:

2.3.1 Ashby's Methodology

To meet the product performance and minimize the cost, Ashby presented a novel method for selection of materials in different applications [35]. Ashby's approach is used here to determine the optimal performance battery for hybrid vehicle applications. Using an objective function, under the influence of some constraints, the desired function is optimized to minimize/maximize the performance; is the basic idea behind the Ashby's approach. This approach optimizes a performance index P_j, based on objective functions are used here to apply in battery selection as in (2.1).

$$P_j = f_j(F, P, M) \tag{2.1}$$

f is functional, i.e. function of a function, *F* is battery functional requirement, *P* is battery properties and *M* is the material.

2.3.2 TOPSIS Method

TOPSIS is a Multi Attribute Decision Making (MADM) method for measuring relative efficiency of alternatives. Yoon and Hwang [36, 37] introduced the TOPSIS method based on the idea that the best alternative should have the shortest distance from an ideal solution. They assumed that if each attribute takes a monotonically increasing or decreasing variation, then it is easy to define an ideal solution. Such a solution is composed of all the best attributes' values achievable, while the worst solution is composed of all the worst attribute's values achievable. The goal is to propose a solution which has the shortest distance from the ideal solution in the Euclidean space. Such a solution may need to simultaneously have the farthest distance from a negative ideal solution [38, 39]. TOPSIS method considers both the distances and tries to choose solutions which are simultaneously close to the ideal solution. The procedure can be followed in six steps:

Step 1: *Construction of decision matrix*: The decision matrix is expressed as (2.2).

$$D=\begin{pmatrix} d_{11} & \cdots & d_{1m} \\ \vdots & \ddots & \vdots \\ d_{n1} & \cdots & d_{nm} \end{pmatrix} \tag{2.2}$$

d_{ij} is the rating of the alternative A_i with respect to the criterion C_j.

Step 2: *Construction of the normalized decision matrix:* Each element r_{ij} is obtained by the Euclidean normalization as (2.3).

$$r_{ij=}\frac{d_i}{\sqrt{\sum_{i=1}^{m} d_{ij}^2}}, i = 1, \ldots . m \text{ and } j = 1, \ldots . n. \tag{2.3}$$

Step 3: *Construction of the weighted normalized decision matrix:* The weighted normalized decision matrix v_{ij} is computed as (2.4): $V_{ij} = w_i * r_{ij}$ where

$$\sum_{i=1}^{m} w = 1 \tag{2.4}$$

Step 4: *Determination of the ideal solution A* and the anti-ideal solution A*$^-$ as (2.5).

$$A^* = [V_1^*, \dots\dots, V_m^*] \text{and } A^- = [V_1^-, \dots\dots, V_m^-] \tag{2.5}$$

- For desirable criteria

$$V_i^* = \max\{v_{ij}, j = 1, \dots\dots, n\}$$
$$V_i^- = \min\{v_{ij}, j = 1, \dots\dots, n\}$$

- For undesirable criteria

$$V_i^* = \min\{v_{ij}, j = 1, \dots\dots, n\}, V_i^- = \max\{v_{ij}, j = 1, \dots\dots, n\}$$

Step 5: Separation of each alternative from ideal and negative ideal solution is calculated as (2.6).

$$\left.\begin{aligned} S_i^* &= \sqrt{\sum_{i=1}^{m}(V_i^* - V_{ij})^2}, j = 1, \dots\dots., n \\ S_i^- &= \sqrt{\sum_{i=1}^{m}(V_i^- - V_{ij})^2}, j = 1, \dots\dots., n \end{aligned}\right\} \tag{2.6}$$

Step 6: *Ranking*: Calculate the relative closeness to the ideal solution of each alternative as (2.7):

$$C_j^* = \frac{S_i^-}{S_i^- + S_i^*}, j = 1, \dots.., n. \tag{2.7}$$

A set of alternatives can be ranked according to the decreasing order of C_j *.

2.3.3 VIKOR Method

The VIKOR which is a means of multi-criteria optimization (MCO) and compromise solution method, was developed by Opricovic and Tzeng [38, 40, 41]. The method can be defined as a multi-criteria optimization of complex systems and it is based on ranking and selecting from a set of alternatives under conflicting criteria. Assuming that each alternative is evaluated according to each criterion function, the compromise ranking could be performed by comparing the measure of closeness to the ideal alternative. The compromise solutions could be the basis for negotiations, involving the preference of decision makers by criteria weights [42]. The VIKOR algorithm also determines the weight stability intervals for the obtained compromise solution with the input weights

given by the expert. This method focuses on ranking and selecting from a set of alternatives in the presence of conflicting criteria.

It introduces the multi criteria ranking index based on the particular measure of 'closeness' to the 'ideal' solution. Development of the VIKOR method started with the following form of Lp-metric [43]:

Step 1: *Determine the normalized decision matrix:* The normalized decision matrix can be expressed as (2.8):

$$\left.\begin{aligned} F &= \left[f_{ij}\right]_{m\times n} \\ f_{ij} &= \frac{x_{ij}}{\sqrt{\sum_{i=1}^{n} x_{ij}^2}}, i = 1, \dots\dots, m, \text{and } j = 1, \dots . n; \end{aligned}\right\} \tag{2.8}$$

and x_{ij} is the performance alternative with respect to the j^{th} criteria.

Step 2: *Determine the ideal and negative ideal solutions:* The ideal solution S* and negative ideal solution S^- are calculated as (2.9):

$$\left.\begin{aligned} S^* &= \{\left(\max f_{ij} I\, j \in J\right) or (= \{\left(\min f_{ij} I\, j \in J\right) I i = 1, \dots\dots, m\} = \{f_1^*, f_2^*, \dots\dots, f_n^*)\} \\ S^- &= \{\left(\min f_{ij} I\, j \in J\right) or (= \{\left(\max f_{ij} I\, j \in J\right) I i = 1, \dots\dots, m\} = \{f_1^-, f_2^-, \dots\dots, f_n^-)\} \end{aligned}\right\} \tag{2.9}$$

where

$$\left.\begin{aligned} J &= \{j = 1,2, \dots . n \; I \; f_{ij}, \text{a larger response is desired}\} \\ J' &= \{j = 1,2, \dots . n \; I \; f_{ij}, \text{a smaller response is desired}\} \end{aligned}\right\} \tag{2.10}$$

Step 3: *Calculate the utility and regret measure:* The utility measure and the regret measure for each alternative are as (2.11):

$$\left.\begin{aligned} S_i &= \sum_{j=1}^{n} w_j \times (f_j^* - f_{ij})/(f_j^* - f_j^-) \\ R_i &= \max_j [w_j \times (\frac{f_j^* - f_{ij}}{f_j^* - f_j^-})] \end{aligned}\right\} \tag{2.11}$$

S_i represents utility measure, R_i represents the regret measure and w_j is the weight of the criteria j.

Step 4: *Calculate the VIKOR index:* The VIKOR index can be calculated as (2.12):

$$Q_i = v\left[\frac{S_i - S^*}{S^- - S^*}\right] + (1 - v)\left[\frac{R_i - R^*}{R^- - R^*}\right] \tag{2.12}$$

Q_i represents the i^{th} alternative VIKOR value i=1,....,m.

$$\text{and} \quad \left.\begin{aligned} S^* &= \min_j S_i \\ S^- &= \max_j S_i \\ R^* &= \min_j S_i \\ R^- &= \max_j S_i \end{aligned}\right\} \tag{2.13}$$

v is usually set to 0.5 [44, 45].

2.4 Result and Discussion

The primary requirement to use an HEV is a large driving range with minimum liquid fuel consumption over the roads. The optimal performance of hybrid vehicle varies with the batteries used during propulsion. Out of various available batteries, battery selection is performed based on various attributes for HEV applications. The selection chart and calculations obtained from various methods are presented in following sections.

2.4.1 Ashby's Methodology

These battery performance indices affect the overall fuel economy of hybrid vehicles and performance. The optimal battery is selected here by placing the battery attributes in selection map. Figure 2.1, 2.2 and 2.3 are plotted using table 2.1's relevant attribute data. Figure 2.1 shows the variation of specific energy and energy density. It is considered that specific energy density should be high to store more energy. From the figure, it is clear that Li-ion battery has significantly higher specific density and specific energy, both as compared to others.

A good battery should have high electrical efficiency and low self discharge rate. Figure 2.2 infers that, Ni-Cd, Pb-acid and Li-ion have a trade off in terms of its electrical efficiencies. Ni-Cd and Pb-acid battery shows higher efficiencies with higher self discharge rate whereas Li-ion battery with very low self discharge rate exhibit good percentage of electrical efficiency.

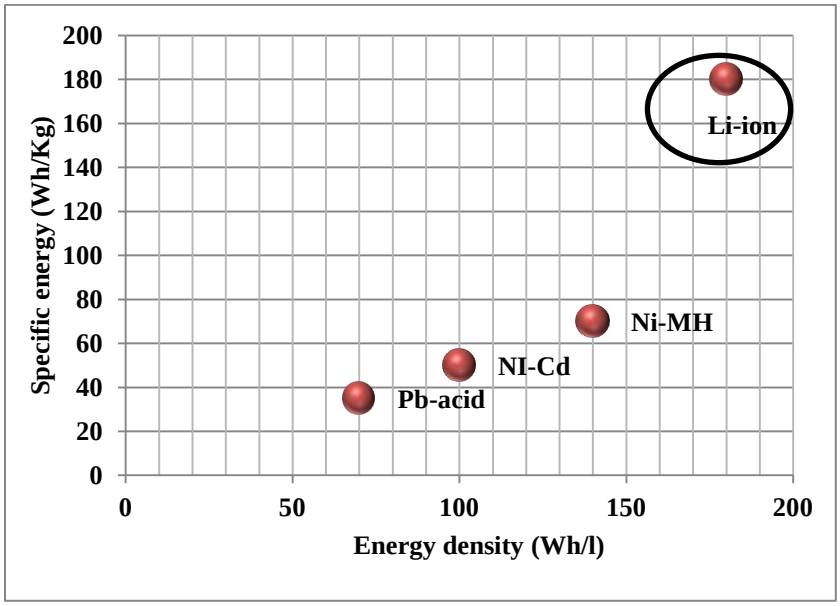

Figure 2.1: Specific energy versus energy density variation

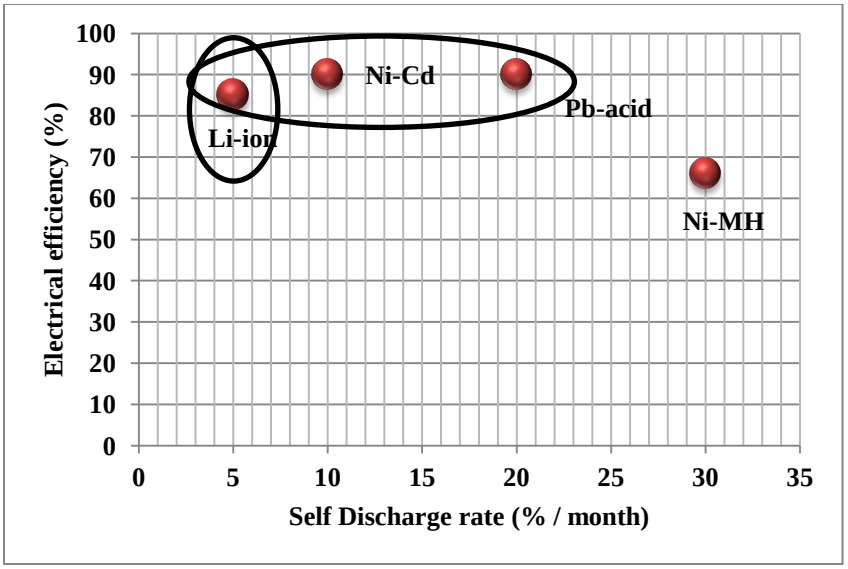

Figure 2.2: Electrical efficiency versus Self discharge plot of different batteries

Figure 2.3 exhibits the energy drawn from the battery in every discharge cycle versus its durability. The Pb-acid battery has a highest 'Watt hour energy per cycle' but lowest durability. As durability reduces the running cost of vehicle increases, hence Pb-acid battery will not be suitable for this application. Ni-Cd has higher durability among all but has very low energy delivery in every cycle. Hybrid vehicles demand high energy from battery; thus Ni-Cd is also not suitable for hybrid vehicle applications. Ni-MH and Li-ion batteries have a trade off in this case with very close values.

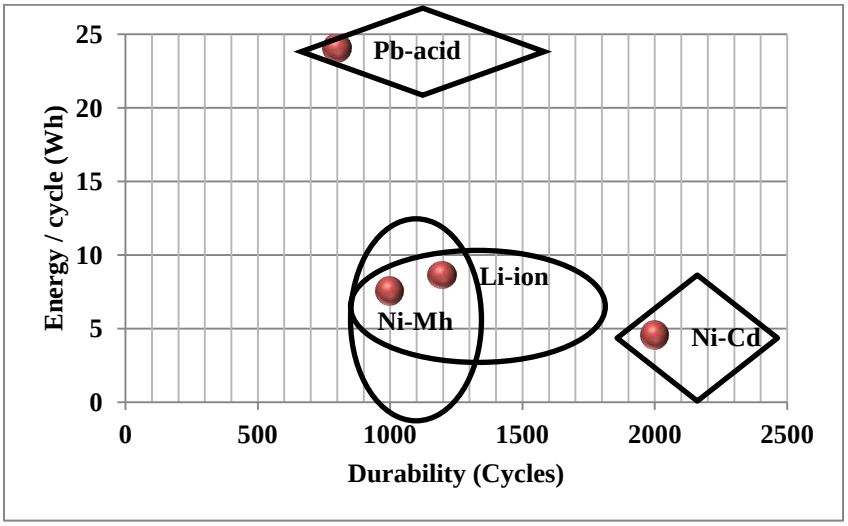

Figure 2.3: Cycle versus durability plot for various batteries

On the basis of the selection charts plotted in figures 2.1, 2.2 and 2.3, Li-ion battery is found to be most promising and Ni-MH ranks as second.

2.4.2 TOPSIS Method

The various available batteries and their attributes are given in table 2.2. Here, self discharge rate and cost are minimization type and rest others are maximization type attributes. The normalized decision matrix is formed using (2.3) and the same is given in table 2.3. Weighting factors of the various attributes are computed using the ratio method and are listed in table 2.4. The weighted normalized decision matrix is obtained using (2.4) and is presented in table 2.5. Ideal and negative ideal solutions are estimated using (2.5) in table 2.6. Distance of each alternative from the ideal and negative ideal solutions is listed in table 2.7 using (2.6). The ranks of batteries are calculated using (2.7) and the same is shown in table 2.8. The table shows that highest score is achieved by Li-ion battery which makes it a best suitable option to use in hybrid vehicle applications. Similarly, Ni-MH ranks second, Ni-Cd ranks third and fourth position is occupied by Pb-acid battery.

Table 2.2: Batteries and Attribute

Parameter / Battery	Energy density	Specific energy	Cell voltage	Electrical efficiency	Self discharge rate	Cost	Energy/cycle
Li-ion	180	180	3.6	85	5	24	8.6
Ni-Mh	140	70	1.2	66	30	18.5	7.5
Ni-Cd	100	50	1.2	90	10	11	4.5
Pb acid	70	35	2	90	20	8.5	24

Table 2.3: Normalized decision matrix

Parameter / Battery	Energy density	Specific energy	Cell voltage	Electrical efficiency	Self discharge rate	Cost	Energy /cycle
Li-ion	0.6959	0.8886	0.8082	0.5099	0.8675	0.2801	0.3190
Ni-MH	0.5412	0.3456	0.2694	0.3959	0.2052	0.4450	0.2782
Ni-Cd	0.3866	0.2468	0.2694	0.5399	0.7350	0.6700	0.1669
Pb acid	0.2706	0.1728	0.4490	0.5399	0.4701	0.7450	0.8904

Table 2.4: Weighting factors of different attributes

Parameter	Energy density	Specific energy	Cell voltage	Electrical efficiency	Self discharge rate	Cost	Energy/ cycle
Weighting factor	0.3668	0.2508	0.0059	0.2478	0.0486	0.0464	0.0333

Table 2.5: Weighted normalized decision matrix

Parameter / Battery	Energy density	Specific energy	Cell voltage	Electrical efficiency	Self discharge rate	Cost	Energy/ cycle
Li-ion	0.2553	0.2229	0.0048	0.1263	0.0422	0.0130	0.0106
Ni-MH	0.1985	0.0866	0.0016	0.0981	0.0099	0.0206	0.0092
Ni-Cd	0.1418	0.0619	0.0016	0.1338	0.0357	0.0311	0.0055
Pb acid	0.0992	0.0433	0.0026	0.1338	0.0228	0.0345	0.0297

Table 2.6: Ideal and negative ideal solution

Parameter	Energy density	Specific energy	Cell voltage	Electrical efficiency	Self discharge rate	Cost	Energy/ cycle
A*	0.2553	0.2229	0.0048	0.1338	0.0099	0.0130	0.02973
A-	0.0992	0.0433	0.0016	0.0981	0.0422	0.0345	0.0055

Table 2.7: Separation of each alternative from ideal and negative ideal solution

Battery	Li-ion	Ni-MH	Ni-Cd	Pb-acid
S^*	0.038185416	0.153411313	0.200946167	0.239213630
S^-	0.240596446	0.113945285	0.059015989	0.047246682

Table 2.8: Battery Ranking

Battery	Li-ion	Ni-MH	Ni-Cd	Pb-acid
C_j	0.863027617	0.426192156	0.227017618	0.164932733

2.4.3 VIKOR Method

The normalized decision matrix table 2.3 is used for step 1 matrix formation as mentioned in (2.8). Determination of ideal and negative ideal solution is presented in table 2.9 using (2.9). Utility and regret measures are collected in table 2.10 using expressions given in (2.11). It finds utility measure S_i and regret measure R_i according to (2.11). The VIKOR index for all the batteries are calculated in table 2.11 using (2.12). The minimum value set of the desired alternative by VIKOR method is for Li-ion battery type. Hence, Li-ion battery will be the best alternative to choose with minimum cost and self discharge rate while maximizing other attributes.

Table 2.9: Determination of ideal and negative ideal solution

Parameter	Energy density	Specific energy	Cell voltage	Electrical efficiency	Self discharge rate	Cost	Energy/ cycle
S^*	0.6959	0.8886	0.8082	0.5399	0.1324	0.2549	0.8904
S^-	0.2706	0.1728	0.2694	0.39597	0.7947	0.7198	0.1669

Table 2.10: Calculation of utility and regret measure

Battery	S_i	R_i
Li-ion	0.124424152	0.051630977
Ni-MH	0.684380212	0.247828691
Ni-Cd	0.548299239	0.266819135
Pb acid	0.650893481	0.366876310

Table 2.11: VIKOR index

Battery	Li-ion	Ni-MH	Ni-Cd	Pb acid
Q_i	0	0.811182583	0.719792283	0.970098787

Ranking outcomes of TOPSIS and VIKOR methods are put together in figure 2.4. Like Ashby, TOPSIS and VIKOR methods also rank Li-ion battery the best. TOPSIS ranks batteries in the order: Li-ion>Ni-MH>Ni-Cd>Pb-acid, whereas VIKOR ranks like Li-ion> Ni-Cd > Ni-MH >Pb-acid.

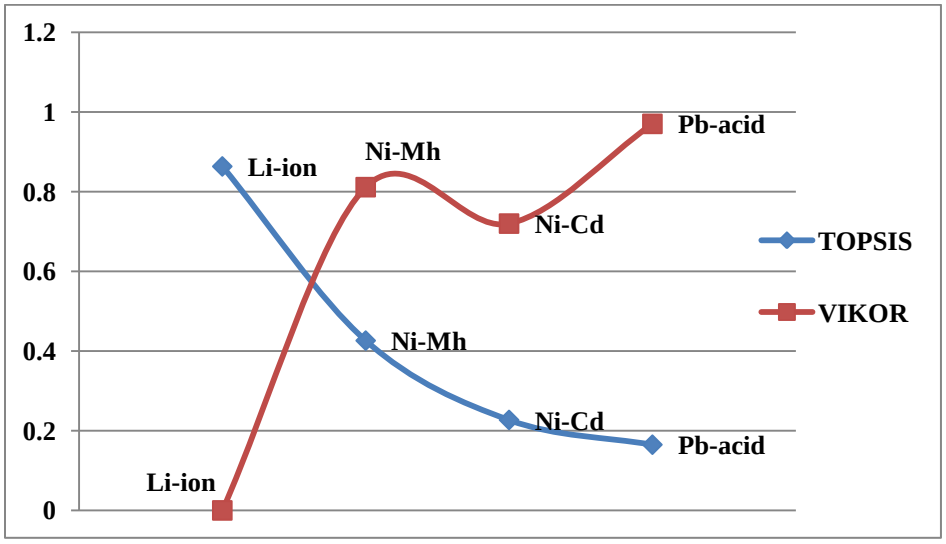

Figure 2.4: Comparison of TOPSIS and VIKOR

The spider web plot in figure 2.5 summarizes all parameters mentioned in table 2.1 which also shows that Li-ion battery is covering a wide range of desirable attributes.

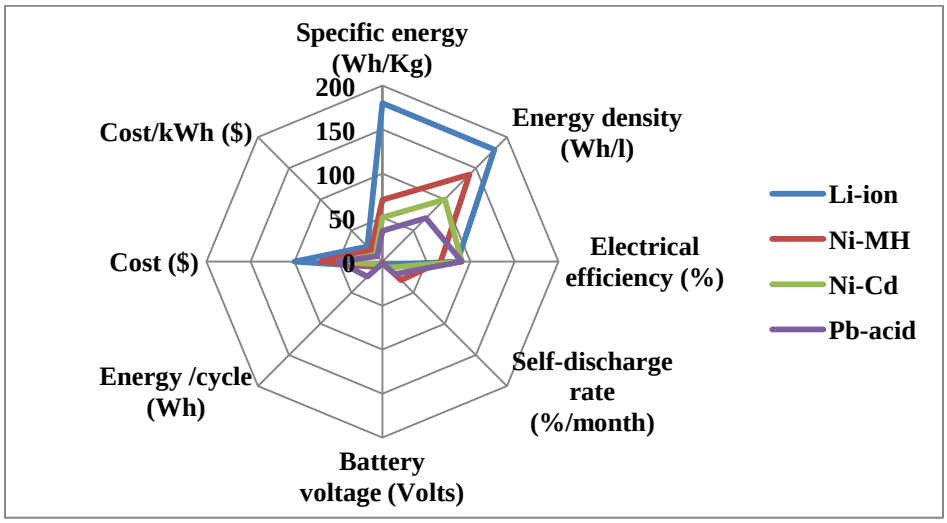

Figure 2.5: Spider web plot for attributes of the different batteries

Aforementioned discussions recommend Li-ion battery as the best suitable option for hybrid vehicle applications followed by Ni-MH.

It is also investigated that the absence or presence of any attribute in any decision making method affects the ranking order. Many combinations are tested and in all cases Li-ion battery proves to be the best except one case. In this particular case, energy density and specific energy are ignored, which leads to lower ranking of Li-ion battery. The sequence of ranking in this case is Pb-acid > Ni-Cd > Li-ion > Ni-MH.

High energy density and high specific energy allow vehicle to perform satisfactorily in case of acceleration and energy regeneration. Further, hybrid vehicles require battery with high energy density to provide a large mileage in one charge cycle. This concludes that for HEV applications, Li-ion battery will be an appropriate choice with respect to good mileage, reliability and durability. Based on this analysis, this thesis work uses Li-ion battery to model and optimize the power of HEV.

Hence, Li-ion battery and Ni-MH battery proves to be descent options for use. The table 2.12 below summarizes the usage of these battery technologies in various hybrid vehicles.

Table 2.12: Overview of battery technology used in several vehicles

Company	Vehicle model	Battery technology
GM	Chevy-Volt	Li-ion
	Saturn Vue Hybrid	Ni-MH
Ford	Escape	Ni-MH
	Fusion	Ni-MH
	MKZ HEV	Ni-MH
	Escape PHEV	Li-ion
Toyota	Prius	Ni-MH
	Lexus	Ni-MH
Honda	Civic	Ni-MH
	Insight	Ni-MH
Hyundai	Sonata	Lithium Polymer
Chrysler	Chrysler 200C EV	Li-ion
BMW	X6	Ni-MH
	Mini E	Li-ion
BYD	E6	Li-ion
Daimler Benz	ML450	Ni-MH
	S400	Ni-MH
	Smart EV	Li-ion
Mitsubishi	iMiEV	Li-ion
Nissan	Altima	Ni-MH
	Leaf EV	Li-ion
Tesla	Roadster	Li-ion
Think	Think EV	Li-ion, Sodium/Metal chloride

2.5 Summary

The optimal battery selection for HEV applications using multi criteria decision making methods like, Ashby, TOPSIS and VIKOR methods are presented. The performance indices of battery are optimized against several battery attributes. On the basis of battery selection charts, it is found that Li-ion and Ni-MH batteries outperform and would serve the purpose in hybrid vehicles. Further, very high specific energy and energy density of Li-ion against Ni-MH battery, advises to opt for Li-ion battery. A powerful battery

management system can be used to increase the performance and life of Li-ion battery. Li-ion batteries are inviting lots of research attention due to its lower self discharge rate, high specific energy density and high specific power. Various technologies are being explored by researchers to manufacture low cost batteries with improved performance. As a result, in near future smaller size, powerful and long live Li-ion battery will attract not only hybrid vehicle manufacturers but manufacturers of all the relevant disciplines with reduced cost.

Chapter 3
Battery Modeling and Formulation of SOC Estimation Method

In hybrid vehicles, battery is one of the propulsive power sources and its effective usage can minimize the liquid fuel consumption. Correct information about its operating conditions are essential, therefore, an accurate battery model is required to predict its I-V characteristic and dynamic behaviour. This chapter presents a highly effective thermo-electric model of Li-ion battery developed in Simulink. An algorithm is proposed for adaptive estimation of State of Charge (SOC) and Open Circuit Voltage (OCV) to notify the accurate charge level for better utilization of battery power and optimal vehicle performance. Thermal behaviour of Li-ion battery is investigated for wide temperature range and its effect on resistance, capacity and OCV is recorded. The threshold SOC level to which battery should be depleted, is calculated using gradient method.

3.1 Overview of Existing Models

Sean proposed PSPICE macromodel to simulate battery with sufficient characterization data. THis model shows voltage dependency on SOC, discharge current, resistance and capacity variation with respect to temperature [46]. This is further used to propose a discrete-time model which is capable of battery lifetime estimation [47]. In 1994, 'National Renewable Energy Laboratory' (NREL) modeled Li-ion battery with a voltage source and internal resistance as a function of SOC, temperature and current flow direction in ADVISOR. Saft America developed the high-power Li-ion cells and implemented 2-capacitance battery model in PSPICE. It shows a slightly better performance in comparison to NREL's model [48]. Chen et al. proposed a model to be used with an equilibrium potential and two internal resistances R_1 and R_2 where R_1 is a function of discharge current, temperature and life cycle and R_2 is a function of SOC and temperature but did not count for transient response of the battery [49].

Gao et al. demonstrated a dynamic model of Li-ion battery which depicts a capacity variation on the basis of C-rate (known as charge and/or discharge current rate

per hour), temperature change, equilibrium potential and transient response of the battery [50]. It consists of equilibrium potential, internal resistance and a capacitor but doesn't account the self discharge current and diffusion effect between electrodes. Tremblay et al. presented a battery model, for dynamic simulation software and added same in the SimPowerSystems library MATLAB/Simulink [51]. It consists of an internal resistance and a voltage source which is a non-linear function of battery SOC. It does not account for self discharge current, Peukert and memory effects as well as temperature variation.

Lee et al. used Li-ion battery model with internal resistance, 1RC combination and a voltage source. They estimated SOC using ampere-hour counting and capacity estimation, neglecting OCV based SOC method [52]. Using lumped model, SOC estimation algorithm is developed at varying temperatures in [53, 54]. It consists of one resistance with two components (series and charge transfer), 1RC ladder (diffusion resistance and capacitance) and voltage source (OCV) but does not account self-discharge current. A circuit based Li-ion battery model using AMESim is developed and the temperature rise in core and the crust was represented. But model considers only particular discharge rate and different temperature and discharge rate factor functions for different rates [55]. [56] combined the electric model developed in [54] and thermal model developed in [55] to derive a thermo-electric analytical model. This model can inspect the behavioural change of battery due to temperature variation, but contains other lacking of [49].

For online SOC estimation, [57] proposed a model with internal resistance, OCV and 2RC circuit combinations. For SOC estimation, only ampere counting is considered and OCV based counting is neglected. The model developed in [58] is a blend of previous models and overcomes few of their limitations. It predicts runtime, steady state and transient response accurately by capturing all the dynamic electrical characteristics of batteries. The RC network is modeled to account the effect of self discharge loss due to long time storage and also includes transient response but does not include thermal effects. [59] used a model developed in [58] and incorporated temperature and capacity fading effect. To determine online SOC of Li-ion battery, estimated electrical parameters with temperature variation are estimated by [60]. Determination of battery SOC using a second order model is introduced in [58, 61].

Kroeze and Krein proposed two models for predicting SOC, terminal voltage and power losses. These are: 1) SOC can be predicted when temperature and cycle number are given and 2) transient behavior of terminal voltage can be figured out where each parameter is a function of SOC [62]. Zhang et al. constructed an equivalent circuit of battery cell which is based on Thevenin's theorem. It describes SOC variation with current [63]. This also neglected self discharge current. Randles' model [64] developed for lead-acid batteries, is remapped by [65]. They implemented an equivalent circuit model to determine state of function of Li-ion battery, but did not consider the temperature effect. Based on experimental results, 2RC battery model is proposed and mathematical modeling is performed, but self discharge current is not considered [66]. References [67, 68, 69, 70] also proposed 2RC battery model, but there is no discussion found with respect to the self discharge current.

3.2 Modeling of Battery

Since batteries play a vital role in HEVs, it is essential to study their behavior before incorporating them as power source. A holistic understanding would result in better performance of the vehicle. The battery can be modeled using electrochemical, mathematical, analytical and stochastic approaches. Impedance based and electrical circuit based modeling can also be performed. The electrical circuit based model depicts the battery behavior easily [71]. Electric circuit based models are of varying degrees of complexity and are able to capture the battery performance with respect to a set of parameters. The parameters are explained in detail in further sections of the chapter.

Here three electric circuit based battery models showing internal resistance, diffusion and double layer effects, self discharge current and temperature dependence of parameters are developed. A thermo-electric Li-ion battery model and effect of thermal behaviour of various battery parameters are studied here. The battery models are designed with Matlab/Simulink which suits for dynamic simulations. Values of electrical components used during modeling are decided using [51, 58]. Battery modeling specifications are given in Table A1 (Appendix A).

3.2.1 Model 1

When the power source delivers the current, output voltage is lower than the no load voltage because there is a voltage drop due to the internal resistance (R_{int}) offered by the battery. This resistance is resultant of hindrance caused by electrolyte in the flow of charged ions. Model 1 consists of a power source and an internal resistance illustrated in figure 3.1. R_{int} consists of both, ohmic resistance and the polarization resistance [72]. OCV will be presented by (3.1) where V(t), V'(t) and i(t) are OCV, output voltage and current respectively at time t.

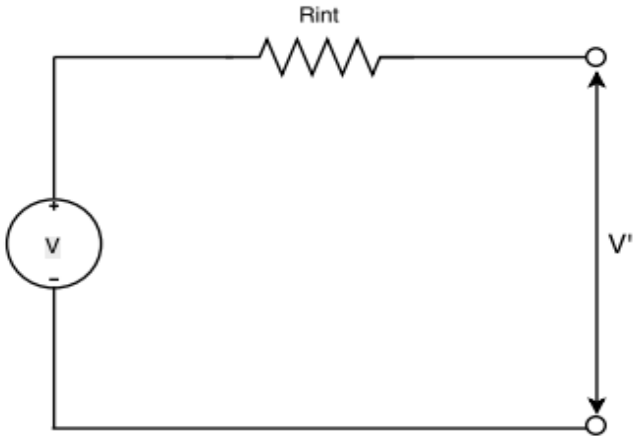

Figure 3.1: Model 1 battery equivalent circuit

$$V'(t) = V(t) - i(t) * R_{int} \tag{3.1}$$

3.2.2 Model 2

Due to the double-layer formation at electrode/electrolyte interface capacitive effects arise [73]. This capacitance consists of purely electrical polarization and diffusion capacitances [74]. The transient response of the battery is influenced by double layer and diffusion capacitances when the rates of reactions are high. This effect is modeled using a single lumped capacitance in parallel with the resistance [75]. To predict the run-time behavior of the battery, transient R_1 and C_1 (in parallel) are connected in series with R_{int} as illustrated in figure 3.2. The time constant characterizes the time varying response of the battery. OCV for figure 3.2 is given as (3.2).

$$V'(t) = V(t) - i(t)\left[R_{int} - \left\{\left(\frac{R_1 + 2R_{int}}{R_1 C_1}\right) e^{-\left(\frac{t}{R_1 C_1}\right)}\right\}\right] \tag{3.2}$$

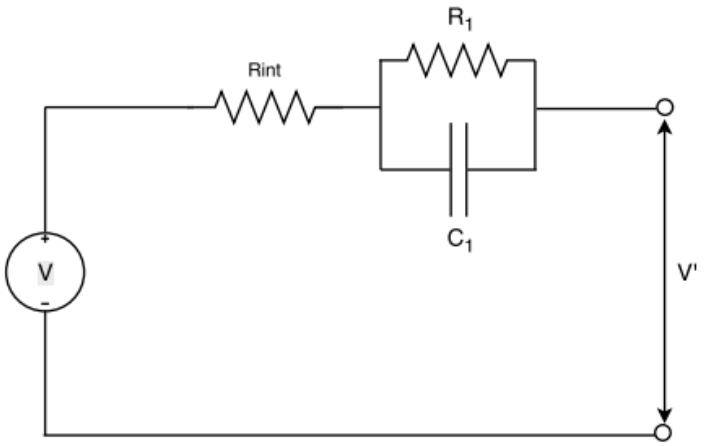

Figure 3.2: Model 2 battery equivalent circuit

3.2.3 Model 3

Double layer and diffusion capacitances in model 2 are represented as R_1 and C_1 combination. But, to represent them separately, 2 of such combinations are employed in model 3. Model 3 is presented in figure 3.3, composed of voltage source which is a function of charge remaining in the battery, internal resistance R_{int}, diffusion and double layer resistances and capacitances R_1, R_2, C_1, and C_2 respectively. Governing equation of OCV for the model 3 is given as (3.3).

$$V'(t) = V(t) - i(t)\left[R_{int} - \left\{\left(\frac{R_1 + 2R_{int}}{R_1 C_1}\right) e^{-\left(\frac{t}{R_1 C_1}\right)}\right\} - \left\{\left(\frac{R_2 + 2R_{int}}{R_2 C_2}\right) e^{-\left(\frac{t}{R_2 C_2}\right)}\right\}\right] \quad (3.3)$$

Equations (3.1), (3.2) and (3.3) demonstrate the open circuit voltages of models 1, 2 and 3 respectively. Temperature effect and self-discharge current considerations will be included and explained in further sections. OCV and current calculations should include both temperature and self discharge current during simulations and analysis to realize the impacts over the performance of the battery. A number of Li-ion cells are connected in series and parallel to simulate a powerful battery to be used in hybrid vehicles.

Knowledge of the amount of charge left in the battery compared with the energy it had when it was full, gives the user an indication of how long a battery will continue to perform before it needs recharging. Next section is dedicated to determine SOC and used the above discussed models for the simulation purposes.

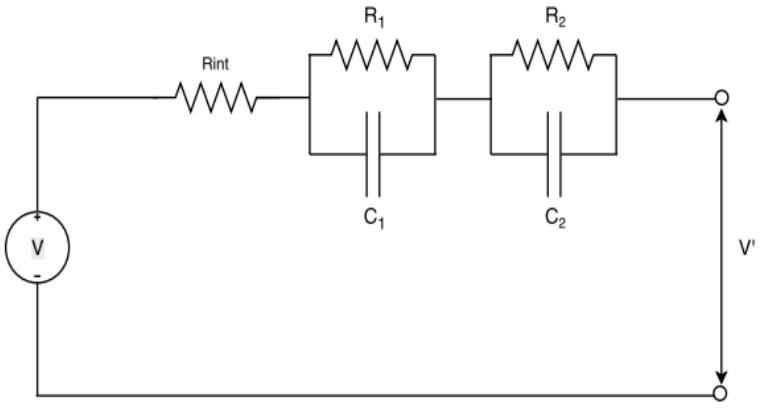

Figure 3.3: Model 3 battery equivalent circuit

3.3 Proposed SOC Estimation Method

The vehicle performance is characterized by SOC of battery, defined as the ratio of remaining capacity to fully charged capacity given as (3.4).

$$SOC = SOC_0 - \frac{1}{SOC_0}\int_{t_0}^{t_f} i(t)\, dt \tag{3.4}$$

SOC_0 is the initial SOC level of battery, $i(t)$ is the current from battery at time t, t_0 Is time from where SOC starts to deplete and t_f is the final time up to which discharge is allowed.

A large number of researchers attempted to calculate exact SOC of the battery. Major methods used are 1) Direct method 2) Specific gravity measurement 3) Voltage based (OCV) and 4) Current based (Ampere hour counting). Direct measurement is not useful because it considers the discharging rate only and specific gravity method is useful for Pb-acid batteries as it measures the changing weight of active materials. Voltage based and current based measurement have been used and suggested by various researchers. Although, they also suffer with some negative effects but have advantages also.

Pang et al. used OCV method to calculate SOC (i.e. SOC_v) of battery [76]. The OCV based SOC estimation technique is advantageous in various aspects like i) OCV versus SOC characteristic is independent of the age of the Li-ion battery [77], ii) this is very accurate, but suffers with a disadvantage that it requires some rest time after full

charge [78]. Ampere-hour counting method (i.e. SOC_i) is a suitable method to estimate SOC of the battery as it is easy, direct and easily implementable. If the current measurement is accurate, then the method is reliable also. But it may have some initial value or accumulated error problems [79]. Initial value problem occurs as knowledge of correct initial SOC is not available generally. Accumulation error problem at an instant is defined as the difference between the analytical and numerical solutions. It is resultant of truncation and round off both. Moreover, the SOC_i calculation needs capacity information of the battery. If calculation gets stuck to any wrong reading, incapability of correcting it advises to go for an alternative SOC estimation method. To overcome the shortcomings of both and to utilize the added advantages, these two methods can be combined together. [80] and [81] identified the contribution of both SOC_v and SOC_i together to estimate accurate SOC of the battery but do not include the effects of temperature. It is appreciable to characterize Li-ion battery to dynamically compute SOC even in case of temperature variation. Li-ion battery is very reactive chemically and gets affected by temperature significantly. Under optimal temperature range batteries behave as prescribed, but outside, battery cell experiences severe loss of capacity. To characterize the battery performance under the influence of temperature, thermal effect during modeling is deemed here for mentioned models. In this thesis work, a generalized SOC estimation method is proposed using both SOC_v and SOC_i. The block diagram of same is given in figure 3.4. This method includes the effect of temperature and self discharge current. The proposed method is applied to all three battery model developed in the previous section. The details of steps involved in SOC estimation are given in coming sections.

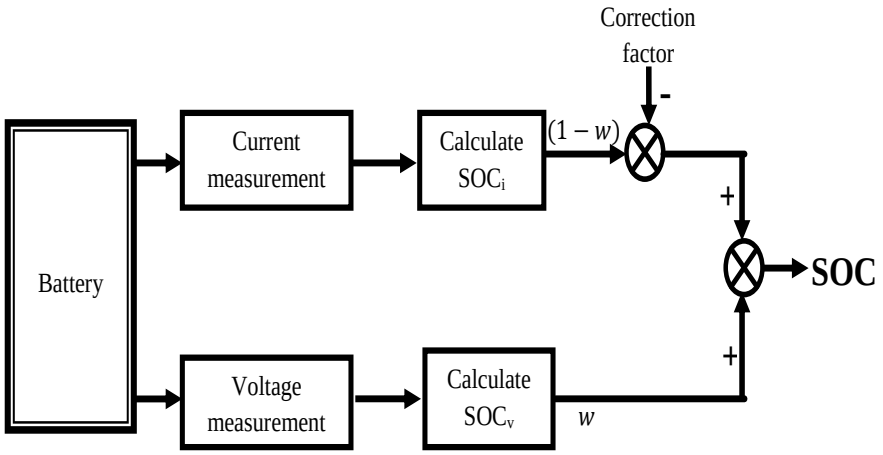

Figure 3.4: Proposed SOC estimation method

3.3.1 SOC_v Calculation

Cell voltage under reversible conditions, i.e. all the reactions are balanced is called equilibrium voltage which is occasionally referred as OCV or rest voltage. With this OCV, voltage based SOC at temperature T can be estimated using equation (3.5).

$$SOC_v(T) = \frac{1}{a_1}(OCV(T) - a_0) \tag{3.5}$$

Where a_0 = battery terminal voltage when SOC = 0% and a_1 = battery terminal voltage when SOC = 100%. Due to change in temperature, equilibrium voltage of battery at any temperature T gets changed as (3.6).

$$V_{(T)} = V_{(298)} + \left(\frac{dV}{dT}\right)(T - 298) => OCV \tag{3.6}$$

$\frac{dV}{dT}$ is temperature coefficient and is constant for the considered temperature range. So the consideration of this OCV with temperature effect will lead to modify SOC_v and will contribute in the absolute SOC computation.

3.3.2 SOC_i Calculation

The Ampere hour involves the current integration flowing through the battery to estimate SOC. SOC_i at temperature any temperature T can be computed as (3.7) considering self discharge current.

$$SOC_i(T) = \frac{1}{C_p}\left(C_p - \int\{i(T) + i_{(s-d)}(T)\}dt\right) \tag{3.7}$$

Cp is battery capacity in Ah.

From the Arrhenius equation, the reaction rate is given as (3.8). During the electron transfer reaction, electrons require the additional amount of energy to surmount the energy barrier is called the activation energy (E_a=J-mol^{-1}) and depends on temperature. As for every 10°C temperature increase current gets double, so for a ΔT temperature change, reaction rate ratio is articulated as (3.9).

$$K = K_0 * e^{\left(-\frac{E_a}{RT}\right)} \tag{3.8}$$

$$\frac{K(T + \Delta T)}{K(T)} = 2^{\left(\frac{\Delta T}{10}\right)} \tag{3.9}$$

K_0 = reaction constant, R = gas constant, Ea = activation energy and T= operating temperature. K is reaction rate (mole/s) and can be expressed as current. Suppose K_1 is the reaction rate at temperature (T+ΔT) i.e. K_1= K (T+ΔT) and K_2 at temperature T i.e. K_2 = K (T). To represent effect of temperature on E_a, (3.8) and (3.9) are equated as (3.10) after taking natural logarithm and then E_a is computed to have effect of temperature on its evaluations as in (3.11).

$$ln\frac{K(T+\Delta T)}{K(T)} = \frac{E_a}{R}\left(\frac{1}{T_T} - \frac{1}{T_{(T+\Delta T)}}\right) = \left(\frac{\Delta T}{10}\right) ln2 \tag{3.10}$$

$$E_a = ln2\left(\frac{R}{10}\right)(T * (T + 10)) \tag{3.11}$$

Li-ion batteries exhibit self discharge phenomena, even at moderate oxidation levels. It is primarily due to losses occurring at the negative electrode, which results from several side reactions, each with their own activation energy and rate constant. From Arrhenius equation (3.8), self discharge current can also be modeled. The battery capacity also affects it; hence self discharge current is sculpted as (3.12) considering the effect of temperature on activation energy from (3.11).

$$i_{(s-d)}(T) = \frac{1}{c_p}K_0(T) * e^{-\left(ln2\left(\frac{R}{10}\right)(T*(T+10))\right)} \tag{3.12}$$

The temperature dependent SOC can be deduced as (3.13) by combining SOC_v and SOC_i with a weighting factor w. Charging and discharging efficiency influences battery dynamics to a great extent and weighting factor allied with SOC_i governs the combined SOC. Correction factor (CF) η is integrated here, which is a function of SOC as (3.14) which helps in getting exact SOC during discharging. Weighting factor calculation is presented in next section in detail.

$$SOC = wSOC_v + (1-w)(SOC_i - \eta) \tag{3.13}$$

$$\eta = \left(1 - \frac{SOC_0}{100}\right) \qquad at\ 25\ ^\circ C \tag{3.14}$$

3.3.3 Weighting Factor Calculation

To calculate the weighting factor, the steady value of OCV and time required to achieve this should be considered because under steady conditions SOC_v has a higher accuracy

[82]. The entire OCV range is divided into 100 sections and each section's weighting value is calculated as (3.15).

$$w_1 = 2 * \mathrm{Ik} - 50\mathrm{I} * \frac{.5}{100}; 1 \leq \mathrm{k} \leq 100 \tag{3.15}$$

From the discharging characteristics, average time taken by OCV to get steady condition is t_s=1278s and time between two samples is t=192.78s. As $t<t_s$, weighting factor w is deduced as (3.16).

$$w = w_1 * \frac{t}{t_s} \tag{3.16}$$

Weighting factors using (3.15) and (3.16) are computed and collected in table 3.1; correction factors corresponding to different SOC levels are also computed at 25 $^{\circ}C$ and cognated with weighting factors in table 3.1.

Table 3.2 brings together the reference SOC values to be generated during discharging and values obtained from the proposed method. The values obtained from proposed method are very close to the reference values for 100 to 50 percent SOC range. The error is very less and is in the range of 0-0.5 percent. From 50-36 percent SOC ranges, the error between the reference and obtained SOC is less than 2 percent but error starts increasing below 35 percent and continues till empty state.

Table 3.1: Weighting factors and correction factors corresponding to varying SOCs

Weighting factors			**Correction factor**
SOC (%)	w	$\mathbf{1-w}$	η
100	0.0420	0.9580	0.0
90	0.0340	0.9600	0.1
80	0.0250	0.9750	0.2
70	0.0171	0.9829	0.3
60	0.0085	0.9915	0.4
50	0.0000	1.0000	0.5
40	0.0085	0.9915	0.6
30	0.0171	0.9829	0.7
20	0.0250	0.9750	0.8
10	0.0340	0.9660	0.9
0	0.0428	0.9571	1.0

Continuous recording of SOC during vehicle propulsion is important to update power management system, which command to toggle between battery and engine for minimum fuel consumption and better energy efficiency. Change in temperature due to any reason (environmental effect or battery pack utilization) alters the characteristic of the battery. Self discharge current and effect of temperature change is considered in the

proposed algorithm. Flow chart of the proposed algorithm is shown in figure 3.5. The simulation data are analyzed to obtain the effect of temperature on OCV, SOC, resistance and capacity of the battery and are discussed in later sections.

Table 3.2: Comparison between reference and obtained values of SOCs

Reference SOC (%)	Obtained SOC (%)	Error (%)	Reference SOC (%)	Obtained SOC (%)	Error (%)
100	100.0	0.0000	36	36.67	1.8611
90	90.09	0.1000	35	35.73	2.0857
80	80.32	0.4000	34	34.79	2.3235
70	70.39	0.5571	33	33.85	2.5758
60	60.28	0.4667	32	32.92	2.875
50	50.00	0.0000	31	31.99	3.1935
40	40.44	1.1000	30	31.05	3.5000
39	39.50	1.2821	20	21.82	9.1000
38	38.55	1.4474	10	12.68	26.800
37	37.61	1.6486	00	1.07E-07	00.000

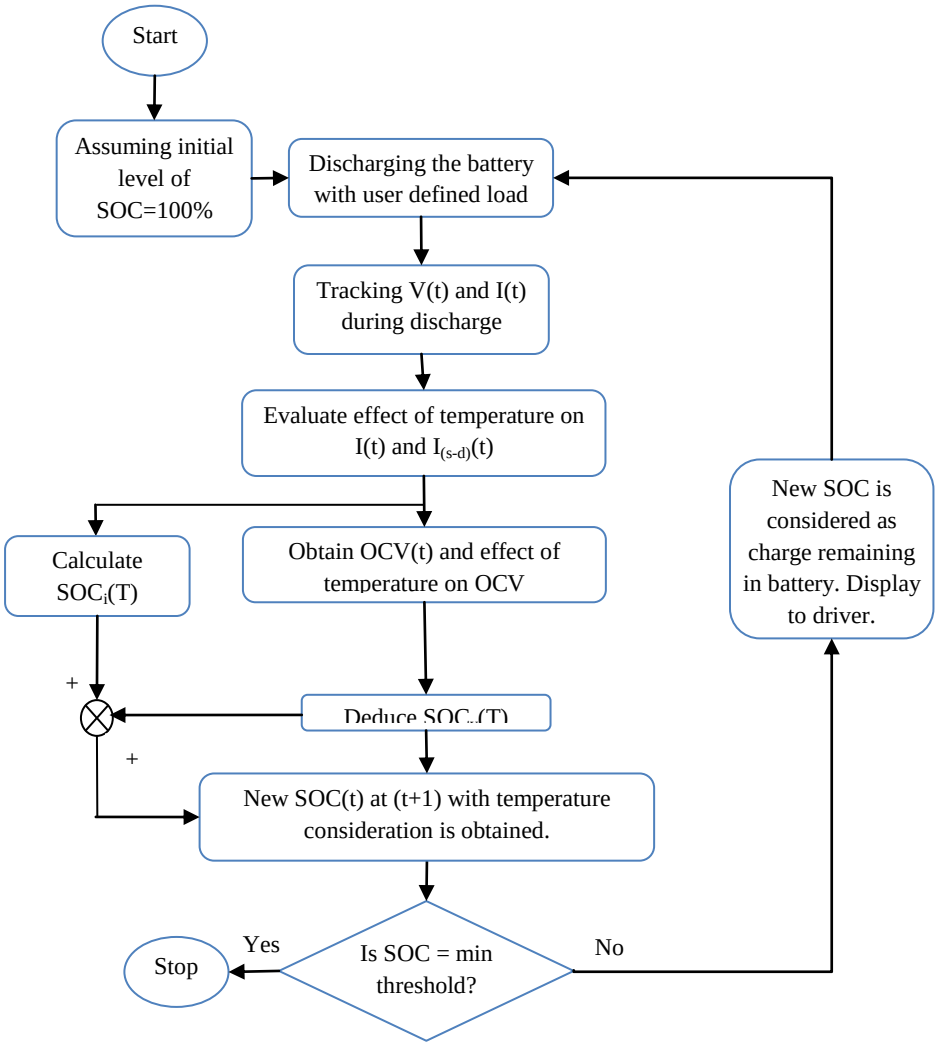

Figure 3.5: Flow diagram of online SOC estimation

3.3.4 Correction Factor Assessment for Varying Temperature

Determination of CF is an important and complex process. As the battery supplies energy to the load (vehicle), at that time accurate SOC information is very important under dynamic state of charge/discharge to the driver and controller both. Under operational conditions, current transfer rate affects the CF. CF is closely related to the charging and discharging rate. The performance of the battery with the load is expected to vary and CF gets modified for the varying conditions. Here variation of CF with SOC and temperature is verified and a mathematical expression is proposed. When battery alone is considered then CF can be estimated as given in (3.14), but as it gets associated with the load, it varies significantly and can alter the performance of the vehicle.

At high SOC levels, the kinetic rates are high due to the presence of more un-reacted active mass and presence of higher level of electrolyte concentration which leads to rapid material conversion. At low SOC levels, the kinetic rates are relatively low and lead to 100 percent charge efficiency [83]. Change in temperature directly influences the rate of reaction and governs the CF. It can be summarized that CF is a function of both temperature and SOC. Simulation results verify the effect of SOC and T over CF. The proposed CF derived can be stored or calculated 'on-the-fly' and applied incrementally to correct the SOC. The CF variation with the SOC and temperature is shown in figure 3.6.

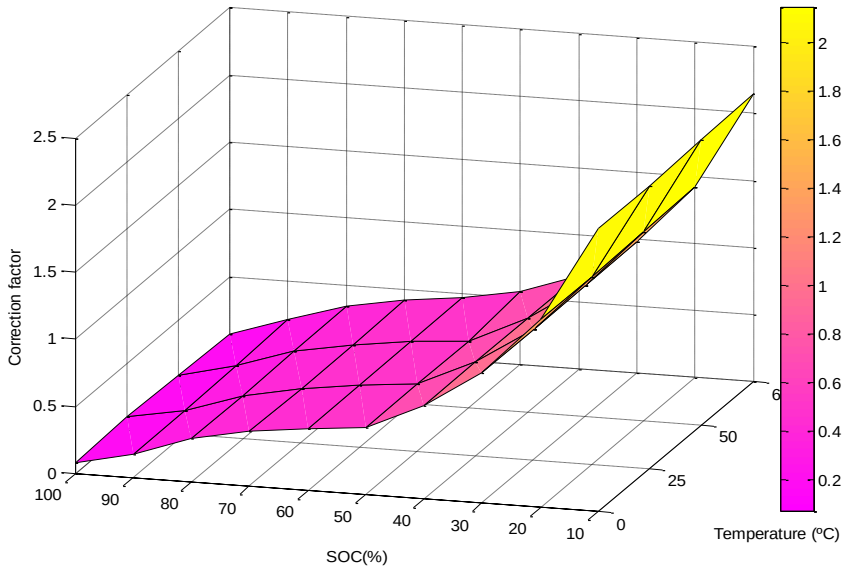

Figure 3.6: Correction factor variation with temperature and SOC

Exploration of CF for the range of SOCs with wide temperature series is performed i.e. 0˚C, 25˚C, 50˚C, 60˚C (very low, room temperature and high) which helps in finding a healthy operating range for the battery. The pattern achieved is more or less follows Cauchy's distribution. At room temperature (25˚C), CF is higher for lower SOCs and becomes low with higher SOC values. The same pattern is observed for 0˚C, 50˚C and 60˚C; only the quantitative measures are changed. Based on the simulation results and extensive mathematical analysis, a modified CF is proposed (at other than room temperature) and given in (3.17). According to this developed relation, CFs are calculated 'on the fly' subsequently SOCs are estimated adaptively and found to be same as reference values. ε is the error tolerance band and is found to be between 0-5 percent. SOC is in percent and T in Kelvin.

$$\eta_{new(T,SOC)} = \eta_{298} + \frac{\left(\frac{SOC}{1000}\right)}{T - 298} \pm \varepsilon \tag{3.17}$$

Table 3.3 collects the correction factors calculated at different temperatures corresponding to varying SOC levels.

Table 3.3: Correction factors at different SOCs

Correction factor at different temperatures				
SOC (%)	0 ˚C	25 ˚C	50 ˚C	60 ˚C
100	1.0996	1.08405	1.09000	1.0740
90	1.0764	1.07670	1.09300	1.1146
80	1.1227	1.12290	1.13200	1.1435
70	1.1067	1.10690	1.11150	1.1177
60	1.0625	1.06145	1.10634	1.0659
50	1.0000	1.00000	1.00000	1.0493
40	1.0960	1.09580	1.09800	1.0999
30	1.2740	1.27440	1.28000	1.2850
20	1.5950	1.59800	1.68080	1.6190
10	2.2110	2.21000	2.22500	2.2450
0	0.0000	0.00000	0.00000	0.0000

3.3.5 Threshold SOC Determination

Li-ion batteries are used extensively in HEVs to propel the vehicle as primary power source, hence it is essential to monitor its SOC continuously. Overcharging and depletion below a specified level deteriorates battery health. Since batteries are expensive, it is compulsory to take care of their health for durability. Battery mainly operates in two modes: 1) charge depletion and 2) charge sustaining. In HEVs both the modes together

are used in such a way that initial and final SOC at the end of the trip are same. Further, batteries get charged either by the engine (indirectly by fuel) or by regenerative braking.

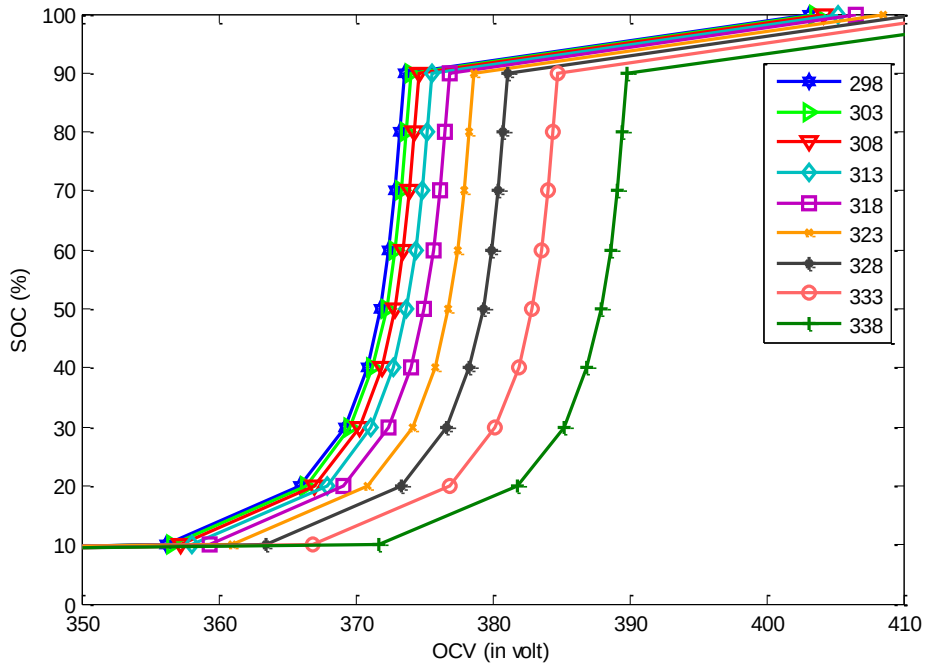

Figure 3.7: SOC vs. OCV at different temperature

In available literatures, no proper justification to choose the lowest SOC level to which battery should be allowed to discharge is found. Based on data collected during discharge from 100 to 0 percent SOC at various temperatures, the threshold SOC level using gradient method is proposed. The curves shown in figure 3.7, are seventh order equation at 25˚C and can be approximated as (3.18).

$$SOC = p1 * z^7 + p2 * z^6 + p3 * z^5 + p4 * z^4 + p5 * z^3 + p6 * z^2 + p7 * z + p8 \qquad (3.18)$$

where p1 = -6.9991e+007, p2 = -8.6071e+007, p3 =2.8379e+008, p4= -2.3169e+008,

p5= 0.0481e+007, p6=1.8831e+007, p7=2.0122e+006, p8 = -86693 and z= OCV.

The rate of SOC variation is linear from 90 to 35 percent SOC range and OCV is constant hence this range is the best for vehicle propulsion. Below 35 percent, a rapid decline in OCV is observed and SOC changes abruptly. These also get authenticated from table 3.2. The proposed threshold level of SOC is 35 percent and operating below this, is not recommended as shown in figure 3.8. This has been analyzed by observing gradient at each and every SOC point. When a battery operates at higher temperatures, threshold occurs sooner and at lower operating temperatures, it occurs later as compared to the

room temperature case, the same can also be observed in figure 3.7. Corresponding to 35 percent threshold SOC, OCVs will be 369.09 V, 370.13 and 372.08 at 278K, 298 K and 313 K respectively.

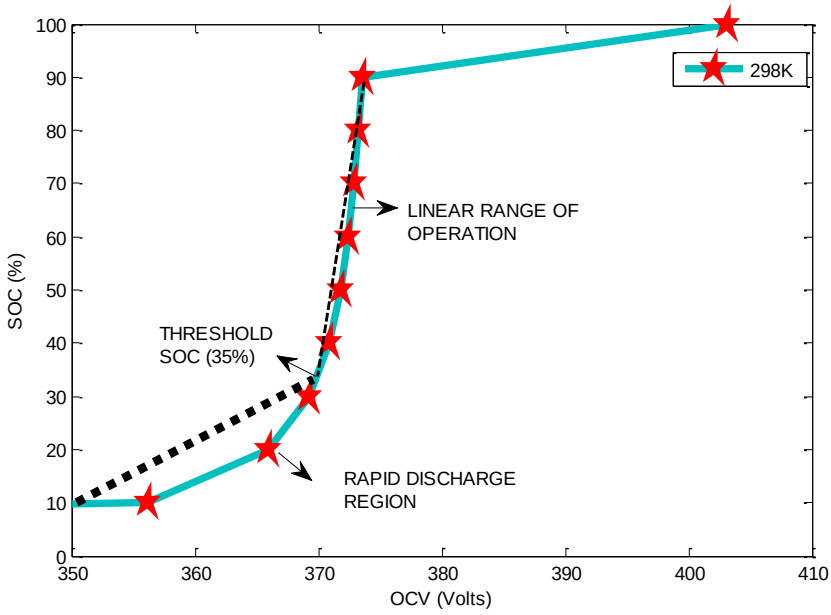

Figure 3.8: Determination of Threshold SOC

3.4 Effect of Temperature on Battery Performance

Li-ion battery performs very well in ambient environment (at room temperature). A change in temperature alters the characteristic of the battery so it is advisable to keep the battery temperature in a limited range. Sometimes, the variation may be so significant that it alters the complete performance characteristic of the battery. To validate the temperature dependent characteristics, the proposed battery models are used with a load set to draw a constant current of 25.6 A, but with the environmental temperature set to various values. The battery was then discharged repeatedly from full SOC to zero SOC at each temperature. The simulation data are analyzed to obtain the relation between the OCV and SOC and effect on internal resistance and capacity of battery as given in the following sections.

3.4.1 Effect on Open Circuit Voltage

Concentration of Li-ions of solid phase with respect to intercalating material represents OCV and gets affected by changes in chemical composition, pressure and temperature as

presented in [84]. OCV represents batteries' chemical reaction phenomenon. In Li-ion batteries concentration of lithium ions of the solid phase with respect to intercalating materials (Li-ions) determines the open circuit potential [85].

Battery SOC consists of OCV as the major component which defines the thermodynamic properties of the battery. To see the effect of temperature on OCV, proposed models are simulated for a wide temperature range from -20°C to 60°C to see the response and corresponding curves are plotted in figure 3.9 (a), (b) and (c). At different SOC values ranging from 10 to 90 percent, a variation in OCV is seen due to temperature change. OCV increases as temperature gets higher than room temperature and decreases with decreasing temperature. From -20°C to 40°C, OCV curves are very close to each other. OCV values changes a lot in comparison to the average OCV after 40°C. Results obtained here are compared with the practical results given [86, 87] and are found to be optimistic.

As temperature increases, OCV values gets differ for considered models at various SOC ranges. Figure 3.10 (a), (b) and (c) shows OCV at 0°C, 25°C and 60°C for all three proposed models respectively. OCVs at 0°C and 25°C don't differ much but beyond 45°C results fluctuate and a large difference is found at 60°C.

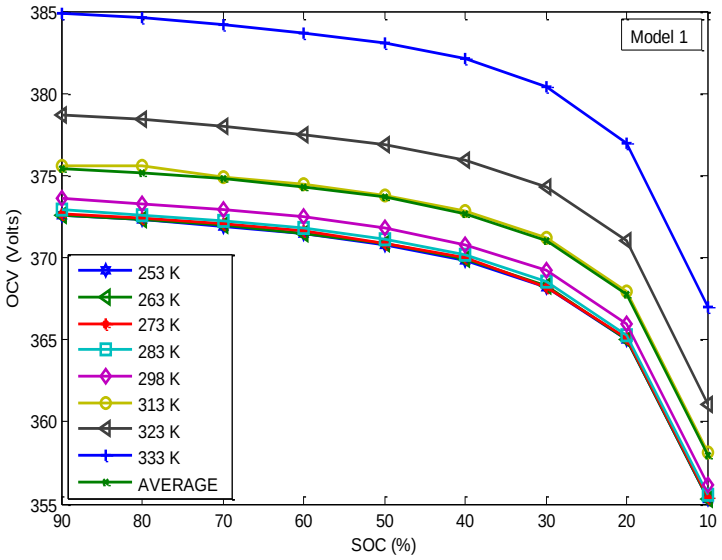

(a)

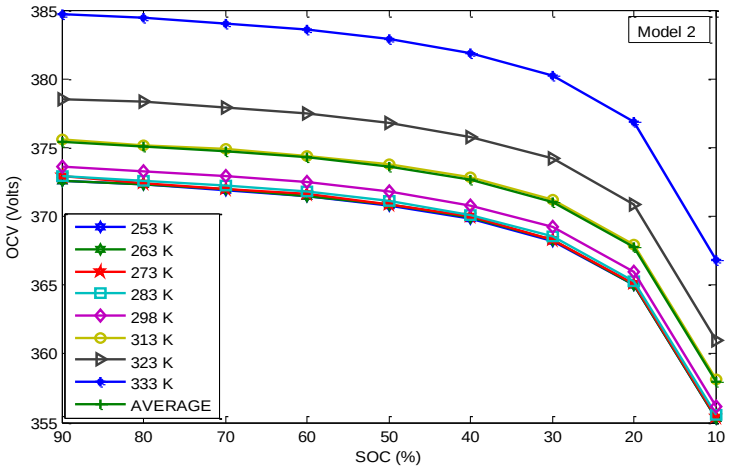

(b)

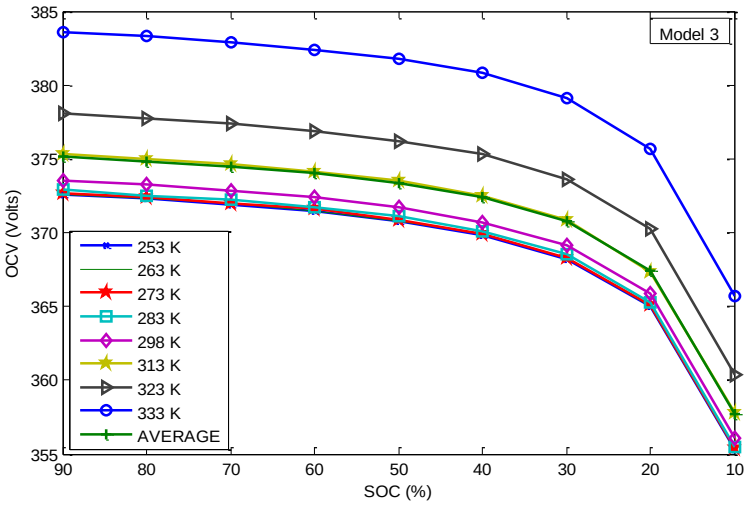

(c)

Figure 3.9: Effect of temperature on OCV (a) model 1, (b) model 2 and (c) model 3

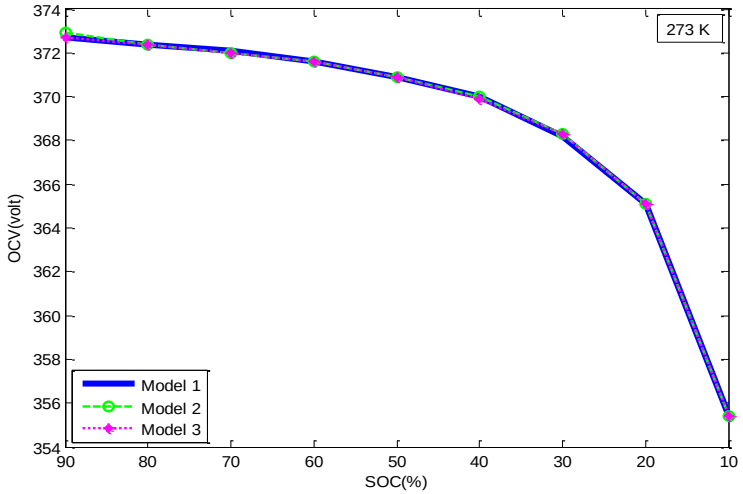

(a)

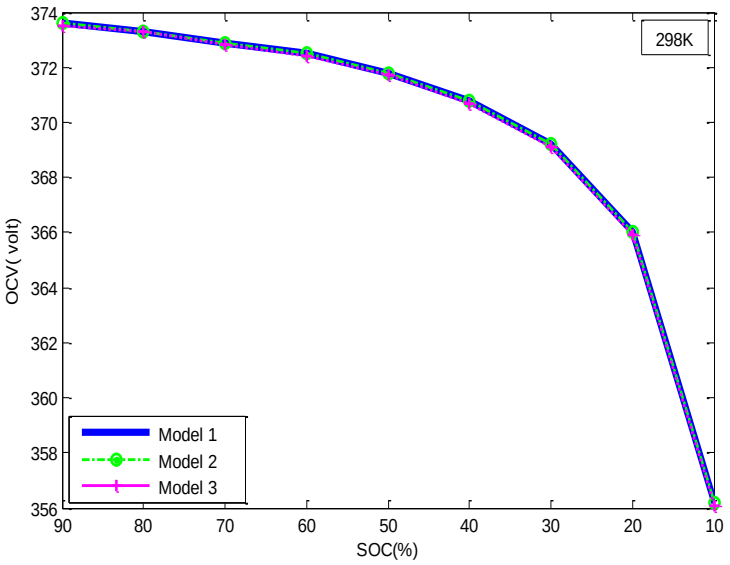

(b)

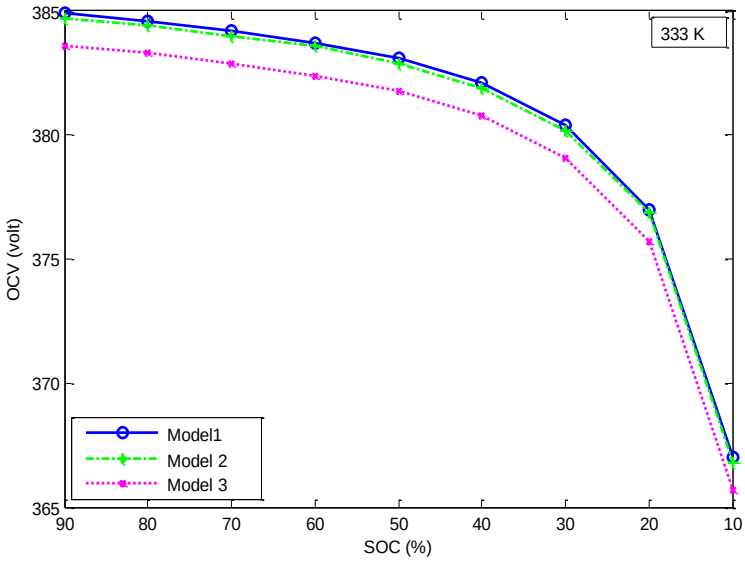

(c)

Figure 3.10: Temperature effect on OCV, (a) model 1 (b) model 2 and (c) model 3

3.4.2 Effect on Capacity

The capacity of battery can be defined as the total electrical charge relinquished by battery from its fully charged state to empty. Amount of charge contained by a battery is its useable capacity. Capacity of the battery extensively varies with operating conditions and strongly depends on the internal impedance of the battery. It gets much influenced by the temperature change. At high temperatures, chemical reaction requires less activation

energy so with a very less amount of energy more intercalation and de-intercalation of lithium ions occur resulting in a higher cell voltage. Due to higher temperatures lithium ions can diffuse faster, which means a higher current can flow, which increases the power and discharge capacity of Li-ion cells. At low temperatures, the intercalation and de-intercalation requires higher activation energy for the chemical reactions. So less lithium ions can participate in the active cell mechanism which results in a temporary loss of capacity [88]. With the increase in temperatures, capacity increases with decrease in resistance. For model 1, 2 and 3 the increase in capacity above room temperature is recorded and presented in table 3.4.

Table 3.4: Temperature effect on capacity

Temperature (°C)	**Increase in Capacity (%)**		
	Model 1	**Model 2**	**Model 3**
35	4.3	4.73	4.52
40	4.88	5.41	5.58
45	6.2	6.27	5.73

With decrease in temperature the capacity of the battery diminishes. At low temperatures, the resistance increases and current drawing capability decreases due to slower reaction rates. Figure 3.11 depicts the actual remaining capacity of battery as temperature decreases. Since self discharge current is also considered, so the battery capacity at room temperature even cannot be achieved to be 100 percent. It will be little bit lower than rated capacity.

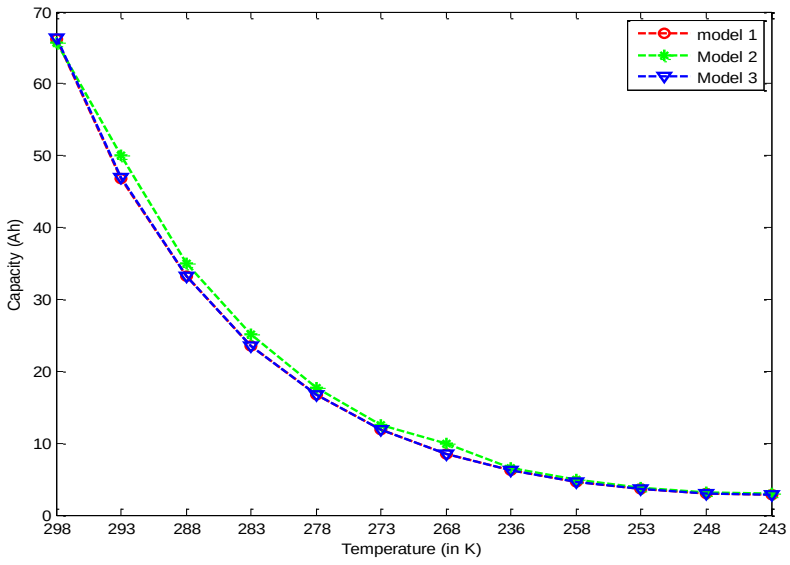

Figure 3.11: Capacity variation over wide temperature range for model 1, 2 and 3

3.4.3 Effect on Resistance

Terminal voltage of cell is lesser than the source voltage and higher voltage is required to charge the cell which reduces its effective capacity as well as decreases its charging/discharging efficiency. It signifies, there is voltage drop offered by internal resistance of cell. Higher discharge rates, give rise to higher internal voltage drops which explains the lower voltage discharge curves at high C-rates [89]. The internal resistance of the battery varies with change in various parameters and can never be considered as constant even though the manufactures label it as constant. It majorly depends on C-rate, SOC and temperature. At low temperatures, cell may be very inefficient due to larger impedance and reduced capacity. But at higher temperature, efficiency improves due to the lesser internal impedance because rate of chemical reactions increases. For lower internal resistance, self discharge rate increases and cycle life deteriorates.

High resistance is observed below room temperature, but as temperature increase resistance decreases rapidly which can be clearly observed here. At and below room temperature resistance experienced by model 1 and 2 are same, but at higher temperatures, resistance of model 3 is greater than model 2. Thus, it is seen that model 3 combination imposes an impact at higher temperatures, but doesn't alter the performance at room temperature and below this. Figure 3.12 (a) shows resistance offered by model 3 is more than others at low temperatures. A magnified view to make it clear is given in figure 3.12 (b).

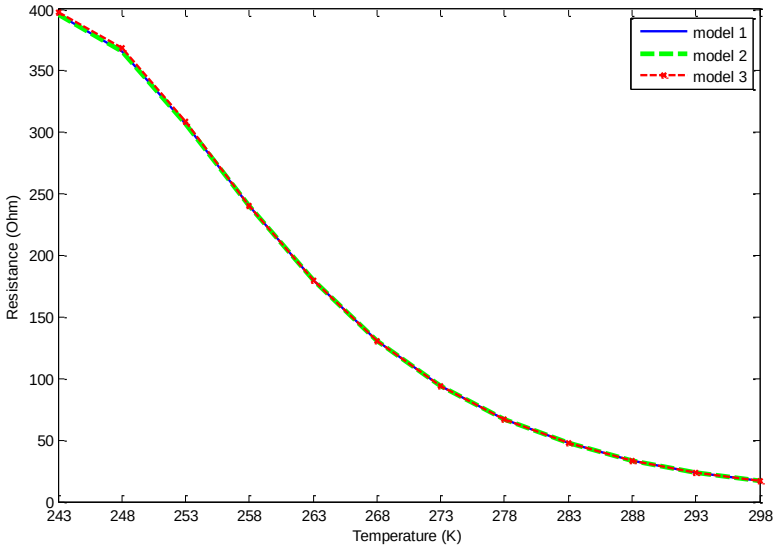

(a)

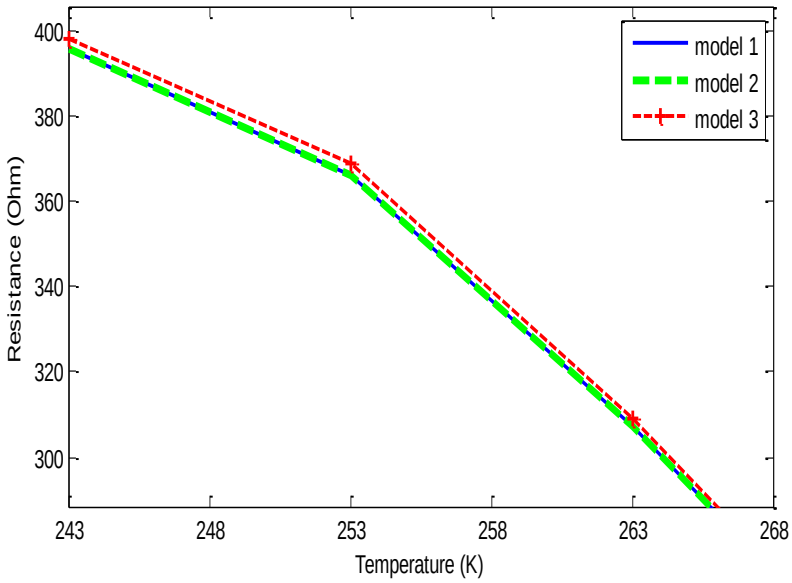

(b)

Figure 3.12: Resistance comparison of models (a) at and below room temperature (b) low temperatures

Figure 3.13 (a) compares resistance variation above room temperature for all the models. The resistance offered by model 3 is lower than model 1 and 2 as figured in 3.13 (b). Behavior of model 3 at all the temperatures are varied compared to model 2 which makes it clear that 2 RC combination imposed during modeling will certainly affect the battery characteristics and hence the performance of HEVs wherever it will be used. The observations at various temperatures demonstrate the similar results as in [90].

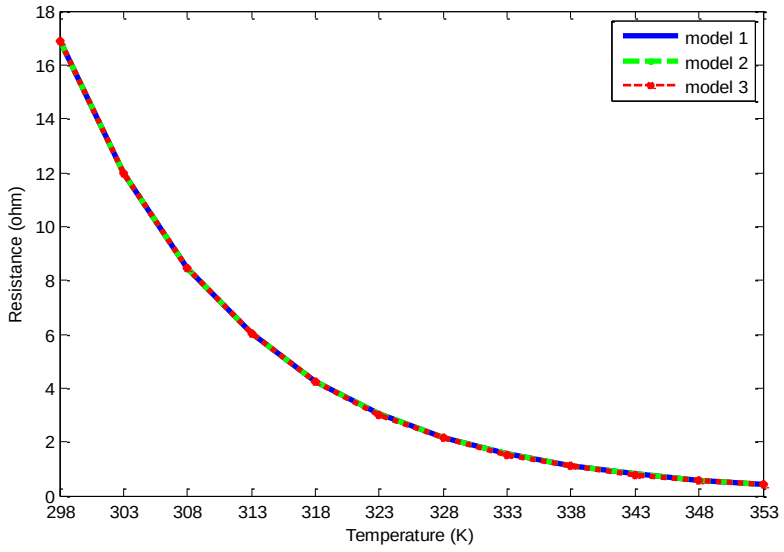

(a)

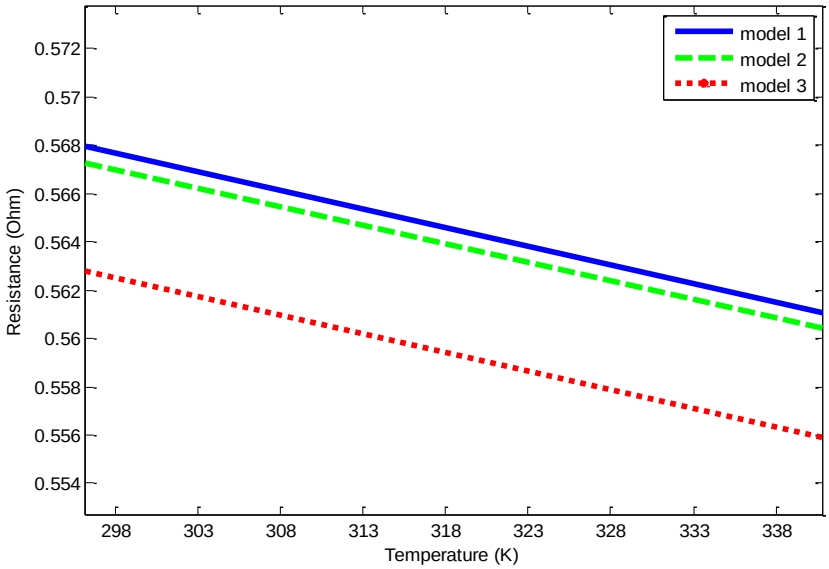

(b)

Figure 3.13: Resistance comparison of models (a) at and above room temperature (b) high temperatures

For the fixed temperature, battery resistance varies minutely or is almost constant for a complete SOC range from 100 to 10 percent [91]. Figure 3.14 (a), (b) and (c) depicts the behavior of resistance over a wide temperature and SOC ranges for model 1, 2 and 3 respectively. At high temperatures, offered resistance is very less compared to the lower temperatures. While discharging battery from the 100 percent SOC level to 10 percent, the resistance offered by models is recorded and shown in figure 3.15 (a), (b) and (c) which portray very clearly that a minute change occurs in resistances in the whole range of SOC variation at any particular temperature. This figure illuminates, as SOCs varies, resistance changes. It elucidate that internal resistance doesn't remain constant during discharging. During vehicle performance analysis, constant internal resistances are generally considered by researcher. In this research work, resistance offered by battery is considered varying with respect to the SOC, not constant. It will lead towards real time mechanism. During modeling, it is assumed that charging and discharging characteristics are same.

For utilizing the larger capacity of the battery, offered resistance should be less because an increase in resistance decreases capacity. Figure 3.16 demonstrate the resistance and capacity variation together for model 3 which is true for rest of the models also.

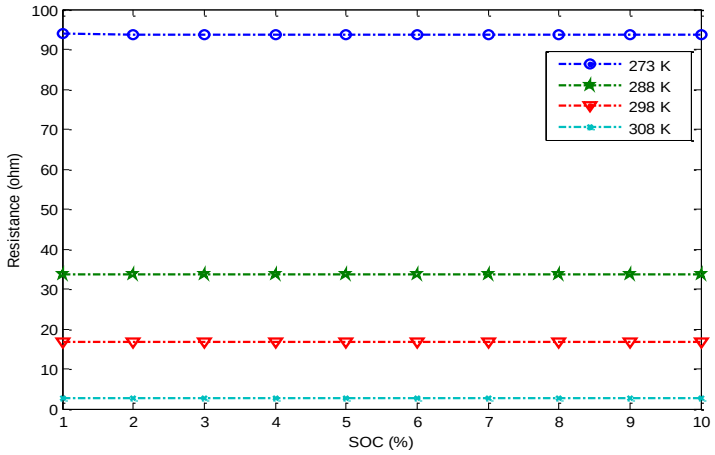

(a)

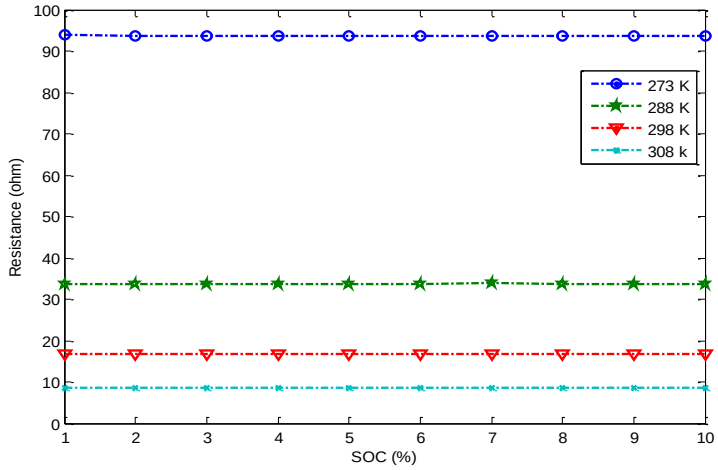

(b)

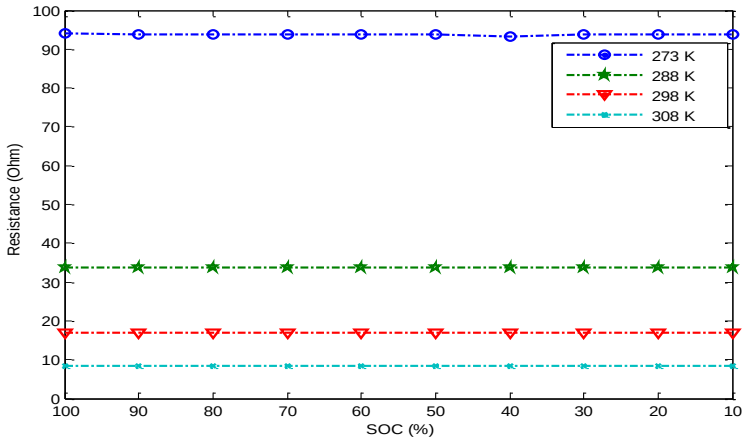

(c)

Figure 3.14: Variation in resistances for different temperatures at different SOC ranges (a) model 1, (b) model 2, and (c) model 3

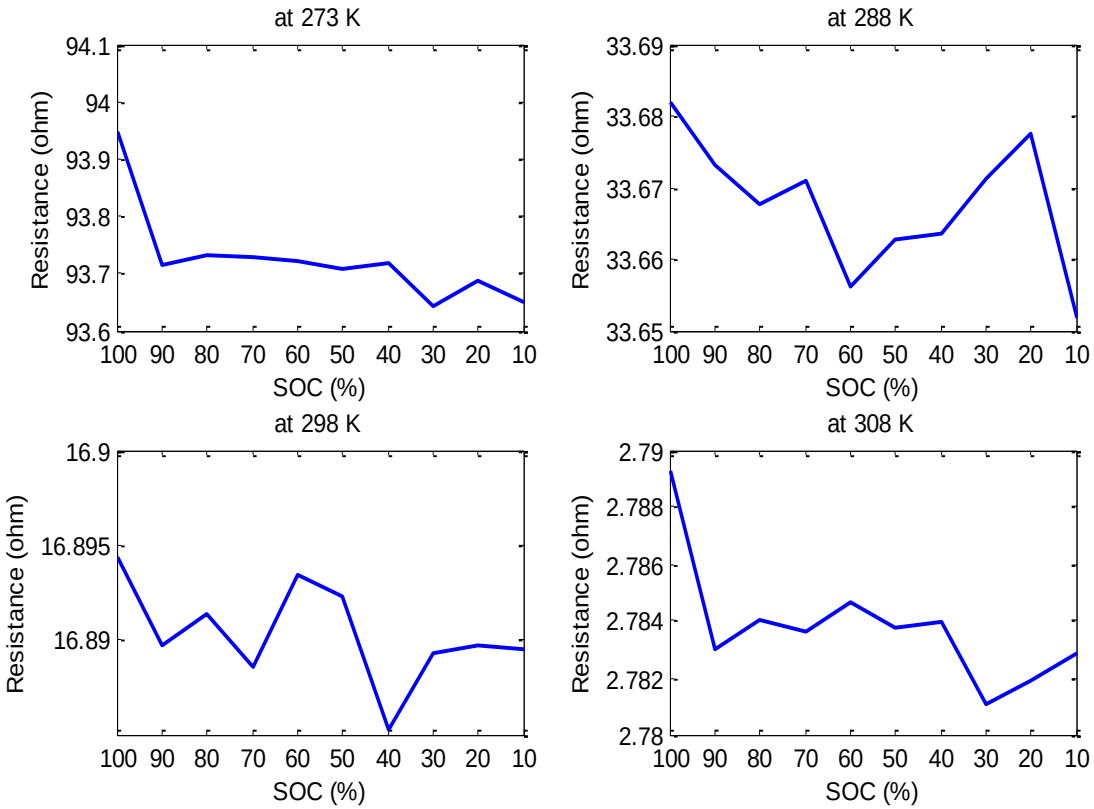
at 273 K
Resistance (ohm)
94.1
94
93.9
93.8
93.7
93.6
100 90 80 70 60 50 40 30 20 10
SOC (%)
at 288 K
Resistance (ohm)
33.69
33.68
33.67
33.66
33.65
100 90 80 70 60 50 40 30 20 10
SOC (%)
at 298 K
Resistance (ohm)
16.9
16.895
16.89
100 90 80 70 60 50 40 30 20 10
SOC (%)
at 308 K
Resistance (ohm)
2.79
2.788
2.786
2.784
2.782
2.78
100 90 80 70 60 50 40 30 20 10
SOC (%)

(a)

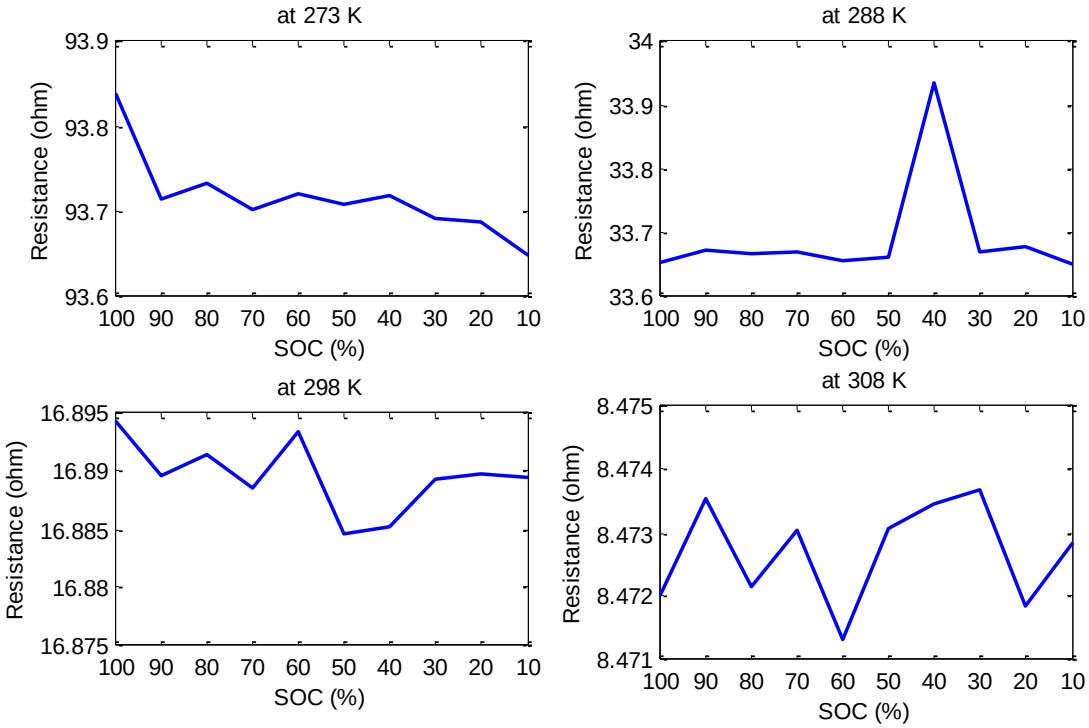
at 273 K
Resistance (ohm)
93.9
93.8
93.7
93.6
100 90 80 70 60 50 40 30 20 10
SOC (%)
at 288 K
Resistance (ohm)
34
33.9
33.8
33.7
33.6
100 90 80 70 60 50 40 30 20 10
SOC (%)
at 298 K
Resistance (ohm)
16.895
16.89
16.885
16.88
16.875
100 90 80 70 60 50 40 30 20 10
SOC (%)
at 308 K
Resistance (ohm)
8.475
8.474
8.473
8.472
8.471
100 90 80 70 60 50 40 30 20 10
SOC (%)

(b)

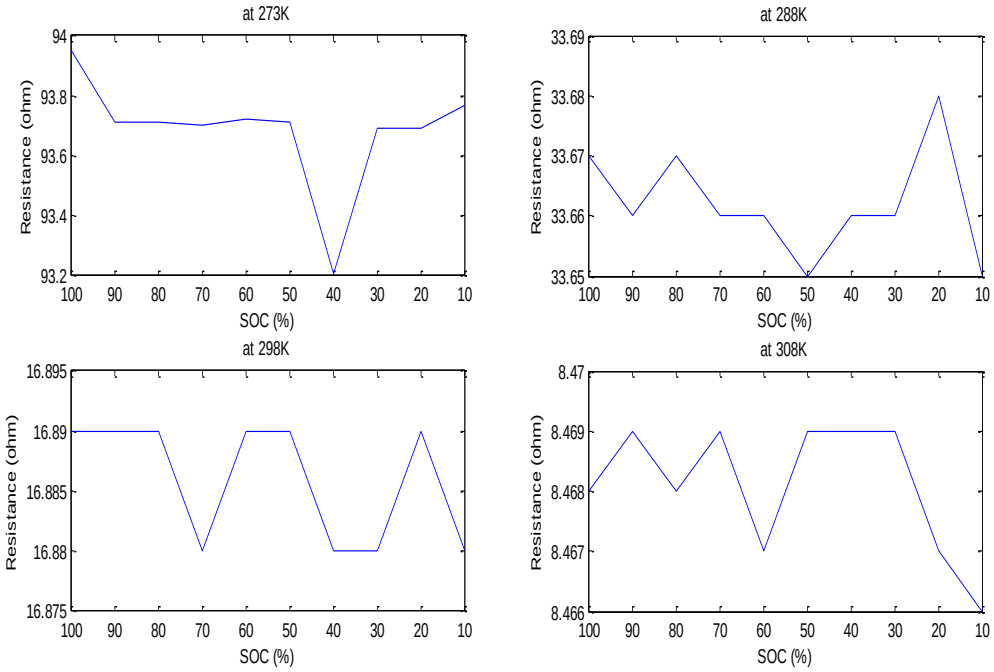

(c)

Figure 3.15: Variation in resistances With respect to temperatures (a) model 1, (b) model 2 and (c) model 3

At low temperatures, battery cell is inefficient due to more impedance, but at higher temperature, efficiency improves because the rate of chemical reactions increases due to lesser impedance offered. Johnson et al. locate an increment of three times in resistance as the temperature drops from ambient to 0˚C [92]. Johnson articulates that resistance can get varied by eight times depending upon discharge rate [89]. Battery capacity extensively varies with operating conditions and strongly depends on its internal impedance. With changing temperature, impedance of a battery varies a lot, hence capacity. At lower temperatures, cell reaction rate decreases, hence low current flows and vice-versa at higher temperatures. Therefore, the usable capacity decreases at low temperatures and increases at high temperatures. At higher temperatures, current drawn from battery increases rapidly, and battery depletes swiftly. Battery operation at enormously high temperatures causes an increase in rate of thermal reactions leading to even higher heat generation. Many electrochemical side reactions are damaged in the process. An efficient convective cooling system can avoid such high temperature excursions during repeated cycling.

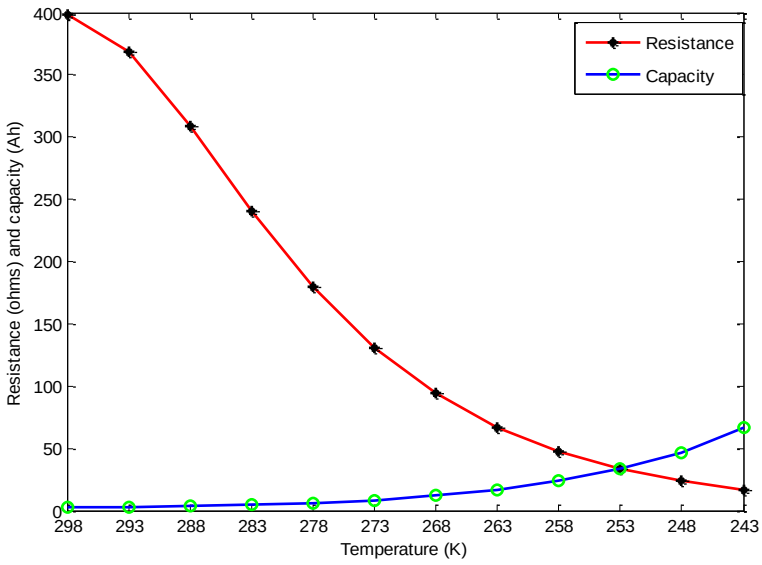

Figure 3.16: Resistance and capacity variation with temperature

3.5 Summary

For HEV applications, researchers have generally used Model 1 along with Ampere hour counting and significance of other battery models is not explored. In this chapter battery models are developed including self discharge current and effect of temperature on battery operation. Further a modified novel SOC estimation algorithm is developed based on Ampere hour counting and OCV. An expression of correction factor is proposed here to take care of temperature effect during SOC calculations. All these developed models along with SOC estimation method will be used in vehicle and impact on vehicle performance will be analyzed in coming chapters.

Chapter 4
Review of Power Optimization Techniques

Various HEV architectures and important components are summarized in this chapter. Input power split architecture is chosen in this thesis work. This architecture features with an ICE, battery and Planetary Gear Set (PGS). Presence of an alternative energy source along with the ICE in HEVs appeals for optimal power split between them for minimum fuel consumption and maximum power utilization. An intelligent energy management strategy along with PGS makes it possible. Energy management algorithms decide the power split between engine and motor in order to improve the fuel economy and optimize the performance. This chapter describes various energy management strategies available in the literature. Considerable amount of research work has been conducted for energy optimization. These control strategies are summarized here in a coherent framework.

4.1 Architecture of HEVs

Hybrid vehicles use electric, hydrogen or fuel cell traction system and an ICE to deliver power during vehicle propulsion. It generally incorporates either two or more energy storage devices on board. An HEV discussed over here consist an electrical battery and ICE and makes its architecture complex and is defined in terms of connection among ICE, battery, motor, generator and PGS. An efficient architecture of HEV should be able to harness desirable characteristics of both sources. This should meet out driver power demand with minimum toxic emissions and maximum fuel economy.

In HEVs, two types of power flow occur: 1) electrical and 2) mechanical. On the basis of power flow directions, they are classified mainly into three categories: 1) series hybrid 2) parallel hybrid and 3) series-parallel (power-split) hybrid. These are discussed in detail as below.

4.1.1 Series Architecture

The series configuration shown in figure 4.1 consists of an electric motor with an ICE without any mechanical connection between them. In this configuration, two electrical powers are added together in the power converter, which functions as an electric power coupler to control the power flows from battery and generator to electric motor or from electric motor to battery. ICE is used for running a generator when the battery doesn't have enough power to drive the vehicle, i.e. ICE drives an electric generator instead of directly driving the wheels. Series hybrids have only one drive train, but require two distinct energy conversion processes for all operations. These two energy conversion processes are gasoline to electricity and electricity to drive wheels. Fisher Karma, Renault Kangoo, Coaster light duty bus, Orion bus, Opel Flexetreme, Swiss auto REX VW polo uses series configuration.

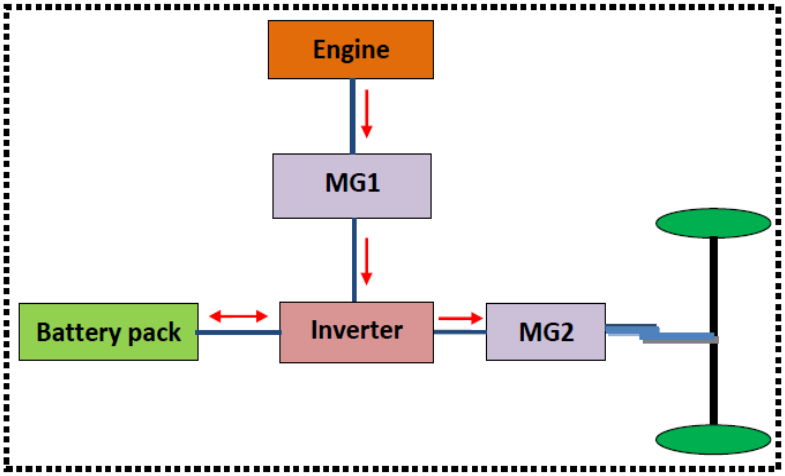

Figure 4.1: Series architecture

4.1.2 Parallel Architecture

In the parallel configuration two mechanical powers are added together in a mechanical coupler and power flow is controlled by both the power plants. Architecture shown in figure 4.2 consists of a single electric motor and ICE in such a way that both individually or together can drive the vehicle. Parallel hybrids allow both power sources to work simultaneously to attain optimum performance. While this strategy allows for greater efficiency and performance, the transmission and drive train are more complicated and expensive. Parallel configuration is more complex than the series, but it is comparatively

advantageous. Honda's Insight, Civic, Accord, General Motors Parallel Hybrid Trucks, BAS Hybrid such as Saturn VAU and Aura Greenline, Chevrolet Mali by hybrids utilize parallel configuration.

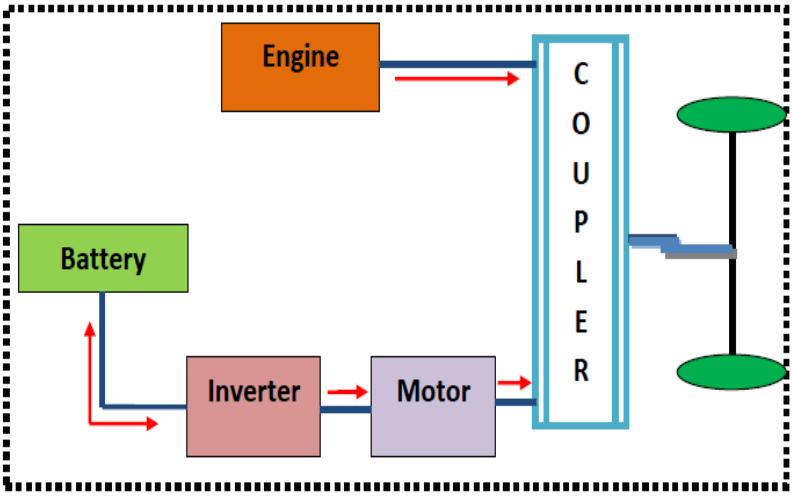

Figure 4.2: Hybrid vehicle configurations

4.1.3 Power-split Architecture

Power split hybrids have a combination of both series and parallel configuration in a single frame. The basic feature of this configuration is that it incorporates two power couplers: electrical and mechanical. In this configuration engine and battery can, either alone or together power the vehicle and battery can be charged simultaneously through the engine. Basically, it extends the All Electric Range (AER) of hybrid vehicle. The current dominant architecture is the power-split configuration which is categorized into two modes 1) one (single) and 2) two (dual) mode. Single mode contains one PGS and dual mode contains two PGS which are required for a compound power split. It is further classified into three types, 1) Input-split, 2) Output-split and 3) compound-split as determined by the method of power delivery.

4.1.3.1 Input-split configuration

In the input-split power configuration or single mode electro-mechanical electronically variable transmission (EVT), planetary gear is located at the input side as shown in figure 4.3. The input power from the ICE is split at the planetary gear. It gives low efficiency at high vehicle speed [93]. Toyota Prius employs an input split power configuration.

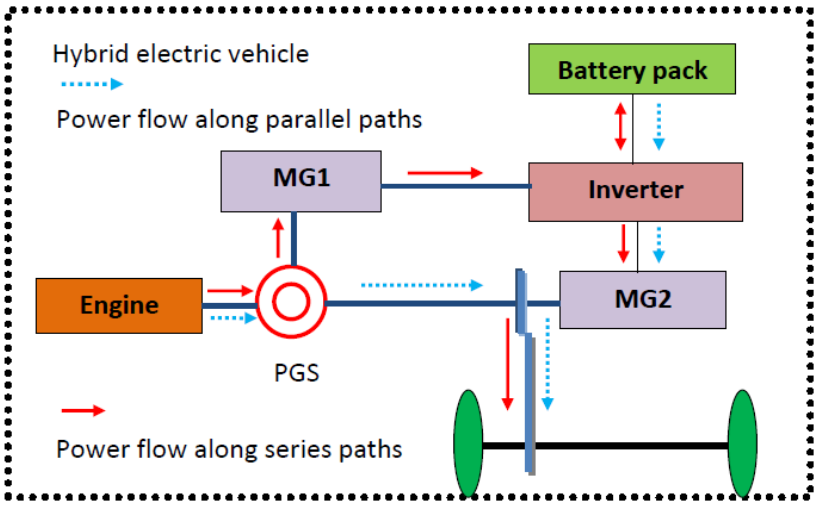

Figure 4.3: Input split configuration

4.1.3.2 Output-split configuration

The output-split power train consists of one planetary gear at the output side as shown in figure 4.4. The output-split system uses power recirculation at low vehicle speed and power splitting at high vehicle speed. Power recirculation means that a portion of the engine power is re-circulated by the charging of any one motor/generator and discharging of the other. Due to charging and discharging efficiency of the motors, re-circulated power negatively affects the system efficiency. Hence output-split power train displays poor performance at low vehicle speed compared to input split [94]. Chevrolet volt uses output split configuration.

4.1.3.3 Compound-split configuration

In compound-split configuration, the two clutches provide a torque advantage of the motor at low speed while fundamentally changing the power flow through the transmission as shown in figure 4.5. When the first clutch is applied and the second clutch is open, the system operates as an input-split. When the second clutch is applied and the first clutch is released, the system operates as a compound-split. This hybrid can shift between these two in a synchronous shift, involving only torque transfer between elements without sharp changes in the speeds of any element. Lexus HS250h, RX400h, Toyota Camry and Highlander, Lexus GS450h, LS600h use compound split configuration. The combination of a compound-split and an input-split enables a two mode hybrid system. The use of dual mode solves the problems of the single mode power train and provides better vehicle performance with respect to fuel economy, acceleration

and motor size. In dual mode, PGS are used for both the input split and compound split [95]. Two mode hybrids includes General Motors two-mode hybrid full-size trucks and SUVs, BMW X6 Active Hybrid and Mercedes ML 450 hybrid, Allison EV Drive, Chrysler Aspen, Chevrolet Tahoe, GMC Yukon hybrid.

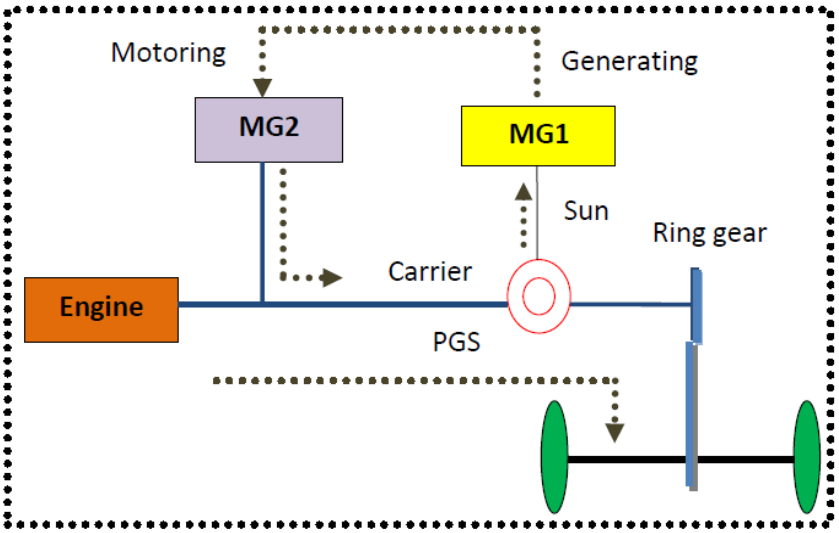

Figure 4.4: Output split configuration

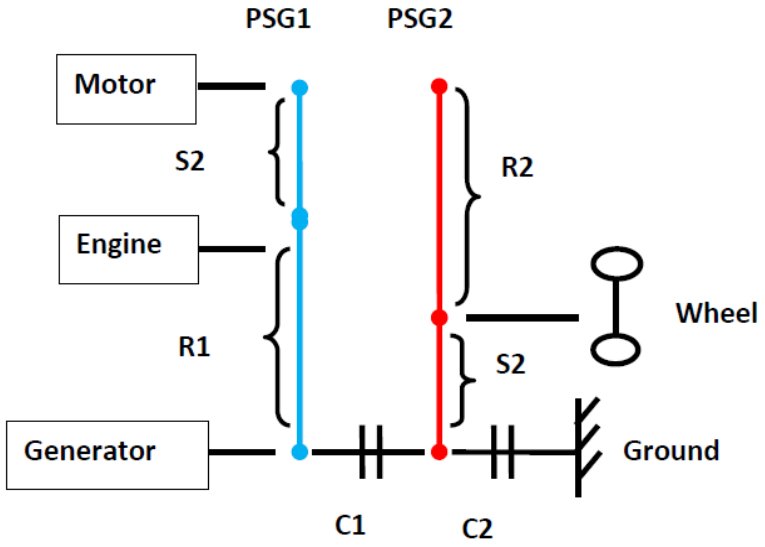

Figure 4.5: Ccompound-split configuration

Toyota Prius is an input split new generation hybrid automotive system introduced in 2003 by Toyota Motor Corporation. It uses an ICE and a battery powered motor for propelling the vehicle. It increases overall fuel economy using following energy saving techniques:

1) Automatically stops the engine during idling.

2) Applies regenerative braking to capture kinetic energy generated during deceleration or braking.

3) ICE and motor works together when cruising.

4) Motor is run during low power requirement but ICE is made on to operate in its most efficient regions for generating electricity [96].

4.1.4 Planetary Gear System

In Toyota hybrid system, PGS is used as a speed coupler. PGS contains carrier, sun, ring and several pinion gears as shown in figure 4.6 form three axis: sun axis, ring axis and carrier axis. Among three shafts any can be indulged as input or output. The ring gear is attached to the motor and final drive, engine to the carrier and generator to the sun. Gear speeds and radii are related as (4.1).

$$\omega_r * r_r = -\omega_s * r_s + \omega_c(r_s + r_r) \tag{4.1}$$

where ω_r, ω_s , ω_c are ring, sun and carrier angular speeds respectively and r_r, r_s are ring and sun radii respectively. Neglecting energy losses in steady state operation, torques acting on sun, ring and carrier have the relationship as (4.2).

$$T_c = -k_{ys}T_s = -k_{yr}T_r \tag{4.2}$$

T_c, T_s and T_r are the torques acting on carrier, sun and ring gear, $k_{yr} = (1 + i_g)/i_g$ and $k_{ys} = (1 + i_g)$ ang i_g is gear ratio. While moving, engine speed ω_e, motor speed ω_m and generator speed ω_g are related as (4.3).

$$\frac{N_r}{N_s + N_r} * \omega_m + \frac{N_s}{N_s + N_r} * \omega_g = \omega_e \tag{4.3}$$

For Prius, N_r =78 and N_s=30, so (4.3) becomes (4.4);

$$7.2222 * \omega_m + .2778 * \omega_g = \omega_e \tag{4.4}$$

This equation describes that ω_m is directly proportional to the linear speed of the vehicle with a quantitative change due to tire radius and final drive ratio [97].

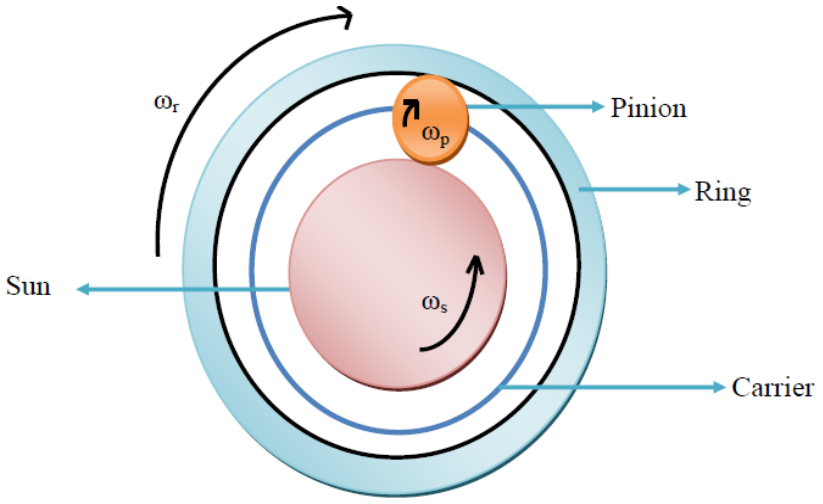

Figure 4.6: Planetary gear system

This chapter includes several powerful methods of energy optimization available in literature. These methods are not mutually exclusive and can be used alone or in combinations. The authors have compiled more than 100 papers cognate to optimal performance of HEVs published till 2013. Figure 4.7 shows the summary of papers published from various refereed journals, conferences and magazines. This data is based on the papers studied and cited in this paper.

4.2 Overview of Different Optimization Strategies

Due to the complex structure of HEVs, the design of control strategies is a challenging task. The preliminary objective of the control strategy is to satisfy the driver's power demand with minimum fuel consumption and toxic emissions. Moreover, fuel economy and emissions minimization are conflicting objectives, a smart control strategy should satisfy a trade-off between them.

Various control strategies are proposed for optimal performance of HEVs. A detailed overview of different existing control strategies along with their merits and demerits is presented. A broad classification of these strategies is given in figure 4.8. All these strategies are compared in terms of structural complexity, computation time, type of solution (real, global, local) and a priori knowledge of driving pattern.

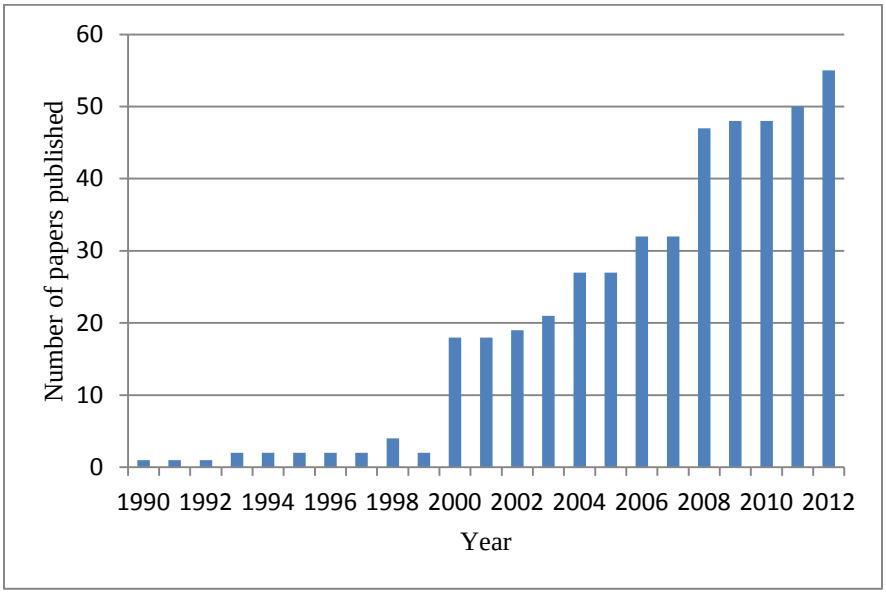

Figure 4.7: Graphical representation of papers published per year

There is no commonly accepted answer for "structural complexity" but the intersection of almost all answers is nonempty. Structural complexity deals with the complexity classes, internal structure of complexity classes and relations between different complexity classes. Complexity class is a set of problems of related source-based complexity and can be characterized in terms of mathematical logic needed to express them. Computation time is the length of time required to perform a computational process. A controller designed for a particular set of parameters is said to be robust if it performs fairly well under a different set of assumptions. To deal with uncertainty, robust controllers are designed to function properly with uncertain parameter set or disturbance set. Locally optimal of an optimization problem is optimal (either maximal or minimal) within a neighbouring set of solutions. A globally optimal, in contrast to local, is the optimal solution amongst all possible solutions of an optimization problem.

Control Strategies are broadly classified into rule-based and optimization-based control strategy and all other subcategories are classified based on these two main categories.

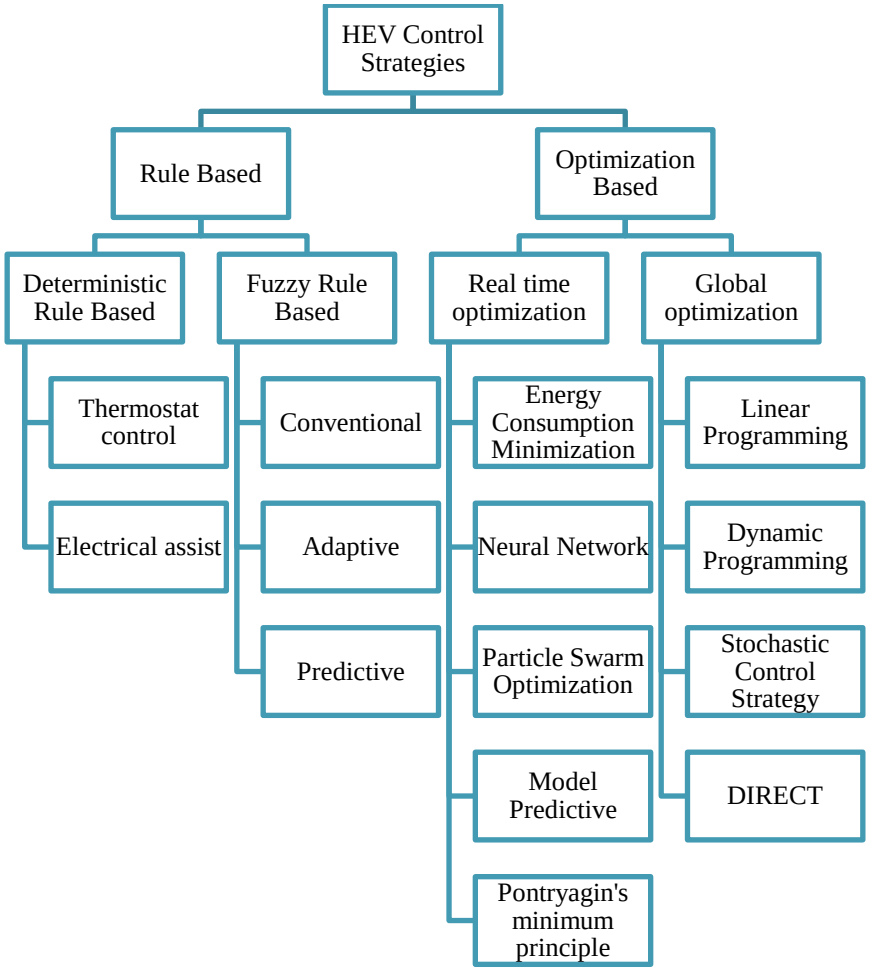

Figure 4.8: Classification of control strategies

4.2.1 Rule-based Control Strategies

Rule-based control strategies are fundamental control schemes that depend on mode of operation. They can be easily implemented with real-time supervisory control to manage the power flow in a hybrid drive train. The rules are determined based on human intelligence, heuristics, or mathematical models and generally, without prior knowledge of a drive cycle.

The rule-based controllers are static controllers. Basically, the operating point of the components (ICE, traction motor and generator etc.) is chosen using rule tables or flowcharts to meet the requirements of the driver and other components (electrical loads and battery) in the most efficient way. The decisions are related to instantaneous inputs only. This strategy is further subcategorized into deterministic rule-based and fuzzy rule-based.

By recognizing the road load, an energy management system for Belt Driven Starter Generator (BSG) type hybrid vehicle is developed by [98]. It gives a good fuel economy as well as launch performance. The dynamic performance and drivability is also improved at the same time. For energy and power management of a multi-source (battery and super-capacitor) hybrid vehicles, a two level of management scheme is formulated. First level uses a certain set of rules to restrict the search area and second level uses a meta-heuristic approach. Trovao et al. provides a quality solution for sharing energy online between the two energy sources with improved range and extended battery life [99].

4.2.1.1 Deterministic rule-based control strategy

The rules are designed with the aid of fuel economy or emission data, ICE operating maps, power flow within the drive train and driving experience. Implementation of rules is performed via lookup tables to share the power demand between the ICE and the electric traction motor. Kim et al. proposed a concept of hybrid optimal operation line for parallel HEV, which is derived based on effective specific fuel consumption with Continuously Varying Transmission (CVT). They determined the optimal values of parameters (such as a CVT gear ratio, motor torque and engine throttle) while maximizing overall system efficiency [100]. For the optimal robust control, [101] developed a rule-based control algorithm and tuned it for different work cycles.

Thermostat control strategy uses the generator and ICE to generate electrical energy used by the vehicle. In this strategy the battery SOC is always maintained between predefined high and low levels, by simply turning on/off the ICE. The strategy is simple, but it is unable to supply necessary power demand in all operating modes.

4.2.1.2 Fuzzy-rule based control strategy

L.A. Zadeh introduced the term fuzzy logic and described the mathematics of fuzzy set theory. Fuzzy logic system is unique to handle numerical data and linguistic knowledge simultaneously. Fuzzy sets represent linguistic labels or term sets such as slow, fast, low, medium, high etc. In fuzzy logic, the truth of any statement is a matter of degree. Fuzzy control is simple, easy to realize and has strong robustness. It can converse experience of designer to control rules directly. Fuzzy logic is a form of multi-valued logic derived from fuzzy set theory to deal with reasoning that is approximate rather than precise.

The knowledge of an expert can be coded in the form of a rule-base and used in decision making. It is a non-linear structure and is especially useful in a complex system such as an advanced power train. In essence, a fuzzy logic controller (FLC) is a natural extension of many rules based controllers implemented (via look-up tables) in many vehicles today. Fuzzy logic based methods are insensitive to model uncertainties and are robust against the measurement of noises and disturbances, but requires a faster microcontroller with larger memory.

a) Traditional fuzzy control strategy

Efficiency is decided based on the selection of input, output and rule-based control strategy. Two operating modes; namely, optimize fuel use and fuzzy efficiency modes, are used to control drive train operation. The FLC accepts battery SOC and the desired ICE torque as inputs. Based on these inputs as well as the selected mode, the ICE operating point is set. The power required by the electric traction motor is the difference of total load power required and power required from ICE.

In the optimum fuel use strategy, the FLC limits instantaneous fuel consumption, calculated from the fuel use map and maintains sufficient battery SOC, while delivering demanded torque. In the fuzzy efficiency strategy, the ICE has operated in its most efficient operating region. The operating points of the ICE are set near the torque region, where efficiency is highest at a particular engine speed. Load balancing is achieved using electric motors. This control strategy uses a motor to force ICE to operate in the region of minimal fuel consumption while maintaining SOC. Load balancing is necessary to meet power demand and avoid unnecessary charging and discharging of the battery. A major drawback of this control strategy is that the peak efficiency points are near high torque region, thereby ICE generates more torque than required, which in turn increases fuel consumption. Also, during load balancing, heavy regeneration overcharges the battery. To avoid this, the control strategy should be used with a downsized ICE.

b) Adaptive fuzzy control strategy

This strategy can optimize both fuel efficiency and emissions simultaneously. However, fuel economy and emissions are conflicting objectives, which means an optimal solution cannot be achieved by satisfying all the objectives. The optimal operating point can be obtained using weighted-sum approach optimization of conflicting objectives. Due to

various driving conditions, appropriate weights have to be tuned for fuel economy and emissions. Considering stringent air pollution laws, operating points with high emissions are heavily penalized. The conflicting objectives within the adaptive fuzzy logic controller include fuel economy, NO_X, CO and HC emissions. In order to measure the interrelationship of the four contending optimizing objectives with a uniform standard, it is essential to normalize the values of fuel economy and emissions by utilizing the optimal values of fuel consumption and emissions at current speed. The optimal values of fuel economy and emissions at particular ICE speed can be obtained from the ICE data map.

The relative weights are adaptively assigned to each parameter based on their importance in different driving environments. Moreover, weights must be selected for each ICE based on their individual data maps. This control strategy is able to control any one of the objectives, by changing the values of relative weights. Further, tremendous reduction in vehicle emission is achieved, with negligible compromise in fuel economy.

c) Predictive fuzzy control strategy

If the information on the driving trip is a priori known, it is extremely trivial to obtain a global optimum solution, to minimize fuel consumption and emissions. However, the primary obstacles entail acquiring further information on planned driving routes and performing real-time control. This problem can be resolved using global positioning system (GPS) which can easily identify the probable obstacles like, heavy traffic or a steep grade. The control strategies can be developed for specific situations, e.g. if a vehicle is running on a highway and will enter into a city (where heavy traffic may be encountered), it is advised to restore more energy by charging the batteries, for later use. General inputs to the predictive FLC are vehicle speed variations, the speed state of the vehicle in a look-ahead window and elevation of sampled points along a predetermined route. Based on the available history of vehicle motion and its variability in the near future, FLC determines the optimal torque that ICE contributes to the current vehicle speed. The predictive FLC outputs a normalized GPS signal in (−1, +1) which informs the master controller to charge or discharge the batteries and to restore enough energy for future vehicle operating modes.

Being robust and fast, it is advised to design FLCs for non-linear and uncertain systems. FLCs result in small overshoot, short adjustment time and good dynamic/static quality. Using mix-modeling approach, Arsie et al. implement an FLC to control the parameters related to the driver-vehicle interaction, torque management and battery recharging strategy [102]. To improve energy conversion efficiency, several fuzzy logic based energy management strategies are implemented [103, 104, 105]. [106] implement a fuzzy logic based proportional integral (PI) controller for nonlinear control of the plants. Lee et al. introduce an FLC for driving strategy implementation. This is useful for nonlinear and uncertain systems and is not affected by vehicle load variation and road pattern [107]. Bauman et al. demonstrate the effectiveness of FLC to increase the fuel economy and show that it works well for a non-linear, multi domain and time-varying plant [108]. Tao and Taur design a less complex PID-like FLC with a heuristic functional scaling which is easy to adjust even in the absence of the plant's complete mathematical model [109]. [110] apply driver command, battery SOC and motor/generator speed as fuzzy sets to design an FLC for parallel HEVs. Patel and Mohan design a very simple PI controller using fuzzy logic with less number of universes of discourse [111]. Bathaee et al. [112], Khoucha et al. [113], Zhang et al. [114] implement an FL based controller for optimal energy management strategy. Poursamad and Montazeri [115] introduce a GA tuned FLC to minimize the fuel consumption and emissions and to improve the driving performance of a parallel HEV. To improve its accuracy, adaptability and robustness, a compressibility factor was used with PSO. Won and Langari propose an IEMA based on the concept of driving situation awareness for parallel HEV. The authors basically implemented an IEMA which gives knowledge about driving situation awareness. They simulated the controller using ADVISOR for the different driving/road conditions and showed a significant reduction in exhaust gases and improvement in fuel economy [116]. Kachroudi et al. design a predictive decision support system for optimal energy flow distribution among engine and other auxiliaries. They determined the global optimum using PSO, which was further, validated using hardware-in-loop (HIL) technique [117].

4.2.2 Optimization-based Control Strategy

In optimization based control strategies, the goal of a controller is to minimize the cost function. The cost function for an HEV may include the emission, fuel consumption and torque depending on the application. Global optimum solutions can be obtained by

performing optimization over a fixed driving cycle (DC). These control techniques do not result in real-time energy management directly, but based on an instantaneous cost function, a real time control strategy can be obtained. This instantaneous cost function relies on the system variables at the current time only. It should include equivalent fuel consumption to guarantee self-sustainability of electrical path. Optimization based control strategies can be divided into two main groups, namely global optimization and real time optimization. These are discussed in the following sections in detail.

4.2.2.1 Global optimization

A global optimization technique for energy management strategy in an HEV requires the knowledge of entire driving pattern which includes battery SOC, driving conditions, driver response and the route. Due to computational complexity, they are not easily implementable for real time applications. Linear programming, dynamic programming and GA, etc. are used here to resolve vehicle energy management issues. Based on optimal control theory and assuming that minimizing the fuel consumption reduces the pollutant emissions, a global optimization algorithm is developed [118]. Delprat et al. proposes a global optimization strategy for HEVs performance analysis, but do not provide optimal results [119]. Delprat et al. suggest a global optimization strategy for known DC and for all SOC ranges. This offers the quick global optimal solution and minimizes the fuel consumption [120]. To get a better optimal solution for HEV design and control, another global optimization technique has been suggested by [121].

a) Linear programming

The fuel economy optimization is considered as a convex nonlinear optimization problem, which is finally approximated by Linear Programming (LP) method. LP is mostly used for fuel efficiency optimization in series HEVs. Formulation of fuel efficiency optimization problem using LP may result in a global optimal solution.

In hybrid power trains, better degree of freedom to control exists. By controlling the gear ratio and torque, an optimized design and control of a series hybrid vehicle is proposed in [122]. The problem is formulated as a non-linear convex optimization problem and approximated as a linear programming problem to find the fuel efficiency. Kleimaier and Schroder propose a convex optimization technique for analysis of

propulsion capabilities using LP, which provides independence from any specific control law [123]. Pisu et al. designed, supervisory control strategies for hybrid electric drive trains to minimize fuel consumption. They designed a stable and robust controller using linear matrix inequalities [124]. Miaohua and Houyu design a sequential quadratic programming based energy management strategy to minimize fuel consumption. They consider balanced SOC as a constraint and showed improved results [125].

b) Dynamic programming

Dynamic Programming (DP) was originally used in 1940 by Richard Bellman to describe the process of solving problems where one needs to find the best decisions successively. DP is both a mathematical optimization method and a computer programming method. In both the contexts, it refers to simplifying a complicated problem by breaking it into simpler sub-problems in a recursive manner.

The very essence of this technique is based on the principle of optimality. Having a dynamical process and the corresponding performance function, there are two ways to approach the optimal solution to the problem. One is the Pontryagin's maximum principle and the other is 'Bellman's dynamic programming'. It has the advantage of being applicable to both linear and nonlinear systems as well as constrained and unconstrained problems. But it also suffers from a severe disadvantage called curse of dimensionality which amplifies the computational burden and limits its application to complicated systems.

Since the knowledge of the duty cycle is required beforehand, the DP algorithm cannot be implemented in real time. However, its outputs can be used to formulate and tune actual controllers. The power management strategy in an HEV is computed through dynamic optimization approach by various researchers as mentioned below.

An adaptive neural-fuzzy inference system (ANFIS) along with DP is used to get the optimal solution to the problem [126]. Using DP and a rule based approach; optimal power split between both of energy sources is obtained for a series HEV [127]. They suggest that to increase computational efficiency, the discrete state formulation approach of DP should be used. To reduce the fuel consumption, a DP based optimal control strategy for a parallel hybrid electric truck is reported in [128]. They developed a feed-forward, parallel HEV simulator in order to maximize fuel efficiency and proposed DP

and rule based power optimization algorithm for sustaining mode of battery operation. Sundstrom et al. study the hybridization ratio of two types of parallel HEVs namely, 1) Torque assist and 2) full hybrid. Further, using DP optimal fuel consumption is achieved for different hybridization ratios. The results show that both fuel consumption and need of hybridization are less in case of the full hybrid model [129]. A medium-duty hybrid electric truck is implemented using DP to optimize the power and fuel economy. It results in 45 percent higher fuel economy than ICE truck. A near optimal power management strategy is obtained using DP, considering sustained SOC as a constraint [130]. Koot et al. proposed an energy management strategy for HEVs and verified it through DP, quadratic programming and modified DP (DP1) strategies [131]. To keep energy levels in a prescribed range without affecting the battery health in HEVs, [132] formulated a finite horizon dynamical optimization problem and solved it using DP. Keulen et al. solve an energy management problem for HEVs and optimize it using DP in charge sustaining mode [133]. Sundstrom et al. propose a generic DP function, to solve discrete time-optimal control problem using Bellman's DP algorithm [134]. [135, 136] use DP and on-board implementable energy consumption minimization strategy (ECMS) for charge depletion mode operation. They conclude that for long distances and large size batteries, ECMS and DP provide a similar fuel economy and SOC profile. Again DP and classical control theory is used by Ngo et al. and they report improvement of 11 percent in fuel economy [137]. Kum et al. firstly found an optimal solution using DP and estimate battery SOC with respect to remaining trip distance using energy-to-distance ratio. Then they implement an adaptive supervisory power train controller to reduce fuel consumption and emissions based on extracted results from EDR and catalyst temperature system [138]. For a multi source HEV containing gen set, [139] proposed a DP for optimizing power management system. In case of known trip distance it can give global optimal solution and save 12.6 percent gasoline. Ravey et al. initially proposes a method to minimize the size of the components (energy source) using GA. Later they use DP to optimize the power management strategy and claim a higher fuel economy [140]. Shams-Zahraei et al. implement an optimal energy management strategy using DP considering the significance of temperature noise factors. With the variation in temperature, fuel efficiency and emissions changes even for the same driving patterns and conditions [141].

c) Stochastic control strategy

Stochastic strategy is a framework for modeling optimization problems that involve uncertainty. In this strategy, an infinite-horizon stochastic dynamic optimization problem is formulated. The power demand from the driver is modeled as a random Markov process. The Markov driver model predicts the future power demands by generating the probability distribution for them. The past decisions are not required for this prediction. The optimal control strategy is then obtained using Stochastic Dynamic Programming (SDP). The obtained control law is in the form of a stationary full-state feedback and can be directly implemented. It is found that the obtained SDP control algorithm outperforms a sub-optimal rule-based control strategy trained from deterministic DP results. As opposed to deterministic optimization over a given DC, the stochastic approach optimizes the control policy over a family of diverse driving patterns.

i. Stochastic Dynamic Programming

Optimization method which uses random variables to formulate an optimization problem is called stochastic optimization. In DP if, either state or decision is known in terms of probability function, it is called SDP. A high performance computing technique is required to solve the stochastic optimal control problem.

For better optimality in comparison to supervisory control strategy, [142] propose an infinite-horizon SDP in which power demand by the driver is modeled as a random Markov process. The control law obtained, is real-time implementable in HEVs. In a parallel hybrid electric truck, both infinite-horizon SDP and Shortest Path SDP (SP-SDP) optimization problems are formulated which yield a time-invariant causal state-feedback controller. In SP-SDP power management strategy variation of battery SOC from a desired set-point is allowed to get a trade-off between fuel consumption and emissions. The SP-SDP based controller is advantageous over SDP as it offers better SOC control and lesser number of parameters to be tuned [143]. Using SDP, [144] formulated a hybrid power optimal control strategy using Engine-in-Loop (EIL) setup, which instantly analyzes the effect of transients on engine emissions. Tate et al. [145] used the SP-SDP to find a trade off between fuel consumption and tailpipe emissions for an HEV, facilitated with a dual mode EVT. With simple methods SP-SDP solution takes eight thousand hours while using linear programming and duality it takes only three hours. Using SP-

SDP, [146] proposed a real-time energy management controller. This considers drive cycle as a stationary-finite scale Markov process. This controller is found to be 11 percent more efficient than an industrial baseline controller. Wang and Sun [147] proposed an SDP-Extremum Seeking algorithm with state-feedback control. It contains the nature of global optimality of SDP and SOC sustainability. Further extremum seeking output feedback compensates for its optimal control error. Opila et al. develop an energy management strategy based on SDP and implemented successfully in a prototype HEV. The feature of this controller is that they run in real-time embedded hardware with classic automotive computing ability and the energy management strategy gets updated very frequently to yield a strong driving characteristic [148].

ii. Genetic Algorithm

GA is a heuristic search algorithm to generate the solution to optimization and search problems. This is a branch of artificial intelligence inspired by Darvin's theory of evolution. GA begins with a set of solutions (chromosomes) called a population. The solutions from one population are taken according to their fitness to form new ones. Most suitable solutions will get a better chance than the poorer solutions to grow and the process is repeated until the desired condition is satisfied. GA is a robust and feasible approach with a wide range of search space and rapidly optimizes the parameters using simple operations. They are proven to be effective to solve complex engineering optimization problems, characterized by nonlinear, multi-modal, non-convex objective functions. GA is efficient at searching the global optima, without getting stuck in local optima.

Unlike the conventional gradient based method, GA technique does not require any strong assumption or additional information about objective parameters. It can also explore the solution space very efficiently. However, this method is very time consuming and does not provide a broader view to the designer.

Piccollo et al. utilize GA for energy management of an on road vehicle and minimize the cost function containing fuel consumption and emission terms [149]. For dynamic and unpredictable driving situations, a fuzzy clustering criterion is used with GA which reduces the computational effort and improves the fuel economy [150]. GA in HEVs is used simultaneously to optimize the component sizes and to minimize the fuel consumption and emissions [151, 152, 153, 154]. A MOGA is further used by [155] to

solve the optimization problem of HEVs which optimizes control system and power train parameters simultaneously and yields a Pareto-optimal solution. MOGA is developed to reduce fuel consumption and emissions as well as to optimize power train component sizing [156]. Using non-dominated sorting GA (NSGA), a pareto-optimal solution is obtained for reduced component sizing, fuel consumption and emissions [157].

GA is a powerful optimization tool which is particularly appropriate to multi objective optimization. The ability to sample trade-off surfaces in a global, efficient and directed way is very important for the extra knowledge it provides. In the case where there are two or more equivalent optima, the GA is known to drift towards one of them in a long term perspective. This phenomenon of genetic drift has been well observed in nature and is due to the populations being finite. It becomes more and more important as the populations get smaller. NSGA varies from GA only in the way the selection operator works. Crossover and mutation operations remain the same. This is similar to the simple GA except the classification of non-dominated fronts and sharing operations. MOGA is a modification of GA at selection level. MOGA may not be able to find the multiple solutions in case where different Pareto-optimal points correspond to the same objective.

d) Dividing Rectangle (DIRECT)

DIRECT is sampling based algorithm and was developed by Donald to find a global minimum and is derivative free. The algorithm starts with the hypercube search space. The function is then sampled at the center point. The hypercube is then divided into smaller hyper rectangles and center points of these rectangles are again sampled. DIRECT identifies sets of optimal rectangle for every iteration. DIRECT is the modification of Lipschitz approach which does not specify the Lipschitz constant. When Lipchitz constant is not used, all the possible searches are performed for a predefined number of iteration [158, 159, 160].

The research target is to improve fuel economy of an input split series-parallel HEV using DIviding RECTangle (DIRECT) algorithm. DIRECT is applied to find the optimal values of parameters to make engine on. No liquid fuel consumption will happen for engine off condition. Among all the non-gradient based techniques DIRECT is good for HEV application [161]. Fellini et al. used DIRECT and complex (derivative free algorithms) to optimize the components sizes used in HEVs and DIRECT was observed better than complex [162]. Dosthosseini et al. used DIRECT method to find the solution

to for power management optimization in HEVs [163]. Zhang et al. proposed DIRECT algorithm for optimizing set of parameters of logic threshold control stratgey realized in HEV. Author claim that DIRECT is useful for off-line parameter optimization and can consume lesser time if used in real vehicle [158]. Wang et al. proposed a power control strategy to optimize fuel consumption and emissions in HEVs using PSO and compared with DIRECT algorithm. By simulating these strategies for several DCs, PSO is found to be better than DIRECT [164]. Gao and Mi investigated studied various optimization methods for the optimization of HEVs. They predict that DIRECT is efficient for HEV related optimization issues [165].

4.2.2.2 Real-time optimization

Due to the causal nature of global optimization techniques, they are not suitable for real-time analysis. Therefore, global criterion is reduced to an instantaneous optimization by introducing a cost function that depends only on the present state of the system parameters. Global optimization techniques do not consider variations of battery SOC in the problem. Hence, a real-time optimization is performed for power split while maintaining the battery charge.

Instantaneous optimization techniques based on simplified model and/or efficiency maps are proposed in [166, 167]. Reference [166] presents the concept of real time control strategy for efficiency and emission optimization of a parallel HEV. It considers all engine-motor torque pairs which forecast the energy consumption and emissions for every given point. [167] developed a control strategy for parallel hybrid vehicle in a charge sustaining mode of operation for instantaneous fuel efficiency optimization. And to implement the global constraint, the authors developed a nonlinear penalty function in terms of battery SOC deviation from its desired value.

a) Equivalent consumption minimization strategy

Paganelli et al. propose the concept of equivalent fuel consumption for energy management strategy. It reduces a global optimization problem into an instantaneous minimization problem and provides solution at each instant. Energy consumption minimization strategy (ECMS) calculates the fuel equivalent as a function of current system status and quantities measurable on board, online. It does not require prior knowledge of driving pattern to get an optimal solution and it is real-time implementable.

ECMS is developed by calculating the total fuel consumption as sum of real fuel consumption by ICE and equivalent fuel consumption of electric motor. This allows a unified representation of both, the energy used in the battery and the ICE fuel consumption. Using this approach, equivalent fuel consumption is calculated on a real-time basis, as a function of the current system measured parameters. No future predictions are necessary and only a few control parameters are required. These parameters may vary from one HEV topology to another as a function of the driving conditions. ECMS can compensate the effect of uncertainties of DP. The only disadvantage of this strategy is that it does not guarantee charge-sustainability of the plant.

Equivalent fuel consumption is calculated based on the assumption that SOC variation in the future is compensated by the engine running at current operating point. Jalil et al. use thermostatic control strategy to turn the engine on/off based on SOC profile but did not yield optimal results [168]. Paganelli et al. implement an ECMS to minimize fuel consumption of HEV by splitting the power between ICE and electric motor. They achieve a reduction in the fuel consumption by 17.5 percent as compared to ICE based vehicle alone [169]. Supina and Awad suggest to on/off the engine according to the battery energy level and thus results in improved fuel efficiency of 1.6 to 5 percent over the thermostat control [170]. Without the knowledge of future driving conditions to find the real-time control of fuel consumption of parallel HV is presented in [171]. It uses ECMS for the instantaneous optimization of the cost function and it depends only upon the current system operation. Won et al. propose an energy management strategy for torque distribution and charge sustenance of HEV using ECMS [172]. In this, a multi-objective torque distribution strategy is formulated first and then it is converted into single objective linear optimization problem. [173, 174] implement a modified ECMS for a series HV configuration with two different energy sources which is a generalization of instantaneous ECMS proposed in [170]. For real-time energy management, [175, 176] propose an adaptive ECMS (A-ECMS). It continuously updates the control parameter according to road load condition and provides a quasi-static solution for supervisory control in comparison to ECMS and rule based strategy. Using ECMS, [177, 178] present real time implementable control strategy which even in the absence of future driving information supply optimal results for fuel consumption minimization and toxic emission

reduction. Tulpule et al. propose an ECMS, which requires knowledge of total trip distance instead of driving pattern information to improve fuel economy [179].

a) Model predictive control

Model Predictive Control (MPC) is a good method for dynamic model of the process which is obtained by system identification. The main feature of the MPC is to allow current time slot to be optimized keeping future time slots into account. This is achieved by optimizing a finite time-horizon and implementing the current time slot only. MPC can anticipate future events and can take control actions accordingly.

Real-time implementable energy management strategy of an HEV using MPC is presented in [180]. In classical MPC, at each step an online optimization problem is required to solve. To address this, an MPC with improved speed is implemented by [181]. Kermani et al. implement a Lagrange formula based global optimization algorithm using MPC [182]. An energy management strategy for a series HEV is proposed by [183] using MPC and quadratic programming. Using a quasi-static simulator developed in the MATLAB environment, MPC algorithm is applied. They also investigate the length and type of predictions. Ripaccioli et al. describes a hybrid MPC strategy to co-ordinate power train subsystem and to enforce state and control constraints. Firstly, authors develop a hybrid dynamical model using linear and piecewise affine identification method; and then design an MPC to reduce emissions [184]. Borhan et al. develop a nonlinear-MPC for HEVs to solve the power split optimization problem online [185]. In the absence of a priori knowledge of driving pattern, [186] presented a stochastic-model predictive control for power management of series HEV. Power demand from the driver is modeled as a Markov chain. This algorithm optimizes over a distribution of future requested power demand from the current demand at each sample time. Borhan et al. proposes an MPC based minimum fuel consumption strategy for power-split hybrid vehicles. The complex energy management problem is divided into two levels. For the first level (supervisory level) MPC is used to calculate future control sequences that minimize a performance index and then is applied to the first element of the computed control sequence of the hybrid vehicle model [187]. For a parallel HEV, an MPC torque-split strategy is developed by [188] considering the effect of the diesel engine transient characteristic. The authors conclude that the MPC based method can improve the fuel economy. For minimization of fuel consumption and to keep the SOC within a specified

range, [189] presented an MPC-based controller which works on torque demand predictions estimated from the desired SOC and desired vehicle speed.

b) Neural Networks

McCulloch and Pitts in 1943 firstly designed the neural network and Hebb in 1949 developed the first learning rule. Artificial Neural Network (ANN) is a network of artificial neurons and is a parallel computation technique consisting of many processing blocks connected together in a specific way to perform a specific task. ANN is a powerful computational method which learns and generalizes from training data. This uses the principle of function approximation. The output of a neuron is a function of the weighted sum of the inputs and a bias. The function of the entire neural network is simply the computation of the outputs of all the neurons.

NN's adaptive structure makes it suitable for any control applications. A well designed network can get fit to any lookup table and can adapt itself by training to update the table data. This feature makes it better than rule based controllers. Recurrent NNs are networked with dynamic feedback which means they can also be modeled as dynamic controller. NN is an effective approach for pattern recognition and function fitting.

Bauman et al. used ANN and fuzzy logic for implementing a load levelling strategy and implemented a supervisory controller, which takes care of fuel economy and reduced emissions in case of different drivers and driving pattern [190]. For analysis and control of power split in a parallel HEV, Arsie et al. modelled a dynamic system with vehicle-driver interaction, ICE and electric motor/generator. Using this, vehicle load estimation is performed using NN to optimize the supervisory control strategy for the optimized performance of the vehicle [191]. Mohebbi et al. presented a neuro-fuzzy controller, which is implemented using ANFIS method. This controller is designed based on 1) torque required for driving and 2) battery SOC; and it maximizes the driving torque and minimizes the fuel consumption [192]. For the nonlinear control system, Jun implemented a high accuracy fuzzy neural network (FNN) controller. The membership function of FNN is optimized using modified GA and error-compensation method and results are found better than the normal FLC [193]. Murphey et al. used NN to predict road and traffic conditions optimal power-split in HEVs. The authors first developed a machine-learning framework for energy optimization in an HEV then they present three

online intelligent energy controllers: 1) IEC_HEV_SISE; 2) IEC_HEV_MISE; and 3) IEC_HEV_MIME. The three online controllers were integrated into the Ford Escape hybrid vehicle model for online performance evaluation. All three online intelligent energy controllers were trained within the machine-learning framework to generate the best combination of engine power and battery power to minimise the total fuel consumption. The performance of IEC_HEV_MISE controller was found best and led to fuel savings ranging from 5 to 19 percent as compared to default Ford Escape controller [194].

c) Particle swarm optimization

Particle swarm optimization (PSO) is a faster, inexpensive, robust stochastic global optimization technique developed by R. Eberhart and J. Kennedy in 1995. This technique is used for continuous non-linear function and was developed based on the swarm in nature as bird [195, 196]. PSO is a heuristic evolutionary search algorithm which is an iterative optimization method using particles (population of candidate solutions), and moving these particles around in the search space according to a mathematical formula over the particle's position and velocity. In PSO, particles move around a search space and are guided by best known positions in the search space as well as entire swarm's best known position. When improved positions are discovered, these will guide the movements of the swarm particles. The process is repeated, but does not guarantee the satisfactory solution.

PSO is a meta-heuristic approach as it makes few or no assumptions about the problem being optimized and can search very large spaces of candidate solutions. However, meta-heuristics such as PSO do not guarantee an optimal solution. More specifically, PSO does not use the gradient of the problem being optimized, which means PSO does not require the optimization problem to be differentiable as is required by classical optimization methods, such as gradient descent and quasi-Newton methods. PSO can therefore also be used on optimization problems that are partially irregular, noisy, change over time, etc.

The multilevel hierarchical control strategy optimized by the improved PSO algorithm can properly determine the direction and quantity of the energy flow in the HEVs and make the main power train components operate at high efficiency so that the fuel consumption can be reduced.

For parallel HEV, a multilevel hierarchical control strategy is proposed by [197, 198] using Matlab/Simulink/Stateflow and optimized it using PSO to get an optimal energy flow between engine and electric motor. Jian et al. implemented an FLC for energy management system. Membership function and the rules of FLC are optimized by using PSO to find improved fuel economy and decreased emissions in HEVs. For a charge sustaining operation this strategy gives better fuel efficiency [199]. Aawar et al. combined PSO and electro-magnetic-team fuzzy logic (EM-TFL) together for the design optimization of the HEV power train system to find best electromechanical component sizes for higher efficiency and reduced fuel consumption [200]. Desai and Williamson optimized both power train and control strategy (objective function and constrained function) parameters using PSO for improved fuel economy and efficiency and reduced emissions [201]. Hegazy and Mierlo conclude that PSO consumes lesser time than GA to obtain a solution and is easier to implement [202]. Varesi and Radan used PSO to find the optimal degree of hybridization in series-parallel HEV using ADVISOR to optimize the vehicle performance with reduced fuel consumption and emissions [203]. To optimize the various components of HEV, EM-TFL with PSO has been used by [204] in the form of a case study which concludes that a smaller size engine, electric motor performance is optimized and fuel economy is improved by 22 percent and reduction in toxic emissions is noticed. Wu et al. optimized the component size and control strategy simultaneously in parallel HEVs. This proposed a self adaptive PSO algorithm and uses applied fuzzy set theory to extract the best suitable solutions [205].

d) Pontryagin's minimum principle

Pontryagin's minimum principle (PMP), formulated in 1956 by the Russian mathematician Lev Semenovich PMP gives the best possible control to take a dynamical system from one state to another state in the presence of constraints for some state or input control. PMP is a special case of Euler-Lagrange equation of 'calculus of variations'. For an optimum solution, PMP provides only necessary conditions and the sufficient conditions are satisfied by Hamilton-Jacobi-Bellman equation. In PMP, the number of nonlinear second-order differential equations linearly increases with the dimension so the control based on PMP takes less computational time for getting an optimal trajectory but it could be a local optimal, not a global solution. Under certain

assumptions optimal trajectory obtained by PMP should be considered as a global optimal trajectory. These are 1) Trajectory obtained from PMP is unique and satisfies the necessary and boundary conditions, 2) Some geometrical properties of the optimal field provide the possibility of optimality clarification and 3) As a general statement of the second approach, the absolute optimality is, mathematically, proven by clear proposition [206].

Geering explains PMP to reduce a global energy optimization problem into a local optimization problem [207]. Serrao and Rizzoni implement an optimal control strategy using PMP to get an optimal solution. They have converted global optimization problem into an instantaneous optimization problem [208]. Stockar et al. used PMP to build an optimal supervisory controller by reducing a global optimization problem into local. The advantage of this is that it reduces computational requirement and gives the freedom to solve the problem in the continuous time domain [209]. For real-time implementation of an energy management strategy, the tools used by [210] consist of PMP based off-line optimizer which results in ECMS and is implementable in real-time environment. A real time optimal control can be obtained using PMP as it uses instantaneous minimization of the Hamiltonian function. Kim et al. state that solution based on PMP can be a global optimal under some certain assumptions [211]. Kim et al. finds that PMP provides a near-optimal solution for optimal power management of HEVs if future driving conditions are known. It is suggested to find proper co-state to keep SOC at a desired and predefined level [212].

As the trajectory derived from PMP might not be a global optimal solution, therefore, the control based on PMP can be considered as inferior to the DP. DP requires more computing time than PMP because DP solves all possible optimal controls to find the optimal field. Since DP is a numerical representation of the HJB equation, it needs a similar computation load as the Hamilton-Jacobi-Bellman equation, which solves a partial differential equation. PMP solves just nonlinear second-order differential equations. The drawback of DP with regards to the computational load becomes compounded due to the “curse of dimensionality”.

4.3 Summary

As HEVs are gaining more popularity, the role of the energy management system in the hybrid drive train is escalating. A thorough description and comparison of all the control strategies to optimize the power split between the primary and secondary sources of HEVs used, is given here. Evolution of control strategies from thermostat to advanced intelligent methods is included in the study.

Rule-based controllers are easily implementable, but the resultant operation may be quite far from optimal, i.e., the power consumption is not optimized for the whole trip. In order to achieve the global optimality priori information of trip is required. Although, real-time energy management is not directly possible using optimization based methods, but an instantaneous cost function based strategy may result in real time optimization. The strategies are real-time implementable and are robust in nature.

The concluding table 4.1 serves as a guide to choose the correct method of optimization. It is suggested that strategies should take less computational time, provide global optimal results and get fit to the dynamic simulation environment.

Table 4.1: Comparison chart for various control strategies

Methods	Structural complexity	Computation time	Type of solution	Requirement of priori knowledge
Fuzzy Logic	N	S	G	Y
Genetic Algorithm	Y	M	G	N
Particle Swarm Optimization	N	M	G	N
Energy Consumption Minimization Strategy	Y	S	L	N
Pontryagin's Minimum Principle	N	S	L	Y
Dynamic Programming	Y	M	G	Y
Model Predictive	N	S	G	N
Stochastic Dynamic Programming	Y	M	G	N
Neural Network	Y	S	G	Y
DIRECT	N	M	G	N

G=Global, L=Local, N=No, Y=Yes, M=More, S=Small

Chapter 5
Development of Power Optimization Strategies

Energy management strategies significantly influence the fuel efficiency of HEVs. They play a crucial role in splitting the power between two sources, ICE and the battery. Intelligent power split between these two will enhance the fuel economy and regulate the power flow. This power split depends on SOC of battery, power required at the wheels and engine's operating range. Various parameters of power train are considered to control the toggling between engine and battery. To achieve parameter optimization, various optimization algorithms are practiced to realize the optimal performance. Vehicle parameter optimization over different battery models with modified SOC estimation algorithm is performed in different situations and a comparative study is presented.

Toyota Prius is an input split new generation hybrid automotive system introduced in 2003 by Toyota Motor Corporation is used here for simulation purposes.

5.1 Modes of Operation

Motor/generator (M/G) sets take or provide power from the PGS according to their mode of operation. Power split HEVs work in four different modes to fulfil driver's power demand and is explained as follows with pictorial diagrams:

5.1.1 Mode 0: Launch and backup

For the duration of key on and moving at low speed, M/G2 supplies the primary tractive energy as (5.1). Motor is powered from the battery. Power flow is shown in figure 5.1 (a).

$$T_{out} = \frac{N_2}{N_1} * \omega_m \tag{5.1}$$

Where N_1, N_2 are number of teeth at input of PGS and T_{out} is output torque provided by motor. In the starting motor propels the vehicles but, if SOC is small, engine may start immediately. As the required vehicle speed increases, the engine starts.

5.1.2 Mode 1: Normal driving conditions

Under normal driving conditions, the engine's power is divided into two paths: one portion drives the wheel as (5.2) and (5.3) and another portion drives the M/G1 to produce electricity as (5.4). The motor doesn't supply power in this condition as (5.5) until cruising is required. Energy flow of mode 1 is shown in figure 5.1 (b).

$$T_r = \frac{N_r}{N_s + N_r} * T_e \tag{5.2}$$

$$T_{out} = \frac{N_2}{N_1} * T_r \tag{5.3}$$

$$T_g = \frac{N_s}{N_s + N_r} * T_e \tag{5.4}$$

$$T_m = 0 \tag{5.5}$$

5.1.3 Mode 2: Full acceleration

In this mode, engine along with M/G2 propels the vehicle and supplies the demand as (5.6). MG2 is supplemented by power from the battery. The power flow is shown in figure 5.1(c).

$$T_{out} = \frac{N_2}{N_1} * (T_r + T_m) \tag{5.6}$$

5.1.4 Mode 3: Deceleration or regenerative braking

MG1 is operating as generator to produce electricity to charge the battery and at the same instant also provide braking torque to the final drive. The braking energy dissipated at high speed is recovered with high generator efficiency. At lower speeds, recovering energy will be low because at low motor rotational speeds, motor electromotive forces are low.

Both, engine and motor participate in supplying the demanded power as per the control strategy used. The engine on/off condition depends on battery SOC, requested power, vehicle and engine speed and coolant temperature. Engine on/off conditions are obtained with the following criteria:

a) If vehicle operates at low speed, coolant temperature is acceptable and if sufficient SOC preserves to deliver demanded power, then vehicle operates in electric mode only.

b) If SOC is more than the targeted SOC and engine is 'on' then engine and motor both provide the demanded power.

c) If SOC is less than targeted SOC value, then engine powers the vehicle and also provides extra power to charge the battery.

d) If requested power goes negative and the engine is 'off', then this entire power is stored in the battery by regenerative braking.

It is targeted to operate the engine in its efficient region to achieve better fuel economy.

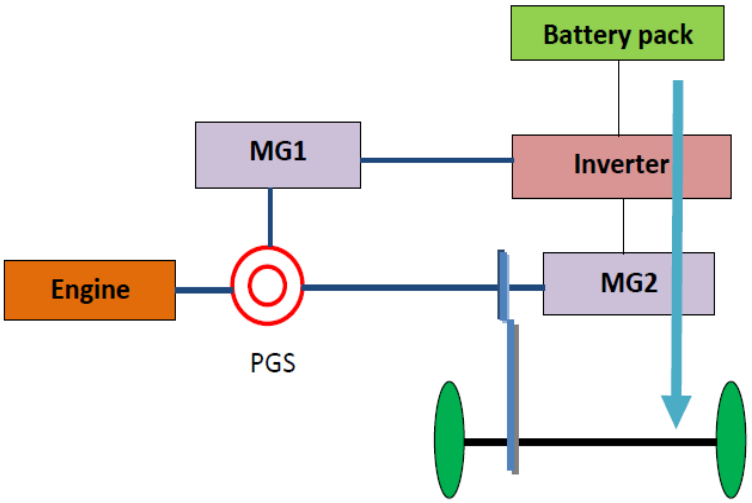

(a)

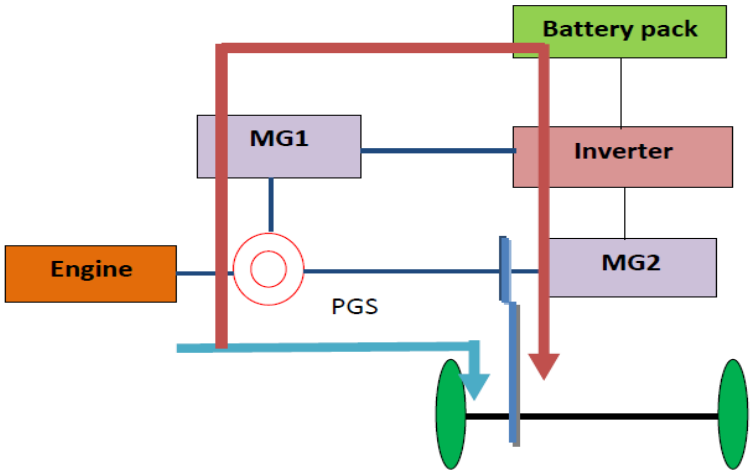

(b)

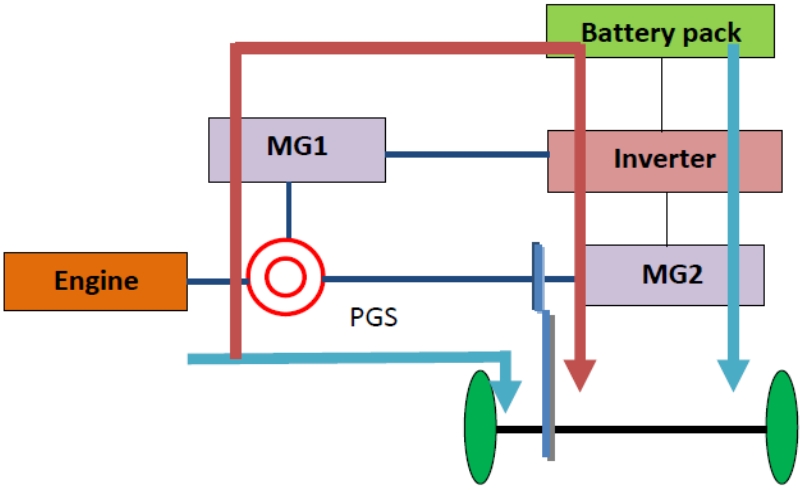

(c)

Figure 5.1: power flow direction in (a) mode 0, (b) mode 1 and (c) mode 2

5.2 Vehicle Power Demand Analysis

Prior knowledge of trip length can estimate tractive force required at wheel as calculated by (5.7). A vehicle of mass M moving with the speed of V on a tilted road with angle α, rolling resistance and aerodynamic drag oppose vehicle's movement. The total force applied to a vehicle to move in the forward direction is given as (5.7).

$$\mathrm{F_r} = \frac{1}{2}\rho \mathrm{A_f} \mathrm{C_D} (\mathrm{V} - \mathrm{V_W})^2 + \mathrm{Pf_r} + \mathrm{Mgsin}\delta \tag{5.7}$$

$\mathrm{A_f}$ is frontal area, $\mathrm{C_D}$ is aerodynamic drag, ρ is air density, V is vehicle speed and $\mathrm{V_w}$ is component of wind speed, $\mathrm{f_r}$ is rolling resistance, δ is road angle and P is force acting on the center of a standstill tire. Torque on driven wheel transmitted from power plant is given as (5.8).

$$\mathrm{T_w} = R_g \zeta \eta_t \mathrm{T_p} \tag{5.8}$$

R is gear ratio of transmission, ζ is gear ratio of drive line, η_t is efficiency of driveline from power plant to the driven wheels and T_p is the torque output from the power plant. $\mathrm{T_p}$ might be the torque of engine or motor or combination of both depending upon the requirement. As per figure 5.2, there might be three different cases, how engine and motor alone or together fulfil the driver's demand. Speed and torque levels are decided based on component's specification. The speed and torque ranges used in this thesis are mentioned in Table A2 and A3 (appendix A).

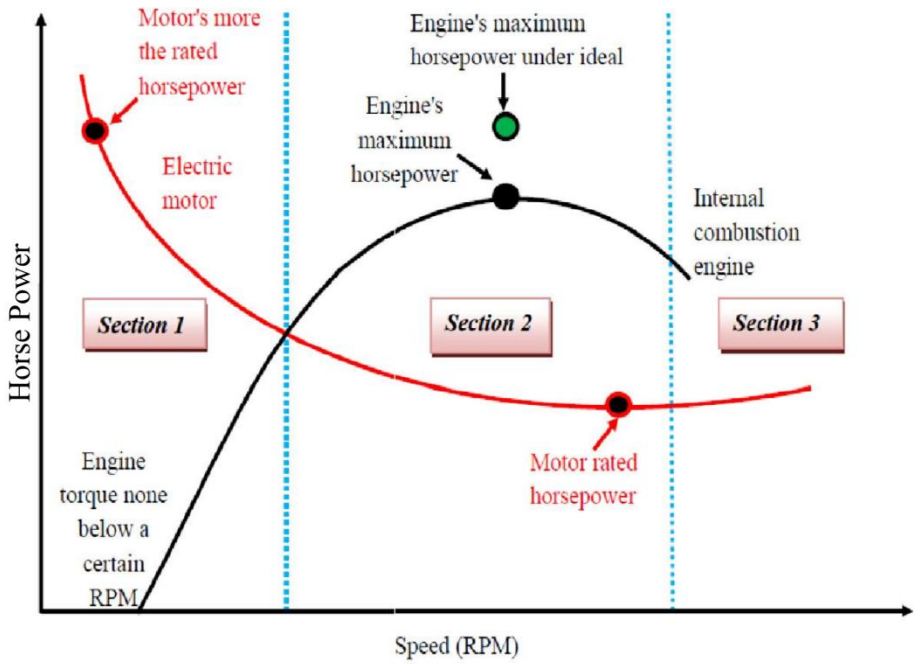

Figure 5.2: Vehicle performance criteria impacted by the engine and motor characteristics

It is clear that high torque is required to start the vehicle. At lower speed, motor's horsepower is 2 to 3 times higher than the rated horsepower and engine's torque is found to be very less. This condition typically suits to the section 1, where the motor is used to start the vehicle and hence no fuel consumption. After certain speed the engine starts up, charges the battery as well as powers the wheels. If the speeds and torques are chosen wisely and engine is chosen to work in its efficient region, then the fuel consumption will be optimum. Mode 1 and mode 2 lies under section 2. In mode 1, by following the speed torque characteristic of engine, it works in the best efficient region; hence performance will be good enough to maximize the fuel efficiency. Charge level in the battery increases through M/G1, which is described as (5.4). M/G2 doesn't work in mode 1. In section 2, in case of cruising, where engine and M/G2 both works, motor and engine both will have good electrical and chemical efficiencies respectively. Supposedly trip requires long hours of cruising at higher speed and engine and motor continue to supply the demanded power, efficiency may go down. This case is best represented by section 3, where both engine and motor will fulfil the demand but will not work in efficient ranges, hence fuel economy will get down and battery will get depleted rapidly. The torque on driven wheel in these three cases is as below:

Case 1: Only motor

Here motor works as power plant and utilizes the charge depletion (CD) mode of operation.

$$T_w = R_g \zeta \eta_t [\, T_l + J \frac{d^2\theta}{dt^2} + B \frac{d\theta}{dt}] \tag{5.9}$$

m_{ep} is mean effective pressure, $V_d$is volumetric density.

Case 2: Only engine

It uses the engine power and acts like conventional ICE based vehicles.

$$T_w = R_g \zeta \eta_t [\frac{m_{ep} V_d}{4pi}] \tag{5.10}$$

T_l is load toque when mechanical load is applied, J is moment of inertia, B is viscous friction and $\frac{d\theta}{dt}$ represents rotation speed.

Case 3: Engine along with motor

This is used in cruising and utilizes charge sustaining (CS) mode of operation.

$$T_w = R_g \zeta \eta_t [\frac{m_{ep} V_d}{4pi} + \, T_l + J \frac{d^2\theta}{dt^2} + B \frac{d\theta}{dt}] \tag{5.11}$$

5.3 Powertrain Control Methodology

Power-split HEVs have the potential to improve in fuel efficiency than series or parallel hybrids because engine speed and torque can be decoupled completely or partially from the driven wheels. By applying a suitable control strategy fuel efficiency can be improved provided it follows the control objectives, like 1) driver torque and speed demand is fulfilled 2) engine operates in its best efficiency region, 3) target SOC level meets at the end of the trip and 4) maximum braking energy is recuperated while braking or decelerating. While making the control strategies different approaches can be followed as elaborated below:

5.3.1 Engine Speed Control Strategy

Vehicle speed ranges are divided into three regions, namely 1) low, 2) medium and 3) high vehicle speed as shown in figure 5.3.

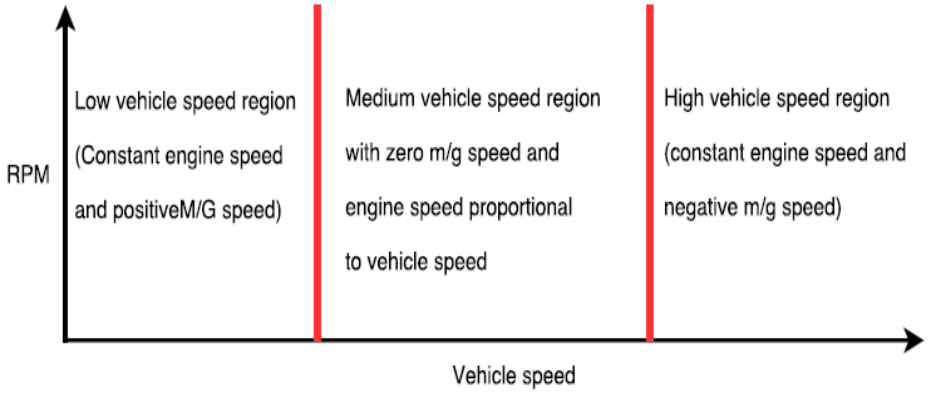

Figure 5.3: Various vehicle speeds ranges

In low speed region, speed coupling mode is used. It avoids the condition to make engine work at too low speeds which is inefficient operation. Low vehicle speed V_L, threshold can be decided by the lowest engine speed allowed with zero M/G speed as in (5.12).

$$V_L = \frac{\pi k_{yr} n_{e\_min} r_w}{30 i_{rw}} \ (\frac{m}{s}) \tag{5.12}$$

Where n_{e_min} is the minimum engine speed allowed, r_w is the wheel radius, $k_{yr} = \frac{1+i_g}{i_g}$ where i_g is the gear ratio and is defined as $\frac{r_r}{r_s}$ and i_{rw} is the gear ratio of the ring gear to drive train wheels. In this region motor/generator operates with a positive speed $n_{M/G}$ as in (5.13).

$$n_{M/G} = k_{ys}\left(n_{e\_min} - \frac{30 i_{rw} V}{\pi k_{yr} r_w}\right) \tag{5.13}$$

V is the vehicle speed in m/s ($V \leq V_L$). From (4.2) torque produced by motor/generator is applied to the sun gear and has direction opposite to its speed. Therefore, M/G absorbs part of the engine power to charge the battery. Power on the M/G shaft $P_{M/G}$ can be expressed as (5.14). $T_{M/G}$ is torque produced by motor/generator.

$$P_{M/G} = \frac{2\pi}{60} T_{M/G} n_{M/G} = \frac{2\pi}{60} T_e n_{e\_min} - \frac{i_{rw}}{k_{yr} r_w} T_e V \tag{5.14}$$

When the vehicle speed is higher than V_L but lower than V_H given by (5.15), M/G is de-energized and sun gear is locked to the stationary frame of the vehicle. Drive train operates in torque coupling mode. Engine speed is proportional to the vehicle speed.

$$V_H = \frac{\pi k_{yr} n_{e\_max} r_w}{30 i_{rw}} \left(\frac{m}{s}\right) \tag{5.15}$$

Where n_{e_max} is the maximum engine RPM allowed. In this medium speed region all the engine power is delivered to the wheels.

When the vehicle speed is higher than V_H, for limiting the engine speed below the maximum engine allowed speed n_{e_max}, M/G has to operate in the direction opposite to the engine speed. It can be expressed as (5.16).

$$n_{M/G} = k_{ys}\left(n_{e\_max} - \frac{30 k_{ys} i_{rw} V}{\pi k_{yr} r_w}\right) \tag{5.16}$$

Where $V \geq V_H$. Then M/G is motoring, and motoring power can be expressed as (5.17).

$$P_{M/G} = \frac{2\pi}{60} T_{M/G} n_{M/G} = \frac{i_{rw}}{k_{yr} r_w} T_e V - \frac{2\pi}{60} \frac{i_{rw}}{k_{yr} r_w} T_e n_{e\_max} \tag{5.17}$$

5.3.2 Traction Torque Control Strategy

In low vehicle speed region when sufficient SOC is available, traction motor torque T_{mt} can be given as (5.18).

$$T_{mt} = \frac{60}{2\pi} \frac{P_{m/g}}{n_{tm}} = \left(\frac{n_{e\_min}}{n_{tm}} - \frac{i_{rw}}{k_{yr} i_{mw}}\right) T_e = -\left(\frac{2\pi r_w}{60 i_{mw}} \frac{n_{e\_min}}{V} - \frac{i_{rw}}{k_{yr} i_{mw}}\right) T_e \tag{5.18}$$

Where i_{mw} is gear ratio from the traction motor to the driven wheels and n_{tm} is traction motor speed.

In case of medium vehicle speed range, torque coupling mode is employed, i.e. sun gear is locked to the vehicle stationary frame and engine speed is proportional to the vehicle speed. In high speed region, engine speed is controlled by n_{e_max} and the M/G works in motoring mode. If the commanded traction torque is higher than the torque that the engine can produce with its optimal throttle at the speed of n_{e_max} and SOC of the battery is lower than SOC_{min} and the battery cannot be discharged any more to support motoring mode, the engine will be forced to operate at the higher speed (beyond the optimal range) to fulfil the driver power demand. In this case, engine alone mode can be used with torque coupling or engine can run at somewhat higher speed so that a M/G

work in generating mode to feed the traction motor to support engine by providing additional torque. For the latter case, n_e can be calculated as in (5.19)

$$n_e > \frac{30 i_{rw} V}{\pi k_{yr} r_w} \tag{5.19}$$

If SOC is higher than SOC_{min}, then the engine should be controlled at its n_{e_max} with optimal throttle and traction motor provides additional torque to engine to support the driver torque demand.

If the commanded traction torque is smaller than the engine torque and SOC is lower than SOC_{min}, engine is operated according to (5.15) and traction motor works in generating mode. If SOC is in between range of SOC_{min} and SOC_{max}, traction motor may be de-energized and engine alone mode can be projected. If SOC is greater than SOC_{max}, engine better shut down and traction motor alone can propel the vehicle.

5.4 Objective Function Formulation and Constraints

Here, the objective of the optimization problem is to maximize the fuel economy. The total fuel consumption in a driving cycle is given by (5.20).

$$J = \dot{m_{ft}} \tag{5.20}$$

Where $\dot{m_{ft}}$ is time rate of total fuel consumption. Fuel consumption is inversely proportional to battery power P_b. A larger battery power will cause vehicle to consume lesser fuel and vice-versa and P_b is directly proportional to SOC. Battery power P_b bears a quadratic equation of V_{oc}, R_b and I_b given as (5.21). The solution of this equation can be given as (5.22).

$$P_b = V_{oc} * I_b - {I_b}^2 * R_b \tag{5.21}$$

$$I_b = \frac{-\left(V_{oc} - \sqrt{{V_{oc}}^2 - R_b * P_b}\right)}{2 * R_b} \tag{5.22}$$

$\dot{SOC}$ is the time rate of SOC and can be expressed as (5.23).

$$\dot{SOC} = -\frac{I_b}{Q_b} \tag{5.23}$$

Further simplifying (5.23) using (5.22) gives relation between battery power P_b and $S\dot{O}C$ as in (5.24).

$$S\dot{O}C = \frac{V_{oc} - \sqrt{{V_{oc}}^2 - 4P_bR_b}}{2R_bQ_b} \tag{5.24}$$

Relations between M/G1, M/G2, engine and requested torques and speeds are summarized in (5.25).

$$\left.\begin{aligned} T_{M/G1} &= -\frac{1}{1+R_g}[T_e] \\ \omega_{M/G1} &= -R_g\zeta\omega_{req} + (1+R_g)\omega_e \\ T_{M/G2} &= -\frac{1}{(1+R_g)}\left[-\frac{(1+R_g)T_{req}}{\zeta} + R_gT_e\right] \\ \omega_{M/G2} &= \zeta\omega_{req} \end{aligned}\right\} \tag{5.25}$$

Where $T_{M/G1}$, $T_{M/G2}$ are torques and $\omega_{M/G1}$, $\omega_{M/G2}$ are speeds of M/G1, M/G2, T_e is engine torque, ω_e is engine speed, ω_{req} requested speed, R_g is gear ratio and ζ is final drive ratio. While solving the objective function for HEVs, following constraints are considered as given in (5.26).

$$\left.\begin{aligned} \omega_{e,min} \le \omega_e \le \omega_{e,max} \\ \omega_{M/G1,min} \le \omega_{M/G1} \le \omega_{M/G1,max} \\ \omega_{M/G2,min} \le \omega_{M/G2} \le \omega_{M/G2,max} \\ T_{e,min} \le T_e \le T_{e,max} \\ T_{M/G1,min} \le T_{mg1} \le T_{M/G1,max} \\ T_{M/G2,min} \le T_{M/G2} \le T_{M/G2,max} \\ SOC_{min} \le SOC \le SOC_{max} \end{aligned}\right\} \tag{5.26}$$

where $\omega_{e,min}$, $\omega_{e,max}$, $\omega_{M/G1,min}$, $\omega_{M/G1,max}$, $\omega_{M/G2,min}$, $\omega_{M/G2,max}$, $T_{e,min}$, $T_{e,max}$, $T_{M/G1,min}$, $T_{M/G1,max}$, $T_{M/G2,min}$, $T_{M/G2,max}$ SOC_{min} and SOC_{max} are the minimum and maximum values of constraints for engine, M/G1, M/G2 and SOC respectively.

Various optimization strategies are introduced here for optimal splitting of power. These strategies are tested on standard driving cycle ECE_EUDC which is shown in figure 5.4. Figure 5.5 shows the force and torque required with respect to the vehicle speed. The positive torque symbolizes power required by the driver and it should be fulfilled either by engine or motor or both together. The negative torque is due to deceleration and indicates that the power is being generated (regenerative braking) during

vehicle propulsion and the battery can get charged. All the developed strategies are verified by checking whether requested speed is met by the achieved speed or not. The best matching promises the validity of the control strategy developed.

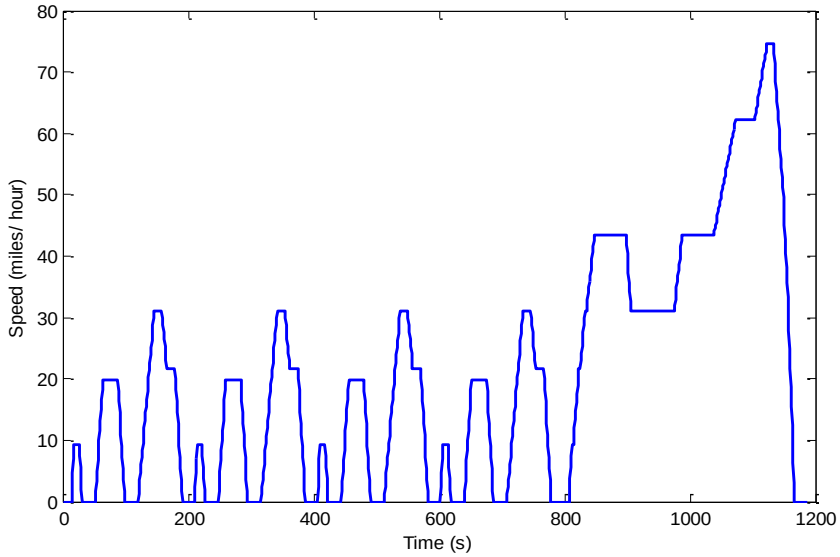

Figure 5.4: ECE_EUDC driving cycle

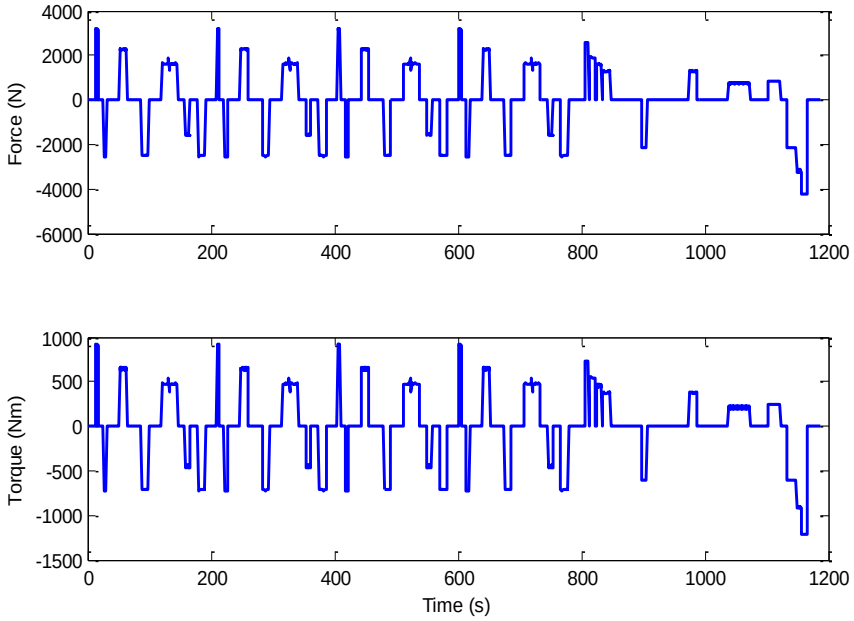

Figure 5.5: Force and torque required by ECE_EUDC

This chapter is divided five parts now onwards. Every part is a presentation of published paper(s). Section heading represents the published article.

5.5 Part 1: Fuel Efficiency Optimization of Input-Split Hybrid Electric Vehicle using DIRECT Algorithm

DIRECT optimizes the 'cs_eng_on_soc', 'cs_min_pwr', 'cs_electric_launch_spd' and 'cs_eng_min_spd'. 'cs_eng_on_soc' is the minimum value of SOC below which the engine must be on. 'cs_min_pwr' is the minimum power commanded of the engine. 'cs_electric_launch_spd' is the vehicle speed threshold; below this speed, the engine is turned off. 'cs_eng_min_spd' is the speed below which engine will be on but does not utilize the fuel. Parameters individually or/and under the influence of each other affects the performance of the vehicle. The analysis is performed on the default R_{int} model provided in ADVISOR and conventional SOC estimation method is used. To analyze this, parameters are grouped in different sets, i.e., Set 1, set 2, set 3 and set 4. Set 1 contains the individual parameters considered, set 2 contains group of two parameters, set 3 contains a group of 3 parameters and set 4 contains group of four parameters. Various sets and the contained parameters are shown in table 5.1. Value selection of these parameters affects the engine on/off status; hence have an impact on fuel consumption.

Table 5.1: List of selected parameters

Set	Parameters	Fuel economy (mpgge)
Set of 1 individual parameter	**cs_eng_on_soc**	44.61
	cs_min_pwr	45.41
	cs_electric_launch_spd	43.43
	cs_eng_min_spd	44.61
Set of 2 parameter	**cs_min_pwr and cs_electric_launch_spd**	43.54
	cs_eng_on_soc and cs_eng_min_spd	42.59
	cs_eng_on_soc and cs_min_pwr	42.59
	cs_eng_on_soc and cs_electric_launch_spd	42.56
	cs_min_pwr and cs_eng_min_spd	43.43
	cs_electric_launch_spd and cs_eng_min_spd	43.39
Set of 3 parameter	**cs_eng_on_soc, cs_min_pwr and cs_electric_launch_spd**	43.28
	cs_eng_on_soc, cs_min_pwr and cs_eng_min_spd	43.35
	cs_eng_on_soc, cs_electric_launch_spd and cs_eng_min_spd	42.19
	cs_min_pwr, cs_electric_launch_spd and cs_eng_min_spd	43.35
Set of 4 parameter	**cs_min_pwr, cs_electric_launch_spd, cs_eng_min_spd and cs_eng_on_soc**	42.89

'cs_min_pwr' shows the highest fuel economy in all the cases considered. The different plots are gathered to verify the authenticity of the proposed discussion. The initial charge on battery cs_init_soc=70 percent and minimum allowable range up to which the battery can be depleted is 30 percent. The variation of SOC over the entire trip is shown in figure 5.6 (a). Figure 5.6 (b) shows the engine off/on status with respect to

varying SOC as shown in figure 5.6 (a). Analyzing figure 5.6 (a) and (b) together, clarify that whenever the engine is off, the SOC is decreasing, i.e. propulsion power is provided by a motor. Similarly, when the engine is on, SOC level is either increasing or held constant, i.e. the battery is getting charged either through regenerative braking or by engine or no effect. Figure 5.6 (c) and (d) show the engine and motor characteristics according to the speed and torque values which have been used during vehicle propulsion over the trip.

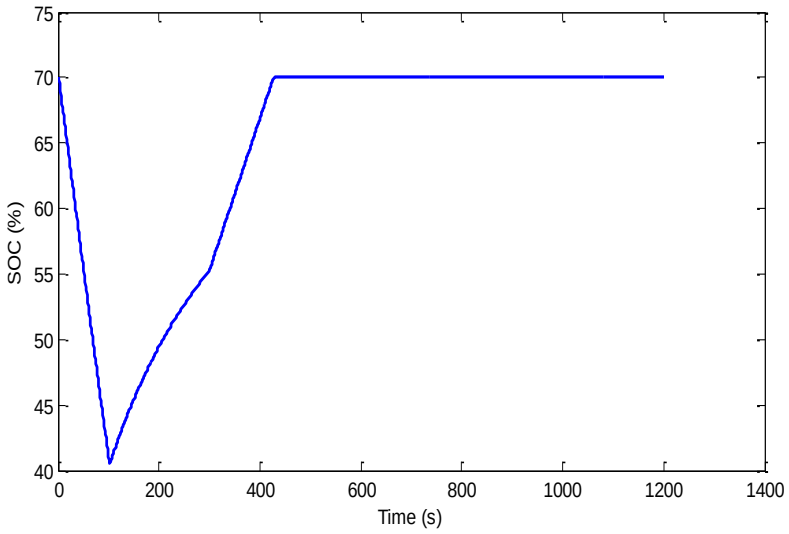

(a)

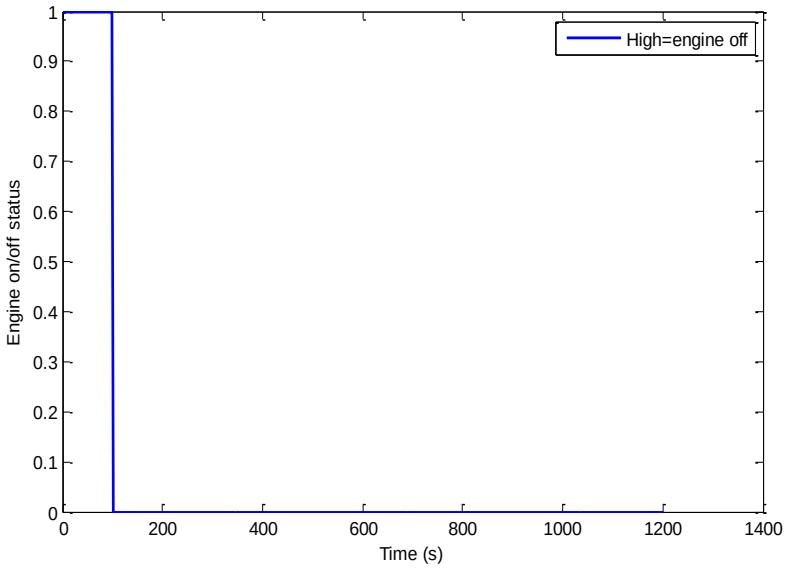

(b)

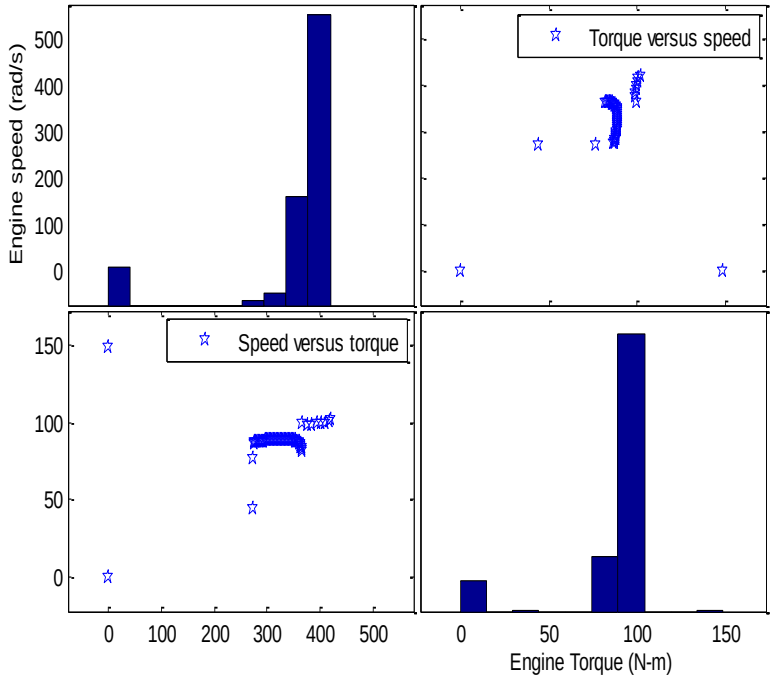

(c)

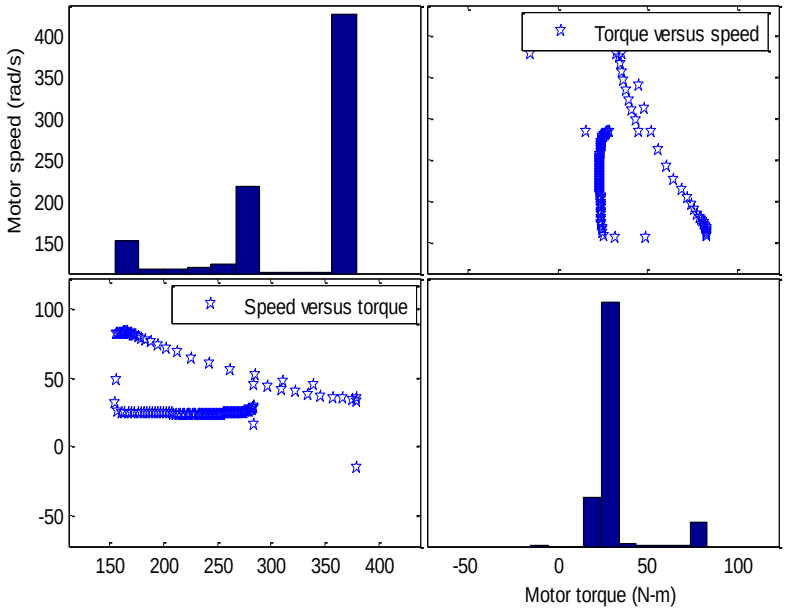

(d)

Figure 5.6: Analysis of DIRECT method (a) SOC variation over entire trip, (b) Engine on/off decision, (c) Engine and (d) Motor speed torque characteristics

24.32, 15.21 and 5.77 mpgge fuel is saved by proposed method compared to [161, 164, 165] respectively. The various vital parameters are optimized here for maximizing the fuel economy and the results of different combinations are tabulated. Detailed

analysis is performed to check the impact of these considered parameters over each other and variation in fuel consumption is observed.

To improve the FE and to check the effect of other battery models, some more optimization techniques are used and given in subsequent sections.

5.6 Part 2: Optimal Fuel Control of Series-Parallel Input Split Hybrid Electric Vehicle using Genetic Algorithm based Control Strategy

The genetic operation includes crossover, mutation, reproduction, gene duplication and gene deletion. After initial random population creation, a fitness test is performed to all individuals and new population is formed by genetic operators like reproduction, crossover and selection. In crossover operation, two parents are combined to form two new offspring. With each generation some of the existing population is selected as offspring and called elitist. Mutation is a genetic operator used to maintain genetic diversity between two succeeding populations. The purpose of mutation is to avoid falling all the solutions in the local region. Fitness evaluation process is iterated till the terminating criterion is met. Benefits of GA are a) parallel processing b) vast solution set can be scanned at a very fast rate c) suitable for complex, discontinuous and noisy fitness function and d) global optima is achieved. The population size, mutation and crossover play a vital role in GA. A wise selection of initial population trims down the computation time. Initialization of the population influences the ultimate solution and makes a significant impact on the convergence speed as well. A vast range random search wastes the time, whereas a very confined area random search may also be not promising as it may turn up with bad genes. High mutation rates provide the facility of wide exploration in search space, but faces problems of finding optimum solutions. On the other hand, lower mutation rates may result in premature convergence. So, here a wide range of mutation rates from low values of 0.1, 0.5 to high mutation rates of 0.1, 0.7, 0.9 are explored to select the mutation rate useful for HEV application.

Figure 5.7 presents the process of finding the optimized solution. Using all the constraints and parameters the fitness function is evaluated and best possible value is determined. This process continues till the terminating conditions are satisfied.

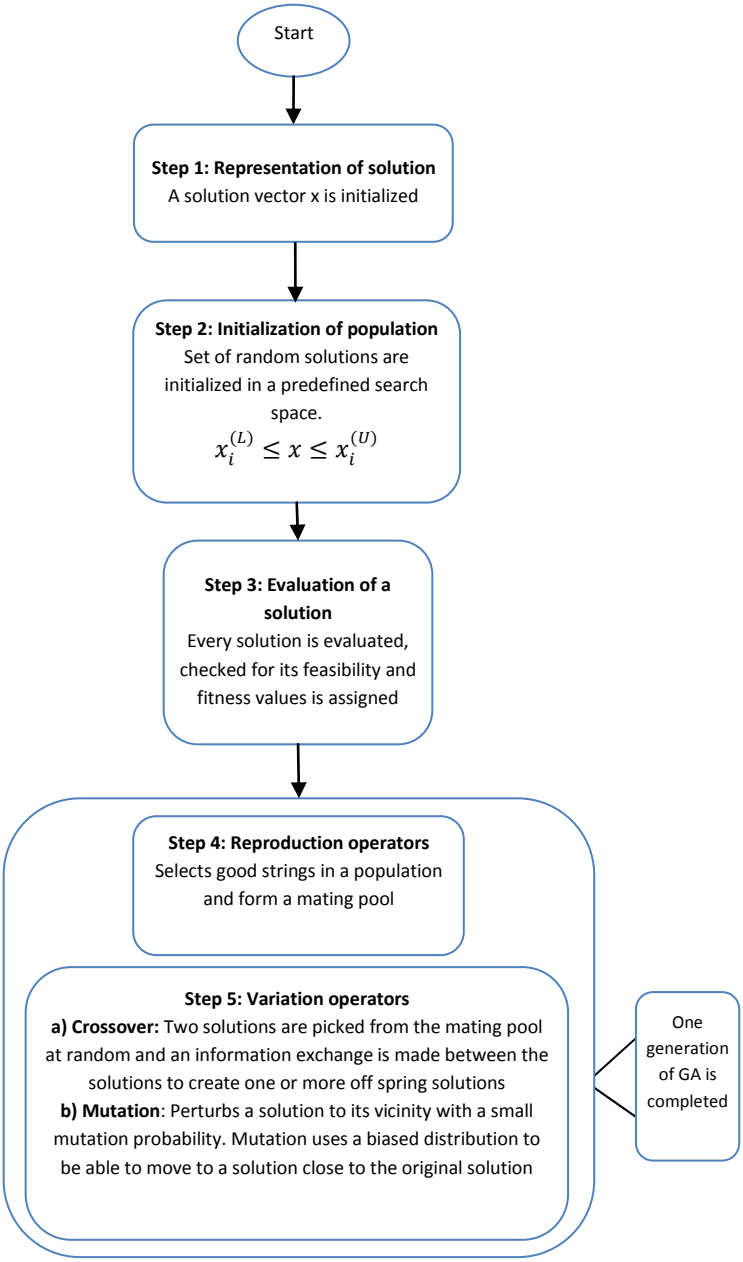

Figure 5.7: Genetic algorithm process flow

Table 5.2 figures out the fuel economies for set of 1 parameter cases, table 5.3 for set of two parameters, table 5.4 for set of parameters of three parameters, table 5.5 for set of four parameters and table 5.6 for set of five parameters. It is observed that mutation rates of 0.1, 0.5 and 0.7 are giving considerable results. Although different mutation rates are also tried, but are not included here in the table because they are either giving similar or deteriorated results. 70 percent mutation rate is chosen to perform the simulations shown in thesis because sometimes it gives considerably much improved fuel economy

than other mutation rates. Population sizes of 5 to 7 times of number of parameters are giving considerable results. Here, 6 times to the number of parameters are chosen.

Table 5.2: Set of one parameter

Set of one Parameter				
		Mutation rates		
Name of parameters	**Population size**	**0.1**	**0.5**	**0.7**
	3	43.04	43.04	43.06
	4	43.04	43.04	43.04
	5	44.34	44.34	44.34
	6	44.34	44.34	44.34
	7	44.34	44.34	44.34
cs_eng_on_soc	8	43.04	43.04	43.04
	3	43.05	43.05	44.09
	4	43.23	43.06	43.05
	5	45.64	45.97	49.69
	6	46.59	42.35	**52.6***
	7	47.1	48.68	47.39
cs_min_off_time	8	46.37	48.8	46.1
	3	40.31	40.31	40.31
	4	40.31	40.31	40.31
	5	42.44	42.44	42.44
	6	42.44	42.44	42.44
	7	42.44	42.44	42.44
cs_min_pwr	8	40.31	40.31	40.31
	3	43.41	43.41	43.41
	4	43.41	43.41	43.41
	5	43.41	43.41	43.41
	6	43.41	43.41	43.41
	7	43.41	43.41	43.41
cs_electric_launch_spd	8	43.41	43.41	43.41
	3	42.45	42.45	42.45
	4	42.45	42.45	42.45
	5	42.45	42.45	42.45
	6	42.45	42.45	42.45
	7	42.45	42.45	42.45
cs_eng_min_spd	8	42.45	42.45	42.45

Table 5.3: Set of two parameters

Set of two Parameters				
		Mutation rate		
Name of parameters	**Population size**	**0.1**	**0.5**	**0.7**
cs_eng_on_soc and cs_min_off_time	7	47.15	46.21	47.15
	8	47.15	46.22	48.97
	9	47.2	47.2	47.2
	10	47.11	47.2	47.11
	11	49.95	47.18	43.49
	12	46.35	46.23	46.35
	13	47.39	46.23	**50.88***
	14	47.38	46.23	47.38
	15	46.37	46.23	46.37
cs_eng_on_soc and cs_min_pwr	8	42.45	42.45	42.45
	9	42.45	42.45	42.45
	10	42.45	42.45	42.45
	11	42.45	42.45	42.45
	12	42.45	42.45	42.45
	13	44.31	42.45	44.31
	14	42.45	42.45	42.45
	15	42.45	42.45	42.45
cs_min_off_time and cs_min_pwr	7	48.21	48.21	48.21
	8	48.21	48.21	50.11
	9	48.17	48.17	**52.75***
	10	48.17	48.17	44.35
	11	48.17	48.17	48.16
	12	47.35	47.31	49.95
	13	43.39	47.31	47.45
	14	47.38	47.38	**52.74***
	15	48.21	47.38	47.38

Table 5.4: Set of three parameters

Set of three Parameters				
		Mutation rate		
Name of parameters	**Population sizes**	**0.1**	**0.5**	**0.7**
cs_eng_on_soc, cs_min_off_time and cs_electric_launch_spd	14	**59.05**	**59.05**	**59.05**
	15	57.51	**59.05**	**59.05**
	16	**59.05**	49.55	49.55
	17	**59.05**	58.93	58.93
	18	**59.05**	50.52	**59.05**
	19	**59.05**	**59.05**	**59.05**
	20	58.55	58.77	**59.05**
cs_eng_on_soc, cs_min_off_time and cs_electric_launch_spd	14	44.16	**44.27**	**44.27**
	15	43.79	44.16	43.8
	16	43.8	44.09	43.73
	17	44.22	44.18	44.18
cs_eng_on_soc, cs_min_off_time and cs_min_pwr	14	46.56	44	46.9
	15	46.66	46.66	**48.58**
	16	47.65	46.59	**48.12**
	17	46.73	46.59	**48.96**
	18	46.47	**48.11**	47.6
cs_eng_on_soc, cs_min_pwr and cs_eng_min_spd	15	43.13	43.26	43.23
	16	43.21	43.23	43.21
	17	43.29	43.21	43.25
	18	43.22	43.23	**43.27***
	19	43.29	43.13	43.13
	20	43.13	43.13	43.13

Table 5.5: Set of four parameters

Set of four Parameters				
		Mutation rates		
Parameters	**Population size**	**0.1**	**0.5**	**0.7**
cs_eng_on_soc, cs_min_off_time, cs_min_pwr, cs_electric_launch_spd and cs_eng_min_spd	20	54.95	54.15	53.77
	22	53.25	**61.17***	54.31
	24	54.82	61.1	53.25
	26	**61.17***	60.98	54.44

Table 5.6: Set of five parameters

Set of five Parameters				
		Mutation rate		
Parameters	**Population size**	**0.1**	**0.5**	**0.7**
cs_eng_on_soc, cs_min_off_time, cs_min_pwr, cs_electric_launch_spd and cs_eng_min_spd	25	53.68	**63.42***	53.68
	27	61.33	53.68	54.04
	29	51.22	62.96	51.69
	30	50.69	54.1	59.55

5.7 Part 3: Hybrid Electric Vehicle Performance Analysis under Various Temperature Conditions

Under varying temperature conditions, battery charging/discharging efficiency changes, hence vehicle performance is affected. To investigate this, proposed modified SOC estimation method along with GA based control strategy is exercised to find the optimal fuel economy for the HEVs at various temperatures.

GA is used to optimize the performance of the vehicle on the basis of some parameters given as 1) cs_eng_on_soc, 2) cs_min_off_time, 3) cs_min_pwr, 4) cs_electric_launch_spd and 5) cs_eng_min_spd. Five different sets corresponds to the individual, group of two, three, four and five named as set 1, set 2, set 3, set 4 and set 5 are considered here. These parameters individually and in the different combinations affect the vehicle operation. Population size is taken six times of the number of parameters considered during simulation with 0.7 mutation rate. Model 1 with modified SOC estimation method is used here. The battery is supposed to have 80 percent initial charge while the trip starts and is assumed to maintain the same at the end of the trip.

Figure 5.8 shows the variation of SOC over the entire DC at different temperatures. At 0˚C battery discharge level is lesser than at 60˚C. A much deeper discharge is observed at 50˚C in comparison to 60˚C, but it should also be noted that during charging, at 60˚C charge level is much higher level than 50˚C. This characteristic can get change as shown in figure 5.9 which depends on the initial charge level and considering the case up to which point battery needs to be (re)charged before finishing the trip.

The observable facts make it clear; at low temperatures the battery energy cannot be utilized properly whereas at higher temperature much deeper discharge level can be

achieved. The continuous usage of battery at higher temperature promises for the good fuel economy but needs frequent charging (either through engine or regenerative braking) to cover the trip using electrical energy. Frequent charging and discharging reduces battery durability. Battery is a costly component and lesser durability may affect the hybrid vehicle's market in terms of economy.

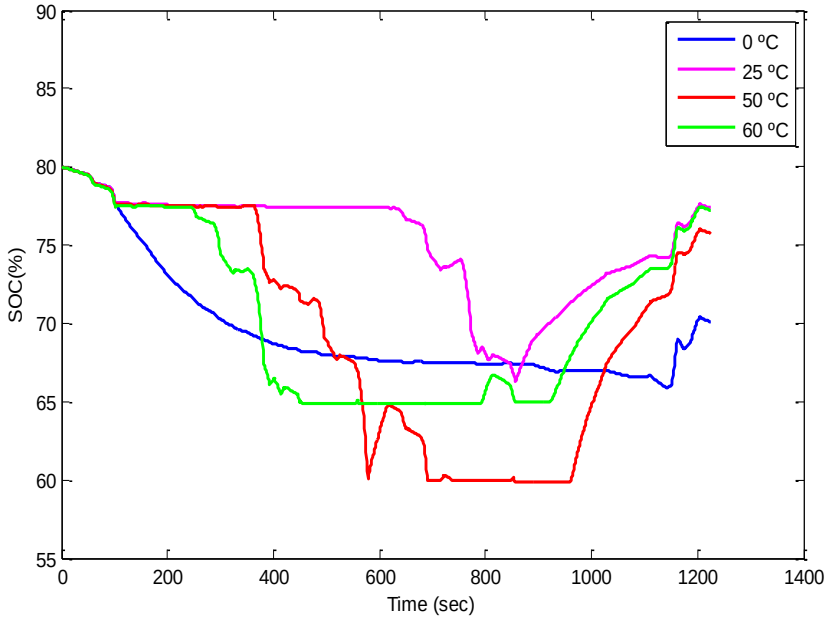

Figure 5.8: SOC variation at different temperatures with 80% initial charge

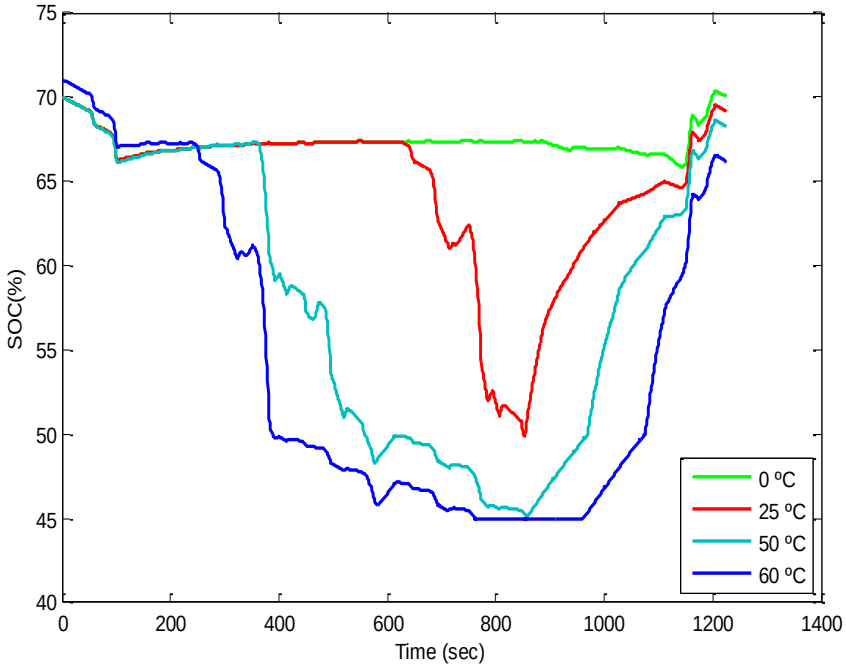

Figure 5.9: SOC variation at different temperatures with 70% initial charge

Engine on/off level corresponds to the battery charging/discharging status is shown in figure 5.10 (a) for 25˚C. The same should be followed for all the cases as well, but at very high and low temperatures it is not observed shown in figure 5.11 (b) and (c). At 0˚C and below as well as at 50˚C and above, the corresponding on/off state of engine doesn't follow the battery charging/discharging sequence, hence using battery at these temperatures may lead to improper execution of the control strategy developed for the vehicle.

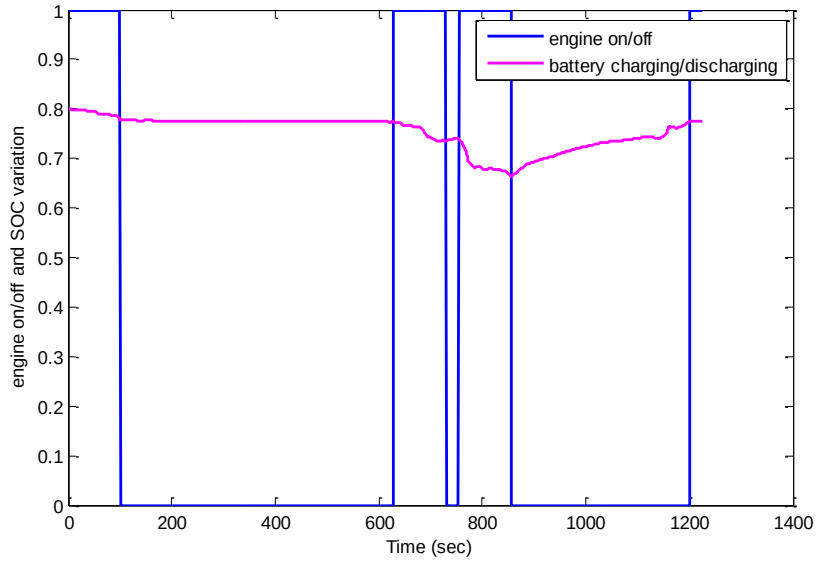

(a)

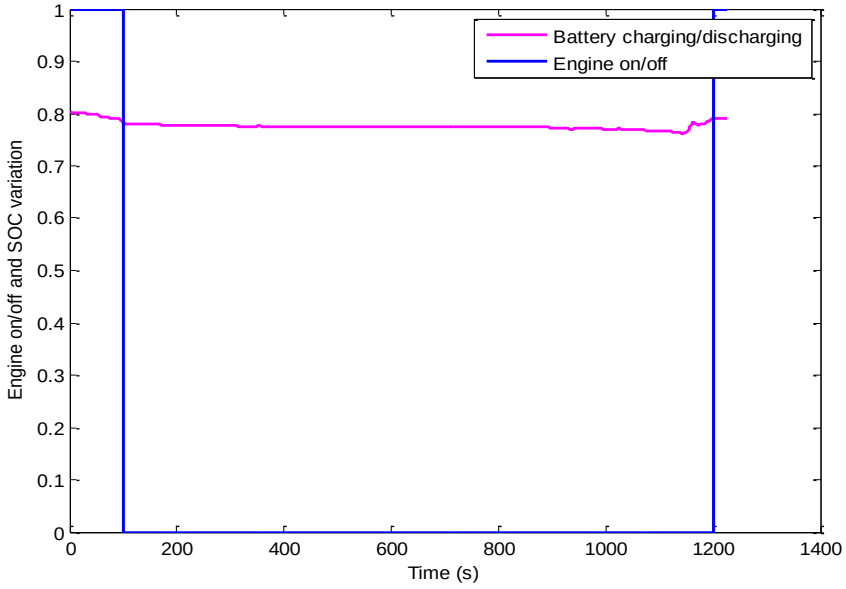

(b)

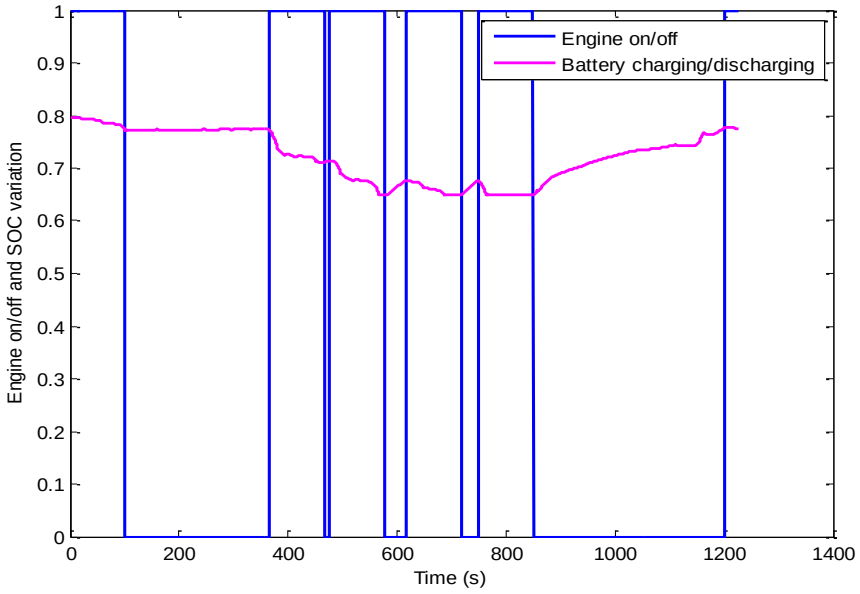

(c)

Figure 5.10: Engine on/off sequence with charge/discharge at (a) 25 ˚C, (b) 0 ˚C and (c) 50 ˚C

Figure 5.11 depicts the engine on/off status i.e., during the trip coverage, at different time instances engine is off/on. A high status symbolizes the engine 'off' condition and low status as engine 'on' state. At 60˚C, on/off transition counts more compared to other lower temperature conditions, results in frequent charging/discharging of battery.

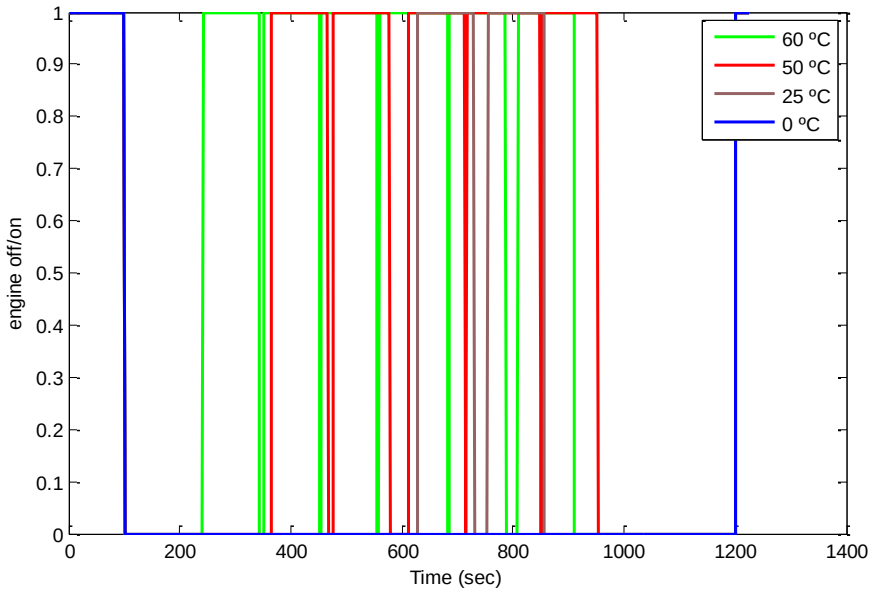

Figure 5.11: Engine on/off sequence at different temperatures

Figure 5.12 shows the current flown in/from battery at 0˚C, 25˚C, 50 ˚C and 60˚C temperatures. At 0˚C the current seems to be minimum but for increased temperature values, the current drawn from battery increases. It again verifies the effect of temperature on impedance offered by battery. Other than 0˚C temperatures, sufficient current exist and can power the motor to propel the wheels. Positive current shows, power is given to wheels and negative current shows that battery is getting charged either through engine or regenerative braking.

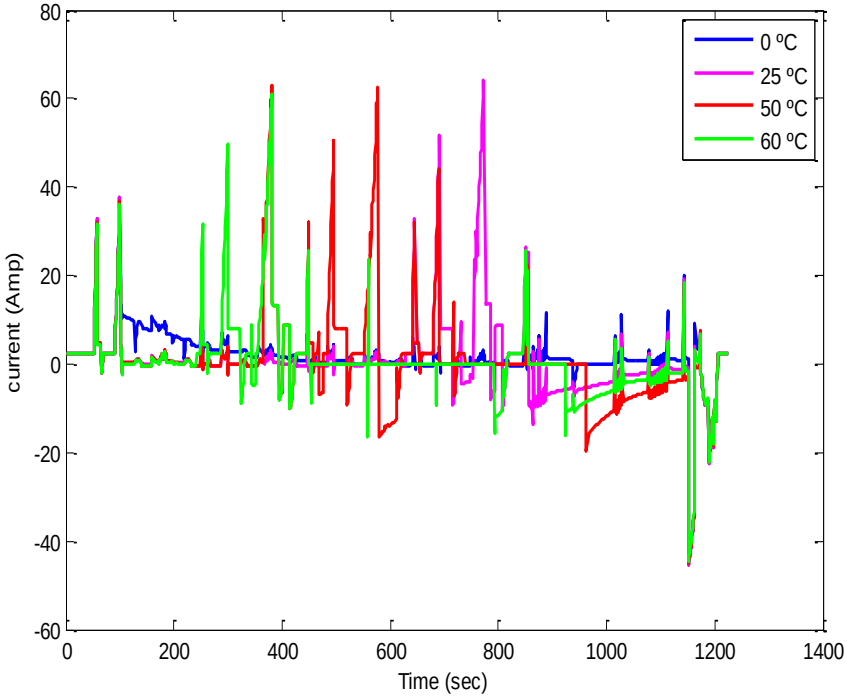

Figure 5.12: Battery current at various temperature

Table 5.7 collects the fuel economies obtained at temperatures 0˚C, 25˚C and 50˚C. Every time it is checked that how correction factor (discussed in chapter 3) is operating. Involving correction factor confirms that the accurate SOC will be measured. Throughout the table contents, it is observed that correction factor is able to measure the exact SOC at start points of simulation. An error between reference and measured SOC values lies in band of 0 to 5 percent.

Table 5.7: SOC and Fuel economy calculation at various temperatures

Set	Temperature / Parameters	0˚C		25˚C		50˚C	
		SOC	mpgge	SOC	mpgge	SOC	mpgge
1	cs_eng_on_soc	79.03	43.80	80.00	47.33	76.65	48.53
	cs_min_off_time	80.20	46.06	80.00	45.51	77.63	47.90
	cs_min_pwr	80.30	44.17	80.00	45.45	76.78	46.84
	cs_electric_launch_spd	79.12	43.91	80.00	47.32	76.64	47.52
	cs_eng_min_spd	79.12	43.91	80.00	47.33	74.50	46.15
2	cs_min_pwr and cs_electric_launch_spd	82.45	44.77	80.00	47.33	80.00	50.80
	cs_eng_on_soc and cs_eng_min_spd	80.00	44.10	80.00	46.85	80.00	49.44
	cs_eng_on_soc and cs_min_pwr	80.00	44.10	80.00	47.33	80.00	50.14
	cs_eng_on_soc and cs_electric_launch_spd	80.00	44.69	80.00	44.52	80.00	45.12
	cs_min_pwr and cs_eng_min_spd	82.45	44.74	80.00	47.33	80.00	50.29
	cs_electric_launch_spd and cs_eng_min_spd	82.45	44.77	80.00	47.33	77.00	46.93
	cs_min_off_time and cs_eng_on_soc	80.30	50.81	80.00	49.20	77.00	51.22
	cs_min_off_time and cs_min_pwr	80.00	52.5	80.00	49.16	80.00	55.21
	cs_min_off_time and cs_electric_launch_spd	80.30	48.08	80.00	52.04	77.00	52.04
	cs_min_off_time and cs_eng_min_spd	80.30	48.94	80.00	53.44	80.00	79.10
3	cs_eng_on_soc, cs_min_pwr and cs_electric_launch_spd	82.45	44.77	80.00	47.33	77.00	48.89
	cs_eng_on_soc, cs_min_pwr and cs_eng_min_spd	82.45	44.74	80.00	47.33	77.00	48.43
	cs_eng_on_soc, cs_electric_launch_spd and cs_eng_min_spd	82.45	44.77	80.00	47.33	77.00	49.09
	cs_min_off_time, cs_electric_launch_spd and cs_eng_min_spd	82.45	57.67	80.00	51.59	80.00	53.66
	cs_min_off_time, cs_min_pwr and cs_electric_launch_spd	82.45	57.67	80.00	52.02	80.00	72.41
	cs_min_off_time, cs_eng_on_soc and cs_min_pwr	82.45	44.71	80.00	51.52	77.00	62.96
	cs_min_pwr, cs_electric_launch_spd and cs_eng_min_spd	82.45	44.77	80.00	47.33	77.00	48.33
	cs_min_off_time, cs_eng_on_soc and cs_electric_launch_spd	82.45	43.07	80.00	51.77	77.00	70.21
	cs_min_off_time, cs_eng_on_soc and cs_eng_min_spd	82.45	57.67	80.00	51.52	79.68	71.30
4	cs_min_pwr, cs_electric_launch_spd, cs_min_off_time and cs_eng_on_soc	80.30	50.62	80.00	51.59	77.00	52.72
	cs_min_pwr, cs_eng_min_spd, cs_min_off_time and cs_eng_on_soc	82.45	51.36	80.00	50.92	77.00	52.43
	cs_min_pwr, cs_electric_launch_spd, cs_eng_min_spd and cs_eng_on_soc	82.45	44.77	80.00	47.36	77.00	49.09
	cs_min_pwr, cs_electric_launch_spd, cs_eng_min_spd and cs_min_off_time	82.45	52.66	80.00	51.77	77.00	49.46
	cs_eng_on_soc, cs_electric_launch_spd, cs_eng_min_spd and cs_min_off_time	82.45	57.67	80.00	49.20	77.00	52.14
5	cs_min_pwr, cs_electric_launch_spd, cs_min_off_time, cs_eng_min_spd and cs_eng_on_soc	82.45	54.33	80.00	51.54	77.00	62.06

5.8 Part 4: Energy Management Strategy for Hybrid Electric Vehicles using Genetic Algorithm

It is observed from an extensive literature survey that for hybrid vehicle applications, model 1 has only used [211, 212, 213, 214, 215, 216, 217, 218, 219, 220, 221, 222, 223]. This simplified battery model is mainly used by researchers to minimize the circuit complexity. The other battery models (model 2 and 3) are accepted by the fraternity to depict the phenomenon of a real battery but are not used in HEV applications. In HEVs, battery is a very important component, thus it is necessary to investigate that how other proposed battery models would affect the HEV performance. This motivated to use the above stated three battery models and then chose one with better efficiency and lesser complexity.

In this section also ECE_EUDC driving cycle is considered but a probability distribution approach is applied to it. Probability distribution approach gives idea about the power requirement (less or more) for different portions of trip. Probability of power demand is analyzed with zero initial and end speed, to predict the nature of the drive cycle. Figure 5.13 explaines the procedure using GA and probability distribution analysis.

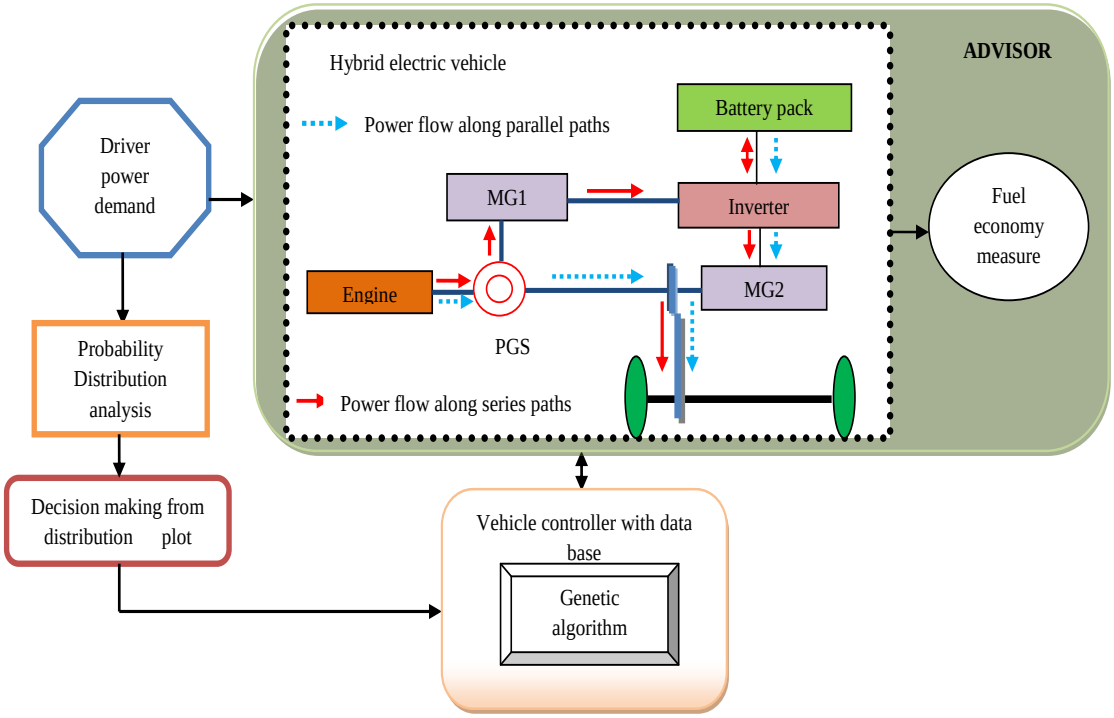

Figure 5.13: Energy management process flow using GA

Probability distribution function for the drive cycle is shown in figure 5.14 up. The distribution follows a Weibull distribution (WD) and is obtained after Kolmogorov-Smirnov and Anderson Darlington tests. This is a continuous probability distribution function [224]. Table 5.8 summarizes the parameters of WD and table 5.9 collects the descriptive statistics.

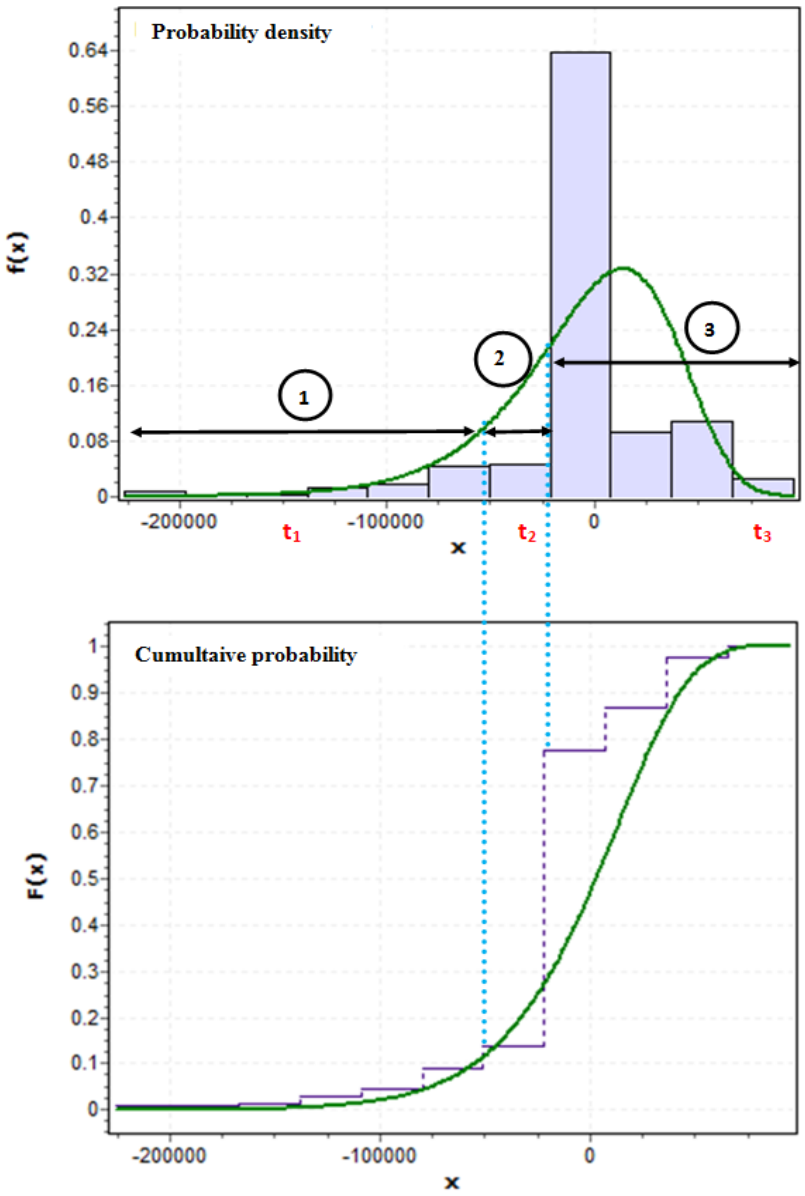

Figure 5.14: Probability density and cumulative probability curves

Table 5.8: Weibull distribution parameters

Parameters	Symbol	Value
Continuous shape parameter	α	22.771
Continuous scale parameter	β	7.50e+5
Continuous location parameter	γ	7.34e+5

Table 5.9: Descriptive statistics of Weibull distribution

Statistics	Value
Sample size	1186
Mean	-1246.2
Variance	1.6503e+9
Standard deviation	40624
Standard error	1179.6
Skewness	-2.0794
Kurtosis	8.8721

The probability distribution function of WD is defined by $f(x)$ as in (5.27). Cumulative distribution function of WD is given by (5.28) and is plotted in 5.14 (down) which predicts the power demand distribution with probability values.

$$f(x) = \frac{\alpha}{\beta}\left(\frac{x-\gamma}{\beta}\right)^{\alpha-1} exp\left(-\left(\frac{x-\gamma}{\beta}\right)^{\alpha}\right) \tag{5.27}$$

$$F(x) = 1 - exp\left(-\left(\frac{x-\gamma}{\beta}\right)^{\alpha}\right) \tag{5.28}$$

5.8.1 Engine on/off Condition Analysis

Figure 5.14 up is divided in three windows, i.e. 't1', 't2' and 't3'. The projections from the cumulative distribution to the probability density signifies that 't1' demands approximately 13 percent of power from the power plant, whereas a leap of approximately 65 percent in power demand is observed in 't2' and rest of the power is demanded in 't3'. This also has the analogy with figure 5.2. For 't1', 't2' and 't3' portions (5.9), (5.10) and (5.11) can be used to calculate the torque at the wheels for considering driving cycle and can be expressed as (5.29), (5.30) and (5.31) respectively.

$$T_{w1} = \int_{t_0}^{t_1} R_g \zeta \eta_t [\, T_l + J\frac{d^2\theta}{dt^2} + B\frac{d\theta}{dt}]\; dt \tag{5.29}$$

$$T_{w2} = \int_{t_1}^{t_2} R_g \zeta \eta_t [\frac{m_{ep} V_d}{4pi}]\; dt \tag{5.30}$$

$$T_{w3} = \int_{t_2}^{t_3} R_g \zeta \eta_t [\frac{m_{ep} V_d}{4pi} + \; T_l + J\frac{d^2\theta}{dt^2} + B\frac{d\theta}{dt}]\, dt \tag{5.31}$$

For optimal operation, engine 'on' threshold point should lie in 't2' and can be obtained using optimization algorithms. Various parameters are optimized to make the engine operate in its efficient range and thus improve the fuel efficiency.

5.8.2 Result Discussion

In the optimization process, parameter 'cs_eng_on_soc', 'cs_min_off_time', 'cs_min_pwr', 'cs_electric_launch_spd' and 'cs_eng_min_spd' are considered individually and also in the set of two, three, four and five respectively as given in table 5.10.

Table 5.10: List of selected parameters

Set name	Parameters
Set of 1 individual parameter	cs_eng_on_soc
	cs_min_off_time
	cs_min_pwr
	cs_electric_launch_spd
	cs_eng_min_spd
Set of 2 parameters	cs_eng_on_soc and cs_min_off_time
	cs_eng_on_soc and cs_min_pwr
	cs_eng_on_soc and cs_electric_launch_spd
	cs_eng_on_soc and cs_eng_min_spd
	cs_min_off_time and cs_min_pwr
	cs_min_off_time and cs_electric_launch_spd
	cs_min_off_time and cs_eng_min_spd
	cs_min_pwr and cs_electric_launch_spd
	cs_min_pwr and cs_eng_min_spd
	cs_electric_launch_spd and cs_eng_min_spd
Set of 3 parameters	cs_eng_on_soc, cs_min_off_time and cs_min_pwr
	cs_eng_on_soc, cs_min_off_time and cs_electric_launch_spd
	cs_eng_on_soc, cs_min_off_time and cs_eng_min_spd
	cs_eng_on_soc, cs_min_pwr and cs_electric_launch_spd
	cs_eng_on_soc, cs_min_pwr and cs_eng_min_spd
	cs_eng_on_soc, cs_electric_launch_spd and cs_eng_min_spd
	cs_min_off_time, cs_min_pwr and cs_electric_launch_spd
	cs_min_off_time, cs_min_pwr and cs_eng_min_spd
	cs_min_off_time, cs_electric_launch_spd and cs_eng_min_spd
	cs_min_pwr, cs_electric_launch_spd and cs_eng_min_spd
Set of 4 parameters	cs_eng_on_soc, cs_min_off_time, cs_min_pwr and cs_electric_launch_spd
	cs_eng_on_soc, cs_min_off_time, cs_min_pwr and cs_eng_min_spd
	cs_min_off_time, cs_min_pwr, cs_electric_launch_spd and cs_eng_min_spd
	cs_min_pwr, cs_electric_launch_spd and cs_eng_min_spd and cs_eng_on_soc
	cs_electric_launch_spd and cs_eng_min_spd, cs_eng_on_soc and cs_min_off_time
Set of 5 parameters	cs_eng_on_soc, cs_min_off_time, cs_min_pwr, cs_electric_launch_spd and cs_eng_min_spd

Based on the parameters to be optimized and constraints, engine 'on' threshold is identified; and corresponding fuel consumption is calculated. The GA is applied to produce the new engine 'on' threshold using selected parameters through succession of elite selection, mutation and crossover. This process continues till the terminating conditions are met. The results obtained for various possible combinations of parameters and battery models with modified SOC estimation method are given in table 5.11. It is clear from the table that the fuel economies are similar at large for battery models 2 and 3. For ease of understanding, in figure 5.15, bar graph is plotted to analyze the fuel

economies for various battery models. Tabulated results contain cases with and without trace miss. Trace miss is defined as that the vehicle does not provide the requested speed and runs at lower than required. By considering the perfect values (cases neglected with trace miss) model 2 is having the highest mean, whereas model 1 and model 3 are inferior. Trace miss can be understood in a generalized way by figure 5.16 (a) and (b). Figure 5.16 (a) shows that requested speed is always achieved by the driver and no trace miss is observed. Figure 5.16 (b) shows the case of trace miss, i.e. requested speed is not achieved at all the instances. There may be various reasons behind traces miss: (a) driving cycle demands such accelerations which cannot be achieved by vehicle, (b) loss of sufficient battery power and (c) under powered vehicle. Here a standard test driving cycle and vehicle of sufficient component sizes are considered. Only battery models are being tested. According to the primary assumption of HEVs that driver's demand should be fulfilled; model 2 is capable enough to execute this criteria and suggested to be used.

Table 5.11: Fuel efficiencies of parameter sets for different battery models

Set name	Model 1 (mpgge)	Model 2 (mpgge)	Model 3 (mpgge)
Set of 1 individual parameter	47.33	51.37	51.12
	45.51	59.80	51.06
	45.45	51.37	51.12
	47.32	51.40	51.41
	47.33	47.33	51.12
Set of 2 parameters	49.20	60.74	65.74
	47.33	51.37	53.23
	44.52	43.93	48.91
	46.85	51.37	51.12
	49.16	60.74	59.13
	52.04	67.52	65.96
	69.59	69.59	65.87
	47.33	51.40	51.41
	51.31	51.37	51.12
	51.40	51.40	51.41
Set of 3 parameters	51.00	65.78	65.49
	56.00	65.83	65.54
	52.72	65.60	65.49
	47.36	53.56	51.39
	47.33	51.37	53.23
	47.33	53.51	53.54
	53.67	65.82	65.52
	51.93	65.70	65.41
	51.95	65.82	65.52
	47.33	51.40	51.41
Set of 4 parameters	51.62	70.65	70.03
	52.13	70.65	70.03
	57.30	65.82	65.52
	54.84	69.81	70.19
	49.84	60.79	60.59
Set of 5 parameters	51.54	69.59	66.16

An efficient control strategy should consider all the governing parameters in optimization. The value of fuel economy for considering all these 5 parameters in model 2 is 52.25 without trace miss and 69.59 with trace miss as against 66.16 for model 3. Thus, model 2 is proposed to use over model 3 due to lesser complexity. It is also apparent; model 2 leads to significant improvement in the fuel economy in HEVs over traditional Model 1. This part considers a modified SOC estimation approach which incorporates the effects of both, voltage and current in SOC estimation; whereas, the most of the literature speaks about the effect of current only. It is verified that, the modified method provides better results over conventional method.

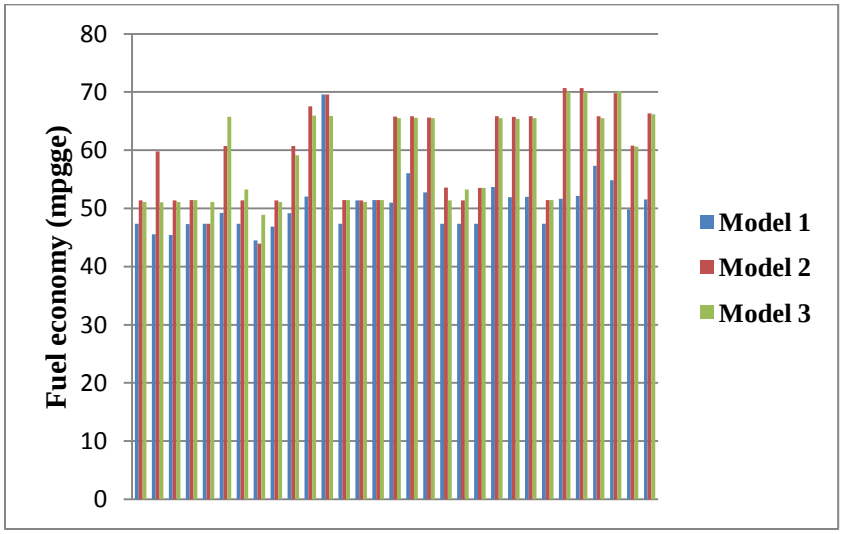

Figure 5.15: Comparison chart of fuel economies for different battery models

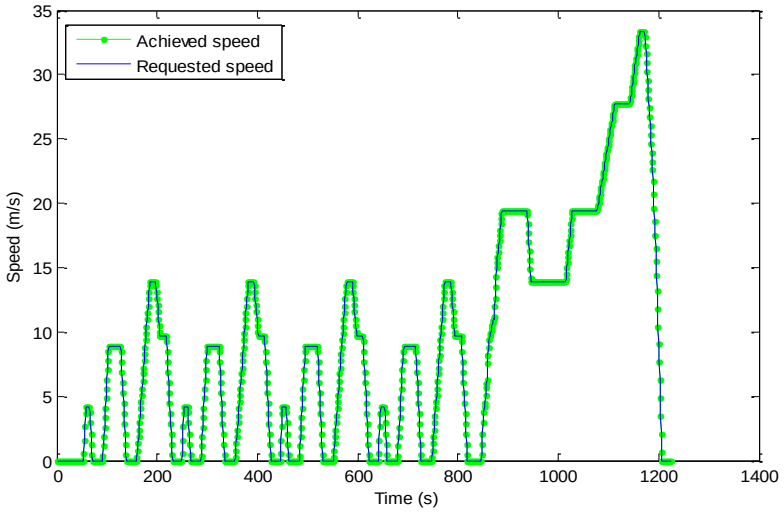

(a)

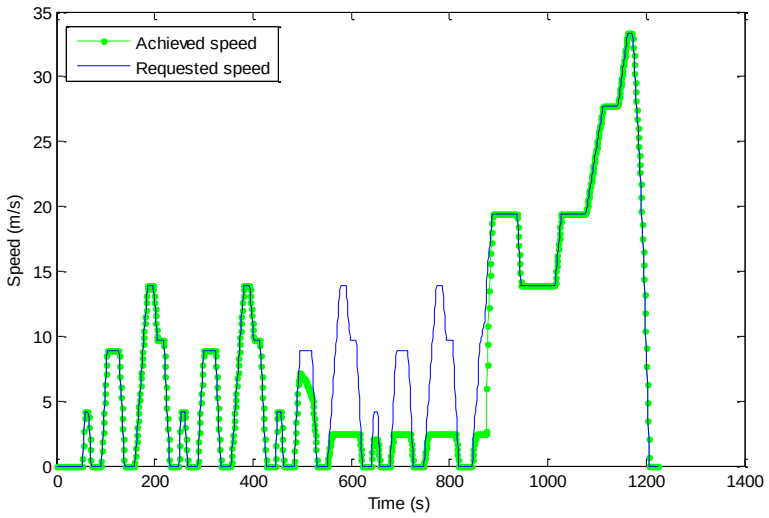

(b)

Figure 5.16: Trace miss analysis (a) no trace miss (b) with trace miss

Figure 5.14 advocates the requested power percentage in three different working windows of engine and motor. The simulation results satisfy driver's power demand by keeping the engine 'on' in its efficient region. Figure 5.17 shows the cumulative distributions plot of achieved power in response to requested power. The resemblance of figure 5.14 (down) and figure 5.17 proves the authenticity of proposed energy management scheme with modified SOC estimation method.

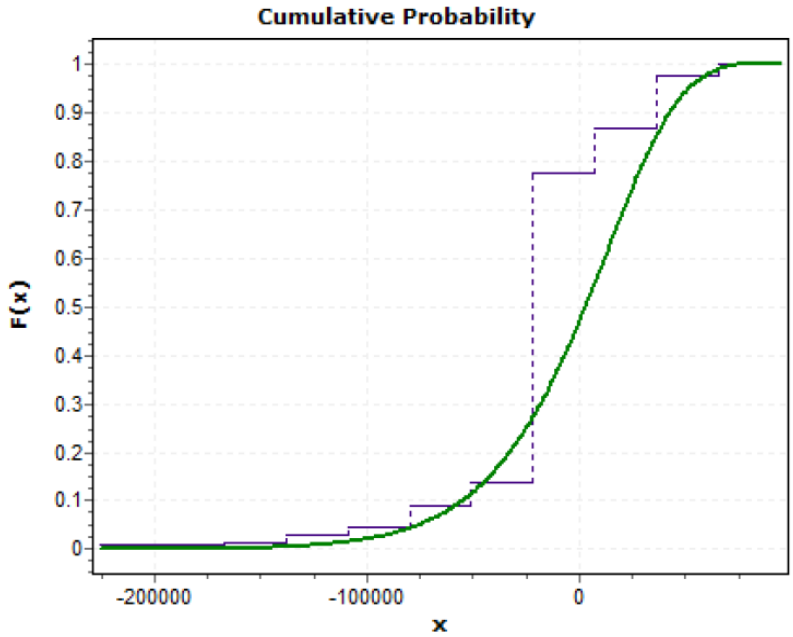

Figure 5.17: Cumulative distribution of achieved power of power plants

From Table 5.12, it is clear that an improvement of 20.25 percent in terms of fuel economy is observed when GA with modified SOC estimation using battery model 2 compared to R_{int} conventional model and Ampere hour counting.

Table 5.12: Fuel economy comparison using GA

Battery model	Fuel economy (mpgge)	Trace miss analysis
R_{int} conventional model	43.45	No trace miss
Model 2*	52.25	No trace miss
*Modified SOC estimation method		

5.9 Part 5: Development of Energy Management Strategy in Hybrid Electric Vehicles using Pontryagin's Minimum Principle and Genetic Algorithm Tuned Controller

PMP is a technique which finds only one trajectory and declares it optimal based on prior calculations, hence features with less computational time against other techniques. PMP provides the facility for implementing real time controller for the relevant operation. PMP based optimal control is applied here to calculate the fuel economies for different battery models with modified SOC estimation approach. The results are compared with the conventional SOC estimation. Four different cases are analyzed here;

1) R_{int} battery model with conventional SOC estimation available in ADVISOR

2) Model 2 with the modified SOC estimation method

5.2.1 Pontryagin's Minimum Principle

To optimize any problem using PMP, the Hamiltonian is formed firstly and minimized with respect to the control input. Then state and co-state equations are obtained by following the set procedure. The flow diagram of PMP is given in figure 5.18.

For the performance measure of the form $J = S(x(t), u(t), t) + \int_{t_0}^{t_f} V(x(t), u(t), t)$ with the terminal cost $S(x(t), u(t), t)$, instantaneous cost $\int_{t_0}^{t_f} V(x(t), u(t), t)$ and the state equation of the form $\dot{x}(t) = f(x(t), u(t), t)$; Hamiltonian constructions involve instantaneous cost and state equation with a time varying vector multiplier λ as in (5.32).

$$H(x(t), u(t), \lambda(t), t) = V(x(t), u(t), t) + \lambda^T(t) * \dot{x}(t) \quad (5.32)$$

According to PMP, optimal control trajectory $u^*(t)$, optimal state trajectory $x^*(t)$ and corresponding optimal co-state trajectory $\lambda^*(t)$ minimize the Hamiltonian such that;

$$H(x^*(t), u^*(t), \lambda^*(t), t) \leq H(x(t), u(t), \lambda(t), t)$$

The following relations and constraints (5.33) must hold with the above condition;

$$\left.\begin{aligned} \dot{x}^*(t) &= \frac{\partial H}{\partial \lambda}(x^*(t), u^*(t), \lambda^*(t), t) \\ \dot{\lambda}^*(t) &= -\frac{\partial H}{\partial x}(x^*(t), u^*(t), \lambda^*(t), t) \end{aligned}\right\} \tag{5.33}$$

Initial condition x_0 and final condition $\left[H^* + \frac{\partial S}{\partial x}\right]_{t_f} \partial t_f + \left[(\frac{\partial S}{\partial x})_* - \lambda^*(t)\right]'_{t_f} \delta x_f$ both are assumed to be zero. If PMP conditions are satisfied, the solution will be extremal and if a global solution exists, it will be the global solution.

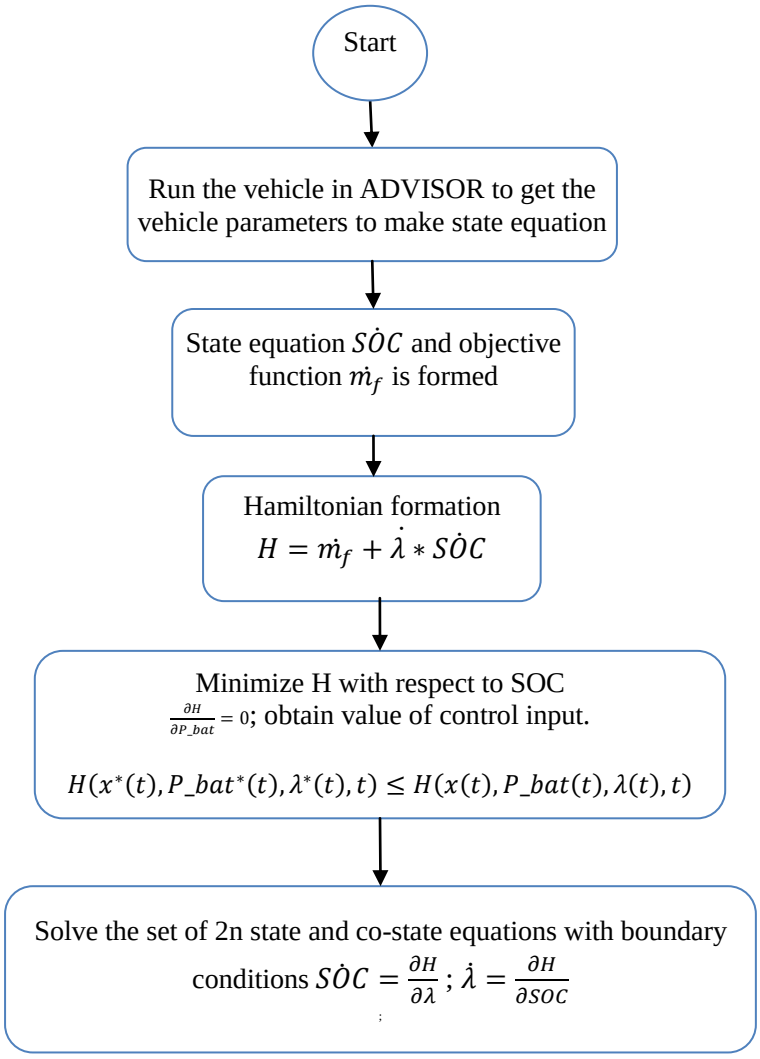

Figure 5.18: PMP process flow

In ADVISOR, Using GA and PMP the power optimization strategy is developed as shown in figure 5-19.

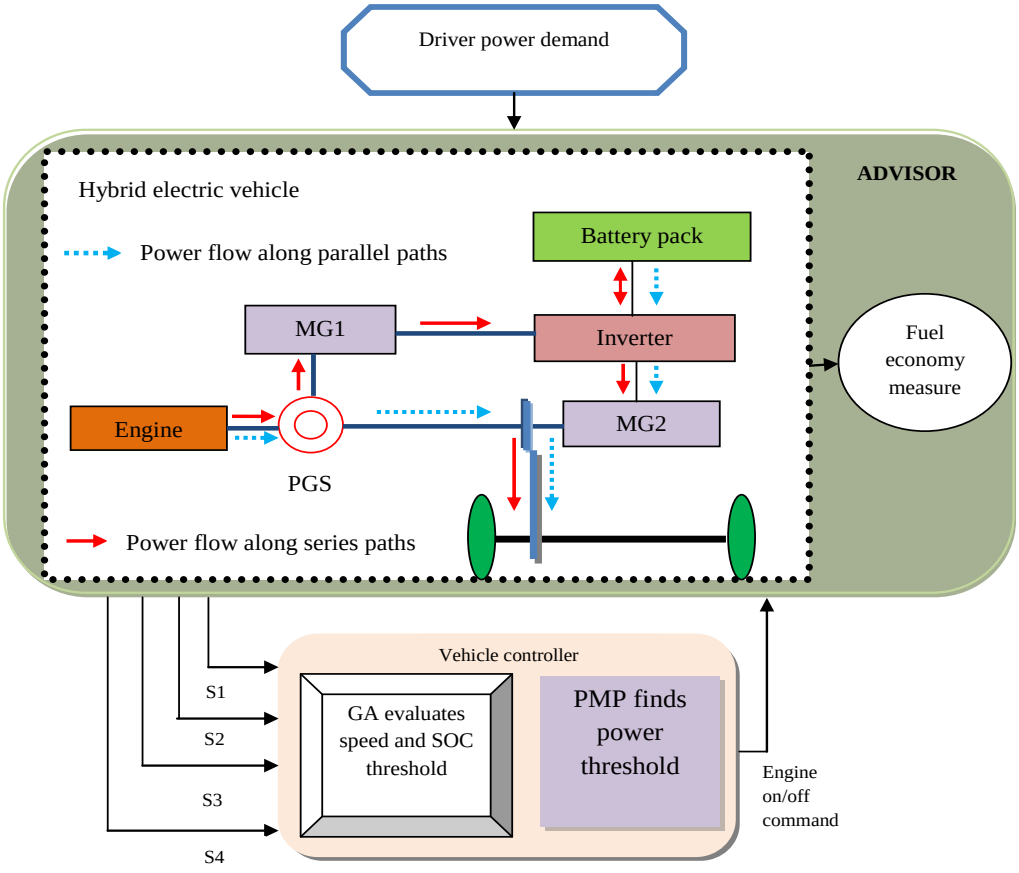

Figure 5.19: Energy management using GA and PMP

5.9.2 State Formation

To distribute the power between engine and motor, torque and speed requirements of driver and SOC play the role of control inputs. Torques and speeds are controlled using certain laws explained in section 5.2 and 5.3. SOC should be considered as unknown control input useful to toggle between engine and motor. SOC is the unknown trajectory obtained after the optimization so battery should be modeled as a dynamical system. And, it can be described as a first order differential equation [225, 226]. First order differential equation of SOC is explained by (5.23) and (5.24).

5.9.3 Observations

Various governing parameters of vehicle are firstly optimized using GA and then a power threshold calculation is performed using PMP. Calculation of thresholds initially using

GA gives a better chance to improve the fuel efficiency. Here, fuel efficiency is derived for different battery models incorporating modified and conventional SOC estimation methods. Fuel efficiency comparison for different battery models with GA and without GA application is shown in table 5.13. By considering all 5 governing parameters, the fuel efficiency of model 2 is improved from 52.8 mpgge to 60.62 mpgge using PMP and criteria of no trace miss is also met. PMP provides an improved result compared to default SOC estimation method. Application of GA has made the fuel economies even better compared to alone PMP. Because GA gets the optimum values of other power train parameters whereas PMP finds the threshold level for power only. As discussed in part 1, five important parameters are selected here to control the engine on/off conditions. The pictorial representation of these is given in figure 5.20.

Table 5.13: Fuel economy comparison for different battery models

Battery model	**Fuel economy (mpgge)**			**Trace analysis**
	With GA	**Without GA**	**Improvement (%)**	
R_{int} conventional model	55.92	44.97	24.32	With trace miss
Model 1*	60.62	51.37	18.00	Without trace miss
* with modified SOC estimation method				

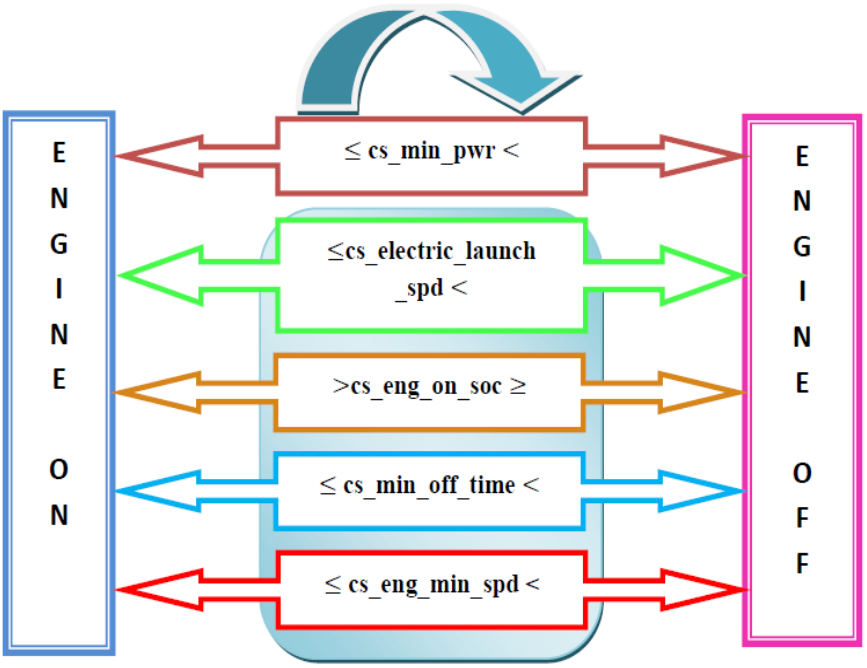

Figure 5.20: Engine on/off decision pictorial representation

To verify the correctness of proposed strategy, requested speed and delivered speed of the vehicle is compared and shown in figure 5.21. The figure infers that these two matches perfectly and there is no trace miss. Vehicle requested power is fulfilled by different components alone or together. Figure 5.5 signifies the time instances of negative torque, i.e. kinetic energy $(=\frac{1}{2}MV^2)$ stored in vehicle's translating mass can be recuperated during these moments. The traction motor operates as generator to recuperate the energy and charges battery as shown in figure 5.22. Positive current flow delivers the current from the battery and negative current signifies the state of battery charging.

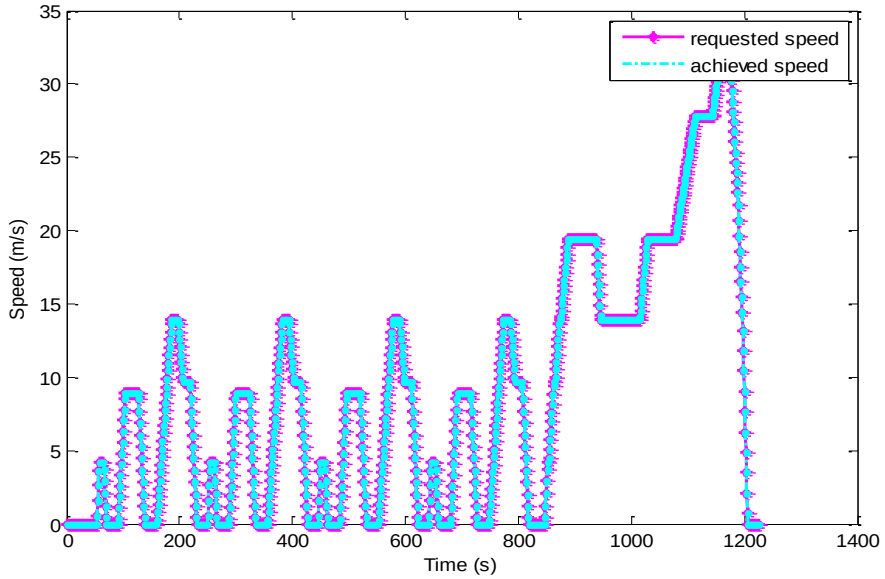

Figure 5.21: Vehicle requested and delivered speed comparison

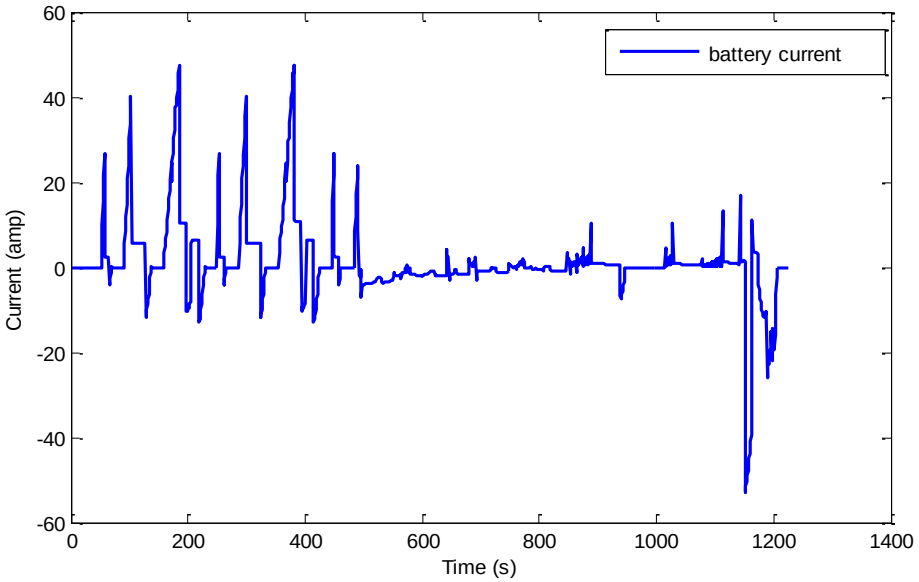

Figure 5.22: Battery current variation

Battery SOC variation over the trip is shown in figure 5.23 at 25ºC with initial SOC as 80 percent and target as 70 percent. An increment in the battery charge (with negative current) is either by engine (to fulfil target SOC requirement) or through regenerative braking (whenever negative torque exists).

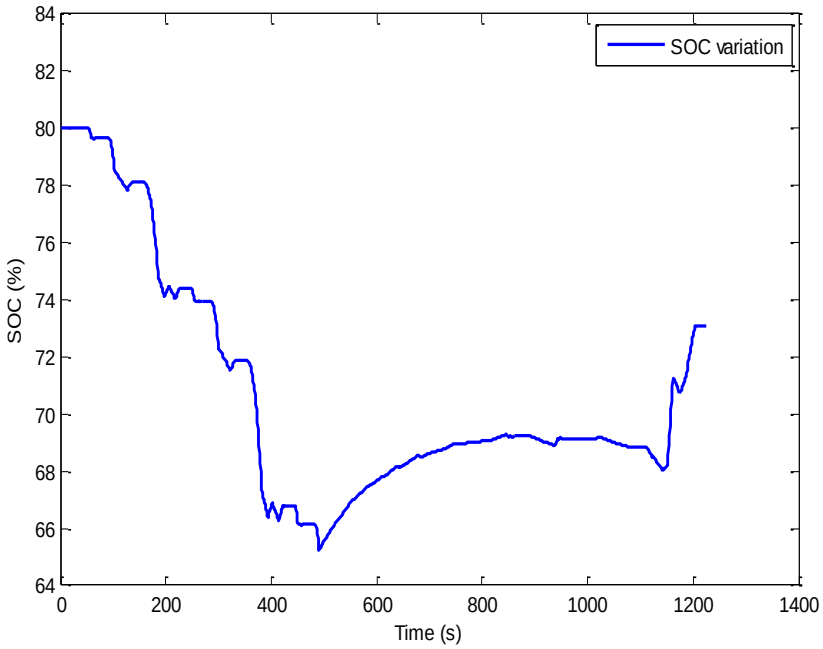

Figure 5.23: SOC variation over the trip

Figure 5.24 shows a combined plot of SOC variation with engine on/off condition. When engine is off in section 1, SOC is decreasing. SOC is constant also in section 1, shows that the speed requested is zero. In section 2, engine is on and battery is charging through generators. When motor is supporting engine during cruising, SOC is decreasing. In section 3, requested speed is zero and engine is off also so no decrease in SOC is observed. Figure 5.25 if analyzed corresponding to figure 5.24, in section 1 engine is off so no fuel is used, in section 2 engine is on fuel usage in liters is keep on increasing and in section 3 its again zero because engine is off. Figure 5.21 and figure 5.23 to 5.26 all synchronized with the driver's demand and supply, proves the suitability of algorithm and control strategy. Table 5.14 collects the time in seconds of trip and actions taken by engine and motor with SOC variation over the entire trip with a closer look.

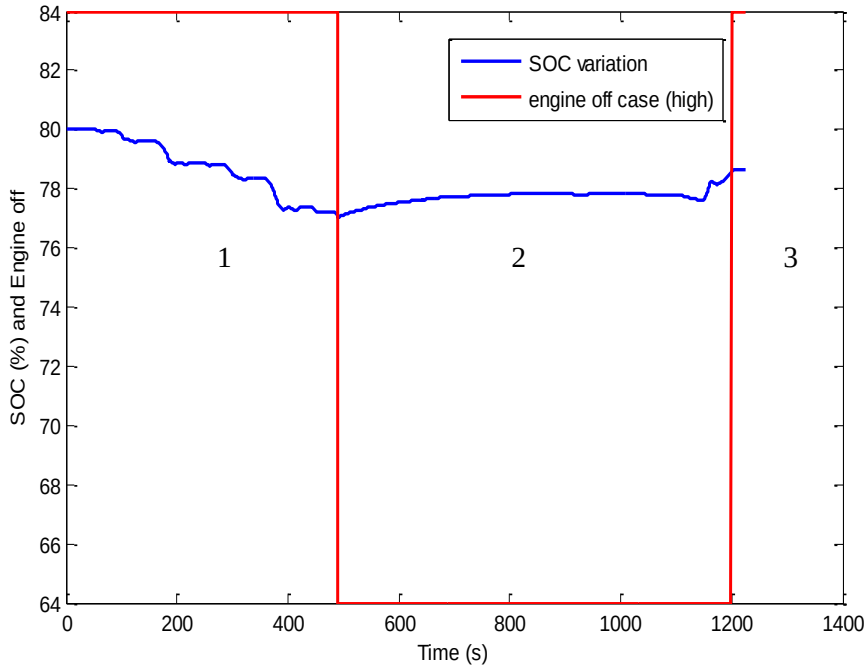

Figure 5.24: SOC variation with engine on/off condition

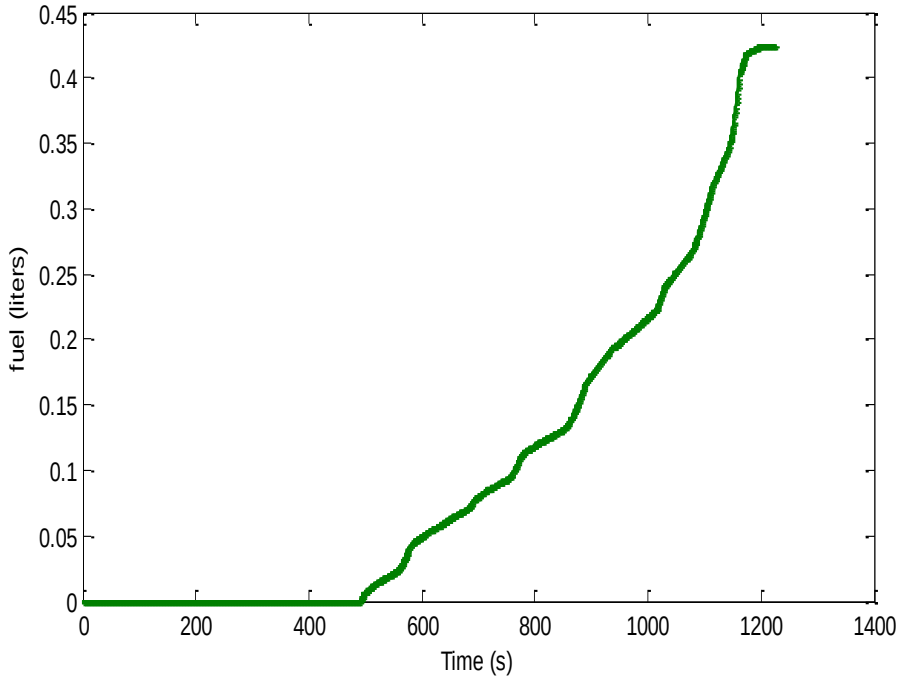

Figure 5.25: Fuel used in liters

Figure 5.24 (a) and (b) shows the engine and motor efficiency points and promise to work in most efficient range possible while acquiring the trace and maintaining SOC.

Table 5.14: Trip analysis with engine and motor state consideration

Time (s)	Engine or motor on/off	Torque analysis	Trend in SOC variation
1-53	Engine off and motor on	Zero	No change
54-65		Positive	Decrease
66-77		Negative	Increase
78-91		Zero	No change
92-128		Positive	Decrease
129-138		Negative	Increase
139-159		Zero	No change
160-197		Positive	Decrease
198-206		Negative	Increase
207-218		Positive	Decrease
219-230		Negative	Increase
231-249		Zero	No change
250-261		Positive	Decrease
262-266		Negative	Increase
267-287		Zero	No change
288-323		Positive	Decrease
324-334		Negative	Increase
335-355		Zero	No change
356-395		Positive	Decrease
396-401		Negative	Increase
402-414		Positive	Decrease
415-426		Negative	Increase
427-445		Zero	No change
446-457		Positive	Decrease
458-462		Negative	Increase
463-483		Zero	No change
484-490		Positive	Decrease
491-847	Engine on and motor off	Positive	Increase
848-859	Engine on and motor on		Decrease
860-873	Engine on and motor off		Increase
874-877	Engine on and motor on		Decrease
878-887	Engine on and motor off		Increase
888-938	Engine on and motor on		Decrease
939-946	Engine on and motor off	Negative	Increase
947-1014	Engine on and motor on	Positive	Decrease
1015-1028	Engine on and motor off		Increase
1029-1144	Engine on and motor on		Decrease
1145-1163	Engine on and motor off	Positive	Increase
1164-1172	Engine on and motor on		Decrease
1173-1199	Engine on and motor off	Negative	Increase
1200-1206	Engine off and motor off		
1207-1226	Engine off and motor off	Zero	No change

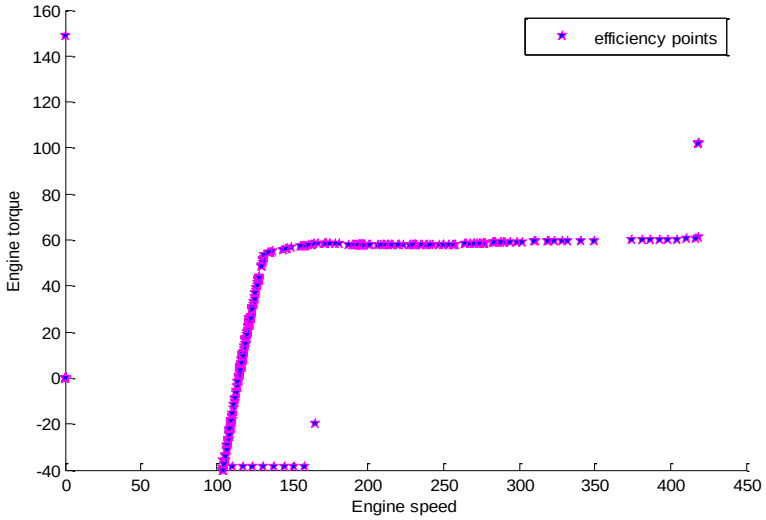

(a)

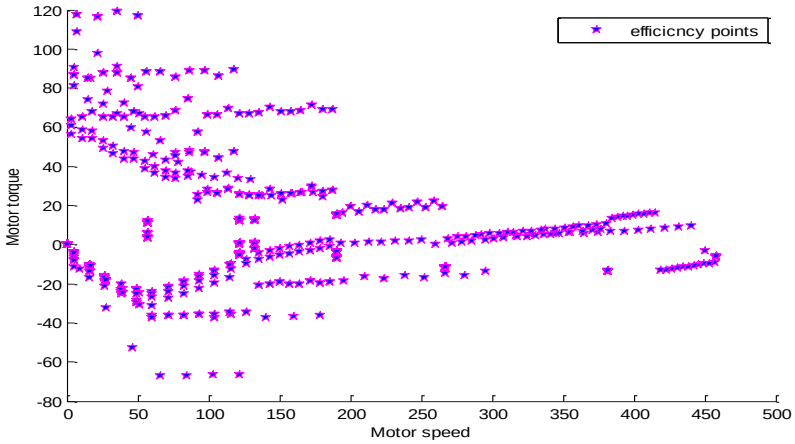

(b)

Figure 5.26: Operating points; (a) engine and (b) motor

5.10 Impact of Engine Idling

Running the engine when vehicle is not moving, is called idling. This condition arises when a vehicle is at red light or waiting while parked. In case of idling engine is on, runs at idle speed and power only engine accessories. The idle speed is the rotation speed when engine is decoupled from the drive train and throttle position is not depressed. An important fact is that engine whether supporting power train or in idling state, emit pollutants and consumes fuel. So, to save fuel and to keep air healthier, idling of engine should be prohibited if possible. A controller collects the information, whether battery need charging, air conditioner need to support, climate control is required, engine or

catalyst temperature are balanced or not and based on these decides to idle the engine [227]. Performance analysis of HEVs including idling is discussed in literature [228, 229, 230]. Interest in exploring the effect of idling and engine shut down rather, and its impact on fuel economy goaded to perform a comparison between these two cases. The results for proposed model are tabulated with and without idling in table 5.15. By excluding the trace miss cases, an improvement in fuel economy of 4 to 4.5 percent on an average is achieved. But, turning the engine on and off very often can reduce the life of engine components.

Table 5.15: Effect on fuel economy with avoided engine idling condition

Set name	With idling	Trace miss analysis	Without idling	Trace miss analysis
Set of 1 individual parameter	51.37	Trace miss persist	53.84	Trace miss persist
	59.80	Trace miss don't exist	53.86	Trace miss don't exist
	51.37	Trace miss persist	54.01	Trace miss persist
	51.40	Trace miss persist	53.84	Trace miss persist
	47.33	Trace miss don't exist	53.84	Trace miss don't exist
Set of 2 parameters	60.74	Trace miss don't exist	69.22	Trace miss don't exist
	51.37	Trace miss persist	53.75	Trace miss persist
	43.93	Trace miss don't exist	48.13	Trace miss don't exist
	51.37	Trace miss don't exist	53.84	Trace miss don't exist
	60.74	Trace miss don't exist	63.48	Trace miss don't exist
	67.52	Trace miss persist	67.03	Trace miss persist
	69.59	Trace miss persist	63.68	Trace miss persist
	51.40	Trace miss persist	53.84	Trace miss persist
	51.37	Trace miss persist	53.97	Trace miss persist
	51.40	Trace miss persist	53.84	Trace miss persist
Set of 3 parameters	65.78	Trace miss persist	70.32	Trace miss persist
	65.83	Trace miss persist	70.92	Trace miss persist
	65.60	Trace miss persist	70.32	Trace miss persist
	53.56	Trace miss don't exist	53.89	Trace miss don't exist
	51.37	Trace miss persist	53.97	Trace miss persist
	53.51	Trace miss don't exist	53.74	Trace miss don't exist
	65.82	Trace miss persist	69.66	Trace miss persist
	65.70	Trace miss persist	69.67	Trace miss persist
	65.82	Trace miss persist	69.69	Trace miss persist
	51.40	Trace miss persist	53.80	Trace miss persist
Set of 4 parameters	70.65	Trace miss persist	75.29	Trace miss persist
	70.65	Trace miss persist	75.29	Trace miss persist
	65.82	Trace miss persist	69.67	Trace miss persist
	69.81	Trace miss persist	69.67	Trace miss persist
	60.79	Trace miss don't exist	63.47	Trace miss don't exist
Set of 5 parameters	52.25	Trace miss don't exist	54.07	Trace miss don't exist

5.11 Summary

Battery modeling and SOC estimation methods are the roots of HEV functioning and play an important role in determining its performance. Their accurate knowledge greatly

decides the engine on/off condition. Available literature talks about various battery models and methods of SOC estimation, but only R_{int} battery models and current based SOC estimation methods are widely used. In this work, various battery models are explored along with modified SOC estimation method to analyze the vehicle performance. Various governing parameters of HEVs are considered in optimization and their optimum values are evaluated using GA and DIRECT based control strategies. The application of GA further improves the fuel economy significantly over classical method. Model 2 and 3 show better fuel economy over battery model 1. Based on the results, model 2 along with modified SOC estimation method should be used further to achieve better HEV performance.

While implementing the strategy, all the important consideration like aerodynamic drag, vehicle glider mass, accessory loads and prescribed SOC level conditions, etc are given utmost attention. PMP along with GA and with modified SOC estimation techniques presents promising energy management system. Various governing parameters of vehicle are firstly optimized using GA and then a power threshold calculation is performed using PMP. Calculation of thresholds initially using GA gives better chance to improve the fuel efficiency.

The performance of the battery varies with the load and temperature, which can be approximated to the nearby true value using a correction factor derived in chapter 3. Temperature variation affects the current, voltage and SOC of the battery which affects the engine transition (on/off) decisions. Effect of temperatures is analyzed to restrict the operating range of the vehicle to achieve the fuel efficient performance along with the longer battery life. As SOC estimation is promising, the proposed method may provide the real time values of fuel economies. At lower temperature fuel economies are lesser and at higher temperature these are high compared to the room's temperature, thus verify the theory of temperature effect on rate of reaction of battery cell. Vehicle performance varies abruptly other than nearby room temperatures and at higher temperature fuel economies are found to be better compared to the lower temperature. But, usage of battery at high temperatures for longer time reduces its life and diminishes vehicle performance.

Chapter 6
Effect of Driving Cycles on HEV Performance

This chapter aims to find the nature and response of a hybrid vehicle on various standard driving cycles. Road profile parameters play an important role in determining the fuel efficiency. Typical parameters of road profile can be reduced to a useful smaller set using principal component analysis and independent component analysis. Resultant data set obtained after size reduction may result in more appropriate and important parameter cluster. With reduced parameter set fuel economies over various driving cycles, are ranked using TOPSIS and VIKOR multi-criteria decision making methods. The ranking trend is then compared with the fuel economies achieved after driving the vehicle over respective roads. Control strategy responsible for power split is optimized using genetic algorithm. Model 2 and modified SOC estimation method are considered for the simulation and improved results compared to default are obtained.

6.1 Need of Driving Cycle Analysis for Fuel Economy Interpretation

HEV's performance will obviously vary over type of road, driver's aggressiveness/behavior, road conditions and weather conditions. Kuhlar [231] and Karstens and Fomunung [232] introduced few parameters which characterize the roads. These parameters have been used to model emissions or fuel economies or others.

These parameters may be able to describe a driving cycle (DC) behavior, but are not able to clearly identify a DC which would result in the best fuel economy (FE). The aim of the study is to find independent parameters of DC able to define the FE. Using size reduction techniques, the few governing parameters are selected and with these parameters DCs are ranked using TOPSIS and VIKOR. Now, the vehicle is run over the different considered DCs to find out their FE using genetic algorithm based control strategy and then ranked accordingly. These two results are compared to get a sense that how DC parameters are linked with FE.

Ten parameters (trip time, average speed, maximum deceleration, average acceleration, idle time during the trip, number of stops, distance, maximum speed,

maximum acceleration and average deceleration) are considered in most of the literatures for DC characterization. These parameters for seven different DCs of city profile are collated in table 6.1. For ease of analysis, numbers of parameters are reduced here. Principle component analysis (PCA) and independent component analysis (ICA) are dimension reduction techniques, but retain the important properties of dataset. PCA developed by Karl [233] and Hotelling [234] is a statistical procedure to un-correlate the variable and reduce the dimension of the data. PCA yields orthogonal vectors of high energy content in terms of covariance. ICA also decomposes the variables into smaller sets and extracts the independent variables from a multivariate dataset. ICA was developed by Jueten and Herault [235] and Comon [236] used to solve cocktail party problems and for blind source separation.

Table 6.1: City driving cycle characteristics

Parameters	UDDS	ECE_EUDC	LA92	US06	Indian	Japan 10-15	WVUCITY
Time (s)	1369	1225	1435	600	2689	660	1408
Distance (miles)	7.45	6.79	9.82	8.01	10.87	2.59	3.3
Maximum speed (mph)	56.7	74.56	67.2	80.3	38.87	43.48	35.82
Average speed (mph)	19.58	19.95	24.61	47.97	14.54	14.09	8.44
Maximum acceleration (ft/s^2)	4.84	3.46	10.12	12.32	5.68	2.6	3.75
Maximum deceleration (ft/s^2)	-4.84	-4.56	-12.91	-10.12	-6.9	-2.73	-10.62
Average acceleration (ft/s^2)	1.66	1.78	2.21	2.2	1.06	1.87	0.97
Average deceleration (ft/s^2)	-1.9	-2.59	-2.47	-2.39	-1.29	-2.12	-1.27
Idle time (s)	259	339	234	45	267	215	427
No of stops	17	13	16	5	52	7	14

Out of these parameters some need to be maximized and the others should be minimized according to their role in defining fuel economy. This requires MCDM measures. Based on the obtained reduced parameters by PCA and ICA, TOPSIS and VIKOR, which are valuable MCDM methods, are applied here to rank the DC in order of their FE.

Further, to support the analysis obtained by these methods, an intelligent power split control strategy is developed using GA to split power between engine and the battery. To control the engine on/off threshold values of governing parameters' values (which are responsible for power split) are obtained using optimization techniques and fuel economy is determined.

6.2 Feature extraction of Driving Cycles

Table 6.1 lists the parameters of seven DCs of city profile considered for study. To extract features of these DCs, PCA and ICA methods are used and explained in the subsequent sections. PCA and ICA are actually performed over 23 different types of DCs and have data strength of [10x23], including the seven used here.

6.2.1 Principal Component Analysis

PCA is useful to the dataset which heavily rely on Gaussian features and utilizes first and second moments of measured data. For the feature extraction, PCA is applied over 23 different DCs and have length of [10x23], including urban and highway. PC8 onward all PCs are zero. PC1, PC2 and PC3 are significant and are considered for interpretation of data. The first principal component PC1 is strongly correlated with eight of the original variables. PC1 can be viewed as a measure of 1) distance, 2) average speed, 3) maximum acceleration, 4) maximum deceleration, 5) average acceleration, 6) average deceleration and 7) number of stops. It would follow that the DCs with good fuel economy would tend to have lesser average speed, maximum acceleration, average acceleration and higher value of maximum deceleration, average deceleration and number of stops. The second principal component (PC2) increases with only one of the values i.e., decreasing distance. This component can be viewed as a measure of how less the distance is covered by vehicle on a driving cycle. The third principal component (PC3) increases if the idle time in the driving cycle increases. This recommends that greater the idle time, the greater the fuel economy. PCs are unit vectors and are orthogonal identity matrix. Identification of the variables of driving cycle through PCA will help to find the required data proved to be useful while analyzing the fuel economy of any vehicle over different driving cycles.

6.2.2 Independent Component Analysis

For the hidden feature extraction, ICA is also used and is popular technique. ICA is statistical and computational technique to identify the meaningful hidden features. Here, ICA is applied on [10x23] size data set where 23 different cycles and 10 different parameters of driving cycles are considered. In contrast to PCA, ICA extracts six parameters significant for the analysis. ICA finds contribution of six parameters of DCs

to be most informative out of ten named as trip time, average speed, maximum deceleration, average acceleration, maximum acceleration and idle time during the trip.

6.3 Nature Identification of Driving Cycles

The driving cycle is the speed trace at each time instant. To know the nature of DCs, probability distribution functions of these are determined. The mean and standard deviations (SD) of the distributions are recorded and listed in table 6.2. It can be observed that no DC follows a normal distribution with mean=0 and SD=1. This enables us to choose ICA for feature extraction as this is fit for non-Gaussian data set. Various DC distributions are plotted in figure 6.1.

Table 6.2: Mean and standard deviations of various distributions

Driving cycle	Mean (Location parameter)	Standard deviation (Scale parameter)	Distribution type
INDIAN	-3.1518	33.79	Generalized Pareto
UDDS	4.2804	5.0278	Gumbel maximum
ECE_EUDC	-1.7264	22.386	Johnson SB
LA92	-1.7373	35.69	Johnson SB
WUVCITY	1.3645	2.4398	Generalized extreme value
US06	-5.1976	80.503	Generalized Pareto
JAPAN 10-15	-1.7264	22.386	Johnson SB

It is observed; DCs chosen here follow non-Gaussian distribution. So, for the feature extraction, techniques useful for non-Gaussian type of data set should be applied. ICA can be used to extract the useful information.

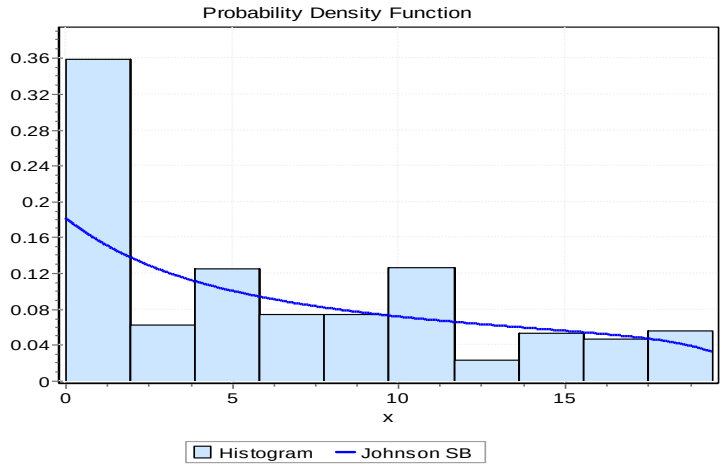

(a)

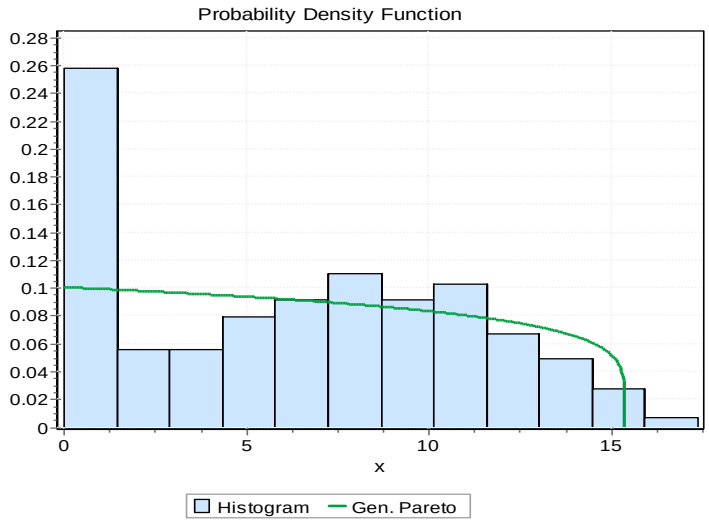
Probability Density Function
0.28
0.26
0.24
0.22
0.2
0.18
0.16
0.14
0.12
0.1
0.08
0.06
0.04
0.02
0
0
5
10
15
x
Histogram
Gen. Pareto

(b)

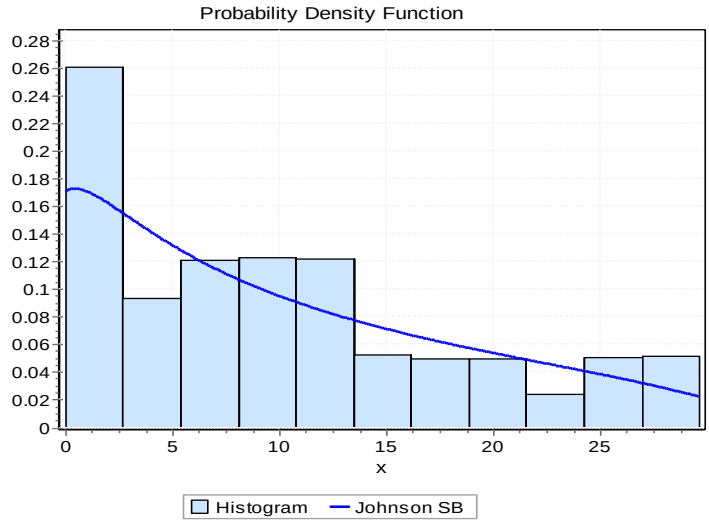
Probability Density Function
0.28
0.26
0.24
0.22
0.2
0.18
0.16
0.14
0.12
0.1
0.08
0.06
0.04
0.02
0
0
5
10
15
20
25
x
Histogram
Johnson SB

(c)

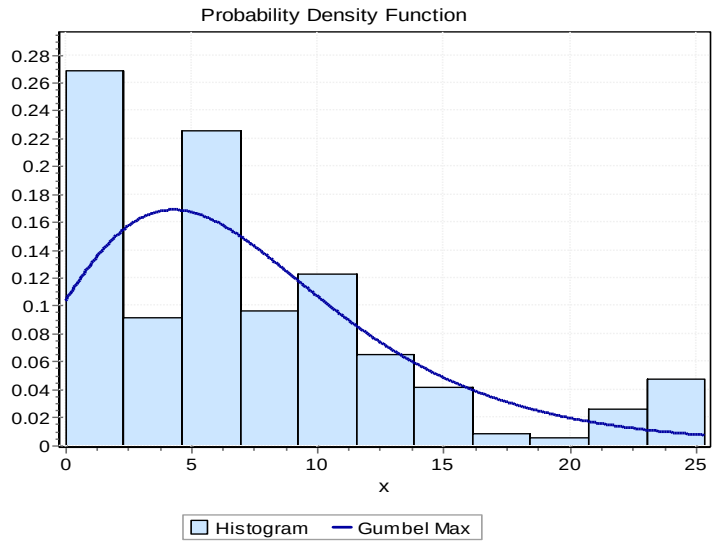
Probability Density Function
0.28
0.26
0.24
0.22
0.2
0.18
0.16
0.14
0.12
0.1
0.08
0.06
0.04
0.02
0
0
5
10
15
20
25
x
Histogram
Gumbel Max

(d)

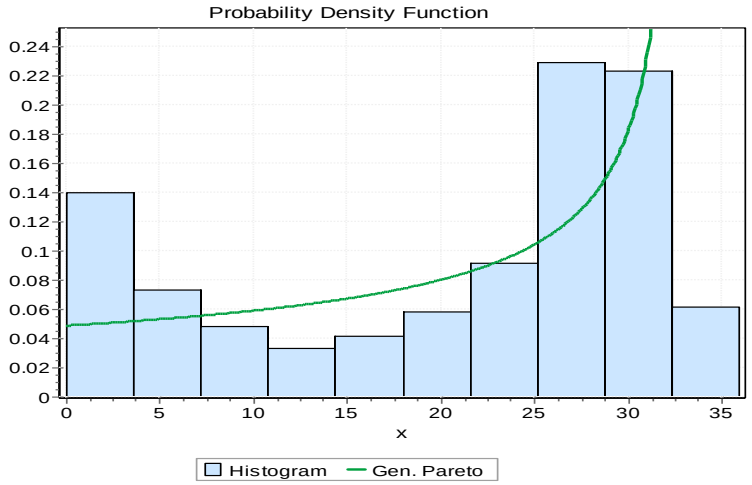

(e)

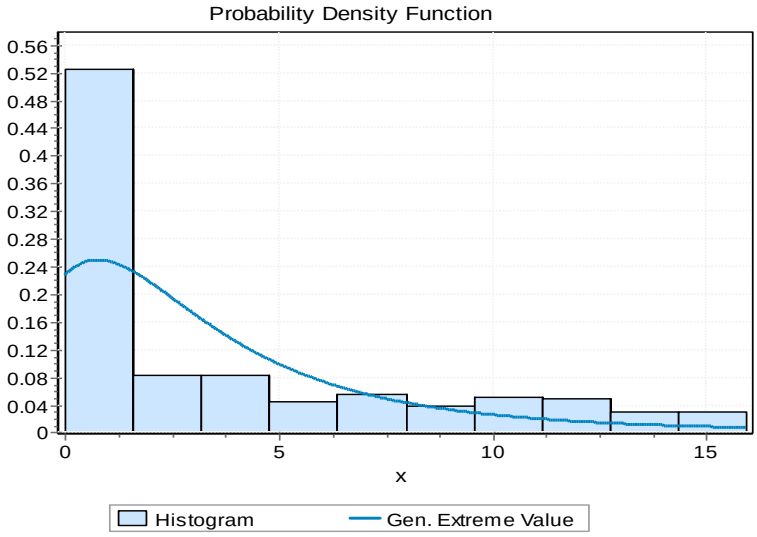

(f)

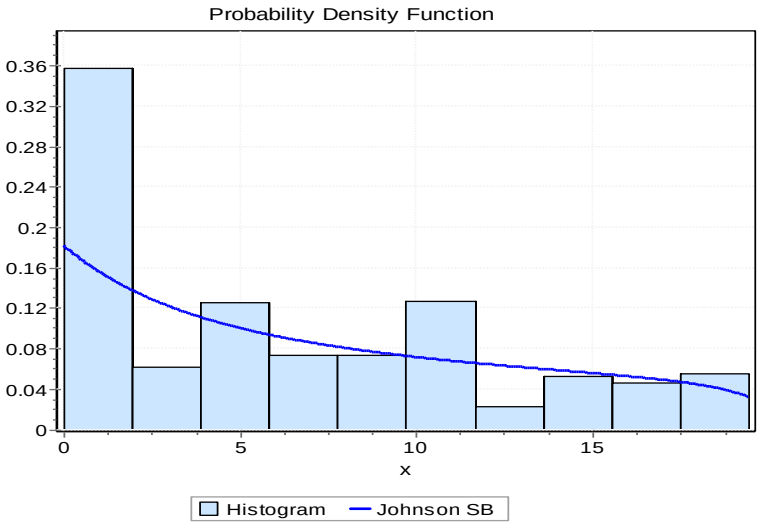

(g)

Figure 6.1: Probability distribution plots of DCs, (a) ECE_EUDC (b) INDIAN (c) LA92 (d) UDDS (e) US06 (f) WVUCITY (g) JAPAN 10-15

6.4 Ranking Method Implication

In order to rank DCs for fuel economy, TOPSIS and VIKOR methods are applied here. VIKOR is multi-criteria optimization and a compromise solution method. It was developed by Opricovic and Tzeng [38, 41, 237]. The method is based on ranking and selecting the alternatives from a set of conflicting norms. Each alternative is estimated according to each criterion function. Ranking is performed by comparing the gauge of closeness to the ideal alternative.

TOPSIS is a multi attribute decision making method. It is used for measuring relative efficiencies of alternatives. Yoon and Hwang [36] and Yoon [37] introduced the TOPSIS method. It is based on the scheme that the prominent alternative has the shortest distance from the ideal solution. If each attribute takes a monotonically escalating or falling variation, ideal solution can be defined simply. Such a solution is composed of all the best attributes' values achievable. Worst solution will be composed of all the worst attributes' values achievable. The shortest distance from the ideal solution in the Euclidean space is the best solution. It may concurrently have the farthest distance from negative ideal solution [39]. So, TOPSIS method chooses the solutions those are all together close to the ideal solution.

VIKOR and TOPSIS are applied to the extracted features from ICA and PCA to rank various DCs in order to get estimation about their FEs without running a vehicle. The results for VIKOR and TOPSIS with ICA and PCA are tabulated in table 6.3. The results infer that Indian DC is getting invariably first position with all the ranking methods. Hence, Indian road conditions are proven to be better for HEVs as they will consume lesser liquid fuel and will further minimize the pollutant emissions. The low acceleration rate, lower speed and frequent start/stops prompt the motor to work more and keep the engine in shut off condition or operate in its most efficient region. This becomes a favorable condition for an efficient HEV. Although other DCs are not found to be same ranked as FE are achieved. A close observation of LA92, UDDS, WVUCITY and ECE_EUDC reveals that most of their parameters are very close to each other, hence taking VIKOR/TOPSIS towards the unintended ranking level.

Table 6.3: Driving cycle ranking by VIKOR and TOPSIS

VIKOR with PCA	VIKOR with ICA	TOPSIS with PCA	TOPSIS with ICA	FE ranking
Indian	Indian	Indian	Indian	Indian
WVUCITY	LA92	WVUCITY	LA92	UDDS
JAPAN 10-15	UDDS	JAPAN 10-15	WVUCITY	ECE_EUDC
UDDS	WVUCITY	UDDS	UDDS	LA92
LA92	ECE_EUDC	ECE_EUDC	ECE_EUDC	WVUCITY
ECE_EUDC	US06	LA92	US06	US06
US06	JAPAN 10-15	US06	JAPAN 10-15	JAPAN 10-15

6.5 Analysis of Fuel Economy over Different Driving Cycles

The presence of two power sources in HEVs focuses on the need of designing an energy management strategy to split power between them. The strategy should be able to minimize the fuel consumption and maximize the power utilization. Fuel economy of Toyota Prius over considered city driving cycles is performed in ADVISOR.

From chapter 5, part 4 discussion model 1 is chosen to use here. Threshold values of deciding parameters, responsible to turn on/off the engine are estimated using GA and fuel economies are recorded. Table 6.4 records the threshold values of 'cs_eng_on_soc', 'cs_min_off_time', 'cs_min_pwr', 'cs_electric_launch_spd' and 'cs_eng_min_spd' obtained after GA simulations. Table 6.5 collects the efficiencies of engine, motor and generator and the fuel economy over various DCs with the threshold values obtained in table 6.4. Among all the driving cycles, Indian urban driving cycle is giving best fuel economies. India being the land of opportunities for automotive industries to invest, the favorable road conditions can be path breaking to bring HEVs on Indian roads as a part of NMEM.

Table 6.4: Optimized parameter values of drive cycles using GA

Drive cycle	SOC (%)	Off time (s)	Power (watt)	Electric speed (rad/s)	Engine speed (rad/s)
UDDS	39.65	9.61	9276.9	10.79	209.43
ECE_EUDC	33.08	6.10	6805.9	12.48	281.66
LA92	38.91	4.26	9306.6	11.08	254.23
US06	38.01	9.80	9318.6	10.63	254.92
Indian	33.60	6.70	9280.2	10.88	252.97
Japan 10-15	33.10	9.71	9762.3	10.64	230.53
WVUCITY	39.11	2.13	9128.3	10.07	230.12

Table 6.5: Efficiency evaluation of components using GA

Drive cycle	Engine efficiency (%)	Motor efficiency (%)	Generator efficiency (%)	Fuel economy (mpgge)
UDDS	30.30	83.65	64.77	59.32
ECE_EUDC	27.32	81.67	92.46	52.25
LA92	31.48	82.59	67.22	48.18
US06	33.08	82.54	60.58	44.72
Indian	30.34	84.17	23.56	61.44
Japan 10-15	19.16	92.89	80.54	43.00
WVUCITY	21.07	79.39	74.63	46.99

Figure 6.2 shows the distance covered in a DC and time taken to complete the route. As time and distance both are more for Indian DC; it seems to have more fuel consumption as compared to others.

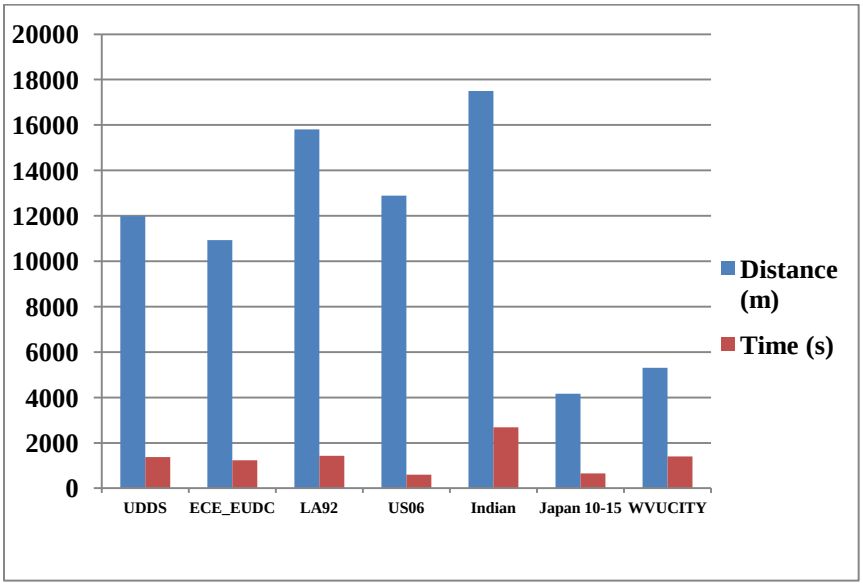

Figure 6.2: Distance covered and time duration of various drive cycles

But, figures 6.3, 6.4 and 6.5 show that average acceleration and average speed are lesser and the 'number of stops' are more for Indian DC as compared to others. If we look deeper into favorable working conditions of HEVs, it can be concluded that low acceleration rate, lower speed, frequent start/stops will motivate motor to work more and will keep the engine in shut off condition or operate in its most efficient region thus minimizing the fuel consumption to a great extent. Further, frequent start/stop will make generators recuperate more energy when the brakes are applied. Therefore, Indian road condition will offer lesser liquid fuel consumption and better utilization of hybridization concept.

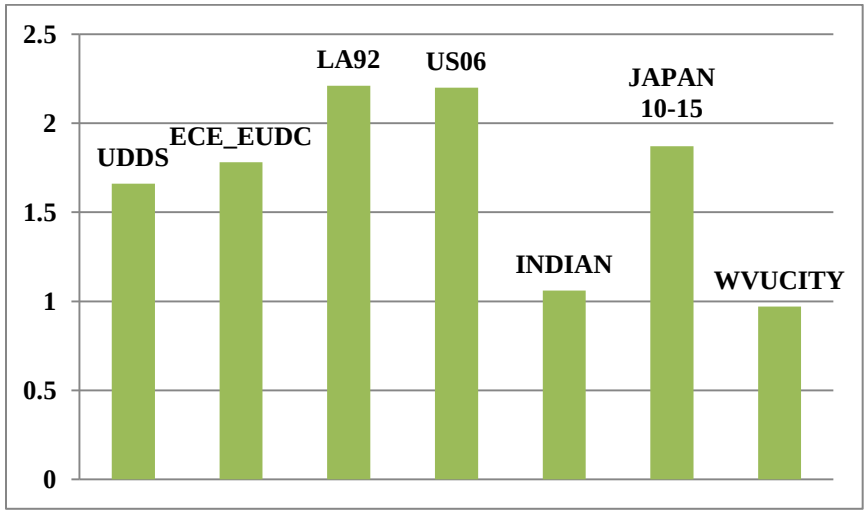

Figure 6.3: Average acceleration plot of various drive cycles

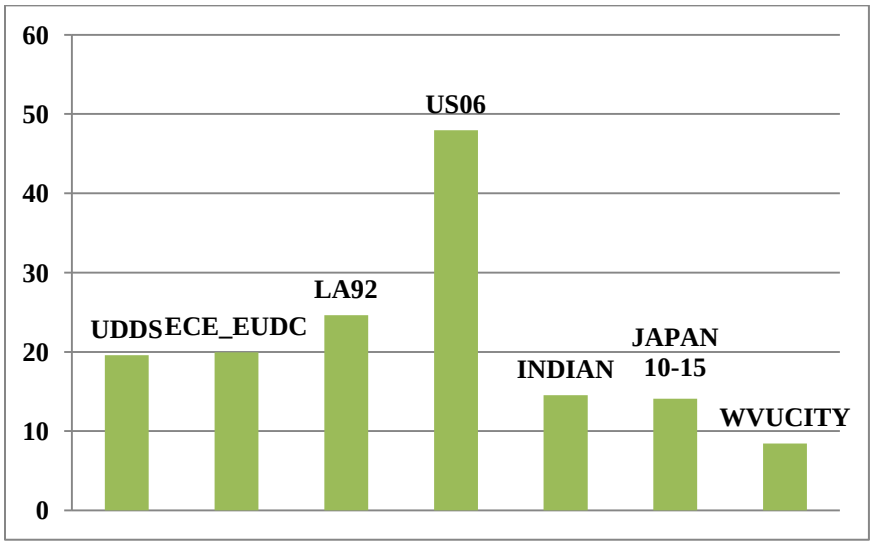

Figure 6.4: Average speed plot of various drive cycles

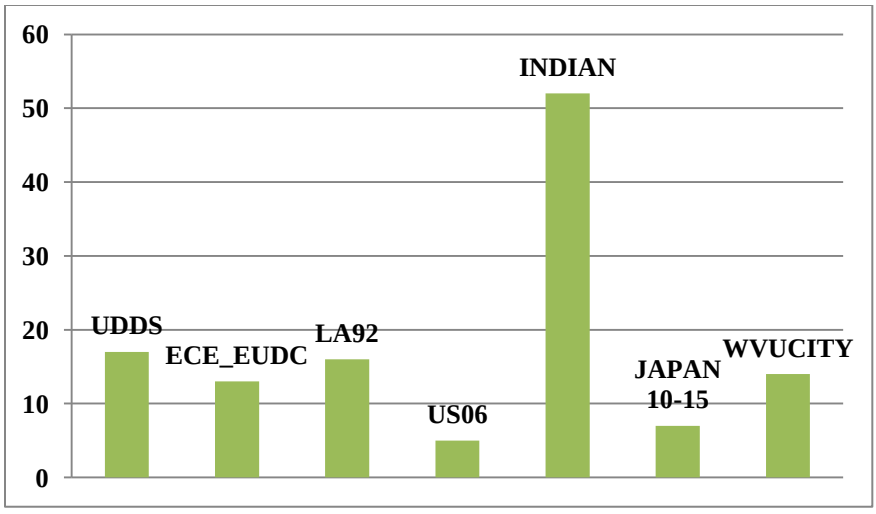

Figure 6.5: Number of stops for various drive cycles

Further simulations are performed with the modified SOC estimation algorithm which promises to give better results in terms of fuel efficiency and speed trace. Table 6.6 performs the comparison between 'default SOC estimation method' with 'R_{int} battery model' and modified SOC estimation method with proposed model 2. The modified SOC estimation algorithm is either improving fuel economy or trace or both.

Vehicle performance is varied much by the idling time of the trip. In general cases, idling are allowed at the stops, i.e., engine runs with some speed to give power to the accessories. But if, idle stopping is implemented (engine shut down rather) the significant amount of fuel can be saved. The comparative study of the fuel economy in case of idle stopping with zero engine speed and engine on is tabulated here. Results in table 6.7 show noteworthy improvement in fuel economies for all DCs and Indian DC is dominating. Two major reasons idle time and number of stops may play momentous functionality. Idle time is considerable, but a high number of stops will recuperate more kinetic energy which will motivate the vehicle to run more on electrical energy, hence improves fuel economy. Highest regenerative efficiency is obtained from Indian DC, shown in table 6.7. Regenerative efficiency is the ratio of energy captured during regenerative braking to the energy generated due to negative forces in a trip.

Table 6.6: Fuel economy comparison with default and modified SOC estimation method

Drive cycle	Fuel economy with default SOC estimation method and Rint model (mpgge)	Fuel economy with modified SOC estimation method and model 2 (mpgge)
UDDS	59 (with trace miss)	59.3291 (without trace miss)
ECE_EUDC	46.7 (without trace miss)	52.2579 (without trace miss)
LA92	44.3 (with trace miss)	48.1884 (without trace miss)
US06	42 (with trace miss)	44.7263 (without trace miss)
Indian	54.7 (with trace miss)	61.4473 (without trace miss)
Japan 10-15	41 (without trace miss)	43.00 (without trace miss)
WVUCITY	46.7 (with trace miss)	46.9988 (without trace miss)

Table 6.7: Fuel economy comparison with and without engine idling

Drive cycle	FE with EI (mpgge)	FE without EI (mpgge)	FE improvement (%)	Idling time (%)	No. of stops	Regenerative efficiency
UDDS	59.32	62.33	5.06	18.9	17	119.59
ECE_EUDC	52.25	54.05	3.44	27.6	13	-78.77
LA92	48.18	50.44	4.69	16.3	16	185.33
US06	44.72	51.58	15.3	7.50	5	217.77
Indian	61.44	85.32	38.8	9.92	52	250.30
Japan 10-15	43.00	44.45	3.37	32.5	7	-381.93
WVUCITY	46.99	48.74	4.61	30.3	14	-193.28

*EI=engine idling

6.5.1 Validation of Control Strategy

The suitability of the proposed control strategy is calculated through numerous simulations performed over different DCs repeated over diverse geographic provinces. The simulations are performed on model 2 with the modified SOC estimation method. In all instances, the demanded power and speeds are met and can be observed from figure 6.6.

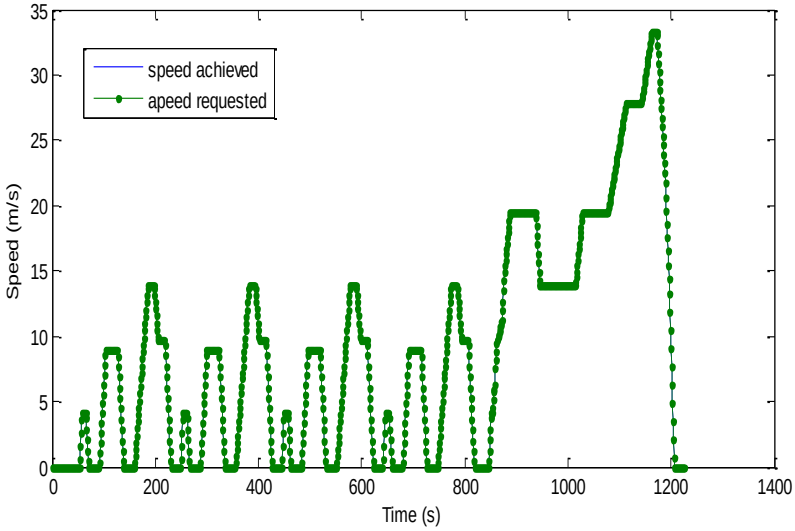

(a)

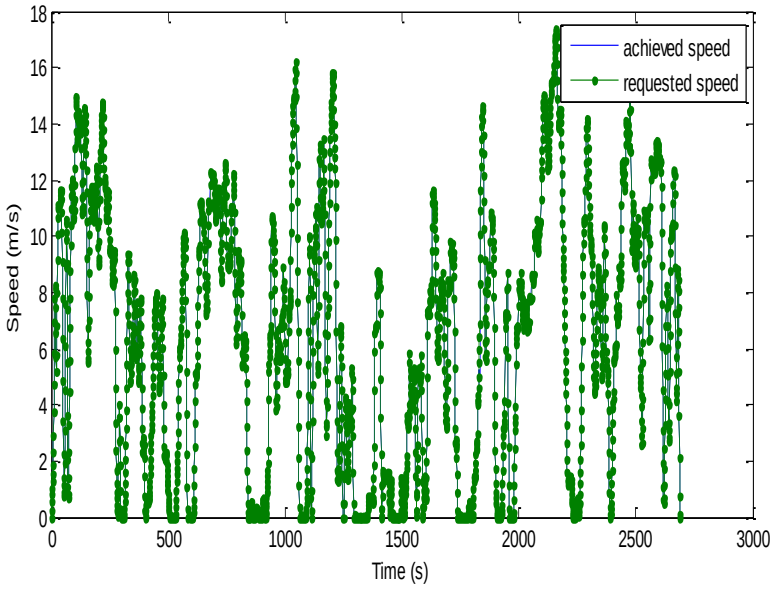

(b)

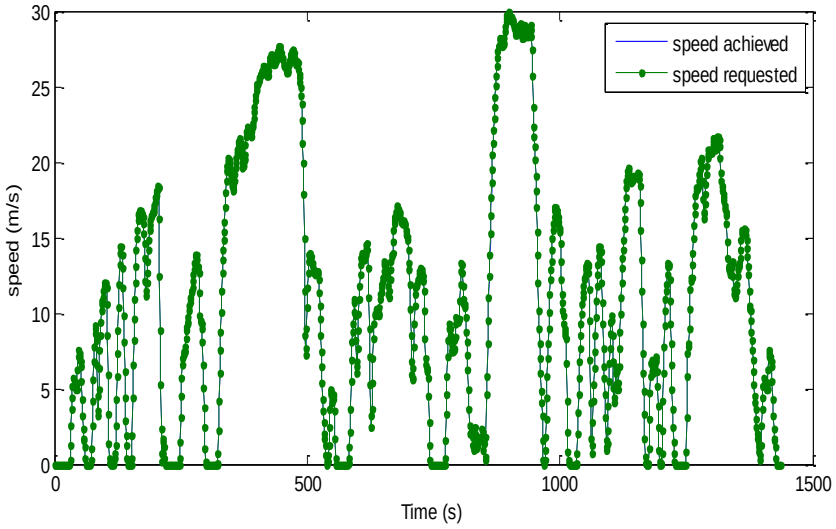
speed achieved
speed requested
speed (m/s)
Time (s)
0
5
10
15
20
25
30
0
500
1000
1500

(c)

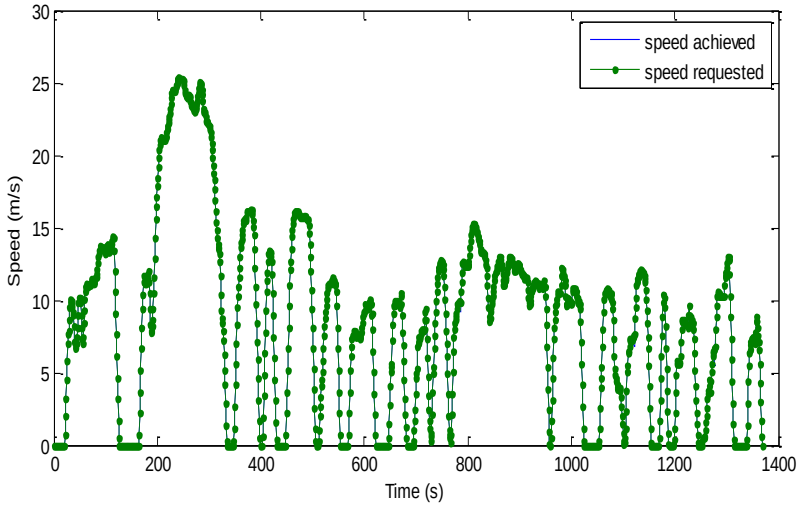
speed achieved
speed requested
Speed (m/s)
Time (s)
0
5
10
15
20
25
30
0
200
400
600
800
1000
1200
1400

(d)

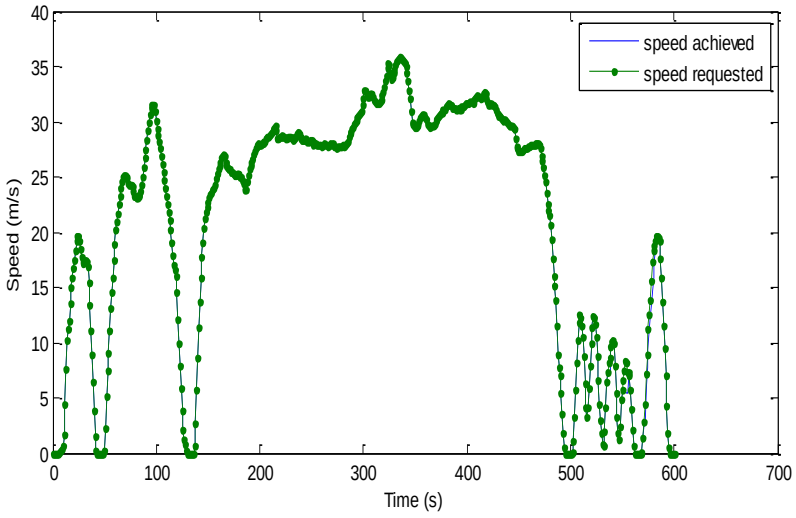
speed achieved
speed requested
Speed (m/s)
Time (s)
0
5
10
15
20
25
30
35
40
0
100
200
300
400
500
600
700

(e)

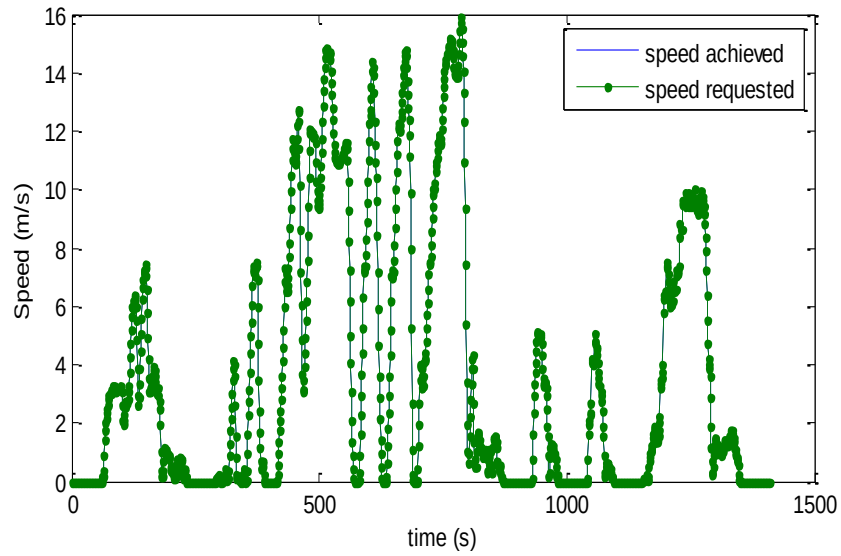

(f)

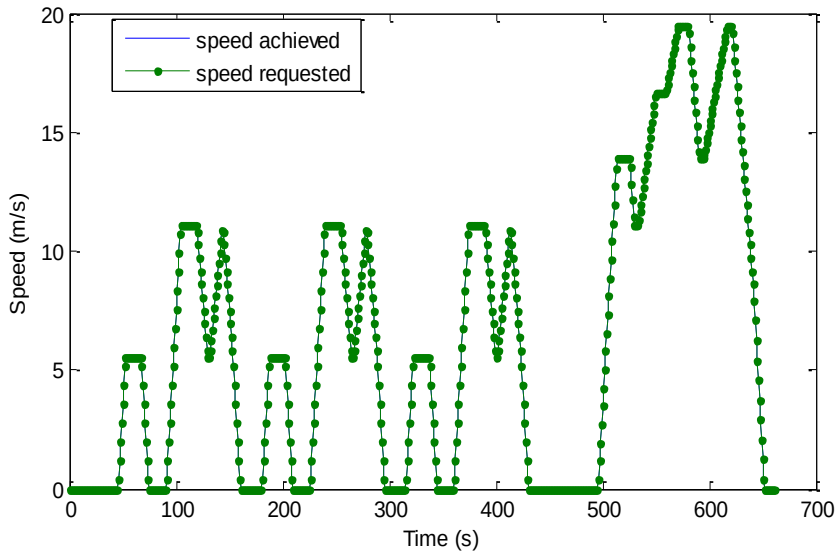

(g)

Figure 6.6: Speed and time traces of driving cycles (a) ECE_EUDC, (b) Indian, (c) LA92, (d) UDDS, (e) US06, (f) WVUCITY and (g) JAPAN 10-15

Various studies also show that HEVs can give better fuel efficiency on Indian roads in comparison to the developed country road [238, 239].

6.7 Summary

The efficiency of an HEV is obviously dependent on the road profiles. A profile is a composition of various parameters. Few vital parameters are identified using size reduction techniques and DCs are ranked in order of their fuel economy using multi

criterion optimization methods. The results are further validated using GA based intelligent power split control strategy. It is concluded that the Indian urban DC is promising and provides higher fuel efficiency for an HEV as compared to other countries. For Indian DC, 61.4437 mpgge FE without engine idling and 85.3290 mpgge with engine idling is achieved. In the automobile sector, the Indian market is ranked second after China with 8.9 percent growth rate. The favorable Indian road profiles will attract more people to use HEVs, thus boom in the automobile manufacturing market is expected. This will further reduce toxic emissions and will contribute to the Indian economy. It is also recommended that ICA should be applied rather than PCA for extracting urban DC parameters to analyze the performance as they follow non-Gaussian distribution. Engine idling should be considered as a powerful feature for improving fuel economy on city roads.

Chapter 7
Conclusion and Future Scope

ICE based vehicles are keystone of the modern transportation system. These vehicles use fossil fuels as a source of energy to propel and let out noxious gases. These gases are harmful for the environment and cause human health problems. Emanation of noxious gases, apace extraction of fossil fuel resources, rising oil prices and increasing concerns regarding energy security; making the ICE based vehicles a reason of environmental pollution and damaging the ecosystem. These concerns encourage the society to discover alternatives for sustainable future transportation.

HEVs are chosen here to fulfil the requirement of the modern transportation system while balancing the petroleum usage and emission of toxic gases. Battery is an important part of HEV and controls the performance over a long run. To achieve real time performance of the vehicle, critical study of battery models should be performed as part and parcel of a vehicle. As the battery gets associated with the vehicle; the load, the vibrations generated during movement, the temperature and the aging effects, all will influence its performance.

7.1 Conclusion

Selection of suitable battery for HEV application is performed using Ashby, TOPSIS and VIKOR methods. Highest relative closeness value (0.863) found out using TOPSIS and minimum index value (0) obtained using VIKOR and from selection charts made by Ashby's approach, Li-ion battery is selected as the best suitable battery. Li-ion battery is rated first, followed by Ni-MH battery using above stated methods. Since Li-ion batteries have high energy density and high specific energy, they are useful for promising HEV performance. They weigh half compared to other batteries, hence will surmount in the future.

Three battery models are developed here to be incorporated into vehicle for propulsion. Effect of temperature on these batteries is studied. Variation in OCV,

resistance and capacity of battery is analyzed for all the three models. From temperature effect analysis, it is observed that the battery should not be operated above 40-45 °C. Increase in temperature increases battery capacity by 4-6 percent which is also observed in practical/experimental data available in literatures of concern. Since self discharge current is included, the battery capacity is not found to be 100 percent as labelled, but it will be a little bit lower than rated capacity.

The threshold SOC level from the SOC-OCV curves at different temperatures is estimated to be 35 percent using gradient method. At lower temperatures this threshold comes later and at higher temperatures his will come sooner compared to room temperature point.

Voltage and current based SOC estimation method is proposed which eliminate the disadvantages of conventional current based method of SOC estimation. A weighting factor associates the voltage and current based SOCs to forecast its precise value. Involving a correction factor reckons the accuracy of SOC calculation in varying temperature and loading conditions. Battery, when placed in the vehicle, deviate from its sterilized behavior. Modification in correction factor is required with load (when battery is place in vehicle to power) and also if operating temperature is varied. A more refined correction factor suitable for loading and varying temperature is proposed. The SOC can be calculated 'on-the-fly' using proposed formula or look up table technique can also be practiced. Proposed SOC estimation method without load is able to estimate SOC with the error band of 0-2 percent above 35 percent SOC level point. As the load gets involved, the error between calculated and reference SOC is found to be in between 0-5 percent band.

To split power between the engine and the battery intelligently, DIRECT, GA and PMP are implemented to determine the fuel economies of vehicle. These optimization techniques help in finding the optimized values of governing parameters of vehicles like power, speed, time of travel and SOC. These optimization techniques are practiced using modified SOC estimation method and a comparison opposite to the conventional SOC estimation method is performed. Proposed method provides significant improvement in fuel economies. It is observed that GA provides an improvement of 21.82 percent over DIRCT method. PMP provides a fuel economy of 60.62 mpgge, which calculates the improvement of 16.01 percent compared to GA. Trace misses are tried to be removed

every time. To have an insightful comparison of applied algorithms with developed battery model and proposed modified SOC estimation method using GA provides 20.25 percent and PMP provides 7.75 percent improvement compared to the default battery and conventional SOC estimation method is observed.

By temperature analysis, it is observed that at lower temperatures fuel economies are lesser and at higher temperature it is high compared to room temperature. Because the current drawn from battery is lesser at low temperatures and at high temperature current drawn is high; vehicle performance varies abruptly other than nearby room temperatures. Continuous charging/discharging of battery at high temperature reduces battery life and diminishes vehicle performance, hence avoided.

Driving cycle parameters are reduced using ICA to a smaller set of six out of ten parameters. TOPSIS and VIKOR methods grade Indian driving cycle first and predict to have a better fuel economy over other driving cycles. These results are further validated using GA based method. In the automobile sector, the Indian market is ranked second after China with 8.9 percent growth rate. The favorable Indian road profiles will attract more people to use HEVs, thus boom in the automobile manufacturing market is expected. This will further reduce toxic emissions and will contribute to the Indian economy.

7.2 Future Work

Considering the battery technology most eminent for the future transportation, following effort can be put in order to improve its performance and hence HEV's fuel efficiency:

1. Analysis and modeling of effects of inhomogeneities like Aging, degradation and failure.
2. Implementation of battery management system is most challenging and demanding for optimized battery operation in HEVs.

In HEVs, lots of scope exist which may help to improve the performance as follows:

1. Implement the proposed algorithm to work in real-time.
2. Implementation of other algorithms to improve the efficiency.
3. Minimize engine emission.

In HEVs, although battery and engine two power sources are present, engine only has to work as power source. Battery gets charged through regenerative braking during deceleration otherwise engine is used to charge the battery. So, indirectly engine only works as power source. A more refined version of hybrid vehicles is PHEV. PHEV consist of a large on-board rechargeable battery along with the smaller size engine. Battery is charged through mains power supply and can be depleted up to its lowest allowable limit. Development of energy management strategies for PHEVs will be next step towards the green transportation.

Vehicle-to-grid (V2G) concept also gets cherished with the concept of PHEVs. With the facilities of large batteries which can be charged at offices, parking lots or at homes during off peak hours can be used to run household appliances and can be sold to grids back during peak hours. An effective two way communication between consumer and grid, smart grid implementation and smart metering infrastructure development, will support the V2G concept to nourish.

References

[1] Jos, G.J., Olivier, G. J.-M., Jeroen, Peters, A.H.W., 2012. Trends in global CO_2 emissions, PBL Netherlands environmental assessment agency.

[2] Environmental impact assessment (EIA), 2013.

[3] Ministry of Environment and Forests, India: greenhouse gas emissions 2007, Government of India, May 2010.

[4] Sharma, S., INCCA Indian network for climate change assessment, India: Greenhouse gas emissions 2007, Ministry of Environment and Forests, Government of India, 2010.

[5] **URL:** http://www.eia.gov/countries/country-data.cfm?fips=IN&trk=m

[6] Schipper, L., Leather, J. and Fabian, H., 2009. Transport and carbon dioxide emissions: forecasts, options analysis, and evaluation.

[7] NOAA, U.S. National Oceanic and Atmospheric Administration (CO2now.org)

[8] IEO (*International energy outlook*), 2013.

[9] IEA, *Transport, energy and CO_2: Moving towards sustainability*, 2009.

[10] Japan automobile manufacturers association Inc., *Reducing CO_2 emissions in the global road transport sector*, 2008.

[11] Singh, A., Gangopadhyay, S., Nanda, P.K., Bhattacharya, S., Sharma, C. and Bhan, C., 2008. Trends of greenhouse gas emissions from the road transport sector in India. *Science of the total environment*, *390*(1), pp.124-131.

[12] Financial express (2010)
URL: http://www.financialexpress.com/news/greenhouse-gas-emissions-up-4.2/947397

[13]**URL:**http://www.commodityonline.com/news/india-october-crude-oil-import-value-jumps-3161-to-$147853-mn-yy-51326-3-51327.html

[14] Annual Energy Outlook 2010 with projections to 2035.
URL:http://www.eia.gov/oiaf/archive/aeo10/woprices.html

[15] Annual energy outlook, 2013.

[16] Annual energy outlook, 2012.

[17] International Energy Outlook, Report Number: DOE/EIA-0484(2011), 2011.
URL:http://www.eia.gov/forecasts/ieo/

[18] EIA Country Analysis Briefs, India- analysis-U.S. Energy information administration, Nov. 2011.
URL: http://www.eia.gov/EMEU/cabs/India/pdf.pdf

[19] **URL:** http://www1.eere.energy.gov/cleancities/about.html

[20] **URL:** http://www.nrel.gov/vehiclesandfuels/energystorage/feature_vision.html

[21] Barnes, J., Walwijk, M.V., Saricks, C., 2009. Hybrid and electric vehicles, the electric drive establishes a market foothold: Progress towards sustainable Transportation. *International Energy Agency*.

[22]**URL:**http://www.kionrightnow.com/story/20578679/electric-vehicles-in-europe-light-duty-hybrid-plug-in-hybrid-and-battery-electric-vehicles-market-analysis-and-forecasts

[23]**URL:**http://indiatransportportal.com/2011/02/government-looking-to-encourage-hybrid-cars-in-indian-market/

[24]**URL:**http://articles.economictimes.indiatimes.com/2012-08-29/news/33476128_1_private-vehicles-electric-vehicles-road-transport

[25]**URL:**http://www.livemint.com/companies/eysinzxlikt4egcw9jbaum/budget-boosts-electric-hybrid-vehicle-industry.html

[26] Morgan, T., 2012. Smart grids and electric vehicles: Made for each other?. International Transport Forum Discussion Paper.

[27] **URL:**http://batteryuniversity.com/learn/article/cost_of_power

[28] Samuel, A.E., 2006. *Make and test projects in engineering design: Creativity, engagement and learning*. Springer Science & Business Media.

[29] Scoullos, M., Vonkeman, G.H., Thornton, I. and Makuch, Z., 2012. *Mercury—Cadmium—Lead Handbook for Sustainable Heavy Metals Policy and Regulation* (Vol. 31). Springer Science & Business Media.

[30] **URL:**http://en.wikipedia.org/wiki/Energy_density (accessed on 30/7/2014)

[31] **URL:**http://www.mpoweruk.com/performance.htm#life (accessed on 30/7/2014)

[32] **URL:**http://en.wikipedia.org/wiki/Battery_(electricity) (accessed on 30/7/2014)

[33] Gears educational system, battey basics: research, test, measure, analyze and select the optimal battery. **URL:** www.gears.com (Retreaved on July 30, 2014)

[34]**URL:**http://batteryuniversity.com/learn/article/cost_of_power, battery university, cost of power.

[35]Ashby, M.F. and Cebon, D., 1993. Materials selection in mechanical design. *Le Journal de Physique IV*, *3*(C7), pp.C7-1.

[36] Hwang, C.L. and Yoon, K., 2012. *Multiple attribute decision making: methods and applications a state-of-the-art survey* (Vol. 186). Springer Science & Business Media.

[37] Yoon, K., 1980. *Systems selection by multiple attribute decision making*. University Microfilms.

[38] Opricovic, S. and Tzeng, G.H., 2004. Compromise solution by MCDM methods: A comparative analysis of VIKOR and TOPSIS. *European journal of operational research*, *156*(2), pp.445-455.
[39] Zeleny, M., 1974. *Linear Multi-Objective Programming*. Springer Verlag.

[40] Tzeng, G.H., Teng, M.H., Chen, J.J. and Opricovic, S., 2002. Multicriteria selection for a restaurant location in Taipei. *International Journal of Hospitality Management*, *21*(2), pp.171-187.

[41] Opricovic, S. and Tzeng, G.H., 2007. Extended VIKOR method in comparison with outranking methods. *European Journal of Operational Research*, *178*(2), pp.514-529.

[42] Opricovic, S., 2009. Compromise in cooperative game and the VIKOR method. *Yugoslav Journal of Operations Research ISSN: 0354-0243 EISSN: 2334-6043*, *19*(2).

[43] Tzeng, G.H., Lin, C.W. and Opricovic, S., 2005. Multi-criteria analysis of alternative-fuel buses for public transportation. *Energy Policy*, *33*(11), pp.1373-1383.

[44] Kackar, R.N., 1989. Off-line quality control, parameter design, and the Taguchi method. In *Quality Control, Robust Design, and the Taguchi Method* (pp. 51-76). Springer US.

[45] Opricovic, S., 1994. Preference stability of compromise solution in multiple decision making. In *Multiple Criteria Decision Making, XIth International Conference,1994*.

[46] Gold, S., 1997, January. A PSPICE macromodel for lithium-ion batteries. In*Battery Conference on Applications and Advances, 1997., Twelfth Annual* (pp. 215-222).

[47] Benini, L., Castelli, G., Macii, A., Macii, E., Poncino, M. and Scarsi, R., 2001. Discrete-time battery models for system-level low-power design. *Very Large Scale Integration (VLSI) Systems, IEEE Transactions on*, *9*(5), pp.630-640.

[48] Johnson, V.H., Pesaran, A.A. and Sack, T., 2001. *Temperature-dependent battery models for high-power lithium-ion batteries*. City of Golden: National Renewable Energy Laboratory.

[49] Chen, S.X., Tseng, K.J. and Choi, S.S., 2009, March. Modeling of lithium-ion battery for energy storage system simulation. In *Power and Energy Engineering Conference, 2009. APPEEC 2009. Asia-Pacific* (pp. 1-4).

[50] Gao, L., Liu, S. and Dougal, R.A., 2002. Dynamic lithium-ion battery model for system simulation. *Components and Packaging Technologies, IEEE Transactions on*, *25*(3), pp.495-505.

[51] Tremblay, O., Dessaint, L.A. and Dekkiche, A.I., 2007, September. A generic battery model for the dynamic simulation of hybrid electric vehicles. In *Vehicle power and propulsion conference, 2007. VPPC 2007. IEEE* (pp. 284-289).

[52] Lee, S., Kim, J., Lee, J. and Cho, B.H., 2008. State-of-charge and capacity estimation of lithium-ion battery using a new open-circuit voltage versus state-of-charge. *Journal of power sources*, *185*(2), pp.1367-1373.

[53] Koo, J.S., Park, S.S., Youn, K.Y. and Kim, C.S., 2001. Development of SOC estimation logic using the steady state DC-IR for SHEV. In *Electric Vehicle, 18th Symposium, 2001*.

[54] Kim, J., Lee, S. and Cho B., The state of charge estimation employing empirical parameters measurements for various temperatures. *IEEE International Power Electronics, Motion, Control Conference*. Wuhan, China, 2009, pp. 939-944.
[55] Bhide, S. and Shim, T., 2009, September. Development of improved Li-ion battery model incorporating thermal and rate factor effects. In *Vehicle Power and Propulsion Conference, 2009. VPPC'09. IEEE* (pp. 544-550).

[56] Tan, Y.K., Mao, J.C. and Tseng, K.J., 2011, December. Modelling of battery temperature effect on electrical characteristics of Li-ion battery in hybrid electric vehicle. In *Power Electronics and Drive Systems (PEDS), 2011 IEEE Ninth International Conference on* (pp. 637-642).

[57] Dai, H., Wei, X. and Sun, Z., 2006, December. Online SOC estimation of high-power lithium-ion batteries used on HEVs. In *Vehicular Electronics and Safety, 2006. ICVES 2006. IEEE International Conference on* (pp. 342-347).

[58] Chen, M. and Rincon-Mora, G.A., 2006. Accurate electrical battery model capable of predicting runtime and IV performance. *Energy conversion, IEEE transactions on*, *21*(2), pp.504-511.

[59] Erdinc, O., Vural, B. and Uzunoglu, M., 2009, June. A dynamic lithium-ion battery model considering the effects of temperature and capacity fading. In *Clean Electrical Power, 2009 International Conference on* (pp. 383-386).

[60] Tang, X., Mao, X., Lin, J. and Koch, B., 2011, June. Li-ion battery parameter estimation for state of charge. In *American Control Conference (ACC), 2011*(pp. 941-946).

[61] Wei, X., Zou, G. and Sun, Z., 2004. Modelling and parameter estimation of Li-ion battery in a fuel cell vehicle. *Chinese Journal of Power Sources*, *28*(10; ISSU 169), pp.605-608.

[62] Kroeze, R.C. and Krein, P.T., 2008, June. Electrical battery model for use in dynamic electric vehicle simulations. In *Power Electronics Specialists Conference, 2008. PESC 2008. IEEE* (pp. 1336-1342).

[63] Zhang, H. and Chow, M.Y., 2010, July. Comprehensive dynamic battery modeling for PHEV applications. In *Power and Energy Society General Meeting, 2010 IEEE* (pp. 1-6).

[64]Vetter, K. J., 1961. *Elecktrochemische KinetiK*. Springer.

[65] Gould, C., Wang, J., Stone, D. and Foster, M., 2012, June. EV/HEV Li-ion battery modelling and State-of-Function determination. In *Power Electronics, Electrical Drives, Automation and Motion (SPEEDAM), 2012 International Symposium on* (pp. 353-358).

[66] Yurkovich, B.J., 2010. *Electrothermal Battery Pack Modeling and Simulation*(Doctoral dissertation, The Ohio State University).

[67] Thanagasundram, S., Arunachala, R., Makinejad, K., Teutsch, T. and Jossen, A., 2012. A cell level model for battery simulation. In *European Electric Vehicle Congress (EEVC), 2012*.

[68] Esfahanian, M., Mahmoodian, A., Amiri, M., Tehrani, M.M., Nehzati, H., Hejabi, M. and Manteghi, A., 2013. Large lithium polymer battery modeling for the simulation of hybrid electric vehicles using the equivalent circuit method. *International Journal of Automotive Engineering*, *3*(4), pp.564-576.

[69] Zhang, C.P., Liu, J.Z., Sharkh, S.M. and Zhang, C.N., 2010. Identification of dynamic model parameters for lithium-ion batteries used in hybrid electric vehicles. *High Technol. Lett.* 16, pp. 6-12.

[70] Junnuri, R.K., Kamat, S., Goyal, N., Annamalai, R., Modak, D., Tashiro, H. and Miwa, N., 2014, August. Modelling of HEV lithium-ion high voltage battery pack using dynamic data. In *Proceedings of the 19th IFAC World Congress* (No. 1).

[71] Lam, L., 2011. *A practical circuit-based model for state of health estimation of li-ion battery cells in electric vehicles* (Doctoral dissertation, TU Delft, Delft University of Technology).

[72] Culcu, H., Verbrugge, B., Omar, N., Van Den Bossche, P. and Van Mierlo, J., 2009. Internal resistance of cells of lithium battery modules with Freedom CAR model. *World Electric Vehicle Journal*, *3*, pp.1-9.

[73] Cliffs, E., 1991. *Electrochemical Systems*, Prentice-Hall.

[74] Conway, B.E., 1991. Transition from "supercapacitor" to "battery" behavior in electrochemical energy storage. *Journal of the Electrochemical Society*,*138*(6), pp.1539-1548.

[75] Chen, M. and Rincon-Mora, G.A., 2006. Accurate electrical battery model capable of predicting runtime and IV performance. *Energy conversion, IEEE transactions on*, *21*(2), pp.504-511.

[76] Pang, S., Farrell, J., Du, J. and Barth, M. (2001). Battery state-of-charge estimation. *Proceedings of 2001 American control conference*, Arlington, VA, Vol. 2, pp. 1644-1649.

[77] Abu-Sharkh, S. and Doerffel, D. (2004). Rapid test and non-linear model characterization of solid-state lithium-ion batteries. *Journal of Power Sources* 130, pp. 266–274.

[78] Lee, S. J., Kim, J. H., Lee, J. M., and Cho B. H. 2007. The state and parameter estimation of li-ion battery using a new OCV-SOC concept. In *Power Electronics Specialists Conference, 2007 International Conference on* (pp. 2799–2803).

[79] Piller, S., Perrin, M.and Jossen, A. (2001). Methods of state of charge determination and their applications. *Journal of Power Sources* 96(1), pp. 113-120.

[80] Tang, X., Mao, X., Lin, J. and Koch, B., 2011, June. Li-ion battery parameter estimation for state of charge. In *American Control Conference (ACC), 2011*(pp. 941-946).

[81] Verbrugge, M., and Tate, E. (2004). Adaptive state of charge algorithm for nickel metal hydride batteries including hysteresis phenomena. *Journal of Power Sources*, 126, pp. 236-249.

[82] Zi-lin, M., Xao-Jian, M., Jun-xi, W., Jia-xi, Q. and Bin, Z., 2008, September. Research on SOC estimated strategy of Ni/MH battery used for hybrid electric vehicle. In *Vehicle power and propulsion conference, 2008. VPPC'08. IEEE* (pp. 1-4).

[83] Kwok, W.Y., Delphi Technologies, Inc., 2001. *Method of calculating dynamic state-of-charge within a battery*. U.S. Patent 6,300,763.

[84] Tagawa, K. and Brodd, R.J., 2009. Production processes for fabrication of lithium-ion batteries. In *Lithium-ion batteries* (pp. 181-194). Springer New York.

[85] Elger, R., 2004. *On the behaviour of the li-ion battery in HEV application*, (Doctoral dissertation, Applied Electrochemistry,Kungliga Tekniska Högskolan).

[86] Markel, T., Brooker, A., Hendricks, T., Johnson, V., Kelly, K., Kramer, B., O'Keefe, M., Sprik, S. and Wipke, K., 2002. ADVISOR: a systems analysis tool for advanced vehicle modeling. *Journal of power sources*, *110*(2), pp.255-266.

[87] Johnson, V.H., Pesaran, A.A. and Sack, T., 2001. *Temperature-dependent battery models for high-power lithium-ion batteries*. City of Golden: National Renewable Energy Laboratory.

[88] Lam, L., 2011. *A practical circuit-based model for state of health estimation of li-ion battery cells in electric vehicles* (Doctoral dissertation, TU Delft, Delft University of Technology).

[89] **URL:** http://www.mpoweruk.com/performance.html

[90] Kim, J., Lee, S. and Cho, B., 2009, May. The state of charge estimation employing empirical parameters measurements for various temperatures. In *Power Electronics and Motion Control Conference, 2009. IPEMC'09. IEEE 6th International* (pp. 939-944).

[91] Kim, J., Lee, S. and Cho, B., 2009, May. The state of charge estimation employing empirical parameters measurements for various temperatures. In *Power Electronics and Motion Control Conference, 2009. IPEMC'09. IEEE 6th International* (pp. 939-944).

[92] Johnson, V.H., 2002. Battery performance models in ADVISOR. *Journal of Power Sources*, *110*(2), pp. 321-329.

[93] Kim, J., Kim, N., Hwang, S., Hori, Y. & Kim, H. (2009). Motor control of input-split hybrid electric vehicles. *International Journal of Automotive Technology*, 10(6), pp. 733−742.

[94] Yang, H., Kim, B., Park, Y., Lim, W. & Cha. S. (2009). Analysis of planetary gear hybrid powertrain system part 2: Output split system. *International Journal of Automotive Technology, 10 (3), pp. 381-390.*

[95] Kim, N., Kwon, J., & Rousseau, A. 2010, Nov. Trade-off between Multi-mode Powertrain Complexity and Fuel Consumption. *In world battery, hybrid and fuel cell electric vehicle, Twenty fifth symposium & exhibition, 2010*.

[96] Staunton, R. H., Ayers, C. W., Marlino, L. D., Chiassonand J. N. and Burress, T. A., Evaluation of 2004 Toyota Prius Htbrid Eleectric Drive System, Report prepared by Oak Ridge National Laboratory, 2006.

[97] Mi, C., Masrur, M.A. and Gao D.W., Hybrid electric vehicles: Principles and applications with practical perspectives, Ch. 4, John Wiley & sons. Ltd., 2011.

[98] Shaohua, L., Changqing, D., Fuwu, Y., Jun, W., Zheng, L. and Yuan, L., 2012, November. A rule-based energy management strategy for a new BSG hybrid electric vehicle. In *Intelligent Systems (GCIS), 2012 Third Global Congress on* (pp. 209-212).

[99] Trovão João, P., Pereirinha Paulo, G. and Jorge Humberto, M., 2013. Antunes Carlos Henggeler. A multi-level energy management system for multi-source electric vehicles–an integrated rule-based meta-heuristic approach. *Appl Energy*, *105*, pp.304-318.

[100] Kim, C., NamGoong, E., Lee, S., Kim, T. and Kim, H., 1999. *Fuel economy optimization for parallel hybrid vehicles with CVT* (No. 1999-01-1148). SAE Technical Paper.

[101] Zaher, M. and Cetinkunt, S., 2013. Real-time energy management control for hybrid electric powertrains. *Journal of Control Science and Engineering*, pp.3.

[102] Arsie, I., Pianese, C., Rizzo, G. and Santoro, M., 2001, July. A model for the energy management in a parallel hybrid vehicle. In *Control and Diagnostics in Automotive Applications, Third International Conference on*, 2001.

[103] Farrall, S.D. and Jones, R.P., 1993, August. Energy management in an automotive electric/heat engine hybrid powertrain using fuzzy decision making. In *Intelligent Control, 1993., Proceedings of the 1993 IEEE International Symposium on* (pp. 463-468).

[104] Cerruto, E., Consoli, A., Raciti, A. and Testa, A., 1994, April. Energy flows management in hybrid vehicles by fuzzy logic controller. In *Electrotechnical, Seventh Mediterranean Conference on,* (pp. 1314-1317).

[105] Cerruto, E., Consoli, A., Raciti, A. and Testa, A., 1994, September. Fuzzy logic based efficiency improvement of an urban electric vehicle. In *Industrial Electronics, Control and Instrumentation, 1994. IECON'94., 20th International Conference on* (Vol. 2, pp. 1304-1309).

[106] Galichet, S. and Foulloy, L., 1995. Fuzzy controllers: synthesis and equivalences. *Fuzzy Systems, IEEE Transactions on*, *3*(2), pp.140-148.

[107] Lee, H.D., Sul, S.K., Kamiya, M., Ikeda, H., Shinohara, S. and Yoshida, H., 2000. Torque control strategy for a parallel-hybrid vehicle using fuzzy logic.*Industry Applications Magazine, IEEE*, *6*(6), pp.33-38.

[108] Baumann, B.M., Washington, G., Glenn, B.C. and Rizzoni, G., 2000. Mechatronic design and control of hybrid electric vehicles. *Mechatronics, IEEE/ASME Transactions on*, *5*(1), pp.58-72.

[109] Tao, C.W. and Taur, J.S., 2000. Flexible complexity reduced PID-like fuzzy controllers. *Systems, Man, and Cybernetics, Part B: Cybernetics, IEEE Transactions on*, *30*(4), pp.510-516.

[110] Schouten, N.J., Salman, M.A. and Kheir, N.A., 2002. Fuzzy logic control for parallel hybrid vehicles. *Control Systems Technology, IEEE Transactions on*, *10*(3), pp.460-468.

[111] Patel, A.V. and Mohan, B.M., 2002. Analytical structures and analysis of the simplest fuzzy PI controllers. *Automatica*, *38*(6), pp.981-993.

[112] Bathaee, S.M.T., Gastaj, A.H., Emami, S.R. and Mohammadian, M., 2005, September. A fuzzy-based supervisory robust control for parallel hybrid electric vehicles. In *Vehicle Power and Propulsion, 2005 IEEE Conference* (pp. 7).

[113] Khoucha, F., Benbouzid, M.E.H. and Kheloui, A., 2010, September. An optimal fuzzy logic power sharing strategy for parallel hybrid electric vehicles. In *Vehicle Power and Propulsion Conference (VPPC), 2010 IEEE* (pp. 1-5).

[114] Zhang, J., Yin, C. and Zhang, J., 2006, June. Use of fuzzy controller for hybrid traction control system in hybrid electric vehicles. In *Mechatronics and Automation, Proceedings of the 2006 IEEE International Conference on* (pp. 1351-1356).

[115] Poursamad, A. and Montazeri, M., 2008. Design of genetic-fuzzy control strategy for parallel hybrid electric vehicles. *Control Engineering Practice*, *16*(7), pp.861-873.

[116] Won, J.S. and Langari, R., 2003, June. Intelligent energy management agent for a parallel hybrid vehicle. In *American Control Conference, 2003. Proceedings of the 2003* (Vol. 3, pp. 2560-2565).

[117] Kachroudi, S., Grossard, M. and Abroug, N., 2012. Predictive driving guidance of full electric vehicles using particle swarm optimization. *Vehicular Technology, IEEE Transactions on*, *61*(9), pp.3909-3919.

[118] Delprat, S., Guerra, T.M., Paganelli, G., Lauber, J. and Delhom, M., 2001. Control strategy optimization for an hybrid parallel powertrain. In *American Control Conference, 2001. Proceedings of the 2001* (Vol. 2, pp. 1315-1320).

[119] Delprat, S., Guerra, T.M. and Rimaux, J., 2002. Optimal control of a parallel powertrain: from global optimization to real time control strategy. In *Vehicular Technology Conference, 2002. VTC Spring 2002. IEEE 55th* (Vol. 4, pp. 2082-2088).

[120] Delprat, S., Guerra, T.M. and Rimaux, J., 2003, October. Control strategies for hybrid vehicles: synthesis and evaluation. In *Vehicular Technology Conference, 2003. VTC 2003-Fall. 2003 IEEE 58th* (Vol. 5, pp. 3246-3250).

[121] Wirasingha, S.G. and Emadi, A., 2011. Classification and review of control strategies for plug-in hybrid electric vehicles. *vehicular Technology, IEEE Transactions on*, *60*(1), pp.111-122.

[122] Tate, E.D. and Boyd, S.P., 2000. Finding ultimate limits of performance for hybrid electric vehicles. *SAE transactions*, *109*(6), pp.2437-2448.

[123] Kleimaier, A. and Schröder, D., 2000, April. Optimization strategy for design and control of a hybrid vehicle. In *Advanced Motion Control, 2000. Proceedings. 6th International Workshop on* (pp. 459-464).

[124] Pisu, P., Silani, E., Rizzoni, G. and Savaresi, S.M., 2003, June. A lmi-based supervisory robust control for hybrid vehicles. In *American Control Conference, 2003. Proceedings of the 2003* (Vol. 6, pp. 4681-4686).

[125] Miaohua, H. and Houyu, Y., 2003. Optimal design of control strategy for series hybrid electric bus. *Journal-Wuhan Transportation University*, *27*(4), pp.440-442.

[126] Jang, J.S.R., Sun, C.T. and Mizutani, E., 1997. Neuro-fuzzy and soft computing: a computational approach to learning and machine intelligence.

[127] Brahma, A., Guezennec, Y. and Rizzoni, G., 2000, September. Optimal energy management in series hybrid electric vehicles. In *American Control Conference, 2000. Proceedings of the 2000* (Vol. 1, No. 6, pp. 60-64).

[128] Lin, C.C., Kang, J.M., Grizzle, J.W. and Peng, H., 2001. Energy management strategy for a parallel hybrid electric truck. In *American Control Conference, 2001. Proceedings of the 2001* (Vol. 4, pp. 2878-2883).

[129] Sundström, O., Guzzella, L. and Soltic, P., 2008, July. Optimal hybridization in two parallel hybrid electric vehicles using dynamic programming. In *Proceedings of the 17th IFAC world congress* (Vol. 17, No. part 1, pp. 4642-4647).

[130] Lin, C.C., Peng, H., Grizzle, J.W. and Kang, J.M., 2003. Power management strategy for a parallel hybrid electric truck. *Control Systems Technology, IEEE Transactions on*, *11*(6), pp.839-849.

[131] Koot, M., Kessels, J.T., De Jager, B., Heemels, W.P.M.H., Van den Bosch, P.P.J. and Steinbuch, M., 2005. Energy management strategies for vehicular electric power systems. *Vehicular Technology, IEEE Transactions on*, *54*(3), pp.771-782.

[133] Van Keulen, T., de Jager, B. and Steinbuch, M., 2008, July. An adaptive sub-optimal energy management strategy for hybrid drive-trains. In *Proc. of the 17th IFAC World Congress* (pp. 102-107).

[134] Sundström, O. and Guzzella, L., 2009, July. A generic dynamic programming Matlab function. In *Control Applications,(CCA) & Intelligent Control,(ISIC), 2009 IEEE* (pp. 1625-1630).

[135] Tulpule, P., Stockar, S., Marano, V. and Rizzoni, G., 2009, January. Optimality assessment of equivalent consumption minimization strategy for PHEV applications. In *Dynamic Systems and Control, 2009 ASME* (pp. 265-272).

[136] Tulpule, P., Marano, V. and Rizzoni, G., 2010. Energy management for plug-in hybrid electric vehicles using equivalent consumption minimisation strategy. *International Journal of Electric and Hybrid Vehicles*, *2*(4), pp.329-350.

[137] Ngo, D.V., Hofman, T., Steinbuch, M. and Serrarens, A.F., 2010, June. An optimal control-based algorithm for hybrid electric vehicle using preview route information. In *American Control Conference (ACC), 2010* (pp. 5818-5823).

[138] Kum, D., Peng, H. and Bucknor, N.K., 2011, June. Optimal catalyst temperature management of plug-in hybrid electric vehicles. In *American Control Conference (ACC), 2011* (pp. 2732-2738).

[139] Zhou, Z., Mi, C., Chen, Z., Masrur, A. and Murphey, Y.L., 2011, September. Power management of passive multi-source hybrid electric vehicle. In*Vehicle Power and Propulsion Conference (VPPC), 2011 IEEE* (pp. 1-4).

[140] Ravey, A., Roche, R., Blunier, B. and Miraoui, A., 2012, June. Combined optimal sizing and energy management of hybrid electric vehicles. In*Transportation Electrification Conference and Expo (ITEC), 2012 IEEE* (pp. 1-6).

[141] Shams-Zahraei, M., Kouzani, A.Z., Kutter, S. and Bäker, B., 2012. Integrated thermal and energy management of plug-in hybrid electric vehicles. *Journal of power sources*, *216*, pp.237-248.

[142] Lin, C.C., Peng, H. and Grizzle, J.W., 2004, June. A stochastic control strategy for hybrid electric vehicles. In *American Control Conference, 2004. Proceedings of the 2004* (Vol. 5, pp. 4710-4715).

[143] Tate, E.D., Grizzle, J.W. and Peng, H., 2008. Shortest path stochastic control for hybrid electric vehicles. *International Journal of Robust and Nonlinear Control*, *18*(14), pp.1409-1429.

[144] Liu, J., Hagena, J., Peng, H. and Filipi, Z.S., 2008. Engine-in-the-loop study of the stochastic dynamic programming optimal control design for a hybrid electric HMMWV. *International Journal of Heavy Vehicle Systems*, *15*(2-4), pp.309-326.

[145] Tate, E.D., Grizzle, J.W. and Peng, H., 2010. SP-SDP for fuel consumption and tailpipe emissions minimization in an EVT hybrid. *Control Systems Technology, IEEE Transactions on*, *18*(3), pp.673-687.

[146] Opila, D.F., Wang, X., McGee, R., Gillespie, R.B., Cook, J.A. and Grizzle, J.W., 2012. An energy management controller to optimally trade off fuel economy and drivability for hybrid vehicles. *Control Systems Technology, IEEE Transactions on*, *20*(6), pp.1490-1505.

[147] Wang, Y. and Sun, Z., 2012, June. SDP-based extremum seeking energy management strategy for a power-split hybrid electric vehicle. In *American Control Conference (ACC), 2012* (pp. 553-558).

[148] Opila, D.F., Wang, X., McGee, R. and Grizzle, J.W., 2013. Real-time implementation and hardware testing of a hybrid vehicle energy management controller based on stochastic dynamic programming. *Journal of Dynamic Systems, Measurement, and Control*, *135*(2), p.021002.

[149] Piccolo, A., Ippolito, L., Galdi, V.Z. and Vaccaro, A., 2001. Optimisation of energy flow management in hybrid electric vehicles via genetic algorithms. In*Advanced Intelligent Mechatronics, 2001. Proceedings. 2001 IEEE/ASME International Conference on* (Vol. 1, pp. 434-439).

[150] Ippolito, L., Loia, V. and Siano, P., 2003. Extended fuzzy C-means and genetic algorithms to optimize power flow management in hybrid electric vehicles. *Fuzzy Optimization and Decision Making*, *2*(4), pp.359-374.

[151] Gao, W. and Porandla, S.K., 2005, September. Design optimization of a parallel hybrid electric powertrain. In *Vehicle Power and Propulsion, 2005 IEEE Conference* (pp. 6).

[152] Montazeri-Gh, M. and Poursamad, A., 2005, January. Optimization of component sizes in parallel hybrid electric vehicles via genetic algorithms. In*ASME 2005 International Mechanical Engineering Congress and Exposition* (pp. 225-231). American Society of Mechanical Engineers.

[153] Montazeri-Gh, M. and Poursamad, A., 2006. Application of genetic algorithm for simultaneous optimisation of HEV component sizing and control strategy.*International Journal of Alternative Propulsion*, *1*(1), pp.63-78.

[154] Zhang, B., Chen, Z., Mi, C. and Murphey, Y.L., 2009, September. Multi-objective parameter optimization of a series hybrid electric vehicle using evolutionary algorithms. In *Vehicle Power and Propulsion Conference, 2009. VPPC'09. IEEE* (pp. 921-925).

[155] Montazeri-Gh, M., Poursamad, A. and Ghalichi, B., 2006. Application of genetic algorithm for optimization of control strategy in parallel hybrid electric vehicles. *Journal of the Franklin Institute*, *343*(4), pp.420-435.

[156] Desai, C. and Williamson, S.S., 2009, September. Optimal design of a parallel hybrid electric vehicle using multi-objective genetic algorithms. In *Vehicle Power and Propulsion Conference, 2009. VPPC'09. IEEE* (pp. 871-876).

[157] Xiaolin, H., Zhongfan, W. and Lianying, L., 2004. Application of Multi-objective Evolutionary Algor ithm in Hybrid Electric Vehicle Design and Control. *Journal-Wuhan Transportation University.*, *28*, pp.384-387.

[158] Zhang, Y., Sun, F. and He, H., 2008, September. Control strategy optimization for hybrid electric vehicle based on DIRECT algorithm. In *Vehicle Power and Propulsion Conference, 2008. VPPC'08. IEEE* (pp. 1-5).

[159] Jones, D.R., 2001. Direct global optimization. In *Encyclopedia of optimization* (pp. 431-440). Springer US.

[160] Björkman, M. and Holmström, K., 1999. Global optimization using DIRECT algorithm in matlab.

[161] Tony, M. and Wipke, T., 2001. Optimization techniques for hybrid electric vehicle analysis using ADVISOR. In *Mechanical Engineering Congress and Exposition, 2001*.

[162] Fellini, R., Michelena, N., Papalambros, P. and Sasena, M., 1999, February. Optimal design of automotive hybrid powertrain systems. In *Environmentally Conscious Design and Inverse Manufacturing, 1999. Proceedings. EcoDesign'99: First International Symposium on* (pp. 400-405).

[163]Dosthosseini, R., Kouzani, A.Z. and Sheikholeslam, F., 2011. Direct method for optimal power management in hybrid electric vehicles. *International journal of automotive technology*, *12*(6), pp.943-950.

[164] Wang, Z., Huang, B., Li, W. and Xu, Y., 2006, December. Particle swarm optimization for operational parameters of series hybrid electric vehicle. In *Robotics and Biomimetics, 2006. ROBIO'06. IEEE International Conference on* (pp. 682-688).

[165] Gao, W. and Mi, C., 2007. Hybrid vehicle design using global optimisation algorithms. *International Journal of Electric and Hybrid Vehicles*, *1*(1), pp.57-70.

[166] Johnson, V.H., Wipke, K.B. and Rausen, D.J., 2000. HEV control strategy for real-time optimization of fuel economy and emissions. *SAE transactions*,*109*(3), pp.1677-1690.

[167] Paganelli, G., Tateno, M., Brahma, A., Rizzoni, G. and Guezennec, Y., 2001. Control development for a hybrid-electric sport-utility vehicle: strategy, implementation and field test results. In *American Control Conference, 2001. Proceedings of the 2001* (Vol. 6, pp. 5064-5069).

[168] Jalil, N., Kheir, N.A. and Salman, M., 1997, June. A rule-based energy management strategy for a series hybrid vehicle. In *American Control Conference, 1997. Proceedings of the 1997* (Vol. 1, pp. 689-693).

[169] Paganelli, G., Delprat, S., Guerra, T.M., Rimaux, J. and Santin, J.J., 2002. Equivalent consumption minimization strategy for parallel hybrid powertrains. In *Vehicular Technology Conference, 2002. VTC Spring* (Vol. 4, pp. 2076-2081).

[170] Supina, J.G. and Awad, S., 2003, December. Optimization of the fuel economy of a hybrid electric vehicle. In *Circuits and Systems, IEEE Forty sixth Midwest Symposium on* (Vol. 2, pp. 876-881).

[171] Sciarretta, A., Back, M. and Guzzella, L., 2004. Optimal control of parallel hybrid electric vehicles. *Control Systems Technology, IEEE Transactions on*, *12*(3), pp.352-363.

[172] Won, J.S., Langari, R. and Ehsani, M., 2005. An energy management and charge sustaining strategy for a parallel hybrid vehicle with CVT. *Control Systems Technology, IEEE Transactions on*, *13*(2), pp.313-320.

[173] Pisu, P. and Rizzoni, G., 2005, September. A supervisory control strategy for series hybrid electric vehicles with two energy storage systems. In *Vehicle Power and Propulsion, 2005 IEEE Conference* (pp. 8).

[174] Pisu, P. and Rizzoni, G., 2005, September. A supervisory control strategy for series hybrid electric vehicles with two energy storage systems. In *Vehicle Power and Propulsion, 2005 IEEE Conference* (pp. 8).

[175] Musardo, C., Rizzoni, G., Guezennec, Y. and Staccia, B., 2005. A-ECMS: An adaptive algorithm for hybrid electric vehicle energy management. *European Journal of Control*, *11*(4), pp.509-524.

[176] Pisu, P. and Rizzoni, G., 2007. A comparative study of supervisory control strategies for hybrid electric vehicles. *Control Systems Technology, IEEE Transactions on*, *15*(3), pp.506-518.

[177] Sinoquet, D., Rousseau, G. and Milhau, Y., 2011. Design optimization and optimal control for hybrid vehicles. *Optimization and Engineering*, *12*(1-2), pp.199-213.

[178] Gao, J.P., Zhu, G.G., Strangas, E.G. and Sun, F.C., 2009. Equivalent fuel consumption optimal control of a series hybrid electric vehicle. *Proceedings of the Institution of Mechanical Engineers, Part D: Journal of Automobile Engineering*, *223*(8), pp.1003-1018.

[179] Tulpule, P., Marano, V. and Rizzoni, G., 2009, June. Effects of different PHEV control strategies on vehicle performance. In *American Control Conference, 2009. ACC'09.* (pp. 3950-3955).

[180] Salman, M.F.C.M., Chang, M.F. and Chen, J.S., 2005, September. Predictive energy management strategies for hybrid vehicles. In *IEEE Vehicle Power and Propulsion Conference, VPPC2005, Illinois Institute of Technology, Chicago, IL, 7-9 Sept*.

[181] Wang, Y. and Boyd, S., 2010. Fast model predictive control using online optimization. *Control Systems Technology, IEEE Transactions on*, *18*(2), pp.267-278.

[182] Kermani, S., Delprat, S., Guerra, T.M. and Trigui, R., 2009, September. Predictive control for HEV energy management: experimental results. In *2009 IEEE Vehicle Power and Propulsion Conference*.

[183] Sampathnarayanan, B., Serrao, L., Onori, S., Rizzoni, G. and Yurkovich, S., 2009, January. Model predictive control as an energy management strategy for hybrid electric vehicles. In *ASME 2009 Dynamic Systems and Control Conference* (pp. 249-256).

[184] Ripaccioli, G., Bemporad, A., Assadian, F., Dextreit, C., Di Cairano, S. and Kolmanovsky, I.V., 2009. Hybrid modeling, identification, and predictive control: An application to hybrid electric vehicle energy management. In *Hybrid Systems: Computation and Control* (pp. 321-335). Springer Berlin Heidelberg.

[185] Borhan, H.A., Zhang, C., Vahidi, A., Phillips, A.M., Kuang, M.L. and Di Cairano, S., 2010, December. Nonlinear model predictive control for power-split hybrid electric vehicles. In *Decision and Control (CDC), 2010 49th IEEE Conference on* (pp. 4890-4895).

[186] Ripaccioli, G., Bernardini, D., Di Cairano, S., Bemporad, A. and Kolmanovsky, I.V., 2010, June. A stochastic model predictive control approach for series hybrid electric vehicle power management. In *American Control Conference (ACC)* (Vol. 2010, pp. 5844-5849).

[187] Borhan, H., Vahidi, A., Phillips, A.M., Kuang, M.L., Kolmanovsky, I.V. and Cairano, S.D., 2012. MPC-based energy management of a power-split hybrid electric vehicle. *Control Systems Technology, IEEE Transactions on*, *20*(3), pp.593-603.

[188] Yan, F., Wang, J. and Huang, K., 2012. Hybrid electric vehicle model predictive control torque-split strategy incorporating engine transient characteristics. *Vehicular Technology, IEEE Transactions on*, *61*(6), pp.2458-2467.

[189] Poramapojana, P. and Chen, B., 2012, July. Minimizing HEV fuel consumption using model predictive control. In *Mechatronics and Embedded Systems and Applications (MESA), 2012 IEEE/ASME International Conference on* (pp. 148-153).

[190] Baumann, B., Rizzoni, G. and Washington, G., 1998. *Intelligent control of hybrid vehicles using neural networks and fuzzy logic* (No. 981061). SAE Technical Paper.

[191] Arsie, I., Graziosi, M., Pianese, C., Rizzo, G. and Sorrentino, M., 2004. Optimization of supervisory control strategy for parallel hybrid vehicle with provisional load estimate. *Proc. of AVEC04*, pp.23-27.

[192] Mohebbi, M., Charkhgard, M. and Farrokhi, M., 2005, September. Optimal neuro-fuzzy control of parallel hybrid electric vehicles. In *Vehicle Power and Propulsion, 2005 IEEE Conference* (pp. 26-30).

[193] Liu, M.J., 2007, July. A fuzzy neural network control system based on improved learning algorithms. In *Zhongguo Dianji Gongcheng Xuebao(Proceedings of the Chinese Society of Electrical Engineering)* (Vol. 27, No. 19, pp. 87-92).

[194] Murphey, Y.L., Park, J., Kiliaris, L., Kuang, M.L., Masrur, M.A., Phillips, A.M. and Wang, Q., 2013. Intelligent hybrid vehicle power control—Part II: Online intelligent energy management. *Vehicular Technology, IEEE Transactions on*, *62*(1), pp.69-79.

[195] Eberhart, R.C. and Kennedy, J., 1995, October. A new optimizer using particle swarm theory. In *Proceedings of the sixth international symposium on micro machine and human science* (Vol. 1, pp. 39-43).

[196] Shi, Y. and Eberhart, R.C., 1998, March. Parameter selection in particle swarm optimization. In *Evolutionary programming VII* (pp. 591-600). Springer Berlin Heidelberg.

[197] Huang, M., 2006, September. Optimal multilevel hierarchical control strategy for parallel hybrid electric vehicle. In *Vehicle Power and Propulsion Conference, 2006. VPPC'06. IEEE* (pp. 1-4).

[198] Huang, M. and Yu, H., 2006, December. Optimal control strategy based on PSO for powertrain of parallel Hybrid Electric Vehicle. In *Vehicular Electronics and Safety, 2006. ICVES 2006. IEEE International Conference on* (pp. 352-355).

[199] Wu, J., Zhang, C.H. and Cui, N.X., 2008. Fuzzy energy management strategy of parallel hybrid electric vehicle based on particle swarm optimization. *Control and Decision*, *23*(1), p.46.

[200] Al-Aawar, N., Hijazi, T.M. and Arkadan, A.A., 2009, May. EM-TFL identification for particle swarm optimization of HEV powertrain. In *Electric Machines and Drives Conference, 2009. IEMDC'09. IEEE International* (pp. 109-112).

[201] Desai, C. and Williamson, S.S., 2010, September. Particle swarm optimization for efficient selection of hybrid electric vehicle design parameters. In *Energy Conversion Congress and Exposition (ECCE), 2010 IEEE* (pp. 1623-1628).

[202] Hegazy, O. and Van Mierlo, J., 2010, May. Particle swarm optimization for optimal powertrain component sizing and design of fuel cell hybrid electric vehicle. In *Optimization of Electrical and Electronic Equipment (OPTIM), 2010 12th International Conference on* (pp. 601-609).

[203] Varesi, K. and Radan, A., 2011, February. A novel PSO based technique for optimizing the DOH in hybrid electric vehicles to improve both the fuel economy and vehicle performance and reduce the emissions. In *Power Electronics, Drive Systems and Technologies Conference (PEDSTC), 2011 2nd* (pp. 342-349).

[204] Al-Aawar, N., Hijazi, T.M. and Arkadan, A.A., 2011. Particle swarm optimization of coupled electromechanical systems. *Magnetics, IEEE Transactions on*, *47*(5), pp.1314-1317.

[205] Wu, L., Wang, Y., Yuan, X. and Chen, Z., 2011. Multiobjective optimization of HEV fuel economy and emissions using the self-adaptive differential evolution algorithm. *Vehicular Technology, IEEE Transactions on*, *60*(6), pp.2458-2470.

[206] Krotov, V., 1995. *Global methods in optimal control theory* (Vol. 195). CRC Press.

[207] Geering, H.P., 2007. *Optimal control with engineering applications* (Vol. 113). Berlin: Springer.

[208] Serrao, L. and Rizzoni, G., 2008, June. Optimal control of power split for a hybrid electric refuse vehicle. In *Proceedings of the 2008 American Control Conference* (pp. 4498-4503).

[209] Stockar, S., Marano, V., Rizzoni, G. and Guzzella, L., 2010, June. Optimal control for plug-in hybrid electric vehicle applications. In *American Control Conference (ACC), 2010* (pp. 5024-5030).

[210] Chasse, A. and Sciarretta, A., 2011. Supervisory control of hybrid powertrains: an experimental benchmark of offline optimization and online energy management. *Control Engineering Practice*, *19*(11), pp.1253-1265.

[211] Kim, N., Cha, S. and Peng, H., 2011. Optimal control of hybrid electric vehicles based on Pontryagin's minimum principle. *Control Systems Technology, IEEE Transactions on*, *19*(5), pp.1279-1287.

[212] Kim, N., Cha, S.W. and Peng, H., 2012. Optimal equivalent fuel consumption for hybrid electric vehicles. *Control Systems Technology, IEEE Transactions on*, *20*(3), pp.817-825.

[213] Li, Y. and Kar, N.C., 2011, September. Advanced design approach of power split device of plug-in hybrid electric vehicles using dynamic programming. In *Vehicle Power and Propulsion Conference (VPPC), 2011 IEEE* (pp. 1-6).

[214] Zhang, C. and Vahidi, A., 2012. Route preview in energy management of plug-in hybrid vehicles. *Control Systems Technology, IEEE Transactions on*, *20*(2), pp.546-553.

[215] Larsson, V., Johannesson, L. and Egardt, B., 2013. Comparing two approaches to precompute discharge strategies for plug-in hybrid electric vehicles. In *Proceedings of the 7th IFAC Symposium on Advances in Automotive Control* (Vol. 7, No. 1, pp. 121-126).

[216] Badin, F., Berr, F.L., Castel, G., Dabadie, J.C., Briki, H., Degeilh, P., and Pasquier, M., 2015. Energy efficiency evaluation of a Plug-in Hybrid Vehicle under European procedure, Worldwide harmonized procedure and actual use. In *Proceedings of EVS28 International Electric Vehicle Symposium and Exhibition* (pp. 1-14).

[217] Sciarretta, A., Serrao, L., Dewangan, P.C., Tona, P., Bergshoeff, E.N.D., Bordons, C., Charmpa, L., Elbert, P., Eriksson, L., Hofman, T. and Hubacher, M., 2014. A control benchmark on the energy management of a plug-in hybrid electric vehicle. *Control Engineering Practice*, *29*, pp.287-298.

[218] Moura, S.J., Stein, J.L. and Fathy, H.K., 2010, September. Battery-health conscious power management for plug-in hybrid electric vehicles via stochastic control. In *Proc. ASME Dyn. Syst. Control Conf* (pp. 1-2).

[219] Banvait, H., Hu, J. and Chen, Y., 2015, July. Design of energy management system of Plug-in Hybrid Electric Vehicle using hybrid systems. In *American Control Conference (ACC), 2015* (pp. 1339-1344).

[220] Zhang, C. and Vahid, A., 2010, June. Real-time optimal control of plug-in hybrid vehicles with trip preview. In *American Control Conference (ACC), 2010* (pp. 6917-6922).

[221] Chen, Z., Xia, B., You, C. and Mi, C.C., 2015. A novel energy management method for series plug-in hybrid electric vehicles. *Applied Energy*, *145*, pp.172-179.

[222] Shankar, R., Marco, J. and Assadian, F., 2012, September. Design of an optimized charge-blended energy management strategy for a plugin hybrid vehicle. In *Control (CONTROL), 2012 UKACC International Conference on* (pp. 619-624).

[223] Liu, J., 2007. *Modeling, configuration and control optimization of power-split hybrid vehicles* (Doctoral dissertation, The University of Michigan).

[224] Lai, C.D., Xie, M. and Murthy, D.N.P., 2003. A modified Weibull distribution.*Reliability, IEEE Transactions on*, *52*(1), pp.33-37.

[225] Guzzella, L., Fahrezeugantriebssysteme. Lecture notes, ETH-Zurich, Switzerland, 2000.

[226] Back, M., Simons, M., Kirschaum, F. and Krebs, V., 2002, July. Predictive control of drivetrains. In *World Congress* (Vol. 15, No. 1, pp. 1506-1506).

[227] Kotre, S.J., Ramaswamy, D., Woestman, J.T. and Breida, M.T., Ford Motor Company, 2003. *Engine on idle arbitration for a hybrid electric vehicle*. U.S. Patent 6,664,651.

[228] Lee, H.D. and Sul, S.K., 1998. Fuzzy-logic-based torque control strategy for parallel-type hybrid electric vehicle. *Industrial Electronics, IEEE Transactions on*, *45*(4), pp.625-632.

[229] Powell, B.K., Bailey, K.E. and Cikanek, S.R., 1998. Dynamic modeling and control of hybrid electric vehicle powertrain systems. *Control Systems, IEEE*, *18*(5), pp.17-33.

[230] Jalil, N., Kheir, N.A. and Salman, M., 1997, June. A rule-based energy management strategy for a series hybrid vehicle. In *American Control Conference, 1997. Proceedings of the 1997* (Vol. 1, pp. 689-693).

[231] Kuhler, M. and Karstens, D., 1978. *Improved driving cycle for testing automotive exhaust emissions* (No. 780650). SAE Technical paper.

[232] Fomunung, I., Washington, S. and Guensler, R., 1999. A statistical model for estimating oxides of nitrogen emissions from light duty motor vehicles.*Transportation Research Part D: Transport and Environment*, *4*(5), pp.333-352.

[233] Pearson, K., 1901. On lines and planes of closest fit to systems of points in space. *The London, Edinburgh, and Dublin Philosophical Magazine and Journal of Science*, *2*(11), pp.559-572.

[234] Hotelling, H., 1933. Analysis of a complex of statistical variables into principal components. *Journal of educational psychology*, *24*(6), p.417.

[235] Jutten, C. and Herault, J., 1991. Blind separation of sources, part I: An adaptive algorithm based on neuromimetic architecture. *Signal processing*, *24*(1), pp.1-10.

[236] Comon, P., 1994. Independent component analysis, a new concept?. *Signal processing*, *36*(3), pp.287-314.

[237] Fu, J., Gao, W. and Song, L., 2009, September. Principal component analysis based on drive cycles for hybrid electric vehicle. In *Vehicle Power and Propulsion Conference, 2009. VPPC'09. IEEE* (pp. 1613-1618).

[238]**URL:**http://www.thehindu.com/news/international/world/untapped-potential-of-hybrid-cars-in-india/article5960835.ece (accessed on 22/01/2016)

[239]**URL:**http://www.ibnlive.com/news/auto/hybrid-vehicles-more-fuel-efficient-in-india-than-us-677898.html (accessed on 22/01/2016)

Appendix A

Table A1: Parameters used during battery modeling

Parameters	Values	Definitions
$\boldsymbol{V}$	345 volts	Battery nominal voltage
$\boldsymbol{C_P}$	69.5Ah	Battery capacity)
Ambient temperature	25^0C=298 K	Room temperature
$\boldsymbol{R}$	8.3143J/mole/K	Gas constant

Table A2: Vehicle parameters used in simulations

Parameters	Values	Definitions
tx_pg_s	78	Number of teeth in ring gear
tx_pg_r	30	Number of teeth in sun gear
wh_1st_rrc	0.009	Rolling resistance coefficient
veh_gravity	9.81 m/s^2	Acceleration imposed by earth
fd_ratio	3.93	Gear ratio of driveline
fc_fuel_den	749 g/l	Volumetric density
fc_min_spd	104.7198 rad/s	Minimum allowable engine speed
wh_radius	0.2870 m	Wheel radius
fc_max_spd	418.8790 rad/s	Maximum allowable engine speed
veh_CD	0.30	Aerodynamic drag coefficient
veh_FA	1.7460 m^2	Vehicle frontal area
veh_air_density	1.2 kg*m^3	Vehicle air density
tx_spd_dep_upshift and tx_spd_dep_dnshift	[0 6.6667 11.1111 17.7778 20.8333 277.7778]	Gear ratio of transmission
vc_idle_bool	1	Idling of engine is allowed
	0	Engine shuts down rather than idle
cs_hi_soc	0.95 (%)	Highest state of charge allowed
cs_lo_soc	0.65 (%)	Lowest state of charge allowed
cs_target_soc	0.70 (%)	Expected state of charge at the end of trip
ess_initial_soc	0.80 (%)	Initial state of charge of battery
mc_inertia	0.0226 kg*m^2	Rotational inertia of motor
mc_inertia	0.0226 kg*m^2	Rotational inertia of generator
fc_air_fuel_ratio	14.5	Air to fuel ratio (on mass basis)
fc_fuel_lhv	42600 (J/g)	Lower heating value
fd_ratio	3.93	Final drive ratio
wh_radius	0.287 m	Rolling radius of tire
mc_mass	56.75 kg	Mass of motor and enclosure
gc_mass	32.7 kg	Mass of machine and enclosure
wh_inertia	3.3807 kg*m^2	Rotational inertia of all wheels, tires, and axles

Table A3: Vehicle components' specifications

Component	Specification
Motor specification	30-kW permanent magnet synchronous motor Torque range=[0 5 35 65 95 125 155 185 215 245 275 305] N-m Speed Range=[0 52.3 104.7 157.0 209.4 261.7 314.1 366.5 418.8 471.2 628.3] rad/s
Engine specification	1.5L Atkinson cycle engine Maximum Power 43kW @4000rpm, Peak Torque 75 lb-ft @ 4000 rpm Torque range =[8.5428 16.9500 25.4928 34.0356 42.4428 50.9856 59.5284 67.9356 76.4784 85.0212 93.4284 101.9712] N-m Speed range=[104.7198 130.8997 157.0796 183.2596 209.4395 235.6194 261.7994 287.9793 314.1593 340.3392 366.5191 418.8790] rad/s
Battery specification	Nominal Cell Voltage: 1.2V Total Cells: 240 (6 cells x 40 modules Nominal Voltage: 288 V Capacity: 6.5 Ah
Generator specification	15-kW permanent magnet synchronous generator Torque range=[0 5 15 25 35 45 55] N-m Speed range=[0 52.35 104.71 157.07 209.43 261.79 314.15] rad/s

List of Publications

Research Articles

[1] **Panday, A.** and Bansal, H.O., 2016. Multi-Objective Optimization in Battery Selection for Hybrid Electric Vehicle Applications, *Journal of Electrical System*, Accepted, in press.

[2] **Panday, A.** and Bansal, H.O., 2016. Development of Energy Management Strategy in Hybrid Electric Vehicles using Pontryagin's Minimum Principle and Genetic Algorithm Tuned Controller. *International Journal of Vehicular*, Article ID 4234261.

[3] **Panday, A.,** Bansal, H.O. and Srinivasan, P., 2016. Thermoelectric Modeling and Online SOC Estimation of Li-Ion Battery for Plug-In Hybrid Electric Vehicles. *Modelling and Simulation in Engineering*, Article ID 2353521.

[4] **Panday, A.** and Bansal, H.O., 2016. Energy management strategy for hybrid electric vehicles using genetic algorithm. *Journal of Renewable and Sustainable Energy*, 8(1), pp.015701.

[5] **Panday, A.** and Bansal, H.O., 2015. Hybrid electric vehicle performance analysis under various temperature conditions. *Energy Procedia*, *75*, pp.1962-1967.

[6] **Panday, A.** and Bansal, H.O., 2014. A review of optimal energy management strategies for hybrid electric vehicle. *International Journal of Vehicular Technology*, Article ID 160510.

[7] **Panday, A.** and Bansal, H.O., 2014. Green transportation: need, technology and challenges. *International Journal of Global Energy Issues*, *37*(5-6), pp.304-318.

Conferences

[1] **Panday, A.** and Bansal, H.O., 2015, March. Optimal fuel control of series-parallel input split hybrid electric vehicle using genetic algorithm based control strategy. In *Energy Economics and Environment (ICEEE), 2015 International Conference on* (pp. 1-5).

[2] Khandelwal, S., **Panday, A.** and Bansal, H.O., 2015, June, Battery Selection to Improve Performance of Plug-in Hybrid Electric Vehicles, In *Advanced Research Applications in Engineering and Technology*, 2015 International Conference on (pp. 1-5).

[3] Pani, P., Athreya, A.R., **Panday, A.,** Bansal, H.O. and Agrawal, H.P., 2015, March. Integration of the vehicle-to-grid technology. In *Energy Economics and Environment (ICEEE), 2015 International Conference on* (pp. 1-5).

[4] **Panday, A.** and Bansal, H.O., 2014, December. Fuel efficiency optimization of input-split hybrid electric vehicle using DIRECT algorithm. In *Industrial and Information Systems (ICIIS), 2014 9th International Conference on* (pp. 1-6).

[5] **Panday, A.** and Bansal, H.O., 2013, January. Temperature dependent circuit-based modeling of high power Li-ion battery for plug-in hybrid electrical vehicles. In *Advances in Technology and Engineering (ICATE), 2013 International Conference on* (pp. 1-6).

[6] **Panday, A.** and Om Bansal, H., 2013, December. Green transportation in India: Need analysis and solution. In *Control, Automation, Robotics and Embedded Systems (CARE), 2013 International Conference on* (pp. 1-5).

Brief Biography of Candidate

Aishwarya Panday received her B. Tech degree from Uttar Pradesh Technical University, Uttar Pradesh and M. Tech degree from Birsa Institute of Technology, Jharkhand, India in 2008 and 2010 respectively. She joined the department of Electrical and Electronics Engineering at B.I.T.S. Pilani, India as a research scholar in 2011. Her area of research interest is modeling of Li-ion battery and power optimization techniques development for hybrid electrical vehicle and plug-in hybrid electric vehicle.

Brief Biography of Supervisor

Hari Om Bansal received his B.E. degree in Electrical Engineering from University of Rajasthan, Jaipur, M.E. degree in Electrical Power Systems from Malviya National Institute of Technology (M.N.I.T), Jaipur and Ph.D. Degree from Birla Institute of Technology & Sciences (B.I.T. S), Pilani, India in 1998, 2000, 2005 respectively. He worked as research assistant in M.N.I.T, Jaipur From 2000 to 2001, then as a Lecturer at the Mody College of Engineering & Technology, Sikar, India. He joined as an Assistant Lecturer in 2001 and worked as Lecturer since 2002-2005 and currently Associate Professor at B.I.T.S, Pilani. His major interest is in research areas as applications of artificial intelligence techniques in Power Systems, Control Systems, distributed generation and solar energy and hybrid vehicle technology. He has written a book chapter on rural electrification and published number of papers in solar thermal system, power distribution generation using artificial techniques.